Optimization of exon skipping therapy for the treatment of Duchenne muscular dystrophy

Flavien Bizot

université PARIS-SACLAY

Optimization of exon skipping therapy for the treatment of Duchenne muscular dystrophy

Optimisation de la stratégie de saut d'exon pour le traitement de la dystrophie musculaire de Duchenne

Thèse de doctorat de l'université Paris-Saclay

École doctorale n° 569, Innovation thérapeutique : du fondamental à l'appliqué (ITFA)
Spécialité de doctorat: pharmacotechnie et biopharmacie
Graduate School : Santé et médicaments.
Référent : Université de Versailles-Saint-Quentin-en-Yvelines

Thèse préparée dans l'unité de recherche **END-ICAP (Université Paris-Saclay, UVSQ, Inserm)**, sous la direction de **Aurelie GOYENVALLE**, directrice de recherche INSERM

Thèse soutenue à Paris-Saclay, le 20 mars 2023, par

Flavien BIZOT

Composition du Jury

Membres du jury avec voix délibérative

Isabelle RICHARD Directrice de Recherche - DR1 CNRS, Genethon - Universite d'Evry val d'Essonne (U951)	Présidente
Virginia ARECHAVALA-GOMEZA Professeur à Ikerbasque (Espagne)	Rapporteur & Examinatrice
Matteo BOVOLENTA Assistant professeur, Université de Ferrara (Italie)	Rapporteur & Examinateur
Matthias TITEUX Chargé de Recherche – CR1 INSERM Institut Imagine (U1163)	Examinateur

THÈSE DE DOCTORAT

NNT : 2023UPASQ007

université PARIS-SACLAY
ÉCOLE DOCTORALE
Innovation thérapeutique
du fondamental à l'appliqué
(ITFA)

Titre : Optimisation de la stratégie de saut d'exon pour le traitement de la dystrophie musculaire de Duchenne

Mots clés : Développement préclinique, Dystrophie musculaire de Duchenne, Oligonucléotides antisens, Thérapie antisens, Maladies neuromusculaires.

Résumé : La dystrophie musculaire de Duchenne (DMD) est une maladie récessive liée à l'X qui touche 20 garçons sur 100 000. Elle se manifeste par une faiblesse musculaire progressive conduisant à une perte de la marche entre 8 et 14 ans puis par le décès des patients autour de 35 ans. La maladie est provoquée par des mutations dans le gène DMD qui conduisent à une absence de la protéine dystrophine. Il n'existe à l'heure actuelle aucun traitement capable de guérir tous les patients. Néanmoins, une stratégie très prometteuse est en développement et repose sur le principe du saut d'exon. Pour ce faire, des oligonucléotides antisens sont utilisés pour moduler l'épissage de l'ARN pré-messager, restaurer le cadre de lecture de l'ARN et ainsi produire une dystrophine fonctionnelle. Cette stratégie a déjà conduit à la mise sur le marché de 4 médicaments aux Etats-Unis mais, en raison de leur faible efficacité, aucun n'a été accepté en Europe. En effet, ces différentes molécules n'ont conduit qu'à des niveaux très faibles de restauration de la dystrophine (de 1 à 6%) ce qui est insuffisants pour espérer un bénéfice thérapeutique significatif chez les patients.

Mon projet de thèse a donc pour objectif d'optimiser l'efficacité de l'approche de saut d'exon en développant des stratégies combinées. Pour ce faire, des oligonucléotides antisens de type tricyclo-DNA développés dans le laboratoire ont été co-administrés avec différentes molécules.

La première combinaison thérapeutique que nous avons testée avait pour objectif de diminuer l'élimination urinaire des oligonucléotides afin d'améliorer leur biodisponibilité. En effet, la majorité des oligonucléotides sont éliminés dans les urines après une administration systémique. Nous avons réalisé une étude histologique et montré une colocalisation entre les oligonucléotides et les transporteurs OAT présents dans les tubes contournés proximaux du rein. Malheureusement, leur inhibition avec le probénécid (un inhibiteur des transporteurs OAT) n'a pas permis d'améliorer l'efficacité de notre traitement antisens.

La seconde combinaison thérapeutique que nous avons testée avait pour objectif d'améliorer le transport intracellulaire des oligonucléotides. Les oligonucléotides entrent en effet dans les cellules par endocytose. Pour pouvoir être actif, ils doivent donc sortir des endosomes et aller dans le noyau cellulaire où se trouve l'ARN pré-messager. Malheureusement, seulement une infime partie d'entre eux y parvient, les autres sont éliminés par la cellule. Afin d'aider les oligonucléotides à sortir des endosomes, une molécule appelée UNC7938 fut utilisée. Cette molécule crée des pores dans les endosomes tardifs permettant ainsi aux oligonucléotides d'en sortir. La combinaison des deux traitements a permis d'augmenter les niveaux de dystrophine restaurée de 31% dans le cœur et de 58% dans le diaphragme. De plus, la fonction cardiaque fut normalisée après 12 semaines de traitement.

La dernière combinaison thérapeutique que nous avons testée avait pour objectif d'augmenter les quantités d'ARN pré-messagers produits afin d'augmenter le nombre potentiel de cibles pour notre traitement. Trois inhibiteurs d'histone deacetylase (HDACi) ont été testés : le givinostat (a pan HDACi déjà utilisé en essai clinique dans DMD), l'acide valproique (un inhibiteur des HDAC de classe I/II) et EX527 (un inhibiteur des classe III). Apres 4 semaines de co-traitement avec notre oligonucléotide, l'acide valproique et le givinostat ont permis d'améliorer l'efficacité des oligonucléotides en augmentant jusqu'à +74% la production de dystrophine. De plus, un co-traitement de 12 semaines avec l'acide valproique a significativement amélioré la fonction musculaire des animaux.

Tous ces résultats ont permis de démontrer la preuve de principe quant à l'utilisation de petites molécules pour améliorer l'efficacité du saut d'exon.

université PARIS-SACLAY
ÉCOLE DOCTORALE
Innovation thérapeutique
du fondamental à l'appliqué
(ITFA)

Title: Optimization of exon skipping therapy for the treatment of Duchenne muscular dystrophy

Keywords: Neuromuscular diseases, Duchenne muscular dystrophy, Antisense oligonucleotides, Antisense therapy, Preclinical development.

Abstract: Duchenne muscular dystrophy (DMD) is an X-linked recessive disorder that affects 20 out of 100,000 boys. It is characterized by progressive muscle weakness leading to loss of ambulation between the ages of 8 and 14 years and a decreased life expectancy (mean age of death: 35 years). DMD is caused by mutations in the DMD gene that lead to an absence of the dystrophin protein. There are currently no curative treatment options available. Nevertheless, promising therapy is under development and is based on the exon skipping strategy. Antisense oligonucleotides are used to modulate the splicing of pre-messenger RNA, restore the RNA open reading frame and thus produce functional dystrophin. This strategy has already led to the approval of 4 drugs in the United States but, due to their low efficacy, none of them have been accepted in Europe. These various molecules led only to very low levels of dystrophin restoration (from 1 to 6%), which are not enough to expect a significant therapeutic benefit in patients

My thesis project therefore aims to optimize the efficacy of the exon-skipping approach by developing combined strategies. To this end, the tricyclo-DNA antisense oligonucleotides developed in my laboratory were co-administered with different molecules.

The first therapeutic combination we tested aimed at reducing the urinary elimination of oligonucleotides in order to improve their bioavailability. It has previously been demonstrated that a large proportion of oligonucleotides are eliminated in the urine. A histological study performed in kidney of treated mice revealed a colocalization between the tricyclo-DNA oligonucleotides and the OAT transporters present in the proximal convoluted tubules of the kidney. Unfortunately, their inhibition with probenecid (a pan OAT transporter inhibitor) did not improve the efficacy of our antisense treatment.

The second therapeutic combination we tested aimed at improving the intracellular transport of the oligonucleotides. Oligonucleotides enter in cells by endocytosis. To perform exon skipping, they must leave the endosomes and go into the cell nucleus where the pre-messenger RNA is located. Unfortunately, only a tiny part of them succeeds, while the majority is eliminated by the cell. To help oligonucleotides to exit endosomes, a molecule called UNC7938 was used. This molecule creates pores in the late endosomes membrane which allows the oligonucleotides to come out. Combination of the two treatments increased restoration of dystrophin levels by 31% in the heart and 58% in the diaphragm. In addition, cardiac function was normalized after 12 weeks of treatment.

The last therapeutic combination we tested aimed to increase the quantity of pre-messenger RNA produced in order to increase the potential number of targets for our treatment. Three histone deacetylase inhibitors (HDACi) were tested: givinostat (a pan HDACi already used in a clinical trial in DMD), valproic acid (a class I/II HDAC inhibitor) and EX527 (a class III inhibitor). After 4 weeks of co-treatment with the oligonucleotide, valproic acid and givinostat improved the effectiveness of oligonucleotides by increasing dystrophin production by up to +74%. Additionally, co-treatment with valproic acid for 12 weeks significantly improved the muscle function of the animals.

In summary, our results establish the proof of principle that combining small molecules to antisense oligonucleotides can improve the efficiency of exon skipping.

RESUME EN FRANCAIS

La dystrophie musculaire de Duchenne (DMD) est une maladie récessive provoquée par des mutations dans le gène DMD présent sur le locus Xp21 du chromosome X. Ces mutations conduisent à l'absence d'une ou plusieurs isoformes de la dystrophine. L'absence de cette protéine dans les muscles induit une faiblesse musculaire progressive conduisant à une perte de la marche entre 8 et 14 ans et au décès des patients autour de 35 ans. Il n'existe à l'heure actuelle aucun traitement capable de guérir tous les patients atteints par cette maladie. Néanmoins, une stratégie très prometteuse est en développement et repose sur le principe du saut d'exon. Pour ce faire, des oligonucléotides antisens sont utilisés pour moduler l'épissage de l'ARN pré-messager, restaurer le cadre de lecture de l'ARN et ainsi produire une dystrophine fonctionnelle. Cette stratégie a déjà conduit à la mise sur le marché de 4 médicaments aux Etats-Unis mais, en raison de leur faible efficacité, aucun n'a été accepté en Europe. En effet, ces différentes molécules n'ont conduit qu'à des niveaux très faibles de restauration de la dystrophine (de 1 à 6%) ce qui est insuffisant pour espérer un bénéfice thérapeutique significatif chez les patients.

L'objectif de ce projet est donc l'optimisation des thérapies de saut d'exon utilisant des oligonucléotides antisens en développant des stratégies combinées. Pour ce faire, des oligonucléotides antisens de type tricyclo-DNA développés dans le laboratoire ont été co-administrés avec des molécules ayant des mécanismes d'action distincts.

La première combinaison thérapeutique que nous avons testée avait pour objectif de diminuer l'élimination urinaire des oligonucléotides afin d'améliorer leur biodisponibilité tissulaire. En effet, l'étude de la biodistribution de nos oligonucléotides post administration intraveineuse nous a montré que la majorité d'entre eux étaient stockés dans le rein avant d'être éliminés dans les urines. Afin de mieux comprendre ce phénomène, une étude histologique fut réalisée et révéla que les oligonucléotides colocalisent avec les transporteurs OAT (pour organic anion transporter) présents dans les tubes contournés proximaux du rein. Afin d'améliorer la distribution des oligonucléotides et d'inhiber cette accumulation rénale,

nous avons utilisé un inhibiteur pharmacologique des canaux OAT : le Probénécid. Malheureusement le Probénécid n'a pas permis d'améliorer la distribution de nos oligonucléotides antisens dans les organes cibles ni la production de dystrophine.

La seconde combinaison thérapeutique que nous avons testée avait pour objectif d'améliorer le transport intracellulaire des oligonucléotides afin d'augmenter la proportion d'oligonucléotide présent dans le noyau des cellules (où se trouve leur cible: l'ARN pré-messager *DMD*). En effet, il est connu dans la litérature que les oligonucléotides entrent dans les cellules par endocytose et, malheureusement, seulement une infime partie d'entre eux parvienent à rejoindre le noyau cellulaire; les autres sont éliminés par la cellule dans les lysosomes. Afin d'aider les oligonucléotides à sortir des endosomes, une molécule appelée UNC7938 fut utilisée. Cette molécule a la propriété de créer des pores spécifiquement dans les endosomes tardifs. Ainsi, la co-administration de cette molécule avec nos oligonucléotides permettrait d'augmenter la proportion d'oligonucléotides atteignant le noyau cellulaire et donc l'efficacité du traitement. L'utilisation de cette combinaison thérapeutique dans un modèle murin a en effet permis d'augmenter les niveaux de dystrophine restaurée de 31% dans le cœur et de 58% dans le diaphragme. De plus, la fonction cardiaque fut normalisée après 12 semaines de traitement. Ce co-traitement, ayant donné des résultats prometteurs, devra etre évaluer plus en détail afin d'envisager dans les année à venir la création de nouveaux médicament chez l'Homme.

La dernière combinaison thérapeutique que nous avons testée avait pour objectif d'augmenter les quantités d'ARN pré-messagers produits. En effet, lors d'étude préliminaire, nous avons constaté une baisse de production d'ARN pré-messagers (la cible de nos oligonucléotides) dans les cellules des animaux modèles de la maladie. Afin de corriger cette faible production, trois inhibiteurs d'histone deacetylase (HDACi) ont été testés: le givinostat (a pan HDACi déjà utilisé en essai clinique dans DMD), l'acide valproique (un inhibiteur des HDAC de classe I/II) et EX527 (un inhibiteur des classe III). Apres 4 semaines de co-traitement avec les oligonucléotides, l'acide valproique et le givinostat ont permis d'augmenter jusqu'à +74% la production de dystrophine dans les muscles. De plus, un co-traitement de 12 semaines avec l'acide valproique a significativement amélioré la fonction musculaire des

animaux. Ces datas permettent de confirmer notre hypothèse de base et prouvent la plus value apportée par les HDACi dans l'efficacité des traitements antisens. Ces résultats sont d'autant plus prometteurs que les molécules testées sont deja utilisées chez l'Homme (acide valproique) ou sont proche de l'être (Givinostat); ce qui facilitera le developement de ce type de bithérapie en clinique.

Pour conclure, l'ensemble des résultats obtenus lors de cette thèse ont permis de démontrer la preuve de principe que l'utilisation de petites molécules pouvait améliorer l'efficacité du saut d'exon induit par des oligonucléotides antisenses, et offrent donc de nouvelles perspectives pour la traitement de la DMD.

ACKNOWLEDGEMENT

First of all, I would like to thank Dr Virginia ARECHAVALA-GOMEZA and Dr Matteo BOVOLENTA for having accepted the heavy task of being reporter of my thesis, despite your busy schedule. I would also like to thank Dr Matthias TITEUX for agreeing to be an examiner of my thesis and Dr Isabelle RICHARD for agreeing to be examiner and president of the jury. Thank you very much; all questions, discussions and advices you give to me make me progress a lot.

Je tiens à remercier Anne GALY qui, en me mettant en relation avec Aurélie et Luis, m'a permis de réaliser cette thèse.

Un grand merci à Aurélie GOYENVALLE, pour m'avoir fait confiance et m'avoir pris en thèse dans son équipe. Ces trois ans ensemble ont été riche d'enseignement et m'ont permis d'évoluer dans le monde de la recherche. Je te remercie pour ta disponibilité et tes conseils qui ont toujours été enrichissants. Je te remercie également de m'avoir permis de participer à de nombreux congres, en ligne pour certains à cause du COVID et en présentiel pour ceux en fin de thèse. Lors de ces évènements, j'ai pu travailler ma communication orale en anglais (ce qui n'était pas donné) ce qui me permet aujourd'hui de présenter ma thèse dans cette langue. Un grand merci également pour toutes les collaborations que nous avons pu mettre en place lors de ma thèse qui m'ont permis d'apprendre beaucoup de chose et qui m'ont fait connaitre à l'étranger.

Merci à Mathilde D et à Amel pour leur aide. Les journées passées tous les trois à sacrifier des animaux dans la bonne humeur resteront à jamais marquées en moi. Merci à Aurélie A qui est toujours de bon conseil. Tes questions et remarques m'ont permis de me remettre en question et de mieux comprendre mon sujet et ses problématiques. Un grand merci pour l'aide apporté durant ma thèse. Je tiens également à remercier Valérie pour sa gentillesse, son aide pour les commandes et ses conseils et astuces en cas de difficultés (et avec le

COVID on en a eu).

Un grand merci à Sonia et à Chloé qui, malgré leur départ peu de temps après mon arrivé, m'ont appris toutes les techniques utiles à la réalisation de ma thèse. Merci à SQY therapeutics et à Thomas plus particulièrement pour la synthèse des oligo. Merci aux responsables de plateformes (Olivier pour l'histologie, Benoit pour la microscopie, Pravina pour l'animalerie et Hendrick pour la génétique) pour l'entretient et la mise à disposition du matériel. Sans vous, aucun résultat n'aurait pu être obtenu.

Un grand merci à Mbarka, ma maman au labo qui a bien pris soin de moi. Tu arrives toujours à me redonner le sourire avec tes blagues et anecdotes en tout genre. Avec l'aide d'Adrien L et des gilets jaunes, tu t'es transformée en cupidon et tu as scellé l'amour franco hollandais en moi.

Merci à François pour sa bonne humeur apportée pendant les repas. Ton humour et tes blagues (toujours en retenue) mettent tous le monde à l'aise et permettent à tous le monde de passer une pose repas détendu.

Un énorme merci à mes co-doctorants préférés Marta, Adrien M, Pauline, Amel, Meriem, Yoann, Adrien L et bien évidemment Valentin. Vous avez été, par vos conseils et votre bonne humeur un vrai moteur pour moi. La disponibilité et la solidarité mutuelle que nous avons mises en place furent exceptionnelles. C'est en s'entraidant que nous avons pu donner le meilleur de nous même. Nos débats nocturnes autour de frites et de bières (ou coca pour certaines ☺) ainsi que nos concours de blagues pas drôle me manquent déjà. J'espère que nous arriverons à nous revoir tous ensemble régulièrement après mon départ. Quoi qu'il en soit, ma porte vous sera toujours ouverte et une canette sera toujours au frais pour vous. Je vous souhaite à tous plein de réussite et de bonheur pour la suite et je souhaite bon courage à ceux qui n'ont pas encore soutenus leur thèse (et à celui qui en débute une seconde). Gardez votre sourire et votre bonne humeur et cette épreuve se passera sans problème pour vous.

Je tiens à remercier encore une fois Valentin qui au fil du temps est devenu un ami, un confident et un psy pour moi. En cas de coup dur, de doute ou de remise en question, tu as toujours répondu présent. Bien que tu sois normand (ca arrive aussi au meilleurs) tu as illuminé mes journées en transformant la pluie en rayon de soleil. Un grand merci pour tout et bravo à toi pour avoir supporter toutes mes blagues ☺. J'espère que tes dernières semaines de thèse se passeront bien et que tu arriveras à mener tous tes projets à bien.

Un grand merci à mes parents et à mon frère qui furent mes premiers soutiens et conseillés. Ils ont pu vivre avec moi les périodes les plus joyeuses et les plus tristes de ma scolarité. Sans vous, je n'aurais pas pu être là où j'en suis aujourd'hui. Merci beaucoup pour tous les coups de mains, aides et conseils que vous m'avez apportés. Je vous aime.

And to conclude, I would like to thanks Karlijn. The little cute girl I met at the lab when she was in internship. Meeting you was the best things that happen during my PhD. Because of you, I made great progress in English and discovered a new country with new customs. Thank you for all your help and advice you gave to me during my PhD (and during the redaction of the manuscript). Our relationship started with a lot of difficulties (COVID crisis, lockdown, long distance relationship, stress of thesis for both of us) but I am happy to have done it with you and I am even happier to come to you now. A big step is passed for us now and other will come soon but I am not scared for it because nothing is impossible when we are together. Love you.

SUMMARY

LIST OF ABBREVIATIONS

2'MOE: 2'O-methoxyethyl ribonucleoside

2'OMe: 2'O-methyl ribonucleoside

6MWT: 6-minute walk test

AAV: adeno associated virus

ACEi: angiotensin converting enzyme inhibitor

ALP: alkaline phosphatase

ALT: Alanine aminotransferase

ASO: antisense oligonucleotides

AST: aspartate aminotransferase

BMD: Becker muscular dystrophy

Cas: CRISPR-associated endonuclease

cDNA: complementary DNA

CK: creatine kinase

CPP: cell-penetrating peptides

CRISPR: clustered regularly interspaced short palindromic repeats

DGC: dystrophin glycoprotein complex

DIA: diaphragm

DMD: Duchenne muscular dystrophy

EDO: enhanced delivery oligo

EMA: European Medicines Agency

ENA: 2'-O,4'-C ethylene bridged nucleic acid

Fab: fragment antigen-binding

FDA: Food and Drug Administration

GAS: gastrocnemius

GRMD: Golden Retriever with Muscular Dystrophy

HDAC: histone deacetylase

HDACi: histone deacetylase inhibitors

HDR: homology-directed repair

KO: knockout

LNA: locked nucleic acid

MRI: magnetic resonance imaging

mRNA: messenger RNA

NHEJ: non-homologous end joining

OAT: organic anion transporter

Palm: palmitic acid

Pip: PNA or PMO internalization peptides

PMO: phophorodiamidate morpholino

PN: phosphoryl guanidine

PO: phosphodiester

PPMO: peptide conjugated-PMO

PS: phosphorothioate

QUAD: quadriceps

RNase H: Ribonuclease H

ROS: reactive oxygen species

sgRNA: single guide RNA

snRNP: small nuclear Ribo Nucleo Protein

TA: Tibialis anterior

TC-DNA: tricyclo-DNA

TfR1: transferrin receptor 1

TRI: triceps

vg: vector genomes

WT: wild-type

LIST OF FIGURES

LIST OF TABLES

INTRODUCTION

1 DUCHENNE MUSCULAR DYSTROPHY

1.1 GENERALITY

1.1.1 Historic of the disease

Duchenne muscular dystrophy (DMD) was described for the first time in 1868 by the doctor Guillaume Duchenne in his book named "De la paralysie musculaire pseudo-hypertrophique ou paralysie myo-sclérosique" (Duchenne 1868). Dr Duchenne described the symptoms of the disease and gave its three main characteristics:

- progressive weakening of the muscle movements until patient became unambulatory
- increase in volume of the paralyzed muscles
- hyperplasia of the interstitial connective tissue of the muscles

In his book, Dr Duchenne gave recommendations for diagnosing the disease. He includes advices to confirm it with the analyses of muscle biopsies to detect muscle fibrosis in young patient and fat droplet in the older. He described the treatment used in 1868 too: the electrical stimulation.

During the following decades, no major discovery was performed. Only the inheritance pattern (X-linked disease) was understood because only men were affected, while their mother was heterozygote and usually asymptomatic for the disease but, in rare cases, resembles the Becker muscular dystrophy symptoms (Duan et al. 2021).

In 1955, doctors Becker and Keiner described a new muscular dystrophy disease with the same symptoms as DMD but with a slower evolution. This disease is the Becker muscular dystrophy (BMD).

During this period, treatment of DMD patients progressed very slowly. In 1974, a new therapy was tested for the first time: the corticosteroids (Drachman, Toyka, and Myer 1974). The administration of prednisone to the patients improved their mobility, gait, and agility, and

reduced serum creatine kinase levels. In 1989, a placebo-controlled trial performed on 103 patients confirmed the effects of prednisone (Mendell et al. 1989). Since then, corticoids are the main treatment of DMD.

In 1977, the locus Xp21 involved in DMD and BMD was discovered in the short arm of the X chromosome. (Greenstein, Reardon, and Chan 1977) but it's only in 1986 that the *DMD* gene was identified (Kunkel et al. 1985; Kunkel et al. 1986; Monaco et al. 1986). The isolation of the protein encoded by the *DMD* gene (namely dystrophin) was performed at the same period (Hoffman, Brown, and Kunkel 1987; Hoffman et al. 1987). Since then, researchers have tried to find a new medicine to restore the dystrophin production in patients as we will see in the section 3 of the manuscript.

1.1.2 Definition

DMD and BMD are both progressive muscle-wasting diseases caused by mutations in the *DMD* gene present on the X chromosome. The difference between the two diseases is the capacity of patients to produce residual amount of the muscular isoform of the dystrophin (Dp427m).

Patients with DMD have a full absence of muscular dystrophin, which leads to severe symptoms including reduced life expectancy. In contrast, patients with BMD are able to produce a mutated but functional dystrophin. The expression of the mutated protein results in a milder phenotype compared to DMD patients with a wide range of disease severity symptoms as we will see in the section 1.4.

1.1.3 Epidemiology

DMD and BMD are X-linked recessive disorders affecting only male population (incidence for female is <1 per million and is limited to case reports of individuals with Turner syndrome) (Duan et al. 2021). The incidence of DMD is around 20 cases per 100,000 life males (Crisafulli et al. 2020; Kariyawasam et al. 2022). Because of the reduced life expectancy of patients, the global prevalence of the disease is reduced in the general population to almost 5 cases per

100,000 males (Crisafulli et al. 2020; Mah et al. 2014). The prevalence of BMD is lower than DMD with only 1.6 cases per 100,000 males (Mah et al. 2014; Salari et al. 2022).

1.2 *DMD* GENE

The *DMD* gene is located on the short arm of the X chromosome at the Xp21.2-p21.1 locus. Since it represents 0.1% of the total genome; it is the longest human gene with a size of approximately 2.4Mb (Den Dunnen et al. 1989). Its full sequence is composed by 79 exons (Roberts et al. 1993) and encodes for a messenger RNA (mRNA) of 14kb (Koenig et al. 1987) (**Figure 1**).

The *DMD* gene is able to encode eight different proteins from different promoters. Proteins differ in their sizes and/or their tissue distribution. The first and most commonly known protein is the Dp427, which is also called full-length dystrophin. This protein has a size of 427kDa and expresses all the 79 exons (**Figure 1**). Dp427 is the only dystrophin with three isoforms of equal size due to three promoters spaced only a few nucleotides apart. The isoforms are:

- The Dp427m: the only dystrophin expressed in the muscle (Klamut et al. 1990; Koenig et al. 1987)
- The Dp427c (also called Dp427b): expressed in the brain (Nudel et al. 1989)
- The Dp427p expressed in the Purkinje cells (Górecki et al. 1992; Holder, Maeda, and Bies 1996)

In addition to the 3 full-length proteins, the DMD gene can produce 5 other dystrophin isoforms:

- Dp260 expressed in the retina (D'Souza et al. 1995)
- Dp140 expressed in the brain and the kidney (Lidov and Kunkel 1997)
- Dp116 expressed in the Schwann cells (Byers, Lidov, and Kunkel 1993)
- Dp71 ubiquitously expressed but with a main role in the brain (Jung et al. 1993) and the retina (Howard et al. 1998)
- Dp40 ubiquitously expressed (García-Cruz et al. 2022; Tinsley, Blake, and Davies 1993)

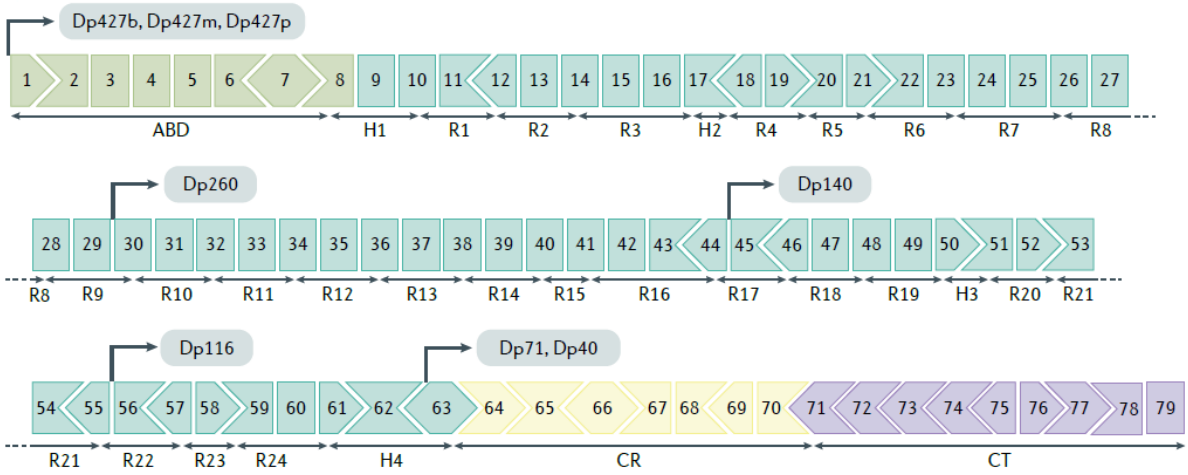

Figure 1: Schematic overview of DMD gene (from *(Duan et al. 2021)**).***
The position of the eight promoters is indicated with the name of the proteins they encode (Dp427b, Dp427m, Dp427p, Dp260, Dp140, Dp116, Dp71 and Dp40). The different exon colors lead to the different part of the protein with in green the N-terminal domain (ABD), in blue: the rod domain divided into 24 spectrin-like repeats (R) and four interspersed hinges (H), in yellow: the cysteine-rich domain (CR) and in purple: the C-terminal domain (CT).

In addition to these 8 main isoforms, other ones are produced from alternative splicing of the gene. This high variability in the sequence of the dystrophin is due to the length of the gene. The gene is so big that it takes 16 hours to be transcribed and, because of its size, many translation errors can be found (Douglas and Wood 2013).

Thousands of different mutations in *DMD* gene have been found in patients with DMD or BMD. The global "TREAT-NMD DMD" database references 7,149 of them with 68.5% of large deletions (deletion of 1 exon or more), 10.97% or large duplications and 10.16% of nonsense point mutations (**Figure 2**).

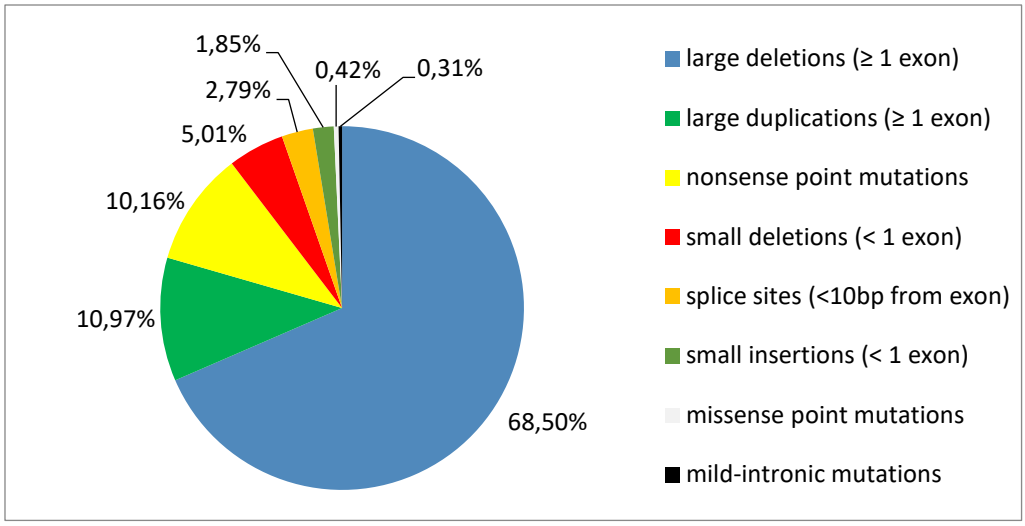

Figure 2: Type and prevalence of mutations causing DMD (data from the TREATNMD DMD Global Database)

66% of the large deletions are localized between the exon 45 to 55 (**Figure 3A**). It can be a deletion of one exon (exon 45 deletion is the most common) to 8 exons (45-52 exons deletion). A second hot spot is localized in the proximal region (exons 2–20) and represents 14% of the deletions (Bladen et al. 2015).

Seven of the eight most commonly reported large duplications are localized in the first exons (from exon 2 to exon 17). The most common one is a duplication of exon 2 which represents 11% of large duplications (**Figure 3B**).

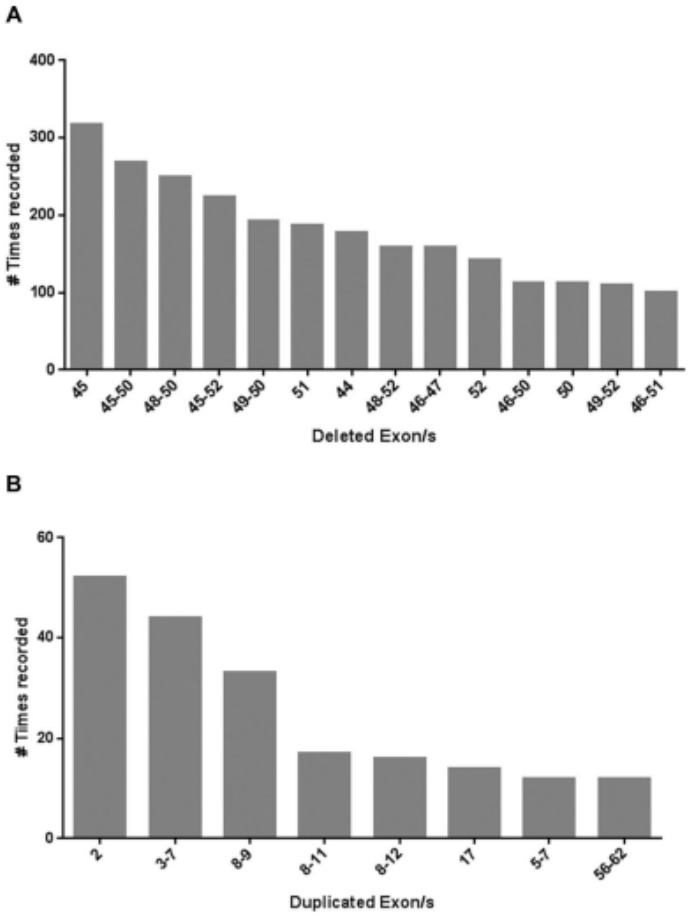

Figure 3: Most commonly reported large mutations (from *(Bladen et al. 2015)***.**
Most commonly reported large deletions (A) and large duplications (B) in the TREAT-NMD DMD Global database.

The severity of the mutation depends on its consequence on the mRNA level. Indeed, a point mutation which leads to the formation of a premature stop codon or an exon deletion/insertion which leads to the disruption of the open reading frame will result in more severe symptoms (i.e. DMD), while a deletion or an insertion of exons that does not disrupt the open reading frame disruption will lead to milder symptoms (i.e. BMD). Based on these observations, new therapies focus on the correction of the open reading frame in order to convert the severe DMD phenotype into the milder BMD one.

The degree of absence of a functional dystrophin protein is not the only factor involved in the severity of the disease. More recently, epigenetic changes have been found in the genome of DMD patients. The histone methylation profile of genes involved in the muscle regeneration process is impacted by the lack of the dystrophin and increases the severity of

the disease (Rugowska, Starosta, and Konieczny 2021). The lack of dystrophin impacts the chromatin conformation of the DMD gene itself with an upregulation of the histone H3K9 methylation (García-Rodríguez et al. 2020). The increase level of this transcriptional repressor leads to decrease *DMD* mRNA production (Chamberlain et al. 1988; Haslett et al. 2002). This phenomenon (called imbalance) is characterized by a normal initiation and by a premature stop of the transcription. Indeed, the comparison of RNA quantity found in muscle of DMD and control patients revealed similar amounts of RNA towards the 5′ end of the sequence and reduced transcript levels towards the 3′ end. During my PhD project, I investigated ways to correct this phenomenon in order to improve the efficacy of exon skipping therapy (Result section, part 3).

1.3 THE DYSTROPHIN: STRUCTURE AND FUNCTION

As previously mentioned, there are 6 main proteins encoded by the *DMD* gene. All proteins are named by their molecular weight. The full length dystrophin (Dp427) is encoded by all the DMD exons which produce 4 domains (**Figure 4**):

- The N terminal actin binding domain
- The rod domain divided into 24 spectrin-like repeats (blue circles in the Figure 4) and four interspersed hinges (blue squares in the Figure 4)
- The cysteine-rich domain (CR)
- The C-terminal domain (CT)

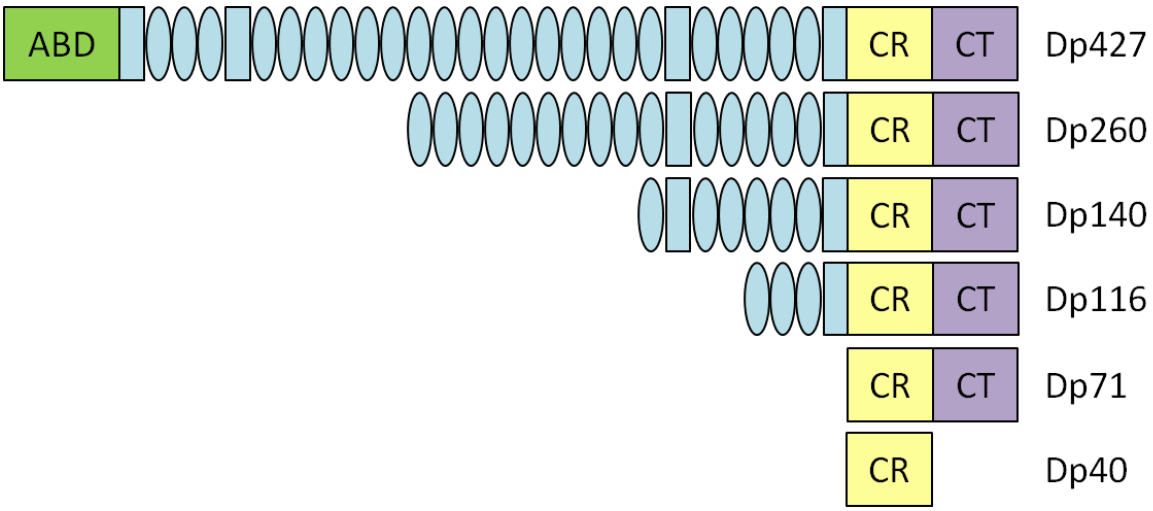

Figure 4: Schematic depiction of dystrophin protein
Composition of the mains dystrophins (Dp427, Dp260, Dp140, Dp116, Dp71 and Dp40). The different colors lead to the different part of the protein with in green the N-terminal domain (ABD), in blue: the rod domain, in yellow: the cysteine-rich domain (CR) and in purple: the C-terminal domain (CT).

Dp260, Dp140, and Dp116 are encoded by different promoters than Dp427. These promoters are localized after the N terminal actin-binding domain so the corresponding proteins do not express this domain but express the three other ones (with more or less rod domain depending on the size of the protein). Dp71 has its promoter even further and contains only the two last domains (Nichols, Takeda, and Yokota 2015). Dp40 has the same promoter as Dp71 but is polyadenylated in intron 70; so it only expresses the cysteine-rich domain (Tinsley, Blake, and Davies 1993).

Dystrophin Dp427 is localized in the sarcolemma of muscle cells where it binds its partners from the dystrophin glycoprotein complex (DGC). The DGC contains dystrophin, calveolin, dystrobrevin, dystroglycan, sarcoglycan, sarcospan, syntrophin, laminin and neuronal nitric oxide synthase (nNOS) (Ervasti and Sonnemann 2008). In the complex, dystrophin links the actin cytoskeleton with its N-terminal domain and the extracellular matrix with its C-terminal domain (**Figure 5**). The bridge established by dystrophin between the two cellular compartments stabilizes the sarcolemma and protects it from disruption during muscle contractions (Pasternak, Wong, and Elson 1995).

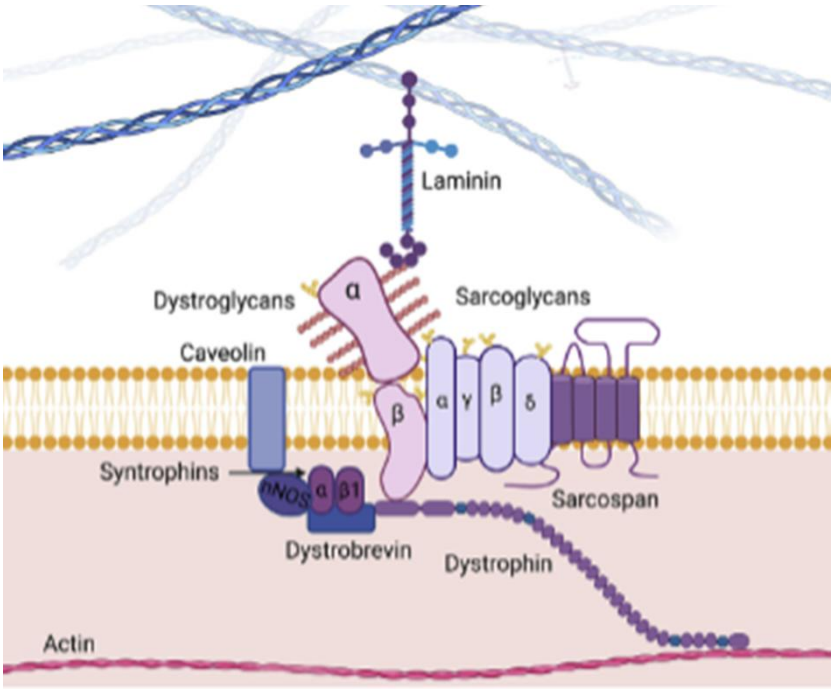

Figure 5: The dystrophin glycoprotein complex (from** (Valera et al. 2021)**)
The DGC is comprised of dystrophin (purple), cytoplasmic actin (pink), dystroglycan (light purple) composed of 2 subunits, α and β, laminin (blue and black), sarcoglycan complex (light blue) composed of 4 subunits (α-, β-, γ-, and δ), sarcospan (purple), dystrobrevin (blue), syntrophins (purple) composed of 2 subunits, α and β, nNOS (dark blue), and caveolin (periwinkle). On the top, in white we have the extracellular matrix and on the bottom in light pink the cytoplasm; in the middle, in orange, there is sarcolemma.

Since the discovery of the DGC, our understanding of dystrophin-interacting partners has improved and binding partners have been identified with the body of the dystrophin. In muscle, the median section of dystrophin can directly link actin or sarcolemma like the terminal section, but it can also bind other proteins involved in the cytosolic signaling pathway like nNOS or PAR1b (also known as MARK2) (Duan et al. 2021). Indeed, the lack of dystrophin has some consequence in all muscle function and interactions. For example, nNOS is involved in the muscle perfusion by decreasing α-adrenergic vasoconstriction in contracting muscles during exercise (Lai et al. 2009). Without dystrophin, nNOS is mislocalized and less active which leads to ischaemic damage in the muscle (Sander et al. 2000). Dystrophin is also involved in the muscle regeneration process. Indeed, PAR1b is involved in the differentiation pathway of satellite cells (the muscle stem cells). Without dystrophin, the expression of PAR1b is down-regulated which leads to a lack of asymmetric

divisions of satellite cells, a reduced production of myogenic progenitors, resulting in a less efficient muscle regeneration (Dumont et al. 2015).

Muscles from DMD patients produce significantly more free radicals than normal muscles. The main free radicals produced in the muscles are the reactive oxygen species (ROS). The mechanical stretching of muscles activates NADPH oxidase 2 and leads to the production of ROS (Prosser, Ward, and Lederer 2011). The absence of dystrophin results in a destabilization of microtubule which becomes dense and disorganized and leads to the production of more ROS (Khairallah et al. 2012).

Dystrophin is a major actor of calcium homeostasis in muscle. The disruption of sarcolemma due to its absence leads to an increase in intracellular calcium level (Turner et al. 1988). Dystrophin is, directly or in combination with the other proteins of the DGC, involved in the deregulation of some calcium channels, plasma membrane Ca2+ ATPase or sodium-calcium exchanger (Allen, Whitehead, and Froehner 2016). Absence of dystrophin can also impact the calcium storage in the sarcoplasmic reticulum by modulating STIM1 and Ora1 channels (Goonasekera et al. 2014). All these phenomena lead to an increase in the activity of calpain, a decrease in the activity of its inhibitor (calpastatin) and to muscle fiber degradation (Kumamoto et al. 1995).

1.4 SYMPTOMS OF THE DISEASE

Dystrophin is produced in a lot of different tissues from muscles to brain and its absence leads to the deregulation of many cellular pathways. In this section, we will describe the symptoms of both DMD and BMD.

1.4.1 Muscular symptoms of DMD

The most commonly known and described symptoms of DMD include the progressive skeletal and cardiac muscle degeneration with fibrous tissue replacement and fatty infiltration. The first symptoms occur between the age of 1 and 3 years-old when children

start walking. They often fall and have difficulties with running. Symptoms increase and boys are commonly diagnosed around 4 years old (Davidson et al. 2014; Magri et al. 2011) Children typically show muscle weakness with muscle hypertrophy and the Gowers' sign when rising up from the ground (illustrate in **Figure 6**). At the age of 8-14 years, muscle weakening progress and patient lost ambulation. Once a patient becomes wheelchair bound, the muscle weakness progresses even faster and abdominal and dorsal symptoms increase. This evolution of the disease leads to scoliosis and joint contractures. Scoliosis reduces the chest cavity volume which leads to increased respiratory problems. The smooth muscles of the digestive tract and of the throat are also affected with time. Transit and swallowing problems will appear and will conduce to food penetration in the laryngeal vestibule or worse in the subglottic area which will induce laryngeal aspiration and asphyxiation (Toussaint et al. 2016).

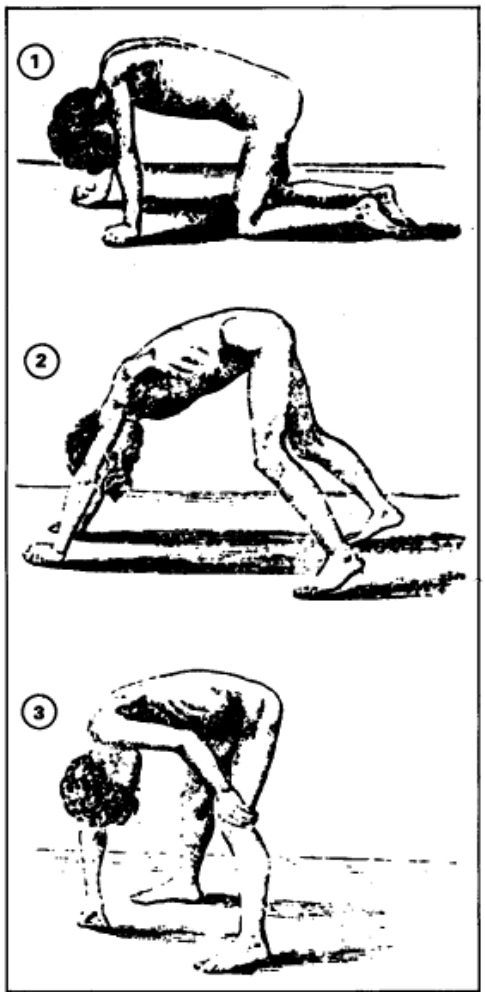

Figure 6: Gowers' sign (from** (Wallace and Newton 1989)**)

In their late teens, DMD patients develop cardiomyopathies which cause the heart chambers to enlarge and the walls to get thinner. Around 20 years-old, breathing problems increase and once the heart and respiratory muscles are damaged, the condition becomes life-threatening (Ryder et al. 2017). DMD patients generally die from cardiac or respiratory failure during their 30s. With good supportive care (presented in section 3.1 of the manuscript), they may survive until their late 30s.

1.4.2 Brain symptoms of DMD

Brain symptoms of DMD patient can be organized in 3 blocks:

- Emotional behavioral problems, such as anxiety, affective disorder, and oppositional/aggressive behavior (Fee and Hinton 2011; Hendriksen et al. 2009).
- Cognitive disorders with a lower intelligence quotient (<70 was found for 27% of patients), learning disability (in 44% of patients), intellectual disability (in 19% of patients) (Banihani et al. 2015)
- Neurodevelopmental disorders with 21% of patients scored above the threshold for autistic spectrum disorder, 24% for hyperactivity, and 44% for inattention. (Ricotti et al. 2016)

Different isoforms of dystrophin are expressed in the brain, at different level, at different developmental stages and in different regions and cells (Doorenweerd et al. 2017):

- Dp427 (c, m) show very low expression during the human foetal brain development, as opposed to DP427p which is not expressed. Dp427c is expressed in the amygdala and hippocampus of adult brain, Dp427p is expressed in adult Purkinje cells and Dp427m is expressed in the cerebellum.
- Dp260 and Dp116 are not expressed in the brain (foetal and adult one).
- Dp140 is express mainly in the foetal brain. In adult brain Dp140 is more expressed in the cerebellum compared to the rest of the brain.
- Dp71 and Dp40 are consistently expressed throughout brain development and in the adult brain (with lower expression in the cerebellum compare to the other regions).

The position of the mutation and the number of dystrophin isoforms impacted are very important for the clinical symptoms of the disease. Mutations affecting Dp71 are associated with severe mental retardation and intellectual disabilities in adult patients (Moizard et al. 2000). Banihani showed that mutations towards the end of the gene lead to worst intellectual symptoms (Banihani et al. 2015). Indeed, patients with a mutation in Dp260 isoform and 5'untranslated region of Dp140 had an intelligence quotient of 85.0, patients with mutation of Dp140 were at 75.0 and patients with a mutation in the Dp71 were <50.0.

1.4.3 Symptoms of Becker muscular dystrophy

In contrast with DMD patients, BMD patients are able to produce some functional dystrophin. This ability leads to a decrease in the symptoms of the disease. For this reason, BMD is often considered as a milder variant of DMD. However BMD has a wide range of disease severity. The most severely affected boys are typically in wheelchair around the age of 16 years (Brandsema and Darras 2015) while the least affected have hardly any symptoms and are still ambulatory at 70 years-old (Yazaki et al. 1999). In addition to the loss of mobility, BMD patients have most of the time increased levels of serum creatine kinase (CK) caused by the muscle damage but to a lesser extent than DMD patients (Gagliardi et al. 2022). Cardiac symptoms are also common in BMD patients with apparition of dilated cardiomyopathy for more than 70% of patients (Del Rio-Pertuz et al. 2022). Dilated cardiomyopathy, followed by arrhythmias, is the most common cause of death in patients with BMD (Connuck et al. 2008).

Some studies have shown emotional-behavioral symptoms in BMD patients but at a lower level than DMD patients. Because of the high variability between studies methodology and patients symptoms, new investigations should be performed to characterize this phenomenon (Ferrero and Rossi 2022).

2 ANIMAL MODELS USED IN RESEARCH

Different animal models can be used to study DMD and investigate new treatments. In this section we will review the most commonly used ones and discuss their advantages and drawbacks (**Table 1**).

2.1 MICE MODELS

2.1.1 Mdx

2.1.1.1 Presentation of the model

The *mdx* mouse also called *C57BL/10ScSn-Dmd^{mdx}/J* has been described for the first time in 1984 (Bulfield et al. 1984). *Mdx* mice have a natural point mutation in the exon 23 of the *Dmd* gene which leads to the apparition of a premature stop codon and the absence of dystrophin Dp427 (the only one expressed in the muscles). This animal model is the first and most frequently used for DMD research and is therefore well-characterized. The absence of dystrophin in the muscle cells of *mdx* mice induces similar symptoms (although milder) than those found in DMD patients, which made the *mdx* mouse model the standard model to study the dystrophin protein and to develop new therapeutics. Indeed, *mdx* mice have; like human; more severe symptoms with age.

One of the first symptoms which appear in *mdx* mice is the muscle degeneration but in contrast with patients (whose progression is continuous over time), in *mx* it progress in cycles in *mdx* (Willmann et al. 2009). Indeed, young mice (2 to 4 weeks) have a high proportion of degenerative and regenerative muscle fibers which conduce to a high proportion of new myofibers; fibers of small size with centralized nuclei. Around 4 to 8 weeks old, necrosis is observed in muscle but it decreases in older mice. The difference between mice and human in muscle degeneration kinetics is a cause of the milder muscular phenotype in mice compare to human. Indeed the absolute muscle force of mice are not poorly reduced with time and mice have, as opposition to human, not difficulties to walk during their all life (Willmann et al. 2009).

The diaphragm of the *mdx* mouse is, in contrast with the other skeletal muscles, the only skeletal muscle which demonstrates a progressive weakness throughout the mouse life span. Indeed, in the diaphragm, histopathological changes are rare in *mdx* mice before 25 days of age and muscle degeneration and regeneration appear around 30 days old (Stedman et al. 1991). At 6 months old, there is necrosis and significant connective tissue proliferation in diaphragm of *mdx* mice and at 16 months old, there is a majority of myofibres loss and fibrosis replacement. Compared to WT mice, the specific diaphragm force of *mdx* mice is decreased by 45% at 2 months old, 58% between 4 and 6 months old and 80% at 24 months old (Chamberlain et al. 2007). This alteration of diaphragm muscle leads to the apparition of respiratory pathology in 16 month-old mice which is not yet present in 4 month-old mice (Gayraud et al. 2007).

Like DMD patient, *mdx* mice have cardiomyopathies but with a less severe phenotype. Indeed, heart symptoms appear later in *mdx* mice with first symptoms around 6 months of age characterized by changes in the electrocardiogram and echocardiogram (Willmann et al. 2009). These symptoms are caused by inflammation processes combined to an increase in myocardial fibrosis and necrosis. The symptoms increase with age and *mdx* of 42 weeks old present dilated, hypertrophied and poorly contracting heart but the symptoms remain less severe as human and are not enough to reduce the life expectancy of mice (Quinlan et al. 2004).

The lack of Dp427 in the brain of *mdx* mice induce, like in patients, some brain, cognitive, and behavioral alterations (Zarrouki et al. 2022). This phenotype is characterized by:

- A learning performance deficit characterized by a delayed acquisition in selective conditioning paradigms involving cue–outcome associative learning, and by deficits in long-term memory in both spatial and non-spatial tasks involving recognition memory.
- An altered emotional reactivity characterized by an enhanced fearfulness in response to mild stress.

These neurological symptoms may be used as phenotypic markers to evaluate the effects of new therapy in the brain.

In summary, the *mdx* mouse model is a correct genetic model to study the DMD gene and the dystrophin expression in all tissues but this model has limit. Indeed, the absence of major clinical signs of muscular dystrophy in young mice (less than 2 months) and its slightly shortened life span make it more difficult to assess the beneficial effects of drug candidates. For this reason, other mice models with more severe symptoms have been developed over the years.

Table 1: Main animal models available to study DMD

Animals	Mutations	Absent dystrophin isoforms
mice		
mdx	stop codon in exon 23	Dp427
D2-mdx	stop codon in exon 23	Dp427
mdx^{2Cv}	mutation in splice acceptor site in intron 42	Dp427 Dp260
mdx^{3Cv}	mutation in splice acceptor site in intron 65	Dp427 Dp260 Dp140 Dp116 Dp71 Dp40
mdx^{4Cv}	stop codon in exon 53	Dp427 Dp260 Dp140
mdx^{5Cv}	stop codon in exon 10	Dp427
mdx52	Deletion of exon 52	Dp427 Dp260 Dp140
HDMD	Addition of human DMD gene	no
del52hDMD/mdx	human DMD gene without exon 52 and stop codon in murine Dmd exon 23	Dp427 (mouse) Human Dp427, Dp260 Dp140
dogs		
GRMD	splicing mutation in intron 6, leading to skipping of exon 7	Dp427
CXMD	splicing mutation in intron 6, leading to skipping of exon 7	Dp427
Delta E50-MD	Deletion of exon 50	Dp427 Dp260
rat		
3	stop codon in exon 3	Dp427
16	stop codon in exon 16	Dp427
Dmd^{mdx}	stop codon in exon 23	Dp427
rabbit		
delta 51	stop codon in exon 51	Dp427 Dp260

2.1.1.2 DBA/2J-mdx or D2-mdx

In order to improve translatability of preclinical studies, a new mouse model with a phenotype closer to the one observed in patients was created. This mouse model is named *D2-mdx*. *D2-mdx* was generated by crossing *BL10-mdx* mice on a *DBA/2J* genetic background (Fukada et al. 2010). The muscle symptoms of this mouse model are more severe than *mdx* with impaired regenerative capacity, inflammation, fibrosis, extensive necrosis and calcifications. However, *D2-mdx* mice still have the same respiratory function as *mdx* mice, and its heart pathology (cardiac calcification) are also found in their WT control (van Putten et al. 2019). The more severe symptoms observed with D2-*mdx* seems to be caused by (van Putten et al. 2019):

- a deletion in the coding region of the Ltbp4 gene which conduce to increase SMAD signaling and fibrosis (mutation also found in human),
- a dysfunctional Anxa6 gene which results in defects in the satellite cells' self-renewal ability, and thus decreased muscle repair
- the presence of the *dyscalc1* gene locus which is responsible of calcifications in skeletal muscles and heart of the mouse model.

While *D2-mdx* has more severe symptoms as the *mdx* ones, its pathology is not progressive and seems to be partially resolves with age (Aartsma-Rus et al. 2023). Because of the disease progression which is different to human, D2-*mdx* is not a perfect model for the development of new drug.

2.1.1.3 mdx^{2Cv}, mdx^{3Cv}, mdx^{4Cv} and mdx^{5Cv}

In 1989, male *C3H.*X_{25} × *C57BL/6Ros* mice treated with a chemical mutagen N-ethylnitrosourea were mating with *mdx* females to produce new mouse models. From this breeding, 4 new mouse lines were created (Chapman et al. 1989):

- mdx^{2Cv} with a mutation in splice acceptor site in intron 42 leading to shift in reading frame
- mdx^{3Cv} with a mutation in splice acceptor site in intron 65 leading to shift in reading

frame

- *mdx*^{4Cv} with a point mutation in exon 53 with formation of premature stop codon
- *mdx*^{5Cv} with a point mutation in exon 10 with formation of new donor splice site, leading to frameshifting deletion

These mice have different mutations that can impact the production of only 1 or all dystrophins, expanding the possibilities for studying the effects of the different dystrophin isoforms.

2.1.2 double knockout models

In an attempt to aggravate the pathology of the *mdx* model and to better understand the role of the dystrophin, mice with double gene knockout (KO) were generated.

2.1.2.1 mdx; utr$^{-/-}$

Utrophin (utr) is a functional autosomal paralogue to dystrophin that shares almost 80% structural homology to the DMD protein (Love et al. 1989). Utrophin is expressed in the sarcolemma of fetal muscles and is progressively replaced by dystrophin during the development (Clerk et al. 1993). Utrophin is also expressed in muscles of adult human, in the neuromuscular and myotendinous junctions, and in regenerative muscle fibres (Pons et al. 1993). In *mdx* mice, the over-expression of utrophin seems to prevent the development of muscular dystrophy symptoms. Consequently and in order to increase the severity of the disease in *mdx* mice, a double KO (DMD and utropin) model was created.

To generate the *mdx; utr*$^{-/-}$ mouse model, female utrophin mutant mice were crossed with male *mdx* mice (Deconinck et al. 1997). Symptoms of this mouse model are closer to those of DMD patient than the *mdx* mice. Indeed, these mice have severe muscle weakness with centrally nucleated fibers at 2 weeks old and adipose and fibrous tissues in mice of 10 weeks old. Diaphragm is altered with necrotic fibers after 6 days of life and cardiac abnormalities were found in mice older than 7 weeks (Grady et al. 1997). *Mdx; utr*$^{-/-}$ mice die from respiratory failure around the age of 20 weeks (Yucel et al. 2018).

This mouse model has shown that *mdx* compensated the lack of dystrophin by a higher production of utrophin. This phenomenon has been shown in DMD and BMD patient too (Janghra et al. 2016).

2.1.2.2 mdx; MyoD$^{-/-}$

MyoD is a muscle-specific transcription factor that plays an important role during muscle regeneration process. *Mdx; MyoD$^{-/-}$* mice have significantly increased disease severity compared to *mdx* mice. Animals have reduced muscle mass, developed cardiomyopathy and scoliosis similar to DMD patients and die prematurely at 12 months of age. In contrast with *mdx* or *MyoD$^{-/-}$* mice, *mdx; MyoD$^{-/-}$* mice presents a hypertrophic heart and increased ventricular diameter by 5 months of age and heart fibrosis by 10 months of age. The severity of the cardiac symptoms makes these mice a good model to study DMD-associated cardiomyopathy (Willmann et al. 2009).

2.1.2.3 mdx; Dtnα$^{-/-}$

α-Dystrobrevin (Dtnα) is a protein which is directly associated to the dystrophin in the DGC and which plays crucial roles as a structural unit and scaffolds for signaling molecules at the sarcolemma of muscle cells. To understand the role of dysrobrevin in the DGC and its possible implication for muscular dystrophy, a double KO dystrophin and α-Dystrobrevin mouse model was created: *mdx*; Dtnα$^{-/-}$ (also named *mdx; αdbn$^{-/-}$*) (Grady et al. 1999). These mice have skeletal muscle myopathy; nuclear cell infiltration and necrosis in heart and 8 to 10 months life expectancy. Symptoms of these mice are milder than *mdx; utr$^{-/-}$* and higher than *mdx* which confirms the importance of dystrobrevin for the integrity of the myofiber sarcolemma and for the NOS-mediated signaling (Grady et al. 1999).

2.1.2.4 mdx; α7-integrin$^{-/-}$

To understand the role of α7-integrin and its interactions with DGC protein, the *mdx; α7-integrin$^{-/-}$* mouse model has been created. These mice exhibit progressive muscle wasting, cardiomyopathy and die 24–27 days after birth from respiratory failure. *Mdx; α7-integrin$^{-/-}$* mouse is a bad model to study DMD cause of its short life expectancy (Mayer et al. 1997).

2.1.3 Other mouse models with mutation in the murin dmd gene

Other mouse models have been created to better understand and treat the mutation found on the *DMD* gene of human patient. For example, *mdx52* were generated in a C57BL/6J backbone without exon 52 (replaced by the neomycin gene) (Araki et al. 1997). Deletion of exon 52 is a common deletion founds in human DMD patients and conduces to the lack of Dp427 (like in *mdx* mice), Dp260 and Dp140. Moreover, exon 52 deletion is a model of exon 51 skipping; exon 51 skipping is the exon skipping therapy applicable to the greatest number of patients.

Other mouse models were created to investigate the consequence of other exon deletion patients have and to develop exon skipping therapy to treat them. To perform it, mice with deletion of 1 (example exon 44, exon 50) or many exons (deletion of exons 52-54 or from 8 to 34 for example) were generated (Zaynitdinova, Lavrov, and Smirnikhina 2021).

2.1.4 HDMD

To be able to test drugs targeting the human DMD gene, a specific mouse model has been created: the *HDMD*. *HDMD* mice are transgenic animals which express a full-length functional copy of the human *DMD* gene as well as a functional mouse *Dmd* gene (Bremmer-Bout et al. 2004). The mice have no phenotype because they can produce all dystrophin (from mice and human) so they cannot be used to test functional recovery. HDMD mice have been crossed with *mdx* mice to generate a new mouse model (*hDMD/mdx*) which express only the human dystrophin in the muscle ('t Hoen et al. 2008). Like *HDMD*, *hDMD/mdx* is a mouse model with no phenotype because cells produce a functional human dystrophin. *HDMD* mouse model has also been used to create the *hDMDdel45*; a model with a human *DMD* gene lacking exon 45 (Young et al. 2017). This mouse model has like the previous one no symptoms because of the production by the cells of a normal murin dystrophin. This model has been used to test the efficacy of exon skipping therapy using human sequence specific to this deletion.

Recently, another mice model has been created with a mutated human DMD gene but in an *mdx* background: *del52hDMD/mdx* (Veltrop et al. 2018). These animals do not produce the mouse dystrophin Dp427 (because of the *mdx* mutation) and produce a human *DMD* mRNA without exon52. The absence of muscle dystrophin makes it a good model to test human sequences for exon 51 or exon 53 skipping. Unfortunately, genetic studies of both *hDMD/mdx* and *hDMDdel52/mdx* showed two copy of the hDMD gene in the chromosome 5 with a tail-to-tail orientation (Yavas et al. 2020). This duplication seems to have taken place during the creation of the hDMD mouse model. Both *hDMD* genes have been KO during the generation of the *hDMDdel52/mdx* mice with the exact same deletion of the first 25 bp of exon 52 but an inverse orientation of intron 51 has been found in both copy of the *hDMD* gene. Luckily, this intronic modification has no consequence on the mRNA sequence. Furthermore, spontaneous skipping of exon 53, leading to restoration of human dystrophin production, has been found in some *hDMDdel52/mdx* mice.

In conclusion hDMD mice are a useful model to test human sequence but some controls should be performed to validate the results and avoid overestimating treatment effects.

2.2 DOG MODEL

2.2.1 GRMD

Dogs, like *mdx* mice, are animals with a natural mutation in the *DMD* gene. Golden Retriever with Muscular Dystrophy (GRMD) is the most characterized dog model. These dogs have a point mutation in the 3' splice site of intron 6, leading to skip exon 7 which alters the reading frame and leads to the apparition of a premature stop codon in exon 8 (Sharp et al. 1992).

Dogs have almost the same symptoms as human DMD patients but with a high heterogeneous severity. Indeed, some animals die after few days, while others are ambulant for months (Ambrósio et al. 2008). Mostly, dogs become less active at 9 months of age and at 12 months respiratory capacity is decreased and pharyngeal and esophageal dysfunctions start to appear. Cardiac atrophy already appears during the neonatal period but systolic dysfunction and left ventricular dilation are detected only after several months (Moise et al. 1991). Because of its "human-like" phenotype, GRMD is a good model to study DMD.

2.2.2 CXMD

As mentioned above, *GRMD* is a good model to evaluate the efficacy of the treatment because of its phenotype close to the human one but this model has a disadvantage: its size. Indeed, GRMD are big dogs so pre-clinical studies performed with them are expensive. To decrease the cost of the pre-clinical studies, a new dog model was created: the *CXMD*. *CXMD* was generated with a cross-breeding between a beagle and a GMRD (Shimatsu et al. 2003). Symptoms of *CXMD* are the same as GMRD without the natal mortality.

2.2.3 DeltaE50-MD dogs or CKCS-MD

Another natural mutation have been found in Cavalier King Charles Spaniels dogs: the *DeltaE50-MD*. The animals have a missense mutation in the 5′ donor splice site of exon 50 that results in deletion of exon 50 in mRNA transcripts (Walmsley et al. 2010). The deletion of the exon 50 makes them a good model to test the effects of exon 51 skipping (the exon skipping able to treat the greatest number of patients). Dogs have almost the same muscular symptoms as human DMD patients. Around 10 months of age tetraplegia symptoms start with high serum level of CK. Dysphagia starts at 3 months of age and dogs die of recurrent aspiration pneumonia around 2 years old. No major cardiology failure has been found in this dog model (Walmsley et al. 2010).

2.3 CAT MODEL

Dystrophin deficient cats were studied for the first time in 1992 (Gaschen et al. 1992). These animals have a more severe disease than humans with hypertrophy of the diaphragm and of the tongue which makes eating and drinking very difficult for them. Cardiac symptoms are different from human too; cats infrequently develop clinical features of heart failure (but humans always have) but develop multifocal mineralizations in the myocardium (humans do not) (Gaschen et al. 1999). For all these reasons cats are not the best animal model to study DMD.

2.4 RAT MODEL

Different rat models have been developed to study DMD. Some Wistar-Imamichi strain rats have been mutated in exons 3 or 16 of the Dmd gene (Nakamura et al. 2014) and Sprague-Dawley rats have a mutation in exon 23 (Larcher et al. 2014). All rats have muscle symptoms similar to the *mdx* mice, but myocardial damages are more severe with fibrosis of the striated cardiac muscles at an earlier age (Zaynitdinova, Lavrov, and Smirnikhina 2021).

2.5 PIG MODEL

To understand the DMD physiological evolution some pig models have been developed. Pig without exon 52 is the first model created (Klymiuk et al. 2013). These animals have a progressive muscle weakness similar to humans but with a faster progression of the disease. All animals died at the age of 14 weeks (before the reproductive age). Pigs with a deletion of exon 51 have been generated too but all animals died after 12 weeks (Zou et al. 2021). Because of the prematury death of all animal before their reproductive age, and to the cost of a breading of pig; no pig model is currently available to study DMD.

2.6 RABBIT MODEL

A DMD rabbit model has been created with a CRISPR-Cas9 targeting the exon 51 (Sui et al. 2018). These rabbits have a high premature mortality; 20% of them die within 2 weeks after birth, and approximately 42.6% within 20 weeks. Muscle phenotypes of 8 weeks old rabbits are similar to the humans with presence of high serum CK levels, muscle degeneration and regeneration, interstitial fibrosis, fatty replacement and mononuclear inflammatory cell infiltrations. Rabbits have cardiomyopathies at 4 months of age with reduced left ventricular ejection fraction and fractional shortening. Cardiac symptoms are the first cause of mortality of the animals.

In conclusion, many animal models of DMD have been studied and generated but none are perfect. Some animals like pigs have more severe symptoms than human, others like cats

have differents symptoms than human and some like mice have only few symptoms. The choice of the animal model must take into account the question to answer. If the question is about the correction of the DMD gene, mouse is one of the best models but if the question is the correction of the DMD symptoms, models like dogs may be more informative.

3 TREATMENT OF THE DISEASE

Major progresses in the treatment of DMD patients were made during the last few years with the approval by the US Food and Drug Administration (FDA) of 4 antisense oligonucleotide drugs: eteplirsen (2016), golodirsen (2019), viltolarsen (2020) and casimersen (2021) respectively targeting exons 51, 53, 53 and 45 and by the European Medicines Agency (EMA) of ataluren (conditional marketing authorization in 2014). These new drugs are very promising but not sufficient for most DMD patients. Symptomatic treatment with corticosteroids combined with cardiac, respiratory, gastrointestinal and orthopedic care is now the basis of the clinical care (HAS 2019; Waldrop and Flanigan 2019). In this section we will describe the symptomatic treatment currently used and the new therapies under development.

3.1 REHABILITATIVE CARE AND SYMPTOMATIC TREATMENT

3.1.1 Corticoid

Corticoid is an anti-inflammatory medicine class used to treat DMD patients. There are currently two corticoid drugs available: prednisolone which is the historical one (used since the 80's (Drachman, Toyka, and Myer 1974)) and deflazacort, an oxazoline derivative of prednisolone. Both drugs are daily administrated (HAS 2019) to patients before they show a decline of the motor functions (which appears around the age of 5-6 years-old) to their death with doses of 0.75 mg/kg/day for prednisone and 0.9 mg/kg/day for deflazacort (Gloss et al. 2016). Both drugs delay the symptoms of the disease but do not cure it. Thereby, this treatment improves muscle function, delays the loss of ambulation from 1.4 to 2.1 years, reduces the need for scoliosis surgery, improves pulmonary function, delays cardiomyopathy onset, and increases survival (HAS 2019; Matthews et al. 2016).

Unfortunately both drugs have side effects. Some are common to all corticoids like immunity or endocrine effects or osteoporosis but other ones seem more drug specific. Deflazacort is also associated with a greater risk of cataracts and prednisone with significant risks of weight

gain, and Cushing's syndrome like appearance (illustrated in the **Figure 7**) (Gloss et al. 2016). To monitor the side effects and prevent their aggravation, annual ophthalmological check-up is recommended and bone density monitoring every 2 years (without context of pathology like fracture or bone pain for example). Some supplementation in calcium and vitamin D are prescribed too (HAS 2019).

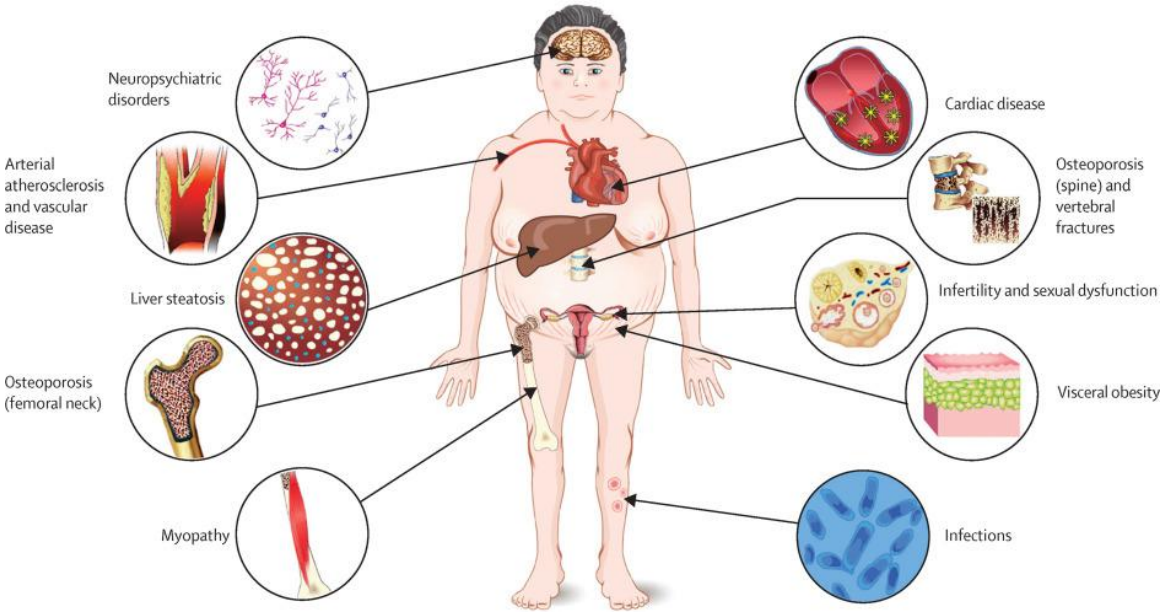

Figure 7: Main comorbidities and clinical complications in patients with Cushing's syndrome (from** (Pivonello et al. 2016)**)

New studies have been performed to optimize this therapy. The first one tried to increase the efficacy by treating young children (before 5 years old) but this increased the risk to develop cardiomyopathy (Kim et al. 2017). The second one tried to decrease the side effects by changing the dosing regimen (with 10 days on, 10 days off instead of daily treatment) but this decreased the treatment efficacy (Guglieri et al. 2022). To decrease side effects and improve treatment efficacy, corticoid therapy is combined with organs/symptoms monitoring and other symptomatic treatments.

3.1.2 Lung treatment

The progressive weakening of the skeletal muscles involved in respiration leads to respiratory compromises and to increase the risk of significant morbidity and mortality events. To prevent it; respiratory function is tested every year from 6 to 12 years-old and every 6 months later. In France, vaccines against flu and pneumococcus are recommended to decrease the severity and the complication of the disease (HAS 2019). Other preventive treatments can be used to delay the respiratory symptoms. The first one is the use of corticoids as previously mentioned (Sawnani et al. 2019). The second one is teaching patients how to initiate lung volume recruitment, cough assist and vest therapies (Waldrop and Flanigan 2019). Nocturnal non-invasive assisted ventilation with back-up rate of breathing are needed when patients have signs of sleep-disordered breathing or when forced vital capacity <50% predicted and maximum inspiratory pressure <60 cm H_2O (Sheehan et al. 2018). If the disease continues to worsen, the combination of spinal surgery and home nocturnal ventilation can be used to improve survival (Eagle et al. 2007). At the end of their life, patients are ventilated 24h per day.

3.1.3 Heart treatment

Cardiomyopathy is, together with pulmonary issues the major cause of morbidity and mortality in DMD. To prevent severe heart damage, cardiac function is controlled yearly upon diagnosis. Cardiac function is screened with electrocardiogram, Holter and echocardiogram or cardiac magnetic resonance imaging (MRI) (Buddhe et al. 2018). The current recommendation is to start heart treatment at 10 years old (before developing abnormal cardiac function) with angiotensin converting enzyme inhibitor (ACEi). This therapy delays cardiac symptoms and improves survival after 10 years of treatment (Duboc et al. 2007). Beta-blockers can be used to treat patient with sinus tachycardia or with ventricular extrasystole (HAS 2019). A clinical trial is in progress to compare beta-blocker with ACEi (Bourke et al. 2018).

A new therapy using allogenic cardiosphere derived cells is currently being tested (Ibrahim, Cheng, and Marbán 2014). These cells have antifibrotic, anti-inflammatory, and regenerative properties. Infusion of 75 million cells to patients decreases fibrosis and improves heart

function at 6 and 12 months post treatment. A randomized blinded trial is in progress to confirm the preliminary results (Taylor et al. 2019).

3.1.4 Orthopedic treatment

Loss of muscle function and osteoporosis are the main symptoms of the disease. To delay it as much as possible, physiotherapy is used. Massage, passive and active muscle stimulations help children to maintain their mobility as long as possible (Carroll et al. 2021) and delay scoliosis. Scoliosis is a frequent complication in the non-ambulatory patients with DMD which may exacerbate the deterioration of respiratory function. For that reason, scoliosis is monitored during every medical check and surgical treatment is undertaken at an early stage of its development (Hsu and Quinlivan 2013).

Decreased bone mineral density is a complication of both the disease and the corticoid therapy which increase the risk of vertebral compression and long bone fractures. Multivitamin supplementation (with vitamin D) in combination with dietary support and physiotherapy are for now the best treatment to maintain bone mineralization. Bisphosphonate supplementation may be used in more severe symptoms too (Waldrop and Flanigan 2019).

3.1.5 Gastrointestinal treatment

Because of the lack of mobility and the absence of dystrophin in the smooth muscle, DMD patients also present gastrointestinal complications. Constipation, reflux and delayed gastric emptying are the more frequent ones. These gastrointestinal complications and the difficulty for DMD boys to eat normally are associated with risk for both obesity and malnutrition (Brumbaugh et al. 2018). Nutritional management with a dietician is strongly advised to decrease these symptoms and osmotic laxatives are used to treat constipation.

3.1.6 Pharmacological therapy in development

As previously discussed, corticoid therapy is currently the first treatment option for DMD but it has many side effects. To decrease the side effects, new compounds with anti-

inflammatory, anti-fibrotic, or antioxidant properties are in development and numerous phase II/III or III trials are ongoing (Deng et al. 2022). One of the molecules of interest is vamorolone; a steroidal anti-inflammatory drug binding the same receptors as corticosteroids. In the long-term extension trial (NCT03038399), Santhera showed that treatment efficacy is similar to corticoids but with an improved safety profile (Santhera 2021). These positive results allowed the validation of its marketing authorization application for the treatment of DMD by the EMA (the October 31, 2022). Santhera is now waiting for the full approval authorization needed for a commercialization in Europe (planned for end of 2023) (Santhera 2022).

Other compounds of interest for treating DMD include sildenatil and tadalafil (phosphodiesterase 5 inhibitors). It was thought that an increase in blood flow could decrease muscle fibrosis in DMD. However, sildenatil has shown heart toxicity during phase II trials (Leung et al. 2014) and tadalafil has shown no improvement in disease outcomes during a phase III trial (Victor et al. 2017).

Givinostat, a histone deacetylase (HDAC) inhibitor, has been shown to change the epigenetic markers of histones in *mdx* mice, which induces the expression of follistatin. Up-regulation of follistatin leads to an increase in muscle regeneration and decrease in inflammation and fibrosis (Consalvi et al. 2013). In phase II trial, 12 months treatment with givinostat was well tolerated and led to a reduction of muscle fibrosis, necrosis, and fatty replacement (Bettica et al. 2016). Givinostat is currently tested in a double blind placebo-controlled phase III study (EPIDYS, NCT02851797) to evaluate its safety and efficacy. The preliminary data showed that givinostat was well tolerated. The drug was also able to delay disease progression by slowing down the decline in time needed to climb four stairs, by maintaining muscle strength and by decreasing fat infiltration by approximately 30% (Action Duchenne 2022). To help its development and speed up its potential approval, both FDA and EMA granted the orphan drug designation to givinostat and FDA gave the rare pediatric disease designation too.

During my PhD, I compared the effects of three HDAC inhibitors (including givinostat) used alone or in combination with ASO therapy. These *in-vivo* protocols performed in *mdx* mice

aim to investigate the effects of HDAC inhibitor on dystrophin RNA production in the different targets organs and the feasibility and the efficacy of a combined therapy using HDAC inhibitor and ASO.

3.2 GENE THERAPY

As previously discussed, DMD is caused by various types of mutations, from only one nucleotide replacement to many exons deletions (**Figure 2**). For this reason, one of the main therapies in development for DMD is gene therapy. This technique aims to treat the disease by providing a functional copy of the DMD gene. In this section, we will study the main strategy in development to correct the *DMD* gene and we will discuss the latest clinical data results.

3.2.1 Additive gene therapy

3.2.1.1 Pre-clinical development

The first solution to possibly cure DMD patients is to introduce a functional copy of the *DMD* gene in all muscle cells. To this aim, a plasmid containing a promoter and the complementary DNA (cDNA) sequence of the DMD gene was created. Injection of plasmids encoding for the full-length dystrophin in mice revealed that this therapy was relatively inefficient with only around 2% of fiber corrected in the injected muscle and no correction in the non-injected ones (Zhang et al. 2004). Intramuscular injection of DNA plasmid in humans showed the same results with less than 10% of muscular fibers partially corrected (Romero et al. 2004). Because of the low restoration level found in the injected muscle and the non-distribution of the plasmid in all muscles, this strategy has some major disadvantages. Vector should be used to carry the cDNA to all muscle cells. The most efficient vectors able to target muscle fibers are the viral vectors but they are generally too small to carry the Dp427 full cDNA sequence (which is 11.5kb long).

In 1990, a BMD patient expressing a dystrophin without exons 17 to 48 was discovered. Although he had a deletion of almost half the coding information, he was still expressing a

functional dystrophin protein and was still ambulant (even one case of 61 years old) (England et al. 1990). Since this case report, other functional mini-dystrophin sequences have been reported with more or less exon deletions. This finding was particularly significant in the context of gene therapy because some viral vectors were able to carry genetic material the size of a mini-dystrophin sequence. This was tested in both adenoviral and retroviral vectors. Unfortunately, adenoviral vectors induced a robust cellular immune response so they could only be efficiently used in immune-compromised animals. Retroviral vectors were also tested in animal models but led to limited efficacy in muscles (Chamberlain 2002).

To be able to treat all muscles, other vectors have been tested and the most promising one was the adeno associated virus (AAV). In the 90s, AAV have been used to treat patients with cystic fibrosis (Wagner et al. 1998) but its ability to treat DMD was limited because of the size of its transgene. Indeed, AAV can only carry 5kb of genetic material and the mini-dystrophin Δ17-48 is 6.5kb big. To solve this problem, some micro-dystrophins (with a size under 4 kb) have been created. The first one was generated in 1997 and was called ΔDysM3 (Yuasa et al. 1997). This sequence encoded for a dystrophin of 3.7kb composed with the N-terminal domain, hinges 1 and 4, a single spectrin-like repeat, the cysteine-rich domain, and C-terminal domain (**Figure 8**). Unfortunately this construct did not manage to treat the *mdx* mice (Takeda 2001).

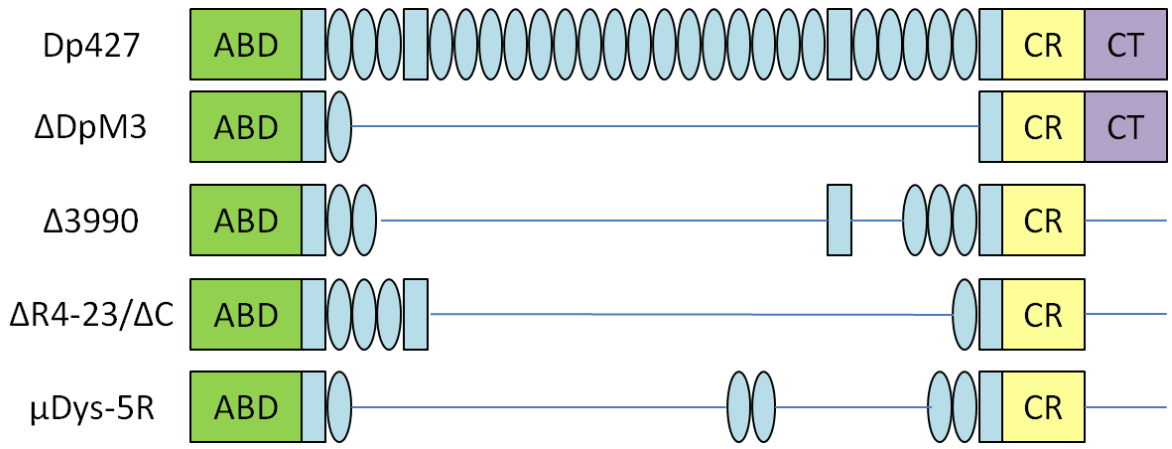

Figure 8: Main microdystrophin sequences used in pre-clinical and clinical trials

Many tests were performed to optimize the sequence of the micro-dystrophin and to find the critical exons to include. Few years later, Xiao lab and Chamberlain lab created AAVs able to restore dystrophin in mouse muscle after local injection. The vector of the first lab contained the micro-dystrophin sequence Δ3990 (Wang, Li, and Xiao 2000) and the second lab the ΔR4-23/ΔC one (Harper et al. 2002). Both sequence encoded for the N terminal domain, the hinges 1 and 4, the spectrin-like repeats 1, 2 and 24 and the cysteine-rich domain. Unlike ΔDysM3, none of them had the C-terminal domain (**Figure 8**). The differences between Δ3990 and ΔR4-23/ΔC are in the central domain of the protein. Δ3990 encodes for the spectrin-like repeats 22 and 23 and the hinge 3 which is not included in the ΔR4-23/ΔC. However Δ3990 does not contain the spectrin-like repeat 3 and the hinge 2 which are include in the ΔR4-23/ΔC.

In March 2006, six boys with frame-shifting deletions in the *DMD* gene were enrolled in the first clinical gene therapy trial for DMD. Patients were treated intramuscularly with an AAV vector coding for a micro-dystrophin (Δ3990). AAV vectors are able to treat the injected muscles cells with an efficiency ranging from 0.01 to 2.56 genome copies per nucleus (cells diploid genome) but none was detected in the untreated contralateral muscles. In this study, three patients (one treated with the lowest dose: 2E10 vg/kg and 2 treated with the highest dose: 1E11 vg/kg) developed T-cell response against the transgene (mini-dystrophin) (Mendell et al. 2012). One hypothesis that may explain the transient T-cell response induced in the patient who made the more severe one is related to the particular mutation of this patient. Indeed, he had a deletion of exons 3 to 17 and Δ3990 express exons 3 to 12 so CD4+ and CD8+ T cells may have reacted against this section of the protein.

During the same period, the dystrophin protein function was getting more and more characterized and the nitric oxide synthase binding domain was discovered. In 2009, the Duan lab created a new micro-dystrophin sequence with the spectrin-like repeats 16 and 17: the μDys-R5 (Lai et al. 2009). Today, the first micro-dystrophins we described (Δ3990, ΔR4-23/ΔC and μDys-R5) are tested in clinic and more than 30 different configurations of synthetic microgenes have been published (Duan 2018).

Table 2: List of AAV serotypes used for gene therapy in neuromuscular disorders (adapted from** (Manini et al. 2021)**)

NA: not available, CNS: central nervous system

Serotype	Glycan recognition	Co-receptor	Target tissues
AAV1	Neu5Aca2-3GalNAcb1-4GlcNAc	NA	Muscle, liver, CNS
AAV2	6-O- and N-sulfated heparin	Fibroblast/hepatocyte growth factor receptor; laminin receptor; integrin aVb5 and a5b1	CNS, liver
AAV3	2-O- and N-sulfated heparin	Hepatocyte growth factor receptor; Laminin receptor	Liver
AAV4	Galb1-4GlcNAcb1-2Mana1-6Manb1-4GlcNAcb1-4GlcNAc	NA	Lung, ependymal cells
AAV5	Neu5Aca2-3(6S)Galb1-4GlcNAc	Platelet-derived growth factor receptor	Muscle, liver, CNS, retina
AAV6	Neu5Aca2-3GalNAcb1-4GlcNAc; N-sulfated heparin	Epidermal growth factor receptor	Muscle, liver, spinal cord
AAV7	NA	NA	Muscle, liver
AAV8	NA	Laminin receptor	Muscle, liver, retina, pancreas
AAV9	Galactose	Laminin receptor	CNS, skeletal and cardiac muscles, liver Human
AAVrh.74	NA	NA	Muscles, spleen, liver

Besides the optimization of the micro-dystrophin sequence itself, additional features of the vector are important including the serotype and the promoter. One of the main challenges is to use an AAV vector able to efficiently target muscle cells following an intravenous injection. To reach this goal many AAV vectors have been screened, tested and classified in terms of their different cell tropisms and receptors. Ten of them are currently used for gene therapy in neuromuscular disorders with more or less efficacy (**Table 2**). AAV6, 8 and 9 were the first AAV vectors that were tested to treat DMD which showed effective whole-body muscle transduction after systemic injection in animal models (rodents and dogs) (Gregorevic et al. 2004; Wang et al. 2005; Yue et al. 2008).

The main limitation of AAV vector is the immune reaction following its administration. Indeed, AAV vector are built with a capsid of commensal virus so patients can be immunized against the vector before the treatment. For example, a study showed that 47 to 96% of patients have pre-existing antibodies against AAV2. Analysis of the seroprevalence of the more efficient AAV vectors (serotypes 8, 9 and rh.74) in DMD patient showed that AAV9 and AAVrh.74 are the less prevalent, thus having the lowest risk for immune reactions (Verma et al. 2022). Based on all this information, some AAV vectors containing micro-dystrophin sequence have been used in clinical trials to treat DMD.

3.2.1.2 Clinical Study

Four clinical trials are currently ongoing to evaluate the safety and the efficacy of systemic injection of AAV micro-dystrophin vectors. Trials are performed by Solid Biosciences, Sarepta Therapeutics, Pfizer and Genethon (**Table 3**). The AAV serotype (8, 9 or rh.74), the muscle specific promoter (MCK, CK8, MHCK7 or Spc5.12) and the micro-dystrophin sequence (Δ3990, µDys-5R or ΔR4-23/ΔC) used in the clinical trials are very variable. These four clinical trials also differ in terms of patient cohort and injected dose. Indeed, ambulatory and not ambulatory patients aged of more than 4 years old have been treated with a dose of 1 or 3E14 vector genomes (vg) per kg during the phase Ib trial of Pfizer. During the clinical trial phase I/II of Solid Biosciences patients (ambulatory or not) of 4 to 17 years old were treated with a doses of 5E13 vg/kg of AVV vector. During the clinical trial phase I/II of Sarepta ambulatory patients of 3 months to 7 years old were treated with a doses of 2E14 vg/kg of AVV vector and during the trial phase I/II of Genethon, ambulatory patients from 6 to 10 years old were included (**Table 3**). In this section we will review the first clinical data obtained with their vectors.

Table 3: Clinical trials ongoing for the treatment of DMD with AAV vector

Drug	**PF06939926 (fordadistrogene movaparvovec)**			**SGT-001**	**SRP-9001**			**GNT 0004**
sponsor	Pfizer			Solid Biosciences	Nationwide Children's/ Sarepta Therapeutics			Genethon
AAV serotype	rAAV9			rAAV9	rAAVrh74			AAV8
promoter	muscle specific			CK8	MHCK7			Spc5.12
transgen	Δ3990			µDys-5R	ΔR4-23/ΔC			ΔR4-23/ΔC
trial number	NCT03362502	NCT04281485	NCT05429372	NCT03368742	NCT03375164	NCT03769116	NCT05096221	2020-002093-27
current stage	Active, not recruiting	Active, recruiting	Active, recruiting	Active, not recruiting	Active, not recruiting	Active, not recruiting	Active, not recruiting	Active, not recruiting
clinical trial phase	Ib	III	II	I/II	I/IIa	II	III	I/II
Patient number	23	99	10	16	4	41	126	51
Patient age	4 years old and older	4 to 7 years old	2-3 years old	4 to 17 years old	3 months to 7 years old	4 to 7 years old		6 to 10 years old
Disease stage	ambulatory and not	ambulatory only	Not applicable	ambulatory and not	ambulatory only			ambulatory only

3.2.1.2.1 PF06939926

PF-06939926 is an AAV vector with a rAAV9 serotype encoding for the microdystrophin Δ3990 under a muscle specific promoter developed by Pfizer. PF-06939926 is currently tested in a phase Ib open-label clinical trial (NCT03362502) to investigate its safety and tolerability in DMD patients. Doses of 1E14 or 3E14 vg/kg are tested and participants will be followed up to 5 years after treatment. In parralel, a multicenter, randomized, double-blind, placebo controlled phase III study is ongoing to monitor the safety and efficacy of the treatment (NCT04281485), in which patients will also be followed until 5 years after treatment.

In May 2020, after injecting 3 patients at the low dose (1E14 vg/kg) and 6 at the high dose (3E14 vg/kg), Pfizer announced that PF-06939926 was well-tolerated during the infusion period and had a good efficacy profile in terms of dystrophin expression (24% restoration with the low dose and 51.6% with the high dose) and motor functions at 12 months post-treatment (Pfizer 2020). Among the 9 treated patients, three serious adverse events were reported but they were all fully resolved within 2 weeks.

In September 2021, three additional serious adverse events were reported and two involved myocarditis. Some mutations in the DMD gene seem to increase the probability to develop this adverse event. For that reason, an amendment was made on the study protocol and patients with a mutation (exon deletion, exon duplication, insertion, or point mutation) affecting exons 9 through 13 or in exon 29 and 30 were excluded from the study (about 15% of the DMD population) (Pfizer 2021a). Few months later, Pfizer announced the unexpected death of a patient, that led the FDA to place a hold on the phase Ib trial (Pfizer 2021b). The company amended the protocol another time and included a 7-days hospitalization period to closely monitor and manage patients just after the treatment and in April 2022, FDA lifted the clinical hold (Philippidis 2022). In June 2022, a phase II trial has been started to evaluate the safety and efficacy of Fordadistrogene Movaparvovec (the new name of PF-06939926) in patient of 2 and 3 years old (NCT05429372).

3.2.1.2.2 SGT-001

SGT-001 is an AAV vector developed by Solid Biosciences with a rAAV9 serotype encoding for the microdystrophin µDys-5R under the promoter CK8. SGT-001 is currently tested in a phase I/II open-label clinical trial (NCT03368742) to investigate its safety and tolerability in DMD patients. In March 2018, the first patient injected with a dose of 5E13 vg/kg was hospitalized due to reduction in platelet and red blood cell counts and to activation of complement (Solid Biosciences 2018a). In February 2019, the quantification of dystrophin restoration level in the 3 injected patients shown a very low efficacy of the treatment (≤5% were detected by western blot in the 3-months biopsy samples) (Solid Biosciences 2019a). Solid Biosciences decided to increase the dose injected to have more dystrophin restored. In November 2019, the third patient injected with 2E14 vg/kg SGT-001 experienced a serious adverse event characterized by complement activation, thrombocytopenia, a decrease in red blood cell count, an acute kidney injury, and cardio-pulmonary insufficiency (Solid Biosciences 2019b). This event caused the FDA to place a clinical hold on the trial. The patient was fully recovered in December 2019, and FDA lifted the clinical hold in October 2020.

In April 2021, the eighth patient injected with 2E14 vg/kg SGT-001, experienced an inflammatory response which was classified as a serious adverse event and considered by the investigator to be drug-related. Dystrophin quantifications in the 3 first patients injected with 2E14 vg/kg SGT-001 were communicated. The values obtained were very heterogeneous (from undetectable to 17.5% at 90 days post treatment) and seemed to increase with time (Solid Biosciences 2021). In March 2022, Solid Biosciences announced the results obtained with the 4^{th}, 5^{th} and 6^{th} patients included in the phase I/II trial NCT03368742 (Solid Biosciences 2022a). Patients have an improved motor function at two years post-infusion as assessed by 6 minute walk test (6MWT) and North Star Ambulatory Assessment and an improved pulmonary function, as measured by forced vital capacity and peak expiratory flow.

In April 2022, Solid Biosciences announced that a second-generation manufacturing product named SGT-003 is planned to enter in clinic in late 2023 (Solid Biosciences 2022b). SGT-003 is composed of a novel muscle-tropic AAV capsid called AAV-SLB101. During the pre-clinical

studies performed on *mdx* mice and non human primates, this new capside was more specific to muscles and less accumulated in the liver compared to the AAV9 one (Solid Biosciences 2022c).

3.2.1.2.3 SRP-9001

SRP-9001 is an AAV vector developed by Sarepta Therapeutics with a rAAVrh74 serotype encoding for the microdystrophin ΔR4-23/ΔC under the promoter MHCK7. SRP-9001 is currently tested in a phase I/IIa, phase II and phase III open-label clinical trials (NCT03375164; NCT03769116 and NCT05096221). Data obtained in the first 4 patients treated with 2E14 vg/kg of SRP-9001 were published in 2020 (Mendell et al. 2020). No serious adverse events were detected post injection. The transduction level efficacy was monitored in muscle biopsies of treated patients and 3 vector copies per nucleus were quantified. The dystrophin restoration level in muscle was at 74.3% 12 weeks after treatment; no data were published for a later time point even if the North Star Ambulatory Assessment is stable during the 365 days following the injection.

In 2021, Sarepta Therapeutics published the data of another phase I clinical trial (NCT04626674). In this study 11 patients were treated with a lower dose of SRP-9001 (1.33E14 vg/kg instead of 2E14). No serious adverse events were found and the mean levels of the dystrophin protein restoration were at 55.4% 12 weeks post treatment (Sarepta 2021a). Data obtain from the phase II trial (NCT03769116) reported in January 2021 showed no improvement of the North Star Ambulatory Assessment in the treated group compared to the placebo one (Sarepta 2021b). Clinical trials are still ongoing to prove the safety and efficacy of the treatment.

3.2.1.2.4 GNT 0004

GNT0004 is an AAV vector developed by Genethon with an AAV8 serotype encoding for the microdystrophin ΔR4-23/ΔC under the promoter Spc5.12. GNT0004 is currently tested in a phase I/II/III open-label clinical trials (2020-002093-27). In April 2021, the first patient was injected (genethon 2021). Because of the apparition of serious side effects, this trial is

temporarily interrupted and the protocol has been amended (genethon 2022).

In conclusion AAV therapy showed promising results during *in-vivo* studies carried out on animals. This technology may, in theory, be able to treat all DMD patients with only one drug (as opposition to the genome editing or the exon skipping therapy that we will review in the next sections). Unfortunately, severe treatment-related adverse reactions, including death have been reported during the clinical trials. A clear understanding of these risks and their mechanisms will be the basis for new drug approval. Indeed, adverse events occurrence may be decreased with a better identification of patients at risk of severe reactions, immunosuppressive regimens, specific follow-up and more specific engineering of capsids (Horton et al. 2022).

Moreover, another limitation of AAV therapy is their inability to be re-administered over time. Therefore, the AAV transgene injected in young patients should be expressed in the target cells of the patient during its all life. The impossibility to make a second injection after some time may be a problem at mild or long term if the production of micro-dystrophin is lost with time, with muscle growth or with muscle physiological remodeling.

3.2.2 Genome editing

3.2.2.1 CRISPR Cas

Clustered regularly interspaced short palindromic repeats (CRISPR) was first identified by Jennifer Doudna and Emmanuelle Charpentier (who won a Nobel prize in 2020 for it) in bacterial. This molecule was used as bacterial immunity. With it, viral DNA was incorporated into the bacterial genome before being transcribed into RNAs. RNA produced may cooperate with the endonuclease to recognize future viral pathogens and mediate to their destruction (Jinek et al. 2012).

CRISPR–Cas9 technology can also be used to induce double- stranded DNA breaks in the *DMD* gene to activate DNA repair systems. To this end, CRISPR/Cas9 system needs two main components:

- a CRISPR-associated endonuclease (Cas)
- a single guide RNA (sgRNA)

The sgRNA contains the complementary sequence of the gene to cut. sgRNA will guide the Cas to the place of interest in the genome and subsequently Cas will cut it. These breaks activate two main repair pathways: the non-homologous end joining (NHEJ) and the homology-directed repair (HDR). In presence of a donor template, the HDR pathway will be activated; in contrast in absence of a donor template, the NHEJ will be activated. The latter is quick and is, in contrast to the HDR pathway, efficient throughout the cell cycle, but may result in insertion or deletions in the DNA sequences. HDR pathway may be used to correct the gene by modifying a point mutation or inserting a missing exon. A major challenge includes the fact that a donor template, which encodes for RNA sequence of interest, should be delivered in the cell at the same time as the CRISPR-Cas system. Moreover muscle fibers are non-dividing cells, which make HDR less efficient as NHEJ.

NHEJ may be used to treat DMD but its effect depends on the localization of the double-stranded DNA breaks (**Figure 9**). It can induce (Aslesh, Erkut, and Yokota 2021; Erkut and Yokota 2022):

- exon skipping if the break is in a splice acceptor site
- exon exclusion with 2 breaks: one before and one after the exon
- exon reframing with a break in the exon sequence

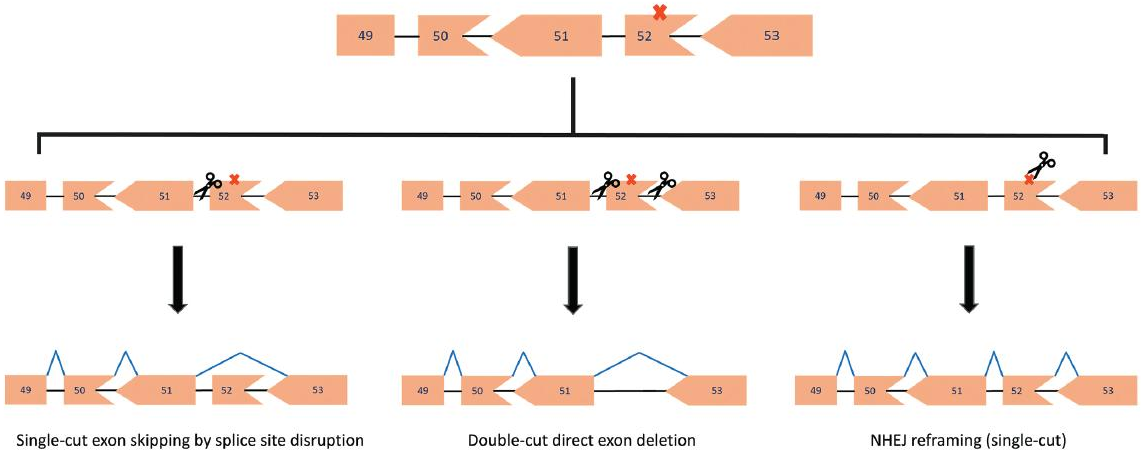

Figure 9: Example of exon 52 skipping mediated by CRISPR/Cas9 gene editing (from *(Aslesh, Erkut, and Yokota 2021)****).***

The single-cut exon-skipping strategy has been tested in vivo in mouse (Amoasii et al. 2017) and dog (Amoasii et al. 2018) models. In mice, this therapy was found to restore dystrophin expression up to 90% of the WT expression level in skeletal and cardiac muscles, to increase muscle force and to normalize CK levels. In deltaE50-MD dogs, single-cut exon-skipping strategy restored dystrophin expression to 60% of WT in muscles and to 90% of WT in heart. These data are very promising and clinical trials are needed to test the safety and efficacy of the drug in humans.

The double cut exon deletion has been tested in both mice and pig models with good results. This method was used to exclude exon 51 in pig delta 52. This deletion leads to the restoration of the open reading frame and to the production of almost 50% of dystrophin in muscles and 10% in heart (Moretti et al. 2020). In mice, this method was used to delete one (Long et al. 2016) or many exons (Bengtsson et al. 2017; Xu et al. 2016). Duchene et al. used this method in mice to connect the exons 47 and 58 by excising all the exons and introns in between (Duchêne et al. 2018). This approach may be applicable to about 40% of the DMD patients. Unfortunately PCR did not detect the hybrid exon junction (47-58) in the tibialis anterior nor in the diaphragm of the treated *del52hDMD/mdx* mice. Only few dystrophin positive fibers were detected in the heart. To confirm the long term efficacy of the double cut - one exon deletion method, Nelson et al analyzed the dystrophin restoration level in mice 1

year after treatment (Nelson et al. 2019). After this period, mice were still able to produce dystrophin in both cardiac and skeletal muscle cells but at a low level (around 5 to 10% of a WT level). Humoral and cellular immune responses have been detected in mice but it may be avoided by treating neonatal mice instead of older one. The double cut exon deletion strategy is currently in development with cell or animal model to be more efficient before being tested in clinic.

For the exon reframing method, Min et al. designed a sgRNA which can insert only a single adenosine in the DNA break (Min et al. 2019). The insertion of a single adenosine in the DNA sequence may restore the open reading frame in exons that are off by only one nucleotide. No *in-vivo* data were found with this specific construction yet.

3.2.2.2 Other methods

Before CRISPR–Cas9, transcription activator-like effector nucleases (TALENs) and zinc-finger nucleases (ZFNs) were used to make double-stranded DNA breaks. Both have been tested for gene editing in DMD, but have major disadvantages (Cai and Kong 2019; Li et al. 2015): ZFNs may induce cytotoxic off-target effects because of its lack of specificity (Zhang et al. 2018) and TALENs have a poor biodistribution in the target cells (Gupta and Musunuru 2014).

3.2.2.3 Genome editing in clinic

Based on its effects in animal models, genome editing seems promising for treatment of DMD. Indeed, unlike the AAV therapy whose transgene must be expressed throughout the patient's life, gene editing technology just needs to be efficient during a short period of time; the time of genome correction. However, the side effects, in particular the off-target ones, should be analyzed carefully. The double-stranded DNA breaks induced in another gene may cause cancer, cell differentiation, or cell apoptosis (depending on the gene and the cells). The modification of germinal cells may transmit the modification to the descendants, leading to ethical issues. The nuclease components (the Cas) are derived from bacteria and therefore the patient may produce an immune response against it. This is of particular interest since this technology is mostly administered with AAV vectors, against which an immune reaction may

be produced too (Robinson-Hamm and Gersbach 2016). In August 2022 the CRD-TMH-001 trial (the first clinical trial using CRISPR to treat DMD patients) was approved by the FDA (NCT05514249) to test this approach on one patient. The patient passed away in November 2022. No details related to the circumstances of this death are currently known (Cure Rare Disease 2022).

In conclusion, even if genome editing showed promising results during *in-vivo* studies carried out on animals, its development and the characterization of its toxic effects (with off target) must be better understood before going into clinic and be approved as medicine.

3.3 MODULATE EXPRESSION OF OTHER GENES

As mentioned in the animal model section, some genes may be up or down regulated to decrease the symptoms of the disease. For example, *dystrophin/ utrophin KO* mouse has more severe symptoms than the *mdx* mouse. For that reason, the modulation of other genes than the *DMD* one can be used to attenuate the disease.

3.3.1 Utrophin up-regulation

As we saw in the animal model section, utrophin is a functional autosomal paralogue to dystrophin which seems to prevent the development of muscular dystrophy symptoms in *mdx* mice. Utrophin upregulation may also be a good strategy to treat DMD patients (Tinsley et al. 1998).

Ezutromid, a small chemical molecule, $C_{19}H_{15}NO_3S$, up-regulated significantly the utrophin level production in the muscle of *mdx* mice and slow down disease progression (Tinsley et al. 2011). Data obtained during the phase I clinical trial showed good tolerability of the compound (Tinsley, Robinson, and Davies 2015). The phase II clinical trial did not show significant efficacy of the drug. In 2018 Summit Therapeutics decided to stop all clinical trials and all developments with this molecule (Summit Therapeutics 2018).

3.3.2 Myostatin inhibition

Myostatin, also known as growth differentiation factor 8 (GDF-8), inhibits the activation of satellite cells and the mTOR pathway which regulates the muscle fiber growth and mass (Yoon 2017). Mice with a KO in myostatin gene have a higher skeletal muscle mass than control mice. In *mdx* mice, the inhibition of myostatin decreases the severity of the disease (Murphy et al. 2010). Domagrozumab and Taldítercept alpha, two myostatin inhibitors, have been tested in phase II trials.

Domagrozumab is a recombinant humanized monoclonal antibody developed by Pfizer. The molecule showed no toxicity of clinical interest during the phase I clinical trial. During the phase II trial no significant effects have been detected which led Pfizer to stop the development of the drug (Wagner et al. 2020).

Taldítercept alpha (also named RG6206) is an anti-myostatin adnectin developed by Roche. Adnectin is an antibody like family proteins with a design based on the framework of the 10th human fibronectin type III domain (Lipovsek 2011). The molecule showed no toxicity of clinical interest during the phase I clinical trial. During the phase II clinical trial no significant effects have been detected, leading to a stop of the drug development by Roche (Roche 2019).

3.4 CELL THERAPY

Gene therapy and gene editing are not the only ways to add a functional DMD gene in muscle cells. Allogenic cells (cells from a donor) or autologous cells (cells from the patient which have been corrected *in-vitro*) may be used to carry the gene in the muscle fibers. To this end, cells need to go into the muscle and fuse with the fibers.

The first cells used for this therapy were satellite cells (muscle stem cells) and myoblasts (the early mononuclear muscle cells able to proliferate or to differentiate in muscular cells). Myoblasts that were injected intramuscularly have shown interesting results in animal models and are currently tested in phase I/II clinical trial (NCT02196467). Although the first results seem promising, one of the major limitations of this technique is the inability of cells to

diffuse to all target organs. Indeed, to cure DMD patient, all muscles, including the heart, should be treated. This is not possible through intramuscular injections. The cells unfortunately failed to treat mice after intra-arterial injections (Skuk and Tremblay 2014).

Mesoangioblast is another cell type able to differentiate into muscle fibers. In contrast with the previous ones, mesoangioblasts are able to do homing to muscle after intra-arterial delivery. A phase I/IIa trial using allogenic cells have been performed in five DMD patients (EudraCT 2011-000176-33). Unfortunately, the dystrophin restoration level was too low to be therapeutically meaningful for the patients (Cossu et al. 2015).

Mesenchymal stem cells are, like the previous cells, able to engraft in skeletal muscle. The advantage of these cells is their possible extraction from umbilical cords (an easy source for allogenic cells collection). During phase I/II trial, mesenchymal stem cells had improved pulmonary function but limb muscle strength was not statistically improved (Dai et al. 2018).

Bone marrow-derived autologous stem cells have been tested in clinical trial (NCT03067831) but their ability to differentiate into muscle fibers was too low to be efficient (Biressi, Filareto, and Rando 2020).

Cardiosphere-derived cells, contrarily to the previous cells, do not differentiate or fuse with muscle cells. Cardiosphere-derived cells secrete vesicles (exomes), which alter the expression profile of macrophages and reprogram fibroblasts. They thus decrease the inflammation and the fibrose. Intracoronary injection of cardiosphere-derived cells was abble to increase the upper limb strength and the heart function of DMD patients (Taylor et al. 2019). A clinical trial phase III is ongoing to confirm the effects of this therapy (NCT05126758).

In conclusion the advantage of cell therapy is the possible multiple administration during the patient life but this technique has many limitations (Sun et al. 2020). One of them is the limited number of cells collected (depending on the cells used for the therapy) which may

impact the efficacy of the treatment. Another limitation is the low engraftment level obtained in the target organs and the accumulation of the cells in the highly vascularized organs such as liver and lungs. To avoid this accumulation, new delivery methods of systemic dissemination should be developed. Furthermore, the transplanted cells should cross the muscle-endothelial barrier to fuse with the regenerating muscle fibers (and treat the disease) and should colonize the satellite cell niche to ensure long-term benefits of the treatment. The last limitation of the autologous cell therapy is the risk of off-target effects induced by the genome editing method used to correct the cell. For all these reasons, cell therapy is not the optimal method to treat DMD patient yet.

3.5 READTHROUGH THERAPY

DMD is caused by a nonsense mutation in the dystrophin gene in about 10% of patients (**Figure 2**). This alteration causes the apparition of a premature stop of translation which results in production of non-functional dystrophin. The aim of readthrough therapy is to restore the production of full length dystrophin by inhibiting the translation termination caused by a point mutation.

Gentamycin was one on the first molecules tested to bypass the premature stop codon generated by a point mutation. This molecule was able to restore functional dystrophin production in the *mdx* mouse model (Barton-Davis et al. 1999). Based on these data, a phase I clinical trial was started (NCT00451074). Three out of four patients who had UGA sequence as stop codon were able to produce dystrophin after the treatment but patients with UAA sequence as stop codon did not. Unfortunately, chronic use of gentamycin increases the risk of nephrotoxicity and ototoxicity (Politano et al. 2003). Due these serious adverse events, the development of this treatment was stopped.

Ataluren, another molecule able to suppress premature termination but without nephrotoxicity and ototoxicity, was able to restore dystrophin production and rescue functional activity of skeletal muscles within 2-8 weeks of treatment in *mdx* mice (Welch et al.

2007). Subsequently, in a phase I trial, sixty-two healthy adults were treated and no adverse events were found, except for only mild headaches, dizziness, and gastrointestinal discomfort at high dose (Hirawat et al. 2007). A randomized, double-blind, placebo-controlled phase II study enrolling 174 DMD patients of 5 years old and older confirmed that ataluren was well-tolerated and showed that the molecule improves the 6MWT after 48 weeks of treatment (Bushby et al. 2014). Based on these results EMA granted a conditional marketing authorization for ataluren in 2014. In 2020, Mercuri et al (Mercuri et al. 2020) compared the results obtained during the phase III trial (STRIDE Registry) in which 217 patients from 11 countries were treated with ataluren with data from 400 untreated patients (from the CINRG DNHS data base). They showed that the main clinical benefit of ataluren was to slow down the disease progression. This effect was found over a mean treatment period of 632 days. They showed that ataluren might delay the worsening of pulmonary function and loss of ambulation but they found no significant improvement of the heart function. Because of its low beneficial effects, the FDA has not approved this drug yet and three clinical trials are ongoing to prove the efficacy of the drug (NCT01247207, NCT03179631, and NCT02369731).

Further analysis of clinical trials data showed that ataluren was more efficient in younger patients (Ruggiero et al. 2018). A phase II clinical trial is ongoing to test the efficacy and tolerability of the treatment in children from 6 month-old to 2 years-old (NCT04336826).

4 SPLICE SWITCHING THERAPY TO TREAT DMD

Splice switching therapy is another therapeutic approach used to restore the dystrophin production in cells. This therapy will not correct the genome (or add a new gene) but will act on the RNA maturation process to produce a functional mRNA and therefore a functional dystrophin.

4.1 INTRODUCTION OF SLICE SWITCHING THERAPY

4.1.1 Splicing mechanism

During transcription, cells produce pre-mRNA from the DNA sequence. To be translated, pre-mRNA needs to undergo a maturation step to exclude the non-coding part of the gene (the introns). This step is the splicing.

The splicing machinery (the spliceosome) is composed of hundreds of proteins which will self-associate to form small nuclear Ribo Nucleo Protein (snRNP). These snRNP will bind the pre-mRNA to put the consecutive exons close from each other before cutting the intron off and link the exons together. To do that, the spliceosome needs to recognize 4 specific sites of the pre-mRNA sequence (**Figure 10**):

- the 5′ splice site (or donor site)
- the 3′ splice site (or acceptor site)
- the branch site (or branch point)
- the polypyrimidine tract

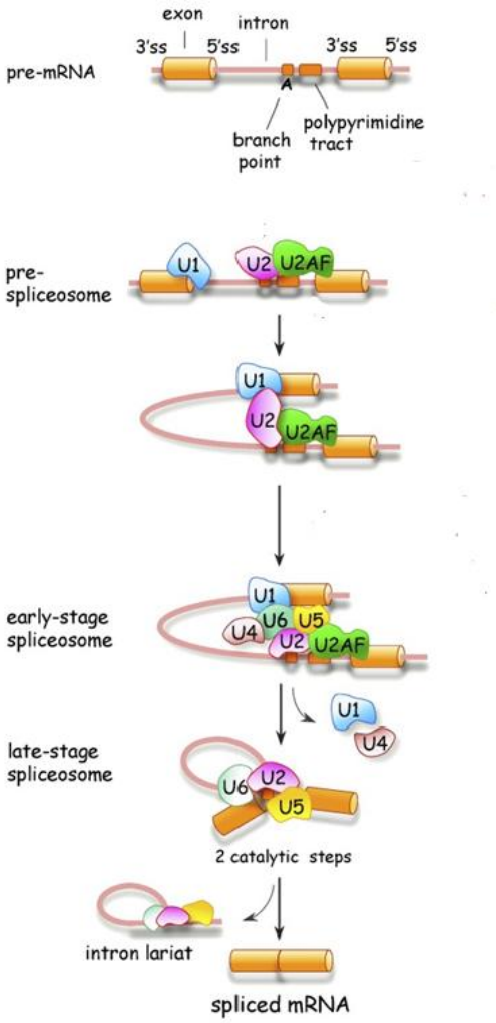

Figure 10: Spliceosome assembly (Adapted from** (Chabot and Shkreta 2016)**)
Pre-mRNA is composed by exons (cylinders), introns (lines), the 5′ splice site (5′ss), the 3′ splice site (3′ss), the branch point, and the polyrimidine tract. The main snRNP involved in the spliceosome appear with their name (U1, U2, U2AF, U4, U5, and U6).

The first snRNPs involved in the spliceosome are U1 (which binds on the 5′ site), and U2 and U2AF (which bind on the 3′site). The combination of these 3 snRNPs with the pre-mRNA forms the pre-spliceosome which initiates the splicing. The snRNP U4, U5 and U6 are next recruited in the spliceosome to exclude the intron of the mRNA sequence (**Figure 10**).

Other proteins may interfere with the spliceosome and modulate the pre-mRNA splicing. For example, the SR proteins (proteins with regions rich in serine and arginine residues) are able to bind to splicing enhancer site of the pre-mRNA to initiate the splicing. By opposition, the heterogeneous nuclear ribonucleo-proteins can bind splicing silencer sites of the pre-mRNA to repress the spicing. A mutation in any of these motifs, disturbing the interaction between the pre-mRNA and the spliceosome interaction sites is able to disturb the pre-mRNA splicing

and conduce to the insertion of an intron or the deletion of an exon in the mRNA sequence (Bergsma et al. 2018). Exon skipping therapy aims at interacting with these domains to modulate the pre-mRNA splicing.

4.1.2 Exon skipping in DMD

The most prevalent mutations causing DMD are deletions of one or more exons which conduce to the disruption of the open reading frame (**Figure 2**). The main aim of exon skipping therapy is to restore the open reading frame by skipping one other exon (or more). In this way, the corrected mRNA will produce a truncated but functional protein, which is similar to the protein found in BMD patients.

Exon skipping therapy is a personalized medicine which should be adapted to the specific mutation of the patient in order to restore the mRNA open reading frame and consequently the production of a functional dystrophin protein. This approach can be applicable to about 55% of DMD patients (80% of patients with a deletion in the gene) (Bladen et al. 2015) but to treat all of these eligible patients many drugs should be developed and produced. The development of eight drugs to skip the eight most prevalent exons would be enough to treat 75% of patients eligible for a single exon skipping therapy (**Figure 11**).

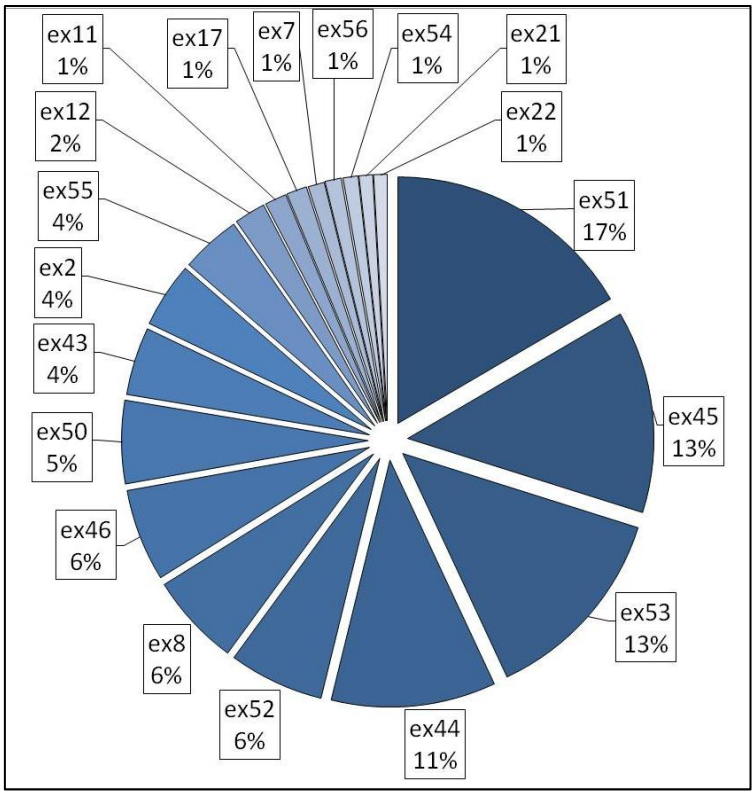

Figure 11: Number of patients potentially rescuable by one exon skipping (data from the UMD-DMD France global database)

1,163 patients from the French database may potentially be treated with only 1 exon skipped. The Figure shows the main exons to skip and the proportion of patients rescuable with it (only exon suitable for 10 patients or more are cited).

The antisense oligonucleotides (ASO) are the more common technology used to perform exon skipping therapy in DMD. To perform it, ASO are composed of an antisense sequence which binds the mRNA at critical splicing sites. In the next section we will describe the ASO currently used and we will then review the results obtained during DMD studies (pre-clinical and clinical trials).

4.2 ANTISENSE OLIGONUCLEOTIDES

ASOs are typically synthetic single-stranded oligonucleotides of 12–30 nucleotides long (Gilar et al. 1997; Griepenburg et al. 2015; Kaur, Wengel, and Maiti 2007), designed to bind to a messenger RNA (mRNA) or non-coding RNA through Watson–Crick base pairing in order to modulate their function/ expression. ASOs were first used in 1978 by Zamecnik and Stephenson as a gene-silencing approach (Zamecnik and Stephenson 1978), but the

technology has rapidly evolved since then with numerous other possible applications making them a valuable tool for genetic-based therapeutics. While the first unmodified ASOs, which were composed of a phosphodiester (PO) backbone and sugar rings, were rapidly degraded within cells and the bloodstream, various modifications have progressively been introduced in their chemical structure in order to protect them from nuclease activity and increase their stability and affinity to target RNA (Wickstrom 1986).

One of the first modifications introduced was the replacement of one of the non-bridging oxygen atoms in the phosphate group with a sulphur atom resulting in phosphorothioate (PS) ASO. This substitution increases the resistance to nuclease degradation and still supports ribonuclease H (RNase H) activity to degrade the target mRNA or mutant toxic mRNA. In addition to their endogenous nuclease resistance, PS modifications offer a significant advantage in terms of pharmacokinetics. Their enhanced affinity for numerous proteins, including plasma, cell surface and intracellular proteins (Crooke et al. 2017; Gaus et al. 2019) facilitates distribution and cellular uptake of PS-ASOs compared to their PO counterparts. However, PS modifications are also known to cause undesirable effects due to plasma protein binding (Iannitti, Morales-Medina, and Palmieri 2014), raising questions for their safety in humans. Acute reactions of PS backbones may include immune-cell activation (Senn, Burel, and Henry 2005), complement activation (Henry et al. 2002) or prolongation of coagulation times (Sheehan and Phan 2001), which are known to be transient and normalize when ASOs are cleared from the bloodstream. Despite these safety concerns, PS backbones remain one of the most largely used chemical modifications to protect ASOs from nuclease activity and increase their stability (Eckstein 2014).

To further improve nuclease resistance and RNA binding affinity, second-generation ASOs were developed with the introduction of a chemical modification in the 2′-position of the sugar moiety such as 2′O-methyl (2′OMe) and 2′O-methoxyethyl (2′MOE). Interestingly 2′-modified ASOs were reported to reduce immune-stimulation side effects compared to PS-modified ASOs (Henry et al. 2000). This generation was the first one tested during clinical trial with the Drisapersen (a 2′OMe ASO tested to treat DMD patient) and the first one approved by the FDA with the Nusinersen (a 2′MOE ASO used to treat spinal muscular atrophy).

Chemical ASO modifications have kept evolving, with substantial changes in the sugar, and have led to a wide variety of designs such as phophodiamidate morpholino (PMO) or locked nucleic acids (LNA).

ASOs can interfere and modulate RNA function via multiple mechanisms that will impact their design and chemical modifications. Briefly, ASOs can be used to promote RNA degradation via the recruitment of RNase H1, which will cleave the mRNA-ASO hetero-duplex while leaving the ASO intact (**Figure 12**, left panel). It is important to note that most sugar-modified ASOs became unable to elicit RNase H1-mediated RNA degradation; hence ASOs must be designed as "gapmers", with a central core of 8–10 consecutive DNA nucleotides to support binding and cleavage by RNase H1. Alternatively, ASOs can be fully modified and work through steric hindrance mechanisms either to modulate splicing, inhibit RNA toxicity through the disruption of RNA structure, impact polyadenylation selection site, inhibit translation, or bind to microRNAs to block their interaction with mRNA (**Figure 12**, right panel).

The variety of mechanisms through which ASO can act and the subsequent therapeutic applications truly represent unique opportunities for the treatment of many conditions. Steady progress in chemistry and design over the years have led to several approved ASOs and numerous others currently being tested in clinical trials, in particular for DMD. In this section we will make an overview of the ASO chemistry tested to treat DMD and we will discuss the results obtained with them during pre-clinical and clinical studies.

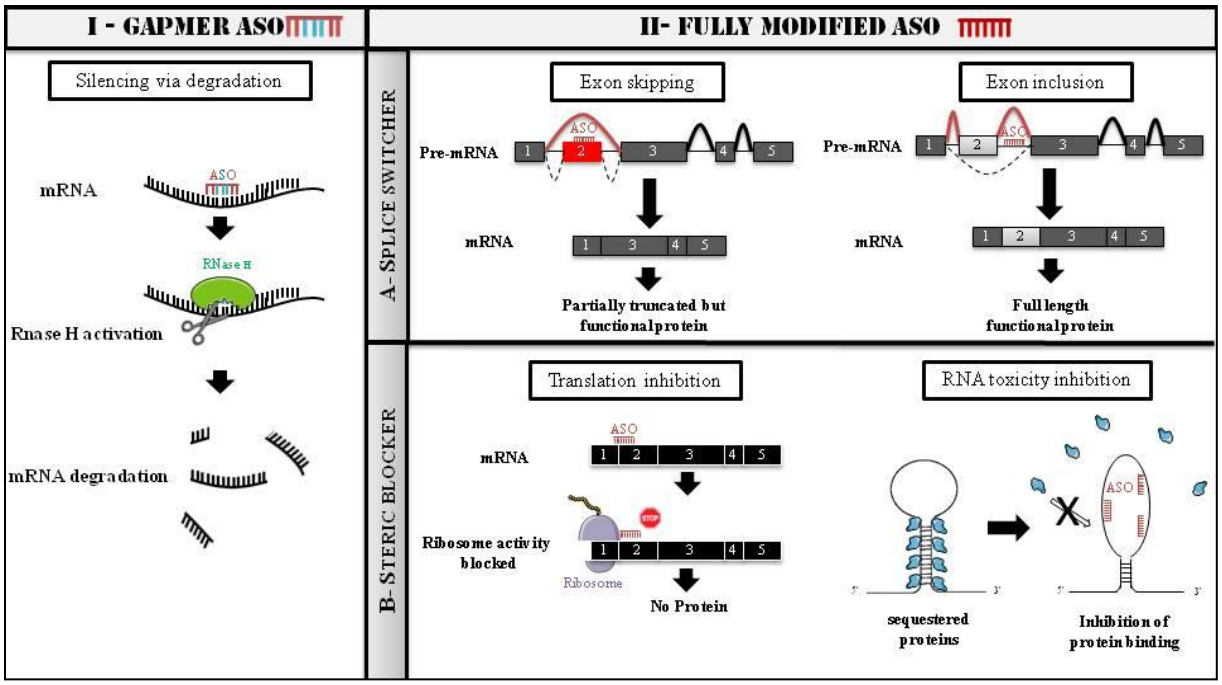

Figure 12: Antisense oligonucleotide (ASO) mechanisms of action *(Bizot, Vulin, and Goyenvalle 2020)***.**
ASOs may exert different effects depending on their structure and design. To induce mRNA degradation via RNase H, ASO must be designed as gapmers (I) with a central core of 8–10 consecutive DNA nucleotides to support binding and cleavage by RNase H1 (in blue), flanked by modified nucleotides for nuclease resistance (in red). Fully modified ASOs (II) are not able to elicit RNase H activity and they are commonly used as splice switchers (A) to manipulate alternative splicing (exon skipping or exon inclusion), or as steric blockers (B) to either block protein translation or inhibit RNA mediated toxicity by competing with protein binding.

4.2.1 2'O-methyl ribonucleoside ASO

While most of the preclinical work using 2'OMe-PS ASO for DMD was produced by the LUMC (Leiden University Medical Center)-based research groups, the first clinical data were actually published by a Japanese group in 2006 using a PS DNA ASO. A single patient, with an exon 20 deletion, was injected with a 31-mer ASO targeting the exon 19 of the DMD gene (named AO19) in the peripheral vein at 0.5 mg/kg four times at 1-week intervals (Takeshima et al. 2006). The treatment was well tolerated and resulted in traces of skipped transcript in biopsied biceps muscle. Nevertheless, the novel transcript did not allow the restoration of quantifiable dystrophin expression and no follow-up studies were ever conducted.

In parallel in Europe, a 20-mer 2'OMe-PS ASO targeting exon 51 was developed and shown to restore significant levels of dystrophin in mouse models of DMD (Lu et al. 2003). Based on these encouraging preclinical data, the Dutch group in collaboration with Prosensa evaluated the intramuscular injection of this ASO named drisapersen in four DMD patients eligible for exon 51 skipping (van Deutekom et al. 2007). The treatment was well tolerated and confirmed the proof of principle of the ASO-mediated exon-skipping approach for DMD since some dystrophin expression was detected, supporting the development of further clinical investigations.

Results of the phase I/IIa trial evaluating the systemic administration of drisapersen were published in 2011 (Goemans et al. 2011). While no serious adverse effects were reported, a total of 120 mild or moderate adverse events occurred, notably proteinuria and several types of reactions at the injection site. Tibialis anterior muscle biopsy samples were analyzed at 2 weeks and 7 weeks after the end of the dose-escalation phase. Exon 51 skipping was observed in all patients receiving 2, 4, or 6 mg/kg/week at both time points but with variable extent. Quantification of western blot shows that dystrophin signal intensity was 1.5–8.2 times greater than the baseline condition (taken from 0.5 mg/kg group of patients) in the groups receiving 4 and 6 mg/kg/week, 2 weeks after the end of the treatment. Following 12 weeks of treatment, no increase in specific muscle force was observed but there was average improvement of 35.2 ± 28.7 m in the 6MWT. Those 12 patients entered a long-term 188-week extension study with subcutaneous injection of 6 mg/kg/week initially (Goemans et al. 2016). Biopsies were taken from the tibialis anterior muscle at week 24 for all subjects and at either week 68 or week 72 for volunteering subjects. Although exon-skipping and dystrophin were detected at both time-points, no formal conclusion could be drawn on potential increase from baseline because no material from pre-treatment biopsies was available. At the end of the treatment, two patients were non-ambulant and two were unable to complete the 6MWT at later visits. Nevertheless, of the eight remaining subjects, the 6MWT appeared improved by a median increase of 64 m (mean = 33) and the cardiac function showed stability; however, on the other hand, muscle strength decreased during the study. Interestingly though, despite the heterogeneity of subjects, some of them who were in a decline stage of the disease, maintained ambulation throughout the study.

Based on these relatively encouraging data, an open-label extension phase III study was launched with 186 ambulant subjects (Goemans et al. 2018). Unfortunately, the slight difference observed in the 6MWT from baseline was found to be non-significant, which was thought to be largely due to subgroup heterogeneity. A post hoc analysis, performed on a subgroup of 80 subjects with a baseline 6MWT between 300 and 400 m, revealed a treatment benefit in 6MWT of 35.4 m (95% CI 1.8–69.0), supporting early intervention. The inability to meet the primary efficacy endpoint (improvement in 6MWT) together with the significant adverse effects (injection-site reactions and renal issues) led to the rejection of the application for drisapersen by the FDA. By mid-2016, Biomarin announced the withdrawal of drisapersen market authorization application in Europe and the discontinuation of all their ASO programs for DMD, which included exons 44, 45, and 53, to invest in research of next generation ASOs.

4.2.2 Phophodiamidate morpholino ASO

In parallel to the 2'OMe-PS ASO development, another chemistry of ASO was developed for DMD: phosphorodiamidate morpholino oligomers (PMO). PMO is a DNA analog whose phosphoribose is replaced by a morpholine ring connected by phosphorodiamidate linkages. Contrary to the PS or PO links that have a negative charge on the sulfur or oxygen atoms, phosphorodiamidate is uncharged so PMO binds less serum proteins which caused the toxicity (Moulton and Jiang 2009). PMO is able to resist to nuclease degradation and bind to RNA sequence without RNase H activation (Hudziak et al. 1996; Summerton 1999). PMO have been shown to be efficient to restore dystrophin production both in cell models, animal models and in human. The results obtained had conduced to the approval of four PMO ASO by the FDA (eteplirsen, golodirsen, viltolarsen and casimersen) (**Table 4**) and one is currently tested in clinic (NS-089/NCNP-02).

Table 4: ASO approved by the FDA (in December 2022)

drug	compagny	ASO chemistry	target exon	FDA date of approval
Eteplirsen	Sarepta Therapeutics	PMO	exon 51	September 2016
Golodersen	Sarepta Therapeutics	PMO	exon 53	December 2019
Viltolarsen	Nippon Shinyaku (NS Pharma)	PMO	exon 53	August 2020
Casimersen	Sarepta Therapeutics	PMO	exon 45	February 2021

4.2.2.1 Eteplirsen

Eteplirsen is the first PMO ASO tested in clinic for DMD. In 2005, a first phase I/II trial started to assess the safety and efficacy of the drug after intra-muscular injection (NCT00159250). Seven DMD patients were treated and no adverse events related to therapy administration and local expression of dystrophin were found (Kinali et al. 2009). In 2009, Sarepta started a second trial phase I/II to test its safety and investigate the clinical effects after intravenous injection (NCT00844597). 19 patients of 5 to 15 years old were included in the study. Eteplirsen was well tolerated as systemic treatment and dystrophin was restored in muscle of treated patients but with a high variability between individuals (Cirak et al. 2011). In 2011, another phase II trial (NCT01396239) enrolled 12 boys with DMD, who received eteplirsen at 30 and 50 mg/kg once weekly for 48 weeks. Patients treated with a dose of 30 mg/kg showed 23% increase in dystrophin positive fiber number after 24 weeks of treatment and 52% after 48 weeks of treatment. Patients treated with the highest dose showed 43% increase in dystrophin positive fiber number after 48 weeks of treatment. These data showed that the duration of the treatment is more important than the dose (Mendell et al. 2013). Moreover, at 36 months, all patients demonstrated a statistically significant advantage on 6MWT and experienced a lower incidence of loss of ambulation compare to untreated patients (Mendell et al. 2016). After 188 weeks of treatment dystrophin restoration level was measured by western blot and revealed an average level of 0.93% for treated patients, compared to 0.08% of untreated patients (Aartsma-Rus and Krieg 2017).

In September 2016, based on the phase II trials results, eteplirsen received accelerated

approval by the FDA but the authorities requested further confirmation on the drug's clinical benefit. In 2018, after reviewing the data, EMA did not approve eteplirsen for the treatment of DMD.

To test the efficacy of the treatment, a phase III trial (NCT02255552) started in November 2014. 79 patients were treated with 30 mg/kg/week of eteplirsen for 96 weeks. At the end of the treatment, dystrophin restoration level was measured by western blot and showed that only 0.63% of normal protein level was restored (versus 0.244% before treatment) (McDonald et al. 2021). The attenuation of decline on the 6WMT over 96 weeks and the attenuation of percent predicted forced vital capacity (based on the use of both standing height and ulnar-calculated height) annual decline were confirmed in the phase III study (McDonald et al. 2021).

Recently, data from 579 patients showed that eteplirsen increases the median survival age of patients, compared to the untreated one (Iff et al. 2022), with a higher effect in young patients. Indeed, patients from 0 to 15 years old showed a 92.9% reduction in the risk of death ($P<0.01$); patients from 15–20 years old showed a 82.1% reduction ($P<0.001$); patients from 20 to 25 years showed a 47.4% reduction ($P<0.05$) and patients older than 28 years old did not show a statistically significant reduction of risk. Furthermore, recent studies suggest that long-term eteplirsen treatment delays loss of ambulation and pulmonary decline (Mitelman et al. 2022).

Currently a phase III trial (NCT03992430) is ongoing to test the safety and efficacy of 144 weeks of treatment with eteplirsen at doses 100 and 200mg/kg/week.

4.2.2.2 Golodirsen

Golodirsen (SRP-4053) is a PMO developed by Sarepta Therapeutics which is specific to exon 53. In 2019, the first results of the phase I/II trial (NCT02310906) were published. Patients that were weekly treated with golodirsen for 48 weeks had, in their muscles, more mRNA with

exon 53 skipped (18.953% versus 2.590% for the control group) and more dystrophin produced with a restoration level of 1.019% versus 0.095% for the placebo group (Frank et al. 2020). Results obtained in the phase I/II trial (NCT02310906) long-term treatment group (3 years treatment) showed that golodirsen was safe (Servais et al. 2022). Moreover, patients treated with golodirsen during 3 years also showed significant beneficial effects for the 6MWT and loss of ambulation.

Based on the increase production of dystrophin found during the phase I/II trial and the safety of the compound (NCT0231096), the FDA granted an accelerated approval to golodirsen in 2019. However, they also asked for further trials to confirm the clinical benefit of the drug. Currently, two phase III studies (NCT02500381 NCT03532542) are recruiting DMD patients to evaluate the efficacy of golodirsen after 144 weeks of treatment.

4.2.2.3 Viltolarsen

In parallel with Sarepta Therapeutics, Nippon Shinyaku had developed a PMO to perform exon 53 skipping. This ASO named Viltolarsen target the same region in the exon 53 as golodirsen but is 21-mer long, whereas golodirsen is a 25-mer oligonucleotide (Aartsma-Rus and Corey 2020). During the phase I trial (NCT02081625) 10 patient have been treated with doses from 1.25 to 20 mg/kg/week for 12 weeks. During this study no specific toxicity was detected and a correlation between the doses injected and the proportion of corrected mRNA was found (Komaki et al. 2018).

In 2016, a phase I/II trial was conducted in Japan (Japic CTI-163291) to evaluate the safety and efficacy of 20, 40 and 80 mg/kg/week of viltolarsen. The weekly injections of 80 mg/kg of viltolarsen led to a higher increase of dystrophin protein production compared to the 40mg/kg/week. Patients treated with the highest dose went from 0.41% (baseline level) to 1.18% of dystrophin produced after 12 weeks of treatment and to 5.21% after 24 of treatment (Komaki et al. 2020). The same year, a phase II trial (NCT02740972) started in the USA to test the safety and efficacy of 40 and 80 mg/kg/week of viltolarsen for 24 weeks. Results obtained in 16 patients showed that the drug was well tolerated but no difference was found in the dystrophin restoration level between the two doses; both restored 5.8% of normal dystrophin level production (Clemens et al. 2020). Furthermore, all treated

participants showed significant improvement in muscle function with for example an improvement in the 6MWT after 25 weeks of treatment (compared to untreated patient) (Clemens et al. 2020). Patients who had participated to the American phase II study (NCT02740972) were enrolled in a long-term phase II study (NCT03167255) with an additional 192 weeks with the same dose of viltolarsen. Analysis performed after 109 weeks of treatment demonstrated significant benefit of the treatment with maintenance of the time needed to raise from the floor from supine position, whereas the control group experienced functional decline (Clemens et al. 2022).

Based on the dystrophin restoration level obtained during the clinical trials and the safety of the compound, the FDA granted an accelerated approval to viltolarsen in August 2020, but asked NS Pharma to confirm the clinical benefit of the drug. Currently, a phase III trial (NCT04060199) is ongoing to evaluate the efficacy of viltolarsen, with an anticipated completion date of December 2024.

4.2.2.4 Casimersen

Casimersen is, like eteplirsen and golodirsen, a PMO developed by Sarepta Therapeutics but specific to the exon 45.

In 2015, a randomized placebo-controlled phase I study (NCT02530905) was started to assess the safety and efficacy of casimersen for 12 weeks in DMD patients. The results showed that casimersen was well tolerated (Wagner et al. 2021). In 2019 a phase II trial started to evaluate the efficacy of the drug, but for now only 3 patients have been included (NCT04179409).

Two phase III studies (NCT02500381 NCT03532542) are currently recruiting DMD patients to evaluate the efficacy of casimersen after 144 weeks of treatment. The preliminary results obtained with the first 43 patients treated for 48 weeks showed that casimersen used at 30 mg/kg/week is able to correct the open reading frame in the mRNA sequence and to increase dystrophin production (1.74% of normal level were restored with the treatment versus 0.93% without) (Iannaccone et al. 2022). Based on these data, FDA granted an accelerated approval to casimersen in 2021, but they also asked further trials to confirm the clinical benefit of the drug. The toxicological analyses performed after 140 weeks of treatment with doses of casimersen from 4 to 30mg/kg/week showed no specific toxicity of

the treatment (Wagner et al. 2021).

4.2.2.5 NS-089/NCNP-02

In order to treat other DMD patients, Nippon Shinyaku Co., Ltd (the industry which commercializes viltolarsen) is developing a new PMO ASO drug designed to skip the exon 44: NS-089/NCNP-02.

In October 2019, a phase I/II trial (NCT04129294) started to assess the safety, tolerability and efficacy of NS-089/NCNP-02. During this trial, patients are treated with doses from 1.62 to 80 mg/kg/wk during 24 weeks. NS-089/NCNP-02 was shown to be well-tolerated and none of the 6 treated patients showed specific side effects. Moreover, all participants showed significant increase in dystrophin production with a restoration level between 10.27% and 15.79% depending on the dose of drug injected (Komaki et al. 2022). NS-089/NCNP-02 is currently tested in phase II trial (NCT05135663) to assess its safety, tolerability and efficacy after 72 weeks of treatment with a dose of 40 or 80 mg/kg/wk.

Despite their approval in USA and Japon, the therapeutic efficacy of PMO remains low with only a small fraction of restored dystrophin in muscle biopsy of treated patient. Other chemistries of ASO are currently in development with the objective to improve the efficacy of ASO based therapy for DMD.

4.2.3 Locked nucleic acid ASO

One of the altrenative chemistry in development for the treatment of DMD is the locked nucleic acid (LNA). LNA have a constrained conformation with a linkage of the 2’ oxygen and the 4’ carbon atom of the ribose ring by one carbon atom. This conformation with bicyclic sugar analog as ribose significantly increases the binding affinity of ASO to its complementary RNA target (Hagedorn et al. 2018).

LNA oligomers of 8 units or longer tend to self-aggregate, which is a cause of toxicity (Khvorova and Watts 2017). To avoid this phenomenon, mixmer composed of both LNA and 2’OMe nucleotides have been generated. These mixmers have efficiently induced exon

skipping and restored synthesis of a functional dystrophin *in-vitro* in both mouse and human muscle cells (Le et al. 2017; Pires et al. 2017). In *mdx* mice, ASO composed of a 30% LNA and 70% 2'OMe nucleotides were significantly more potent than full 2'OMe ASO in inducing exon skipping and dystrophin restoration (Georgiadou et al. 2021). Further experimentations are needed to evaluate the benefit-toxicity profile of LNA/2'OMe mixmer ASO following systemic delivery.

4.2.4 2'-O,4'-C ethylene bridged nucleic acid ASO

Another chemistry in development for the treatment of DMD is 2'-O,4'-C ethylene bridged nucleic acid (ENA). Like LNA, ENA have a restricted conformation with not one but two carbon atom in the 2'O-4'C link. This conformation has the same properties as the previous one and should be mixed with 2'OMe nucleotides to avoid self-aggregation too (Koizumi 2004). 2'OMe/ENA mixmer has efficiently induced exon skipping and restored synthesis of a functional dystrophin *in-vitro* in both mouse and human cells. Systemic delivery of 2'OMe/ENA ASO in mice showed no specific toxicity (Lee et al. 2017).

In January 2016, a phase I/II trial (NCT02667483) started to study the safety, tolerability and efficacy of renadirsen (or DS-5141): a 2'OMe/ENA ASO mediated the exon 45 skipping. In this trial, seven DMD patients from 5 to 10 years old were subcutaneously injected with doses of renadirsen from 0.1 to 6 mg/kg/wk during 2 weeks. No specific side effects were found during this study (Daiichi Sankyo 2021). Renadirsen is currently tested in a phase II trial (NCT04433234) to evaluate the safety and efficacy of long-term treatment with 2 or 6 mg/kg/wk of renadirsen for 2 years. No data for this clinical trial are available yet.

4.2.5 Tricyclo-DNA ASO.

Another chemistry developed for the treatment of DMD is tricyclo-DNA (TC-DNA). TC-DNA have been developed in the late 1990s and present, like the previously mentioned ASO, a constrained conformation. They are composed by an ethylene bridge between the 3'C and 5'C of the ribose rigidified by a cyclopropane unit. This construction gives to TC-DNA a strong resistance to nucleases degradation and a high binding affinity to its complementary

RNA target (Renneberg et al. 2002). Similar to the other ribose modification chemistry, TC-DNA may be combined with PS linkages to decrease its kidney elimination and increase its efficacy in vivo in mice (Murray et al. 2012).

During the preliminary studies performed in *mdx* and *mdx; utr*$^{-/-}$ mice, my host laboratory showed that systemic delivery of TC-DNA PS ASO was able to skip the Dmd exon 23 in both skeletal muscles and heart (Goyenvalle et al. 2015). The exon skipping levels obtained in these organs were 5 to 6 fold higher than the ones obtained with 2′OMe and PMO ASOs. Moreover, TC-DNA PS ASO was able to correct the open reading frame in the brain. It was the first time that an ASO was able to cross the blood brain barrier and significantly treat brain after systemic delivery. The RNA correction levels obtained with the TC-DNA PS ASO were enough to restore the production of Dp427 in all organs. It was concluded that, because of the muscle, heart and pulmonary functions improvements and the emotional/cognitive deficiency correction, the dystrophin produced was functional and that TC-DNA PS ASO may be a good candidate for drug development.

To confirm its capacity to become a new treatment for DMD, the safety profile of TC-DNA PS ASO was then evaluated (Relizani et al. 2017). After 12 weeks treatment with a dose of 200 mg/kg/week, no major toxicity was found. No acute pro-inflammatory response was detected; a normal level of both complement activation and pro-inflammatory cytokine were obtained in the serum of treated mice. The only toxicities found were typical of the PS ASO backbone accumulation in kidneys (Echevarría et al. 2019) with minimal glomerular changes and few cell necroses in proximal tubules.

PS links are known to induce toxicities because of complement cascade activation (Iannitti, Morales-Medina, and Palmieri 2014), immune cell activation (Senn, Burel, and Henry 2005), or prolongation of clotting times (Sheehan and Phan 2001). To decrease this toxicity, PS linkages should be replaced by PO ones. This change will not modify the nuclease resistance capacity of the TC-DNA ASO or its affinity to its RNA target sequence. Unfortunately, the biodistrbution and the efficacy of TC-DNA ASO in the target tissue is decreased with the

substitution (Echevarría et al. 2019). To improve the biodistribution and the efficacy of the TC-DNA PO ASO, a second generation was developped. This generation is composed of a full PO TC-DNA ASO conjugated to a palmitic acid (palm) group on its 5' end. The conjugation of palm to TC-DNA aims at compensating the absence of PS links and facilitate the delivery of the ASO from the bloodstream to the interstitium of the skeletal and cardiac muscles (Relizani et al. 2022). The systemic injection of Palm-TC-DNA PO ASO in *mdx* mice showed similar or higher efficacy than previous TC-DNA PS ASO, but without the PS specific toxicity. Palm-conjugated TC-DNA with a full PO backbone therefore present a more favorable risk-benefit balance than the previous compounds with a proved effective with a particularly encouraging safety profile. These properties offer new perspectives for the clinical development of TC-DNA ASO for neuromuscular diseases.

A phase I/IIa trial will start in 2023 to evaluate the safety and efficacy of intravenous injection of SQY51 (EU CT 2022-500703-49-01). SQY51 is a palm-TC-DNA ASO targeting the exon 51 of the DMD gene. This study will enroll pediatric and adult patients divided in 2 groups: one group of patients will have a multiple-ascending dose to test the safety and tolerability of the drug after 13 weeks of treatment and the other will be included in the phase II trial to be treated during 32 weeks with the optimal dose.

The palm-TC-DNA-PO ASO is the chemistry of ASO I used during my thesis with the objective to improve even further their potency for the treatment of DMD.

4.2.6 Stereopure ASO

Stereoisomers are molecules that have identical chemical composition and sequence of bonded atoms, but differ in their tridimensional orientation. The PS linkage used to increase ASO efficacy converts the achiral PO linkage into a chiral PS center having two distinct stereochemical configurations so two distinct 3-dimensional confirmation. Consequently, an ASO of 20 nucleotides long (with 19 PS link) has over half a million (2^{19}) individual stereoisomers. The comparison of different stereoisomers revealed that PS stereochemistry affects both physicochemical and pharmacological properties of the ASO. Therefore, the development of an optimal position-specific stereochemistry is able to increase the activity of

the ASO both in vitro and in vivo (Iwamoto et al. 2017).

Wave life Sciences is a pharmaceutical company that develops stereopure ASO to treat various genetic diseases including DMD. During pre-clinical studies, stereopure ASOs targeting exon 51 induced higher levels of exon skipping and dystrophin restoration than eteplirsen or drisapersen (Echevarría, Aupy, and Goyenvalle 2018). WVE-210201 (also named suvodirsen) is the ASO developed to skip the exon 51 of the DMD gene which has been tested in clinic. In the phase I trial (NCT03508947), 36 ambulatory and non-ambulatory patients from 5 to 18 years old were enrolled to evaluate the safety and tolerability of the drug. No specific toxicity was found (Wagner et al. 2019) and a phase II/III trial (NCT03907072) was initiated to ensure the efficacy of the drug. In December 2019, Wave Life Sciences stopped the development of suvodirsen since no dystrophin expression improvement was obtained in the muscle biopsies of patients treated during the phase II trial with either the 3.5 mg/kg or 5 mg/kg doses (Wave Life Sciences 2019).

4.2.7 Phosphoryl guanidine ASO

To avoid the toxicity caused by the PS link Wave life Sciences has developed a new ASO chemistry with the replacement of non-bridging oxygen atom present in the phosphate linkage by a phosphoryl guanidine (PN). In contrast with the PO and PS backbones, PN is more stable to nuclease degradation and is not charged. *In-vivo* study performed in *mdx* mice showed that PN ASO have a superior pharmacology and activity profiles compared to PS and PO ASO (Kandasamy et al. 2022).

WVE-N531 is a PN-modified splicing oligonucleotide targeting the exon 53 of the DMD gene developed by Wave Life Sciences This ASO is currently evaluated in phase I/II trial (NCT04906460). In this trial, patients are divided in 2 groups, one having ascending doses of WVE-N531 to test the safety and tolerability of the drug and the other having multiple injections of the most optimal dose. In November 2022, Wave Life Sciences announced that dose escalation was completed and multi-dosing was underway with 10 mg/kg doses of WVE-N531 (Wave Life Sciences 2022A). In December 2022, results obtained during the dose

escalation clinical trial performed on three ambulatory patients were reported (Wave Life Sciences 2022b). Muscle biopsy was taken two weeks after the last injection of WVE-N531 (six weeks after the first dose) and exon skipping and dystrophin restoration levels were monitored. The quantification of exon skipping level by RT-PCR showed that a high proportion of RNA was corrected in the muscles cells of patient (means 53%, range: 48-62%). However, almost no dystrophin was found in the muscle biopsie by western-blot (0.27% was measured, which was below the level of quantification: 1%). During this study, no serious adverse events, no trends in labs, and no oligonucleotide class-related safety events were found which tends to validate the safety of the compound. Furthermore, plasma concentrations and other pharmacokinetic parameters following a single dose of 10 mg/kg have demonstrated an ASO half-life of 25 days, which may support monthly dosing (and not a weekly one like during the trial).

4.2.8 Peptide conjugated-PMO

PMO, which are uncharged and therefore unable to efficiently bind serum proteins (causing their rapid elimination in the urine) (Alter et al. 2006). In order to improve their biodistribution, peptides conjugated-PMO (PPMO) have been engineered. There is currently two PPMO ASO tested in clinic: Vesleteplirsen (developed by Sarepta Therapeutics) and PGN-EDO051 (developed by Pepgen).

4.2.8.1 Vesleteplirsen (SRP-5051)

Vesleteplirsen is a PPMO developed by Sarepta Therapeutics to skip the exon 51 of DMD gene. In fact, vesleteplirsen is the eteplirsen PMO conjugated to an arginine-rich cell-penetrating peptides (CPP) (Sheikh and Yokota 2022).

In *mdx* mice, systemic injection of PMO combined to arginine rich CPP led to sustained expression of the dystrophin protein in whole-body muscles, including cardiac muscle, without detectable toxicity (Jearawiriyapaisarn et al. 2008). In healthy cynomolgus monkey, weekly intravenous injection of these PPMO during 4 weeks induced an average of 40%, 25%, and 2% exon-skipped product in diaphragm, quadriceps, and heart respectively. These data

were promising for the dystrophin correction in muscle but dose dependent toxicity was detected with mild tubular degeneration in the kidneys of monkeys (Moulton and Moulton 2010). To avoid its toxicity, new peptides have been tested with less arginin residues and lowest doses of ASO have been tested (Tsoumpra et al. 2019).

In 2018 a phase I trial (NCT03375255) was initiated to evaluate the safety of the drug. 15 patients received a single injection of vesleteplirsen and no specific side effect was found. Based on these results, patients were enrolled in a phase I/II trial (NCT03675126) to evaluate the safety of multiple injections of the drug. In December 2020, Sarepta announced that once-monthly dosing of vesleteplirsen during 12 weeks produced more exon-skipping (1.6-fold increase) and dystrophin restoration (5-fold increase) than 24 weeks of treatment with 30 mg/kg/week of eteplirsen (Sarepta Therapeutics 2020). A phase II trial NCT04004065 has started to assess the efficacy and the safety of a long period (2 years) of treatment. The first results obtained in the phase II trial showed 10.79% of corrected mRNA and 6.55% of restored dystrophin production in muscle biopsies of patients treated 12 weeks with vesleteplirsen at 30 mg/kg/month (Sarepta Therapeutics 2021C). However, treatment with vesleteplirsen was associated with a major side effect, hypomagnesemia, which was resolved with magnesium supplementation (Sheikh and Yokota 2022).

In June 2022 Sarepta Therapeutics announced that the FDA has placed a clinical hold on vesleteplirsen because of this serious adverse event of hypomagnesemia which occurred during the phase II trial (Sarepta Therapeutics 2022A). In September 2022, the FDA lifted the clinical hold after Sarepta Therapeutics changed the protocol to include expanded monitoring of urine biomarkers (Sarepta Therapeutics 2022B).

4.2.8.2 PGN-EDO51

Another PPMO developed for the treatment of DMD combined PMO with Pip (peptide nucleic acid / PMO internalization peptides). Different Pips have been developed with time but all derived from the R6-penetratin peptide: a derivative of penetratin peptide in which six arginine residues were added to the N-terminus of the CPP. Many pip tested in vivo in *mdx*

mice are able to increase the exon skipping level mediated by PMO (Betts et al. 2012; Ivanova et al. 2008; Yin et al. 2011). In *mdx* mice, the Pip6 series combined to a PMO was able to restore 28% of dystrophin in heart (measured by western-blot after 5 weeks of treatment) which prevented the onset of exercised-induced dilated cardiomyopathy and maintained cardiac function (Betts et al. 2015). Moreover, in a spinal muscular atrophy mouse model, systemic injections of Pip6-PMOs were not only able to treat skeletal muscles and heart but also the brain which is very promising for DMD patients (Hammond et al. 2016). Unfortunately, nephrotoxicity was observed with Pip6-PMO. New pips which are less toxic have been developed (Gait et al. 2019) and the pharmaceutical company Pepgen was created to continue the development of PPMO drug candidate using this technology.

The new pip developped by Pepgen are named enhanced delivery oligo (EDO) and are more efficient than polyarginine peptide to improve PMO efficacy (Holland et al. 2021). PGN-EDO51 is the PMO ASO conjugated with an EDO tested in clinic for the skip of the exon 51 of DMD gene. During preclinical studies, a single dose of 60mg/kg of PGN-EDO51 was able to correct the open reading frame of almost 80% of the mRNA in tibialis anterior, diaphragm and heart of non-human primates (Holland et al. 2021). Moreover, PGN-EDO51 was also able to cross the blood brain barrier and diffuse in the brain after intravenous injection. Based on these data, a phase I trial was initiated in Canada (Mellion et al. 2022). This trial was performed in 32 healthy people to ensure the safety and tolerability of the drug. Data obtained showed no specific toxicity after a single dose of PGN-EDO51 from 1 to 15 mg/kg (PepGen 2022a). A phase II trial is planned for the first half of 2023 to evaluate the safety and efficacy of the drug in DMD patient.

In November 2022, Pepgen announced the development of three other PPMO for the treatment of DMD: PGN-EDO53 to induce exon 53 skipping, PGN-EDO45 to induce exon 45 skipping and PGN-EDO44 to induce exon 44 skipping (PepGen 2022b). PGN-EDO53 has been tested in non-human primate and 36.4% of exon skipping was detected in the biceps biopsy of animals 8 days after the first injection. No *in-vivo* data with the two other PPMO are available yet.

4.2.9 Antibody conjugated PMO

Conjugation of ASO to monoclonal antibodies may increase the muscle uptake of ASO. An antibody against transferrin receptor 1 (TfR1) has been developed to this end. TfR1 is critical receptor for iron uptake in skeletal and cardiac muscle cells. This receptor controls cellular iron homeostasis by mediating endocytosis of iron-bound transferrin (Daniels et al. 2006). To increase endocytosis of ASO in muscles, a fragment antigen-binding (Fab) region targeting Tfr1 has been conjugated to a PMO using a valine-citrulline linker. This linker is stable in plasma and is cleaved in the endosomal compartment to release the oligonucleotide in the cytosol (McCombs and Owen 2015). In *mdx* mice, a single systemic injection of the TfR1-Fab PMO was able to produce dose-dependent exon skipping and dystrophin restoration. The 30 mg/kg dose induced dystrophin expression reached peaks of 72%, 90%, and 77% of WT levels in tibialis anterior, diaphragm, and heart respectively (Desjardins et al. 2022).

Currently, two antibody-conjugated PMOs are tested in clinic: DYNE-251 developed by Dyne therapeutics and AOC1044 developed by Avidity Biosciences.

4.2.9.1 DYNE-251

DYNE-251 is a PMO conjugated to a Fab binding the TfR1 developed by Dyne therapeutics to skip the exon 51 of DMD gene. In September 2022, the phase I/II trial NCT05524883 was initiated to evaluate the safety, tolerability, and efficacy of multiple intravenous doses of DYNE-251. Dyne therapeutics has planned to include in this study 46 ambulant and non-ambulant patients divided into 2 groups:

- One group of patients will have a multiple-ascending dose to test the safety and tolerability of the drug. Patients will be injected 6 times over 24 weeks (1 injection every 4 weeks)
- The second group will have a placebo with the same injection number as the previous group.

Patients in the placebo group will be included in the long-term extension study at the end of

the 24-week study. In this study, patients will be injected 30 times with the ASO over 120 weeks (1 injection every 4 weeks).

No clinical data are available yet.

4.2.9.2 AOC 1044

AOC 1044 is a PMO conjugated to a monoclonal antibody binding the TfR1 developed by Avidity Biosciences to skip the exon 44 of DMD gene. Preclinical study performed on cynomolgus monkeys showed that AOC 1044 is able to perform exon skipping in both skeletal muscle (gastrocnemius, quadriceps and diaphragm) and heart (Karamanlidis et al. 2022). In October 2022, Avidity Biosciences started the phase I/II trial (EXPLORE44) to evaluate the safety, tolerability, pharmacokinetics, and pharmacodynamic effects of single and multiple ascending doses of AOC 1044 administered intravenously in both healty volunteers and DMD patients (Avidity Biosciences 2022).

No data for this clinical trial are available yet.

In conclusion, exon skipping therapy mediated by ASO has made a lot of progress since 2006 (years of the publication of its first clinical data results). Some of them failed to restore sufficient levels of dystrophin in DMD patients, some were approved as medicine in USA and Japan but not in Europe because of their limited efficacy and others are currently tested in clinic. A summary of the on-going trials is provided below in **Table 5**.

Table 5: Clinical trials phase I and II using ASOs for the treatment of DMD

drug	sponsor	ASO chemistry	target exon	trial number	current stage	trial phase	Dose	Patient number	Patient age
NS-089 (NCNP-02)	Nippon Shinyaku	PMO	exon 44	NCT04129294	completed	phase I/II	1.62, 10, 40 or 80 mg/kg/wk for 24 weeks	6	4-17 years old
				NCT05135663	active, not recruiting	phase II	40 or 80 mg/kg/wk for 72 weeks	6	all ages
Renadirsen (DS-5141b)	Daiichi Sankyo	ENA/2'OMe	exon 45	NCT02667483	completed	phase I/II	2 Subcutaneous injection from 0.1 to 6 mg/kg/wk	7	5-10 years old
				NCT04433234	active, not recruiting	phase II	Subcutaneous injection: 2 or 6 mg/kg/wk	8	5 Years and older
SQY51	SQY therapeutics	TC-DNA	exon 51	EU CT 2022-500703-49-01	planned for 2023	phase I/II			Children and adult
WVE-N531	Wave Life Sciences	PN ASO	exon 53	NCT04906460	recruting	phase I/II	dose escalation with a maximum of 7 total doses	15	5-18 years old
Vesleteplirsen (SRP-5051)	Sarepta Therapeutics	PPMO	exon 51	NCT03375255	completed	phase I	single dose from 0,3 to 6 mg/kg	15	12 Years and older
				NCT03675126	terminated	phase I/II	unknow	15	4 Years and older
				NCT04004065	recruting	phase II	1 injection per 4 weeks up to 72 weeks or 2 years	60	7-21 years old
PGN-ED051	Pepgen	PPMO	exon 51	Canada	completed	phase I	single dose of 1, 5, 10 or 15 mg/kg	32	Healthy people only
DYNE -251	Dyne therapeutics	Fab PMO	exon 51	NCT05524883	recruting	phase I/II	1 injection per 4 weeks during 24 or 120 weeks	46	4-16 years old
AOC 1044	Avidity Bioscience	antibody PMO	exon 53	EXPLORE44™	approved	phase I/II		40 healthy and 24 DMD patients	7-27 years old

4.3 AAV-U7snRNA

ASO are not the only technology that has been developed to achieve exon skipping in DMD; another one is based on the use of the AAV-U7snRNA system. U7snRNA is a single strand RNA molecule composed of a complementary sequence to the histone pre-mRNA, a binding site for Sm protein and a hairpin structure at the 3' end. The combination of U7snRNA and seven Sm proteins forms a ribonucleoprotein particle (U7 snRNP) that is involved in the processing of the 3' end of histone pre-mRNAs. The modification of the complementary sequence to the histone pre-mRNA by an appropriate antisense sequences changed its function to an effecter of alternative splicing of pre-messager RNA (Gorman et al. 1998). In the 2000s, this approach was shown to correct the mRNA of both human and mouse DMD cells (Brun et al. 2003; De Angelis et al. 2002).

In order to let U7snRNA diffuse efficiently from the blood to the muscles, AAV vectors have then be used (Goyenvalle et al. 2004). Both intramuscular and systemic administration of AAV-U7snRNA in mice resulted in dystrophin expression and correction of muscle physiologic defects (Simmons et al. 2021). A study performed in nonhuman primates showed no significant toxicity (Gushchina et al. 2021). A phase I/II clinical trial (NCT04240314) was thus performed to study the safety and the efficacy of this therapy in DMD patients with exon 2 duplication which is the more commun duplication found in DMD patient (**Figure 3B**). In contrast with approaches aiming at skipping exon 51 as described just before, this U7snRNA targeting the duplication of exon 2 aims to restore a complete (with all exon included) and therefore a fully functional dystrophin. Muscle biopsy perfomed 3 months after the injection of 3E13 vg/kg of AAV-U7snRNA showed, in the first two injected patients, a reexpression of respectively 5.8% and 1.4% of dystrophin and a decrease of serum creatine kinase levels (typically high in patients with DMD) (Waldrop et al. 2020). The last clinical results have been presented at the 2022 Annual Meeting of the American Society of Gene and Cell Therapy. By 4 months post-injection, a biopsy showed that muscle of the youngest patient produced full-length dystrophin at 70% of normal amounts. The two other patients have lowest protein levels (quantification not communicated) (Nationwide Children's Hospital 2022).

Even if AAV-U7snRNA showed promising results, its effects need to be tempered. Indeed, like

AAV therapy, this technology used AAV vector with can not be reinjected due to the immune reactivity against them (Lorain et al. 2008). The impossibility to make multi-injections during the patient life may be a major limitation of this therapy because in long term studies, progressive loss of AAV vector (and its transgene) has been reported in muscle fibers which conduced to a progressive decrease in dystrophin expression. This progressive loss of treatment efficacy is even higher in animal models with severe muscle damage close to humans (Vulin et al. 2012; Le Hir et al. 2013).

OBJECTIVES

Antisense-mediated exon-skipping is one of the most promising therapeutic strategies for DMD. As mentioned in the introduction, several ASO-based exon skipping drugs have already been approved by the FDA for the treatment of DMD (eteplirsen, golodirsen, viltolarsen and casimersen targeting exons 51, 53, 53 and 45). Approval was based on safety and increased dystrophin expression in muscle biopsies of treated patients at relatively low levels (up to ~5.9% following exon 53 skipping) but clinical trials are still ongoing to assess functional outcomes for each of the compounds. However, the efficacy of exon-skipping strategies is still limited by several challenges, leaving large room for improvement.

The most recognized challenges of ASO-mediated exon skipping are:

- The distribution of ASO into the target tissues
- The cell trafficking of ASOs into the nucleus
- The limited amount of target mRNA

Many efforts have already been made to improve ASO efficacy, mostly through the development of alternative chemistries or various conjugates. My team has in particular worked on the development of the TC-DNA chemistry and further conjugated it with palmitic acid to enhance their therapeutic potential. However ASO biodistribution and efficacy still need to be improved in order to stop the disease progression and achieve meaningful clinical benefit in patients.

The overall objective of my thesis project was to improve exon skipping therapy for the treatment of Duchenne muscular dystrophy. To this end, I focused my research on combined therapies and evaluated molecules with three different mechanisms. Each of them was used in combination with TC-DNA ASO in the *mdx* mouse model as a proof of principle.

1- Limit the renal elimination of ASO

It has previously been demonstrated that the major proportion of ASO are eliminated in the urine (Hammond et al. 2021). To improve ASO bioavailability, we have, in the first study, tried to reduce its urinary elimination with probenecid. Probenecid is a pan organic anion transporter (OAT) inhibitor that has previously been used to improve the efficacy of different drugs like anti-cancer or antibiotics. Since TC-DNA ASOs are negatively charged, we

hypothesized that their elimination is mediated by the OAT channel. To confirm the co-localization between the ASO and the OAT channel, histological stainings were performed on kidney sections of mice treated with TC-DNA ASO. Furthermore, to validate our hypothesis, mice were co-treated with both probenecid and TC-DNA ASO. Urine were collected and ASO quantity eliminated in the first 24h was measured. To investigate the therapeutic benefit of the bi-therapy, tissues were harvested at different time points (24h post 1 co-injection and 2 weeks post 4 weeks of treatment) and TC-DNA biodistribution and efficacy were measured.

2- Improve endosomal escape

It has previously been shown that ASO enter in cells by endocytosis. To achieve exon skipping, they must leave the endosomes in order to enter the cell nucleus where the pre-messenger RNA is located. Unfortunately, only a small part of them succeeds, while the majority is eliminated by the cell. Consequently, to increase the proportion of ASO ultimately reaching the the nucleus, we used an endosomal escape promoter called UNC7938. To maximize its efficacy, UNC7938 was injected in mice 24h after the TC-DNA so that ASO had time to diffuse in the target organs and penetrate the endosomes. To examine whether this combination improves the ASO therapy, 3 studies were performed. In the first one, we measured exon skipping and protein restoration levels 2 weeks after a 4-week treatment to investigate the potential therapeutic of the combination. In the second one, we tried to understand the kinetics of UNC7938 effects on the ASO biodistribution and efficacy and in the last one, we studied the long term efficacy of the treatment.

3- Increase the amount of target mRNA

The last therapeutic combination we tested aimed at increasing the quantity of DMD pre-mRNA produced in order to increase the efficacy of ASO treatment. Indeed, transcriptional studies have shown that dystrophin mRNA levels are reduced in muscle when a mutation is present. Moreover, a strong 5'-3' imbalance in mutated transcripts have been shown in both human cells and mouse organs. To restore a normal mRNA production, three histone deacetylase inhibitors (HDACi) were tested: givinostat (a pan HDACi already used in a clinical trial in DMD), valproic acid (a class I/II HDAC inhibitor) and EX527 (a class III inhibitor). Mice

were sacrificed and organs were collected 2 weeks after 4 weeks of co-treatment to investigate the effects of HDACi on both RNA production, exon skipping and protein restoration levels.

This thesis work has led to the publication of 3 manuscripts:

1. One review article published in 2020 in Drugs:

   Bizot F, Vulin A, and Goyenvalle A. 2020. "Current Status of Antisense Oligonucleotide-Based Therapy in Neuromuscular Disorders." Drugs 80(14):1397–1415. doi: 10.1007/s40265-020-01363-3
2. One research article pusblished in Molecular Therapy Nucleic Acids in 2022:

   Bizot F, Goossens R, Tensorer T, Dmitriev S, Garcia L, Aartsma-Rus A, Spitali P, and Goyenvalle A. 2022. "Histone Deacetylase Inhibitors Improve Antisense-Mediated Exon-Skipping Efficacy in *Mdx* Mice." Molecular Therapy. Nucleic Acids 30:606–20. doi: 10.1016/j.omtn.2022.11.017.
3. One research article currently in revision in Cells:

   Bizot F, Fayssoil A, Gastaldi C, Irawan T, Phongsavanh X, Mansart A, Tensorer T, Brisebard E, Garcia L, L Juliano R, and Goyenvalle A. 2023 "Oligonucleotide enhancing compound increases tricyclo-DNA mediated exon-skipping efficacy in the *mdx* mouse model" Cells.

A brief communication is currently in preparation with the data presented in the result section focusing on the limitation of ASO renal elimination:

Bizot F, Tensorer T, Garcia L, and Goyenvalle A. "Inhibition of organic anion transporter to improve antisense mediated exon-skipping efficacy for DMD".

RESULTS

1 LIMIT THE RENAL ELIMINATION OF ASO

Context:

To improve ASO bioavailability, we aimed reduce the rapid elimination of ASO through urine and for that purpose, we used probenecid. Probenecid is a pan OAT inhibitor previously used to improve the efficacy of different drugs like anti-cancer or antibiotic.

Methods:

Mdx mice were co-treated with TC-DNA ASO (intravenous, 30mg/kg) and probenecid (intraperitoneal, 50mg/kg) just after the injection of ASO.

The biodistribution of ASO was measured in urine and target organs 24h after 1 co injection. A kinetic was also performed with quantification of ASO content in plasma during the first 48h.

A midterm study (4 weeks of treatment) was then performed to ensure the biodistribution effects of probenecid and to investigate the consequence of the bi-therapy on exon skipping and protein restoration levels.

Main Results

The colocalization between the TC-DNA ASO and OAT in the proximal convoluted tubules was confirmed by immunostaining. The biodistribution of the ASO was not significantly impacted by probenecid. The only tendency found was a small increase in the TC-DNA half-life in blood and a higher accumulation of the ASO in the Bowman's capsule of the kidney. Probenecid did not impact exon skipping and protein restoration levels after 4 weeks of treatment.

Conclusion:

Treatment with probenecid failed to improve TC-DNA efficacy in the *mdx* mouse model.

Inhibition of organic anion transporter to increase tricyclo-DNA mediated exon-skipping efficacy in the *mdx* mouse model

Flavien Bizot[1], Thomas Tensorer[2], Luis Garcia[1] and Aurélie Goyenvalle[1]

[1] Université Paris-Saclay, UVSQ, Inserm, END-ICAP, 78000 Versailles, France

[2] SQY Therapeutics, UVSQ, END-ICAP, 78180 Montigny le Bretonneux, France.

Short title: Inhibition of OAT to improve exon-skipping therapy

Keywords: Antisense oligonucleotides, exon-skipping, OAT, Duchenne muscular dystrophy, probenecid

ABSTRACT

Antisense-mediated exon-skipping is one of the most promising therapeutic strategies for Duchenne muscular dystrophy (DMD) and some antisense oligonucleotide (ASO) drugs have already been approved by the US FDA for DMD. The potential of this therapy is still limited by several challenges including the poor distribution of ASOs to target tissues (skeletal muscles, heart and brain).

To improve the ASO uptake in the target organs, tricyclo-DNA (TC-DNA) chemistry has been developed and has shown interesting biodistribution properties in particular to the cardiac muscle and to a lower extent the central nervous system. However, like most ASO chemistry TC-DNA accumulates in the kidney and tend to be rapidly eliminated after systemic delivery. We hypothesized here that inhibiting/preventing renal clearance of ASO using organic anion transporter (OAT) inhibitor could increase the bioavailability of TC-DNA ASO and thus their distribution to target tissues and ultimately their efficacy in muscles. *Mdx* mice were therefore treated with TC-DNA ASO with or without the OAT inhibitor named probenecid. Analysis of ASOs distribution in the different tissues and serum revealed no effect of the OAT inhibitor. Similarly, no differences in exon skipping levels were detected in the muscles from both treatment groups. These findings indicate that OAT inhibition, or at least using probenecid does not improve the therapeutic potential of exon skipping approaches mediated by TC-DNA ASO for the treatment of DMD.

INTRODUCTION

Antisense Oligonucleotides (ASOs)-based therapeutics is one of the main strategies in development for the treatment of a variety of diseases. This approach has already led to new drugs approved by the US FDA and many more are currently tested in preclinical or clinical trials[1]. Systemically delivered ASOs mostly distribute to liver, kidney and spleen, while other tissues of interest such as skeletal and cardiac muscles remain challenging targets[2]. This distribution is one of the main limitations of ASO to treat Duchenne muscular dystrophy (DMD). Indeed, even the ASO that have been approved by the US FDA for the treatment of DMD and that are currently used in clinic, induce only a few percent of dystrophin restoration in patients biopsies[3].

To increase the effect of the treatment, new generations of ASO have been developed with various conjugates or alternative chemistry, such as the tricyclo-DNA (TC-DNA) oligonucleotide. TC-DNA ASOs present many advantages amongst which a particularly interesting distribution to cardiac muscle and central nervous system (CNS) after systemic administration in mouse models of DMD[4,5]. Moreover, recent development had led to a second generation of TC-DNA conjugates that does not contain phosphorothioate linkages and which therefore present a much better therapeutic index[6]. Despite these promising developments, a large proportion of injected ASO does not reach the target tissues and ends up eliminated in the urine.

Rapid elimination in the urine is indeed one of the main reasons underlying the limited efficacy of current ASO chemistries. For example, the phosphorodiamidate morpholino oligomer (PMO) chemistry which has been approved by the FDA for the treatment of DMD is very largely excreted in the urine following administration, with approximately 65%, 60%,

and 93% found in the first 24 hours urine for eteplirsen, golodirsen, and vitolarsen respectively[7]. This elimination mainly occurs during the four hours following the intravenous injection[7,8]. The main cause of this fast renal clearance is the uncharged chemistry of PMO which makes it difficult to bind to proteins in the circulation[9]. To increase the blood protein binding and the bioavailability of ASO drugs, charged chemistries have been used. However, even if their relative charges help them to bind blood proteins, their urinary elimination remains high with almost 33% of injected 2'-methoxy-ethyl (MOE) ASOs found in the urines (over 24h) following a single 10 mg/kg intravenous infusion performed on cynomolgus monkeys[10]. In order to reduce the fraction eliminated in the urine and to increase the blood half-life of ASOs, they have been linked to various conjugates such as fatty acids[11,12]. Despite these improvements, a high proportion of ASOs are still quickly eliminated in the urine. The objective of this study is to improve ASO bioavailability and efficacy by blocking their rapid renal clearance.

Since the TC-DNA ASOs that we use are positively charged, we hypothesize that their elimination was mediated by the organic anion transporters (OAT). OATs are localized in the physiological barriers of multiple tissues, such as kidney, liver, brain, placenta, retina, and olfactory mucosa and are critical for physiological and pathological processes in the body[13]. They also play a major role in absorption, distribution, metabolism, and elimination of clinical therapeutics, thus affecting the pharmacokinetics and pharmacodynamics of the drug profile[13].

To test our hypothesis, we selected the OAT chemical inhibitor probenecid. Probenecid is a drug approved for the treatment of gout (commercial name: Santuril®) which inhibits the OAT, the organic anion transporting polypeptides (OATP) and the multidrug resistance proteins (MRP)[14]. The effects of probenecid on kidney transporters have previously been used

to monitor the urine elimination and improve the efficacy of different treatments like α-difluoromethylornithine (an anti-cancer)[15], flucloxacillin (an anti-viral)[16] and β-lactam antibiotics[17]. Therefore, we investigated in this study whether inhibition of OAT with probenecid could decrease TC-DNA ASO elimination in the urine and increase its biodistribution and efficacy in the other organs.

RESULTS

General distribution of TC-DNA ASO in *mdx* mice

We first studied the overall distribution of the tricyclo-DNA oligonucleotides (TC-DNA ASOs) in *mdx* mice. Adult *mdx* mice were treated weekly with TC-DNA ASO (50mg/kg/wk) during 4 weeks and sacrificed 2 weeks after the last injection. ASOs were quantified in both target organs (muscles) and off target ones (kidney, liver and spleen) and we found that TC-DNA accumulate more in the kidney than in other organs (fold change of ~100 compared to the muscle) as previously shown for other chemistries (Figure 1A). To estimate how much ASO was eliminated in the urine directly after injection, we collected the urines in the first 40h after the first administration of 50mg/kg of TC-DNA (corresponding to a total amount of 1250µg for a mouse of 25 g). Quantification of the TC-DNA ASOs in the urine revealed that approximately 20% of the injected amount was eliminated in the first 40h after injection (Figure 1B). The ASO localization in the kidney was next assessed on tissue sections using a fluorescent probe (Cy3-DNA) complementary to the ASO (Figure 1C). ASO were found localized in the cortex of the kidney, especially in the proximal convoluted tubules and not in the other area (glomerulus, distal convoluted tubules or in the medulla).

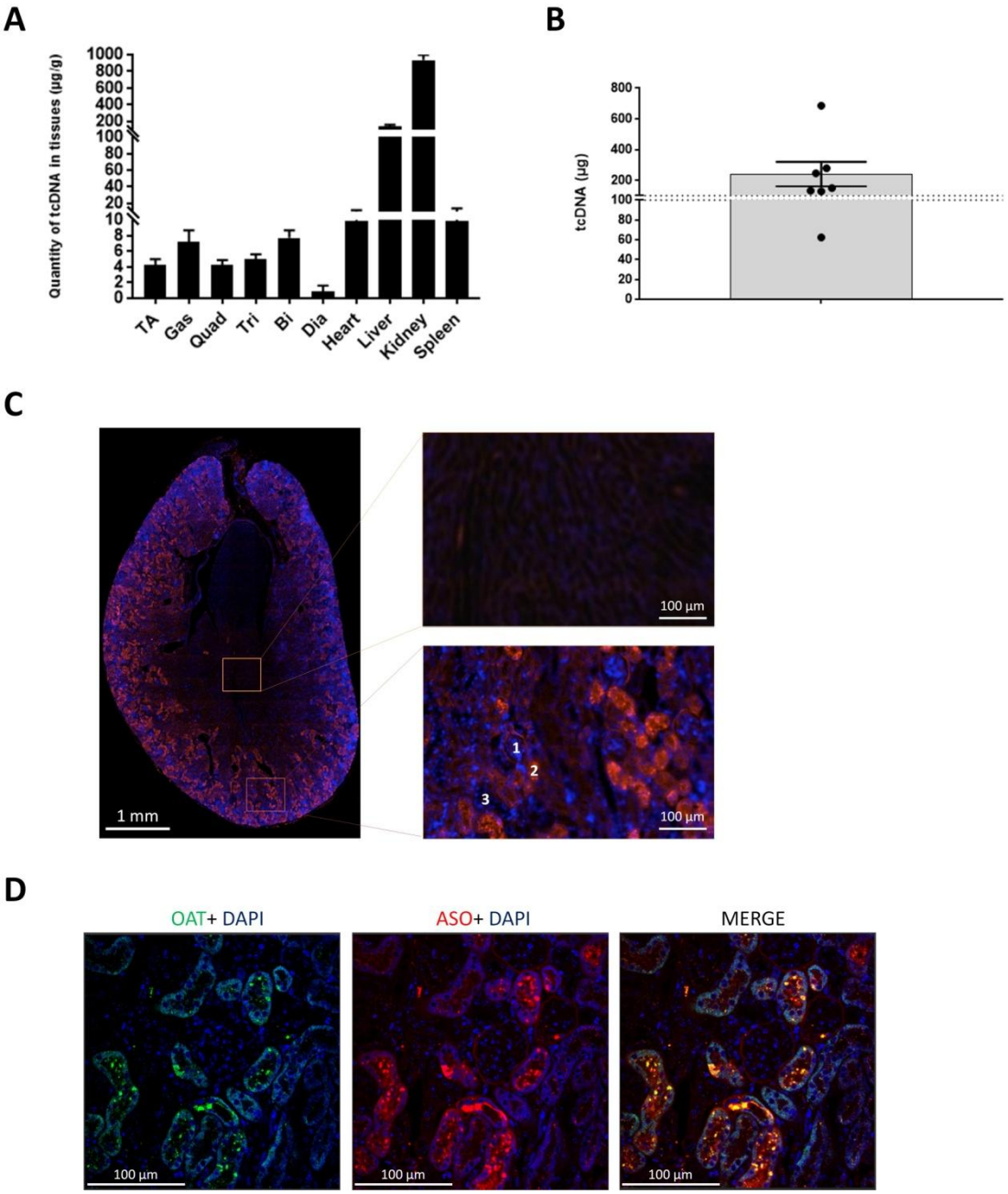

Figure 1: General distribution of TC-DNA ASO in mdx mice

A: Quantification of ASO in the different muscles tissues (Tibialis anterior (TA), gastrocnemius (GAS), quadriceps (QUAD), triceps (TRI), biceps (BI), diaphragm (DIA) and heat) and off target organs (kidney, liver and spleen) after 4 weeks of ASO treatment. N=4 mice. B: ASO quantification in the urine produce during the 40h following a single ASO injection of 1250µg. N=7 mice. C: Detection of the ASO (red staining) by *in-situ* hybridization on transverse sections of kidneys from *mdx* mice treated with ASO. 1 is glomerulus, 2 is proximal convoluted tub and 3 is distal convoluted tub. Nuclei are labelled in blue (DAPI) in the entire kidney sections (left panels) and the zoomed-in regions (right panels). The orange and pink scares indicate the localization of the zoomed region. D: Detection of the OAT1 (green staining) and ASO (red staining) by *in-situ* hybridization on transverse sections of kidneys from *mdx* mice treated with ASO. Nuclei are labelled in blue (DAPI). In the merge, the combined signal of OAT1 and ASO is yellow.

The proximal convoluted tube is, in the kidney, the second area involved in the transfer of molecules from the blood to the urine (after the glomerulus). Because of all its transporters, this tube is where the vast majority of all charged molecules are eliminated by the kidney[18]. One of the main transporter family involved in the transition from blood to urine of anionic molecules are the organic anion transporters (OAT). A co-staining with an antibody anti-OAT1 and the ASO probe was performed in the kidney to investigate the colocalization of both which would support the hypothesis that OATs are involved in the elimination process of TC-DNA ASO (Figure 1D). This staining indicated that OAT are indeed localized only in the proximal convoluted tubules and confirmed the colocalization with TC-DNA.

These results confirmed that TC-DNA elimination in the kidney is likely mediated by OATs and we therefore evaluated the impact of the OAT inhibitor probenecid on the efficacy of ASO treatment.

Impact of short term treatment with probenecid on TC-DNA ASO biodistribution

To investigate the effect of OAT inhibition on TC-DNA ASO biodistribution a short study was performed in *mdx* mice. Mice were treated with intravenous injections of TC-DNA ASO at 50mg/kg followed by an intraperitoneal injection of probenecid at 50mg/kg. Blood was collected at different time points from 30 min to 48h post injection and ASO were quantified (Figure 2A). The pharmacokinetic analysis revealed a slightly higher half-life of TC-DNA in the circulation when probenecid was co-administered (5.8h) compared with TC-DNA treatment alone (4.9h) although this difference did not reach statistical significance. To confirm this data and to ensure it was caused by lower kidney elimination, ASO were

quantified in the urines of injected mice collected in the first 40h post injection. Surprisingly, we found slightly more TC-DNA ASO in the urine of animals co-treated with probenecid compared treatment with ASO only (485 versus 323µg, *P value*=0.4000) (Figure 2B).

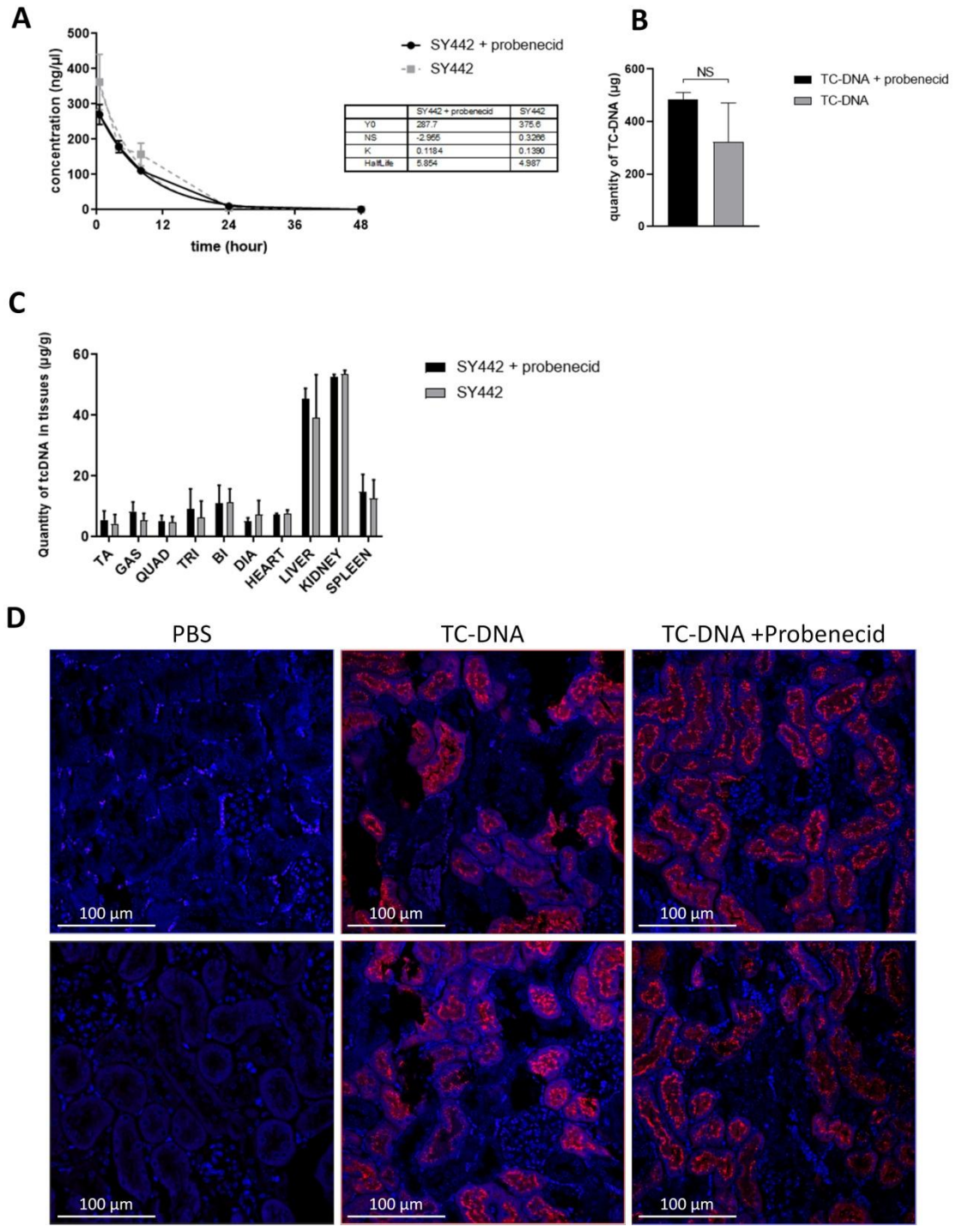

Figure 2: Short term efficacy of probenecid on TC-DNA ASO biodistribution
A: Quantification of TC-DNA ASO in the serum of mice after the injection of 50 mg/kg of TC-DNA alone or combined with an injection of 50 mg/kg of probenecid. N=3 mice.

B: Quantification of TC-DNA ASO in the urine of injected mice in the 24h following the injection of ASO combined or not with probenecid. N=3 mice. C: Quantification of ASO in the different muscles tissues (Tibialis anterior (TA), gastrocnemius (GAS), quadriceps (QUAD), triceps (TRI), biceps (BI), diaphragm (DIA) and heat) and off target organs (kidney, liver and spleen) 24h after treatment with ASO combined or not with probenecid. N=3 mice. D: Detection of the ASO (red staining) by *in-situ* hybridization on transverse sections of kidneys (cortex) from *mdx* mice treated with ASO +/- probenecid. Nuclei are labelled in blue (DAPI)

We next monitored TC-DNA ASO biodistribution in muscles and off target organs like liver, kidney and spleen and found no significant difference between the 2 treated groups (with or with probenecid, globale *P value*= 0.5971) (Figure 2C). The localization of TC-DNA in kidney was also analyzed on sections and revealed the same localization in proximal convoluted tubules and similar signal intensity for both groups of mice (Figure 2D).

Mild term efficacy of probenecid on TC-DNA ASO biodistribution and efficacy.

To further investigate the potential impact of probenecid on ASO efficacy, we performed a repeated dose study, hypothesizing that the effects resulting from OAT inhibition may take longer than 24h to be detectable. In this protocol, *mdx* mice were treated weekly during 4 weeks with either TC-DNA only or TC-DNA + probenecid (same doses as the first study) and analyzed 2 weeks after the last injection. The analysis of TC-DNA biodistribution revealed a similar accumulation profile in both treated group, indicating no effect of the probenecid (Figure 3A). However, the localization of TC-DNA ASO detected with a complementary probe on kidney sections appeared slightly different in both groups. In the kidney of mice co-treated with probenecid, TC-DNA ASO appeared more accumulated in the Bowman's capsules (area around the glomerulus) compared with mice treated with ASO alone (Figure

3B). This suggests that inhibiting the OAT with probenecid may have relocated the ASO within the kidney.

To assess the potential effect of probenecid on ASO efficacy, we quantified the exon skipping level in muscles from both groups of mice (Figure 3C) and found no significant difference between the 2 treatments (Global *P value*= 0.1789).

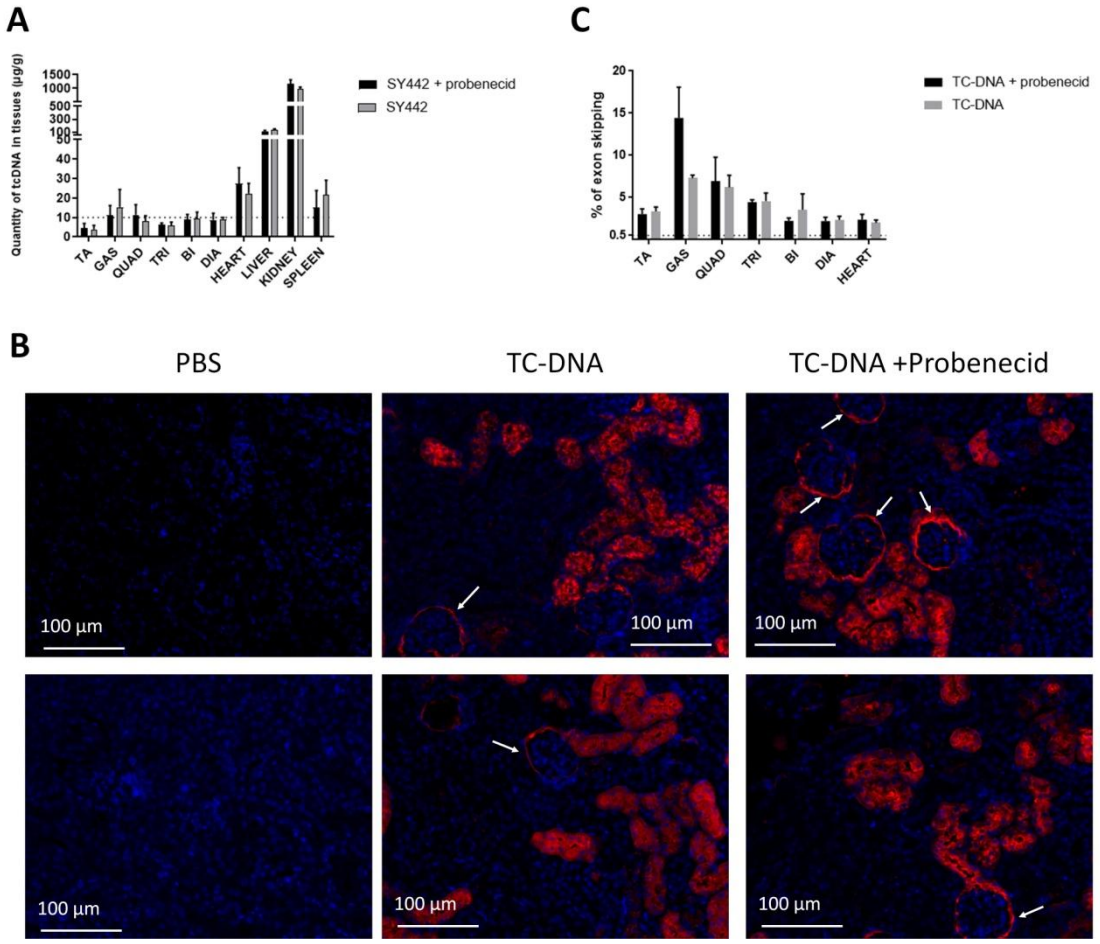

Figure 3: Mild term efficacy of probenecid on TC-DNA ASO biodistribution
A: Quantification of ASO in the different muscles tissues (Tibialis anterior (TA), gastrocnemius (GAS), quadriceps (QUAD), triceps (TRI), biceps (BI), diaphragm (DIA) and heat) and off target organs (kidney, liver and spleen) 2 weeks after 4 weeks treatment with ASO combined or not with probenecid. N=3 mice. B: Detection of the ASO (red staining) by *in-situ* hybridization on transverse sections of kidneys (cortex) from *mdx* mice treated 4 weeks with ASO +/- probenecid. Nuclei are labelled in blue (DAPI) C: Effect of probenecid on exon skipping level. qPCR quantification of exon 23 using taqman qPCR in the different muscle tissues. Tibialis anterior (TA), gastrocnemius (GAS), quadriceps (QUAD), triceps (TRI), biceps (BI), diaphragm (DIA) and heart. N=3 mice per group.

DISCUSSION

In this study, we aimed to improve the bioavailability and biodistribution of TC-DNA ASO in order to enhance the overall exon-skipping efficacy. We first determined that approximately 20% of the injected TC-DNA ASO was eliminated in the first 24h after administration and we characterized the accumulation of TC-DNA ASO in kidneys.

After 4 weeks treatment with TC-DNA ASO, kidneys from injected *mdx* mice were collected and sectioned to determine the ASO localization. The detection of the TC-DNA ASOs with a fluorescent and complementary probe showed that ASOs were localized in the proximal convoluted tubules. This localization was expected because TC-DNA ASO are negatively charged at physiological pH and most of the anions elimination in the kidney occurred by tubular secretion[19]. This is also in line with previous studies showing that charged ASO (such as locked nucleic acid) also accumulate in the proximal convoluted tubules[20]. To make the transition from blood to kidney, most of anion molecules go through the organic anion transporters (OAT) localized at the basolateral membrane of renal epithelial cells (the membrane in contact with the blood)[19]. In this study, we showed that TC-DNA ASOs are co-localized with the OAT channel (OAT1). This preliminary result confirms that the elimination of TC-DNA ASO in the kidney may indeed be mediated by OAT.

We hypothesized here that blocking the early renal elimination of ASO may improve the bioavailability and biodistribution of TC-DNA ASO and ultimately help them reach their target tissue. We therefore treated *mdx* mice with a combination of TC-DNA ASO and probenecid, a competitive inhibitor of all OAT. The analysis of ASO biodistribution at both early time points (24h post 1 injection) and later time points (2 weeks post 4 injections) showed no effect of probenecid on TC-DNA accumulation in tissues. Similarly, no differences were detected by qPCR when measuring exon skipping levels in muscles from

mice treated with ASO or ASO + probenecid. Both distribution and efficacy data indicate that probenecid does not improve TC-DNA ASO potency.

The only difference reported between the 2 treatments is a change in the localization of TC-DNA in the kidney of mice co-treated with probenecid for 4 weeks. We indeed found more ASO accumulated in the Bowman's capsules. This area is for anion molecule involved in almost 10% of the kidney elimination process[19]. An increasing level of TC-DNA ASO in the Bowman's capsules may be a compensation process resulting from the OAT inhibition. This finding suggests that failure to improve ASO therapy by blocking OAT might be caused by the activation of other processes involved in renal elimination (normal one or toxic one).

Overall, this study suggests that blocking OAT in order to decrease rapid ASO elimination through the kidney does not allow a better bioavailability of ASO nor higher exon skipping efficacy.

MATERIAL AND METHODS

Antisense oligonucleotides and animal experiments

Animal procedures were performed in accordance with national and European legislation, approved by the French government (ministère de l'enseignement supérieur et de la recherche, autorisation APAFiS #6518). *Mdx* (C57BL/10ScSc-Dmdmdx/J) mice were bred in our animal facility at the Plateforme 2Care, UFR des Sciences de la santé, université de Versailles Saint Quentin and were maintained in a standard 12-hour light/dark cycle with free access to food and water. Mice were weaned at weeks 4-5 postnatal and 2-5 individuals were housed per cage.

TC-DNA ASO targeting the donor splice site of exon 23 of the mouse dystrophin pre-mRNA[5] was synthesized by SQY Therapeutics (Montigny le Bretonneux, France). Palmitic acid was

conjugated at the 5'end of TC-DNA-PO via a C6-amino linker and a phosphorothioate bond as previously described[6]. Mice were treated with ASO (one intravenous injection per week at 50mg/kg/wk under general anesthesia using 2% isoflurane). The inhibitor of organic anion transporter: probenecid (Bio-Techne reference: 4107) was dissolved in phosphate-buffered saline (PBS). M*dx* mice were treated intraperitoneally with probenecid at 50mg/kg/week just after the ASO injection. Age-matched *mdx* groups receiving an equivalent volume of sterile saline were included as controls and C57BL/10 mice were included as wild-type controls.

Animals were euthanized 24h after the first co-injection or 2 weeks after the end of the protocol of 4 weeks treatment and muscles and tissues were harvested and snap-frozen in liquid nitrogen–cooled isopentane and stored at −80 °C before further analysis. Kidney were sampled at the end of the protocols, fixed in 10% neutral buffered formalin, and embedded in paraffin wax for histological staining.

ASO quantification by fluorescent hybridization assay

Tissues were homogenized using the Precellys 24 (Bertin Instruments, France) in lysis buffer (100 mmol/l Tris–HCl, pH 8.5, 200 mmol/l NaCl, 5 mmol/l EDTA, 0.2% sodium dodecyl sulfate) containing 2 mg/ml of proteinase K (Invitrogen) (50mg tissue/ ml of buffer), followed by incubation overnight at 55 °C in a hybridization oven. After centrifugation at 7000 g (Sorval ST 8R centrifuge, 75005719 rotor) for 15 min, the supernatant was used in the assay. Quantification of ASO was performed using a hybridization assay with a molecular beacon probe, as previously described[21]. Briefly, 10 µl of tissue lysates, serum or urine were incubated with a 5' Cy3-DNA complementary probe conjugated with HBQ quencher at 3' in black non-binding 96-well plates (Fischer Scientific). PBS was added to a final volume of 100 µl per well and fluorescence was measured on a spectrophotometer (Ex 544 nm/ Em 590 nm

using FluoStar Omega). The amount of TC-DNA ASO in tissues was determined using a standard curve build on the measurement of known TC-DNA ASO quantities dissolved in the respective tissue lysates/urine/serum of mock-injected animals.

RNA analysis

Total RNA was isolated from snap-frozen muscle tissues using TRIzol reagent according to the manufacturer's instructions (ThermoFisher Scientific, USA). Exon 23 skipping levels were quantified using real-time quantitative PCR using Taqman assays designed against the exon 23-24 junction and exon 22-24 junction as previously described[6]. 70 ng of cDNA was used as input per reaction and all assays were carried out in triplicate. Assays were performed under fast cycling conditions on a Biorad CFX384 Touch Real-Time PCR Detection System, and all data were analyzed using the absolute copy number method. For a given sample the copy number of skipped product (exon 22-24 assay) and unskipped product (exon 23-24 assay) were determined using the standards Ex20-26 and Ex20-26Delta23 respectively (gBlocks gene fragments from Integrated DNA technology). Exon 23 skipping was then expressed as a percentage of total dystrophin (calculated by the addition of exon 22-23 and exon 22-24 copy numbers).

Immunohistochemistry analysis

Kidney section of 7 µm were de-waxed with 3 xylen baths of 5 min and 3 ethanol 100% baths of 3 min and 1 water acid bath of 1 min. slide were rehydrated in PBS during 10 min at room temperature (RT) before saturation in goat serum 5% during 1h at RT. Primary antibody: rabbit polyclonal antibody OAT1 (dilution 1:500, Abcam ab131087) is incubated 2h at RT. After wash in PBS, secondary antibody (goat anti rabbit cy5: abcam ab6564, dilution 1:500) is incubate 1h at RT. Slide were washed in PSB and incubated with ASO probe coupled with

alexafluor 594 (dilution 1:2500 in PBS, 30 min at RT). After PSB wash, DAPI staining is performed followed by another wash and mounting (Fluoromount ®).Controls prepared by omitting primary antibody showed no specific staining. Images were taken at equivalent locations and exposure times using a Leica white light laser TCS SP8-X (Leica Microsystem, Wetzlar, Germany).

The protocol for ASO staining alone in the kidney is the same as for the co-staining labeling: de-wax, rehydratation, incubation with prob, wash, incubation with DAPI, wash and mounting. Kidneys were scan with a Zeiss Axio Imager with an Orkan camera (Hamamatsu) and AxioVision software.

Statistical analysis

All *in vivo* data were analysed with the GraphPad Prism8 software (San Diego, California, USA) and expressed as means ± S.E.M. The "n" refers to the number of mice per group.

Group comparisons were performed using one and two-way analyses of variance (ANOVA) with repeated-measure comparisons when needed (effects in different muscle tissues for example), followed by post-hoc Dunnett's or Sidak's multiple comparisons when appropriate. The Kruskal-Wallis test was used to compare groups that do not follow a normal distribution (assessed with the Shapiro-Wilk test). Significant levels were set at *$p < 0.05$, **$p < 0.01$, ***$p < 0.001$, ****$p<0.0001$.

ACKNOWLEDGEMENT

We would like to thank the personnel of the plateforme 2CARE for taking care of the animals used in this work and of the plateforme Cymages for the microscopy.

FUNDING

This work was supported by the Institut National de la santé et la recherche médicale (INSERM), the Association Monegasque contre les myopathies (AMM), the Paris Ile-de-France Region and the Fondation UVSQ. F. Bizot is the recipient of a MESRI thesis fellowship.

AUTHOR CONTRIBUTIONS

Conceptualization, F.B. and A.G.; Methodology, F.B. and A.G.; Investigation, F.B. and T.T.; Writing, F.B. and A.G.; Funding Acquisition, L.G. and A.G.; Resources, L.G. and A.G; Supervision, A.G.

CONFLICT OF INTEREST STATEMENT

LG is co-founder of SQY Therapeutics, which produces tricyclo-DNA oligomers. TT is employee of SQY Therapeutics.

REFERENCES

1. Saoudi, A., and Goyenvalle, A. (2021). [RNA splicing modulation: Therapeutic progress and perspectives]. Med Sci (Paris) *37*, 625–631. 10.1051/medsci/2021091.

2. Hammond, S.M., Aartsma-Rus, A., Alves, S., Borgos, S.E., Buijsen, R.A.M., Collin, R.W.J., Covello, G., Denti, M.A., Desviat, L.R., Echevarría, L., et al. (2021). Delivery of oligonucleotide-based therapeutics: challenges and opportunities. EMBO Mol Med *13*, e13243. 10.15252/emmm.202013243.

3. Bizot, F., Vulin, A., and Goyenvalle, A. (2020). Current Status of Antisense Oligonucleotide-Based Therapy in Neuromuscular Disorders. Drugs *80*, 1397–1415. 10.1007/s40265-020-01363-3.

4. Goyenvalle, A., Griffith, G., Babbs, A., El Andaloussi, S., Ezzat, K., Avril, A., Dugovic, B., Chaussenot, R., Ferry, A., Voit, T., et al. (2015). Functional correction in mouse models of muscular dystrophy using exon-skipping tricyclo-DNA oligomers. Nat Med *21*, 270–275. 10.1038/nm.3765.

5. Relizani, K., Griffith, G., Echevarría, L., Zarrouki, F., Facchinetti, P., Vaillend, C., Leumann, C., Garcia, L., and Goyenvalle, A. (2017). Efficacy and Safety Profile of Tricyclo-DNA Antisense Oligonucleotides in Duchenne Muscular Dystrophy Mouse Model. Mol Ther Nucleic Acids *8*, 144–157. 10.1016/j.omtn.2017.06.013.

6. Relizani, K., Echevarría, L., Zarrouki, F., Gastaldi, C., Dambrune, C., Aupy, P., Haeberli, A., Komisarski, M., Tensorer, T., Larcher, T., et al. (2022). Palmitic acid conjugation enhances potency of tricyclo-DNA splice switching oligonucleotides. Nucleic Acids Res *50*, 17–34. 10.1093/nar/gkab1199.

7. Wagner, K.R., Kuntz, N.L., Koenig, E., East, L., Upadhyay, S., Han, B., and Shieh, P.B. (2021). Safety, tolerability, and pharmacokinetics of casimersen in patients with Duchenne muscular dystrophy amenable to exon 45 skipping: A randomized, double-blind, placebo-controlled, dose-titration trial. Muscle Nerve *64*, 285–292. 10.1002/mus.27347.

8. Mercuri, E., Seferian, A.M., Servais, L., Deconinck, N., Stevenson, H., East, L., Zhang, W., Upadhyay, S., and Muntoni, F. (2022). Safety, Tolerability, and Pharmacokinetics of Eteplirsen in Patients 6–48 Months Old With Duchenne Muscular Dystrophy Amenable to Exon 51 Skipping. Muscular Dystrophy Association Clinical & Scientific Conference.

9. Shadid, M., Badawi, M., and Abulrob, A. (2021). Antisense oligonucleotides: absorption, distribution, metabolism, and excretion. Expert Opin Drug Metab Toxicol *17*, 1281–1292. 10.1080/17425255.2021.1992382.

10. Yu, R.Z., Geary, R.S., Monteith, D.K., Matson, J., Truong, L., Fitchett, J., and Levin, A.A. (2004). Tissue disposition of 2'-O-(2-methoxy) ethyl modified antisense oligonucleotides in monkeys. J Pharm Sci *93*, 48–59. 10.1002/jps.10473.

11. Prakash, T.P., Mullick, A.E., Lee, R.G., Yu, J., Yeh, S.T., Low, A., Chappell, A.E., Østergaard, M.E., Murray, S., Gaus, H.J., et al. (2019). Fatty acid conjugation enhances potency of antisense oligonucleotides in muscle. Nucleic Acids Res *47*, 6029–6044. 10.1093/nar/gkz354.

12. Chappell, A.E., Gaus, H.J., Berdeja, A., Gupta, R., Jo, M., Prakash, T.P., Oestergaard, M., Swayze, E.E., and Seth, P.P. (2020). Mechanisms of palmitic acid-conjugated antisense oligonucleotide distribution in mice. Nucleic Acids Res *48*, 4382–4395. 10.1093/nar/gkaa164.

13. Zhang, J., Wang, H., Fan, Y., Yu, Z., and You, G. (2021). Regulation of organic anion transporters: role in physiology, pathophysiology, and drug elimination. Pharmacol Ther *217*, 107647. 10.1016/j.pharmthera.2020.107647.

14. Töllner, K., Brandt, C., Römermann, K., and Löscher, W. (2015). The organic anion transport inhibitor probenecid increases brain concentrations of the NKCC1 inhibitor bumetanide. Eur J Pharmacol *746*, 167–173. 10.1016/j.ejphar.2014.11.019.

15. Schultz, C.R., Swanson, M.A., Dowling, T.C., and Bachmann, A.S. (2021). Probenecid increases renal retention and antitumor activity of DFMO in neuroblastoma. Cancer Chemother Pharmacol *88*, 607–617. 10.1007/s00280-021-04309-y.

16. Everts, R.J., Begg, R., Gardiner, S.J., Zhang, M., Turnidge, J., Chambers, S.T., and Begg, E.J. (2020). Probenecid and food effects on flucloxacillin pharmacokinetics and pharmacodynamics in healthy volunteers. J Infect *80*, 42–53. 10.1016/j.jinf.2019.09.004.

17. Wilson, R.C., Arkell, P., Riezk, A., Gilchrist, M., Wheeler, G., Hope, W., Holmes, A.H., and Rawson, T.M. (2022). Addition of probenecid to oral β-lactam antibiotics: a systematic review and meta-analysis. J Antimicrob Chemother *77*, 2364–2372. 10.1093/jac/dkac200.

18. Yin, J., and Wang, J. (2016). Renal drug transporters and their significance in drug-drug interactions. Acta Pharm Sin B *6*, 363–373. 10.1016/j.apsb.2016.07.013.

19. Dresser, M.J., Leabman, M.K., and Giacomini, K.M. (2001). Transporters involved in the elimination of drugs in the kidney: organic anion transporters and organic cation transporters. J Pharm Sci *90*, 397–421. 10.1002/1520-6017(200104)90:4<397::aid-jps1000>3.0.co;2-d.

20. Moisan, A., Gubler, M., Zhang, J.D., Tessier, Y., Dumong Erichsen, K., Sewing, S., Gérard, R., Avignon, B., Huber, S., Benmansour, F., et al. (2017). Inhibition of EGF Uptake by Nephrotoxic Antisense Drugs In Vitro and Implications for Preclinical Safety Profiling. Mol Ther Nucleic Acids *6*, 89–105. 10.1016/j.omtn.2016.11.006.

21. Echevarría, L., Aupy, P., Relizani, K., Bestetti, T., Griffith, G., Blandel, F., Komisarski, M., Haeberli, A., Svinartchouk, F., Garcia, L., et al. (2019). Evaluating the Impact of Variable Phosphorothioate Content in Tricyclo-DNA Antisense Oligonucleotides in a Duchenne Muscular Dystrophy Mouse Model. Nucleic Acid Ther *29*, 148–160. 10.1089/nat.2018.0773.

2 IMPROVE ENDOSOMAL ESCAPE

Context:

One of the main challenges of ASO-mediated exon skipping is the delivery of ASOs to the nucleus of the target. To increase the biodistribution of the ASO, my lab has developped a second generation of ASO: the palm-TC-DNA. Despite the improved properties of this chemistry, the amount of ASO ultimately reaching the nucleus is still limited. This is caused by the entrapment of ASO in the endosomal compartment of the cells and their degradation before they can reach the nucleus (the target compartment for splice switching ASO). To improve the intracellular transport of ASOs in the target cells and the level o ASOs reaching the nucleus, we used an endosomal escape promoter called UNC7938. UNC7938 is a 3-deazapteridine analog developped at the university of North Carolina (Yang et al. 2015) which destabilizes the membrane of late endosomes by binding to lysobisphosphatidic acid (Allen et al. 2019; Juliano 2021).

Methods:

Mdx mice were co-treated with TC-DNA ASO (intravenous, 30mg/kg/week) and UNC7938 (intravenous, 15mg/kg/week) which was injected 24 hours after the ASO treatment.

After 4 weeks of treatment mice were sacrificed at different time points (from 72h to 6 weeks) and tissues were collected to analyze the effects of UNC7938 on distribution and efficacy of the ASOs.

A long term study of 12 weeks was then performed to confirm the effects of UNC7938 on ASO efficacy. One week after the last injection echocardiography was performed to investigate the potential therapeutic benefit of the co-treatment on cardiac function.

Main Results

UNC7938, combined to TC-DNA ASO, was able to increase the exon skipping efficacy with particular strong effects few days after the end of the treatment. The protein level in the diaphragm and heart was particularly improved, with an increase of 31% and 58%

respectively after 12 weeks of treatment compared to treatment with TC-DNA alone. In addition, the combined therapy was able to normalize the cardiac function after 12 weeks of treatment.

Conclusion:

By promoting endosomal escape, UNC7938 is able to improve the efficacy of ASO therapy. However, these effects were particularly strong at early time points after injection and tended to fade over time, highlighting the importance of the "depot effect" resulting from the otherwise slow release of ASO from endosomes.

Moreover, additional studies should be performed to investigate further the toxicity profile of this therapy and to assess the feasibility of a simultaneous injection of the two molecules.

cells

MDPI

Article

Oligonucleotide Enhancing Compound Increases Tricyclo-DNA Mediated Exon-Skipping Efficacy in the Mdx Mouse Model

Flavien Bizot [1], Abdallah Fayssoil [1,2], Cécile Gastaldi [3,4], Tabitha Irawan [1], Xaysongkhame Phongsavanh [1], Arnaud Mansart [5], Thomas Tensorer [6], Elise Brisebard [7], Luis Garcia [1,4], Rudolph L Juliano [8] and Aurélie Goyenvalle [1,4,*]

1 Université Paris-Saclay, UVSQ, Inserm, END-ICAP, 78000 Versailles, France
2 Raymond Poincaré Hospital, APHP, 78266 Garches, France
3 Medical Biology Department, Centre Scientifique de Monaco, Monaco 98000, Monaco
4 LIA BAHN, CSM-UVSQ, Monaco 98000, Monaco
5 Université Paris-Saclay, UVSQ, INSERM U1173, 2I, 78000 Versailles, France
6 SQY Therapeutics, UVSQ, END-ICAP, 78000 Versailles, France
7 INRAE Oniris, UMR 703 PAnTher, 44307 Nantes, France
8 Initos Pharmaceuticals LLC, UNC Eshelman School of Pharmacy, University of North Carolina, Chapel Hill, NC 27599, USA
* Correspondence: aurelie.goyenvalle@uvsq.fr; Tel.: +33-170429432

Abstract: Nucleic acid-based therapeutics hold great promise for the treatment of numerous diseases, including neuromuscular disorders, such as Duchenne muscular dystrophy (DMD). Some antisense oligonucleotide (ASO) drugs have already been approved by the US FDA for DMD, but the potential of this therapy is still limited by several challenges, including the poor distribution of ASOs to target tissues, but also the entrapment of ASO in the endosomal compartment. Endosomal escape is a well recognized limitation that prevents ASO from reaching their target pre-mRNA in the nucleus. Small molecules named oligonucleotide-enhancing compounds (OEC) have been shown to release ASO from endosomal entrapment, thus increasing ASO nuclear concentration and ultimately correcting more pre-mRNA targets. In this study, we evaluated the impact of a therapy combining ASO and OEC on dystrophin restoration in *mdx* mice. Analysis of exon-skipping levels at different time points after the co-treatment revealed improved efficacy, particularly at early time points, reaching up to 4.4-fold increase at 72 h post treatment in the heart compared to treatment with ASO alone. Significantly higher levels of dystrophin restoration were detected two weeks after the end of the combined therapy, reaching up to 2.7-fold increase in the heart compared to mice treated with ASO alone. Moreover, we demonstrated a normalization of cardiac function in *mdx* mice after a 12-week-long treatment with the combined ASO + OEC therapy. Altogether, these findings indicate that compounds facilitating endosomal escape can significantly improve the therapeutic potential of exon-skipping approaches offering promising perspectives for the treatment of DMD.

Keywords: antisense oligonucleotides; exon-skipping; endosomal escape; duchenne muscular dystrophy; UNC7938; tricyclo-DNA

Citation: Bizot, F.; Fayssoil, A.; Gastaldi, C.; Irawan, T.; Phongsavanh, X.; Mansart, A.; Tensorer, T.; Brisebard, E.; Garcia, L.; Juliano, R.L.; et al. Oligonucleotide Enhancing Compound Increases Tricyclo-DNA Mediated Exon-Skipping Efficacy in the Mdx Mouse Model. *Cells* **2023**, *12*, 702. https://doi.org/10.3390/cells12050702

Academic Editor: Peter Droge

Received: 6 January 2023
Revised: 16 February 2023
Accepted: 20 February 2023
Published: 23 February 2023

1. Introduction

Duchenne muscular dystrophy (DMD) is the most common muscular dystrophy in the paediatric population. It is caused by various pathogenic mutations in the DMD gene, which mostly disrupt the open reading frame and thus lead to an absence of functional dystrophin protein. The exon-skipping approach has been developed to restore the reading frame of the gene and is based on the use of antisense oligonucleotides (ASO). ASOs aim to eliminate one or several exons by masking key splicing sites and therefore induce the expression of an internally deleted but functional dystrophin protein. Several ASO-based drugs have already been approved by the US FDA for the treatment of DMD (eteplirsen,

golodirsen, viltolarsen and casimersen targeting exons 51, 53 and 45) [1]. Approval was mostly based on safety, and a small percentage of dystrophin restoration was observed in muscle biopsies of treated patients. However, the clinical benefit is still marginal, and there is a critical need to improve the level of dystrophin being restored in DMD patients.

One of the most recognized challenges of ASO-mediated exon skipping is the delivery of ASOs to the nucleus of the target tissues [2,3]. To achieve this goal, second generations of ASO have been developed with alternative chemistries or various conjugates [4,5]. Amongst these, we have been working with one particular chemical substance named tricyclo-DNA (tcDNA), and we recently demonstrated that conjugation of palmitic acid to tcDNA significantly enhances its delivery to target tissues [6]. Despite these improvements, the quantity of ASO ending up in the nucleus to bind their pre-mRNA target remains extremely low. Indeed, even when ASOs reach the correct target tissues/cells, most of them end up trapped in the endosomal compartment and are degraded in the lysosomes before they can enter the cytoplasm and the nucleus (e.g., the ultimate target compartment) [2]. Previous studies have focused on ASO cellular trafficking to better characterize the mechanisms and improve the intracytoplasmic delivery of ASOs [3,7]. A number of studies have aimed at influencing ASO pharmacological effect by manipulating components of the endosomal machinery, specifically by targeting proteins involved in endomembrane trafficking, such as GCC2, M6PR, or COPII Golgi coat proteins [8–10].

Overall, these studies confirmed that components of the endosomal trafficking machinery are intimately involved in the subcellular fate and thus the pharmacological effectiveness of ASOs [11].

Several strategies have been considered to allow ASOs to cross the biological barriers and cell membranes. Among them, the conjugation of ASO to a cell penetration peptide (CPP) has been widely used. CPPs are relatively short peptides, from four to forty amino acids, which can induce endocytosis or promote the intracellular effects of ASO [12]. Given that CPPs are charged molecules, they are often conjugated with charge neutral ASOs, such as phosphorodiamidate morpholino oligomers (PMO) [13], and cannot be used with charged ASO like tcDNA. Other approaches based on the use of nanotechnology have been extensively studied, from DNA nanostructures to exosome-like nanocarriers to spherical nucleic acids or lipid nanoparticles (LNPs), all described in recent reviews [5,13,14]. An alternative option is to use small molecules named oligonucleotide enhancing compounds (OEC), which were discovered through high throughput screening and which selectively release oligonucleotides from non-productive entrapment in endosomal compartments [15–17]. Because they are not directly linked to the ASO, OECs may be used with all types of ASOs (charged or uncharged) to facilitate their access to the cytosol and thus improve the probability to reach the nucleus to substantially enhance pharmacological effects [11].

Different types of OECs have been characterized, depending on their mechanism of action: the first one, which has been known for decades is a "proton sponge action", characteristic of lysosomotropic drugs, leads to an influx of water molecules, swelling, and disruption of the endosomal compartment [18]. Alternative mechanisms include disrupting the interaction with the proteins of the endosomal membrane (such as Retro-1, which affects Rab7/9 positive late endosomes) [19]. The more recently identified OEC, named UNC7938, was shown to selectively release oligonucleotides from late endosomes, with only little effect on lysosomal pH, thus emphasizing the distinction between the OECs and typical lysosomotropic compounds [11,17].

In this study, we report the impact of OEC UNC7938 administration on exon-skipping efficacy mediated by tcDNA-ASO in *mdx* mice and characterize the kinetics of the effect. Adult *mdx* mice were treated with a tcDNA-ASO aiming at skipping the *Dmd* exon 23 with or without UNC7938, and these were analyzed at different time points. The combined therapy appeared to be particularly efficient at early time points, as well as in the cardiac muscle, leading to a normalization of cardiac function after three months of treatment.

2. Materials and Methods

2.1. Antisense Oligonucleotides and Animal Experiments

Animal procedures were performed in accordance with national and European legislation, approved by the French government (Ministère de l'Enseignement supérieur et de la Recherche, Autorisation APAFiS #6518). Mdx (C57BL/10ScSc-Dmdmdx/J) mice were bred in our animal facility at the Plateforme 2Care, UFR des Sciences de la santé, Université de Versailles Saint Quentin and were maintained in a standard 12-h light/dark cycle with free access to food and water. Mice were weaned at week four to five (postnatal), and two to five individuals were housed per cage.

TcDNA-ASO, targeting the donor splice site of exon 23 of the mouse dystrophin pre-mRNA [20], was synthesized by SQY Therapeutics (Montigny le Bretonneux, France). Palmitic acid was conjugated at the 5′end of tcDNA-PO via a C6-amino linker and a phosphorothioate bond as previously described (Figure S1) [6]. Mice were injected intravenously with 30 mg/kg/wk of the tcDNA-ASO (one intravenous injection per week under general anesthesia using 2% isoflurane). The oligonucleotide enhancing compound UNC7938 was produced by Initos Pharmaceuticals LLC (Chapel Hill, NC, USA). *Mdx* mice were treated with UNC7938 at 15 mg/kg/wk under general anesthesia using 2% isoflurane 24 h after the ASO injection (every week or every four weeks, depending on the protocol). Age-matched *mdx* groups receiving an equivalent volume of sterile saline were included as controls, and C57BL/10 mice were included as wild-type controls.

Animals were euthanized at different time points according to the different protocols and muscles and tissues were harvested and snap-frozen in liquid nitrogen-cooled isopentane and stored at −80 °C before further analysis.

To assess the safety of UNC7938, liver and kidney were sampled at the end of the 12-wk protocol (two weeks after the last dose), fixed in 10% neutral buffered formalin, and embedded in paraffin wax. Thick sections of 4 µm were then routinely stained with hematoxylin-eosin-saffron (HES) for histopathological evaluation, which was further performed by a veterinary pathologist blind to treatment.

2.2. Echocardiography Procedure

The procedure was performed under isoflurane anesthesia. Anesthesia doses were kept to the lowest possible levels, usually 5% isoflurane for induction and 2.5–3% isoflurane during measurements. Animals were placed on a heating pad to maintain a constant body temperature (37 °C), and their rectal temperature was monitored throughout the experiment. Doppler-echocardiography was performed using a high-resolution ultrasound system (Logiq 9, GE, France) with a 36-MHz scan head. Each animal was shaven from the left sternal border to the left axillary line with depilatory cream before the examination. Each set of measurements was obtained from the same cardiac cycle. At least three sets of measurements were obtained from three different cardiac cycles. The left ventricular end-diastolic diameter (LVEDD), end-diastolic posterior wall thickness, and end-diastolic interventricular septal wall thickness were measured using the leading-edge convention of the American Society of Echocardiography from M mode. The LVEDD was measured, from a M-mode short-axis view of the left ventricle at the papillary muscle level. Left ventricular shortening fraction (RF) and left ventricular ejection fraction (LVEF) were calculated from the M mode. Aortic velocity time integral (VTI) was recorded during the procedure from Doppler echocardiography. Mitral inflow Doppler pattern was recorded (peak E, peak A, and deceleration time) from a four-chamber apical view. The left ventricular systolic intervals of the isovolumic contraction time (IVCT), the ventricular ejection time (ET), and the diastolic interval of the isovolumic relaxation time (IVRT) were measured for the Tei index calculation. Measurements were made for aortic and mitral blood flows recorded from an apical four-chamber modified view using pulsed Doppler, and the sample was placed between the tip of the mitral and the Left ventricular outflow tract. The Tei index was calculated as the ratio of (IVCT + IVRT) to systolic ejection time. Cardiac output (CO) was defined as stroke volume x heart rate. The shortening fraction (%) was calculated by

the formula: (LVEDD-LVESD)/LVEDD × 100. LV end-diastolic (EDV) and end-systolic (ESV) volumes were calculated using a half ellipsoid model of the LV. From these volumes, LV ejection fraction (%) was calculated using the formula: (EDV-ESV)/EDV × 100. These experiments were performed in blind.

2.3. ASO Quantification by Fluorescent Hybridization Assay

Tissues were homogenized using the Precellys 24 (Bertin Instruments, Montigny le Bretonneux, France) at a final concentration of 50 mg/mL of lysis buffer (100 mmol/L Tris–HCl, pH 8.5, 200 mmol/L NaCl, 5 mmol/L EDTA, 0.2% sodium dodecyl sulfate) containing 2 mg/mL of proteinase K (Invitrogen, Germany) and incubated overnight at 55 °C in a hybridization oven. After centrifugation at 7000× *g* (Sorval ST 8R centrifuge, 75005719 rotor) for 15 min, the supernatant was used in the assay. Quantification of ASO was performed using a hybridization assay with a molecular beacon probe, as previously described [21].

2.4. Cell Fractionation and Western Blot Validation

Cell fractionation from freshly dissected gluteus muscles and protein extraction were performed as described previously (Dimauro et al., 2012). Then, 35 µg of protein were loaded onto 4–20% Mini-PROTEAN® TGX™ Precast Protein Gels (BioRad, Carlsbad, CA, USA). The PVDF membranes were probed with primary polyclonal antibodies directed against histone H3 (Cell Signaling Technology, Danvers, MA USA, 1:1000) or primary monoclonal antibodies directed against EEA1 (Sigma Aldrich, Saint Louis, MI, USA, 1:1000) followed by incubation with a goat anti-mouse secondary antibody (IRDye 800 CW Goat anti-mouse IgG, Li-Cor, Germany, dilution 1/20,000) or goat anti-rabbit secondary antibody (IRDye 800 CW Goat anti-rabbit IgG, Li-Cor, Germany, dilution 1/20,000). Bands were visualized using the Odyssey CLx system (Li-Cor, Germany).

2.5. RNA Analysis

Total RNA was isolated from snap-frozen muscle tissues using TRIzol reagent, according to the manufacturer's instructions (ThermoFisher Scientific, Carlsbad, CA USA). To visualize exon skipping levels, aliquots of 500 ng of total RNA were used for RT-PCR analysis using the Access RT-PCR System (Promega, Madison, WI, USA), as previously described [6].

Exon 23 skipping levels were also quantified using real-time quantitative PCR using Taqman assays designed against the exon 23–24 junction and exon 22–24 junction, as previously described [6].

2.6. Western Blot Analysis

Protein lysates were obtained from intervening muscle sections collected during cryosection using the Precellys 24 (Bertin Instruments, Montigny le Bretonneux, France) in RIPA buffer (ThermoFisher Scientific, Rockford, IL, USA) complemented with SDS powder (5% final) (Bio-Rad, Marnes-la-coquette, France) and protease inhibitor cocktail (ThermoFisher Scientific, Rockford, IL, USA). An amount of 25 µg of protein were loaded onto NuPAGE 3–8% Tris-Acetate Protein gels (Invitrogen, Carlsbad, CA, USA), following manufacturer instructions. Dystrophin protein was detected with NCL-DYS1 primary monoclonal antibody (NCL-DYS1; Novocastra, Newcastle, UK, dilution 1/200), as prevsiously described [6]. Quantification was performed using the Empiria Studio software (Li-Cor, Bad Homburg, Germany) based on a standard curve made from pooled lysates from C57BL10 (WT) and *mdx* control for each tissue.

2.7. Serum and Urine Analysis

Blood samples were collected at the end of the treatment for biochemistry analysis. Analyses of serum alanine aminotransferase (ALT), aspartate aminotransferase (AST), alkaline phosphatase (ALP), bilirubin, creatinine, urea, and albumin levels were performed

by the pathology laboratory at Mary Lyon Centre, Medical Research Council, Harwell, Oxfordshire, UK.

Urine was collected using metabolic cages over 24 h, and urine creatinine and total protein were measured, as previously described [22].

2.8. Immunohistochemistry Analysis

Sections of 10 µm at 120 µm intervals were cut from triceps, diaphragm, and heart and examined for dystrophin expression using a rabbit polyclonal antibody Dystrophin (dilution 1:500; cat. number RB-9024-P ThermoScientific, Fremont, CA, USA), which was then detected by goat anti-rabbit IgGs Alexa Fluor 488 (dilution 1/500; A11070, Invitrogen, Eugene, OR, USA). Images were cropped, and scale bars of 100 µm were added using ImageJ software.

2.9. Statistical Analysis

All in vivo data were analyzed with the GraphPad Prism8 software (San Diego, CA, USA) and expressed as means ± S.E.M. The "*n*" refers to the number of mice per group.

Group comparisons were performed using one and two-way analyses of variance (ANOVA) with repeated-measure comparisons when needed (effects in different muscle tissues for example), followed by post-hoc Dunnett's or Sidak's multiple comparisons when appropriate. The Kruskal-Wallis test was used to compare groups that do not follow a normal distribution (assessed with the Shapiro-Wilk test). Significance levels were set at * $p < 0.05$, ** $p < 0.01$, *** $p < 0.001$, **** $p < 0.0001$.

3. Results

3.1. Effect of UNC7938 during a Short Term Exon Skipping Therapy in Mdx Mice

We first studied the effects of the oligonucleotide enhancing compound (OEC) UNC7938 over a relatively short period of four weeks of treatment. In this protocol schematized in Figure 1A, *mdx* mice were treated for four weeks with the previously described palm-tcDNA-ASO targeting the *Dmd* exon 23, which has demonstrated an enhanced therapeutic index in this mouse model [6] and the OEC weekly. UNC7938 was administered intravenously at 15 mg/kg [23] 24 h after each ASO injection, and tissues were collected and analyzed two weeks after the last ASO injection (Figure 1A). Exon 23 skipping levels were quantified by RT-qPCR in several skeletal muscles, including tibialis anterior, gastrocnemius, quadriceps, triceps, and diaphragm, as well as the cardiac muscle. Results revealed an overall improvement of the ASO therapy with UNC7938 compared to tcDNA-ASO alone ($p = 0.0152$, RM two-way ANOVA, ASO vs. ASO + 7938) with a higher effect in the heart ($p = 0.0016$) (Figure 1B).

We next assessed the levels of dystrophin restoration in the different tissues and found higher dystrophin levels in mice treated with the ASO + OEC than in mice treated with the ASO alone ($p = 0.0067$, RM two-way ANOVA, ASO vs. ASO + 7938) with a particular strong effect in the heart reaching a 2.75 fold-increase ($p < 0.0001$) and in the diaphragm (2.75 fold-increase but not statistically significant $p = 0.1680$) (Figure 1C). The amount of tcDNA-ASO in the different muscles and off-target organs were measured, and we found that the overall content of ASO in tissue lysates was not impacted by UNC7938 treatment (Figure 1D) (treatment effect $p = 0.6661$ and 0.1183 for muscles and organs, respectively, analyzed by RM two-way ANOVA).

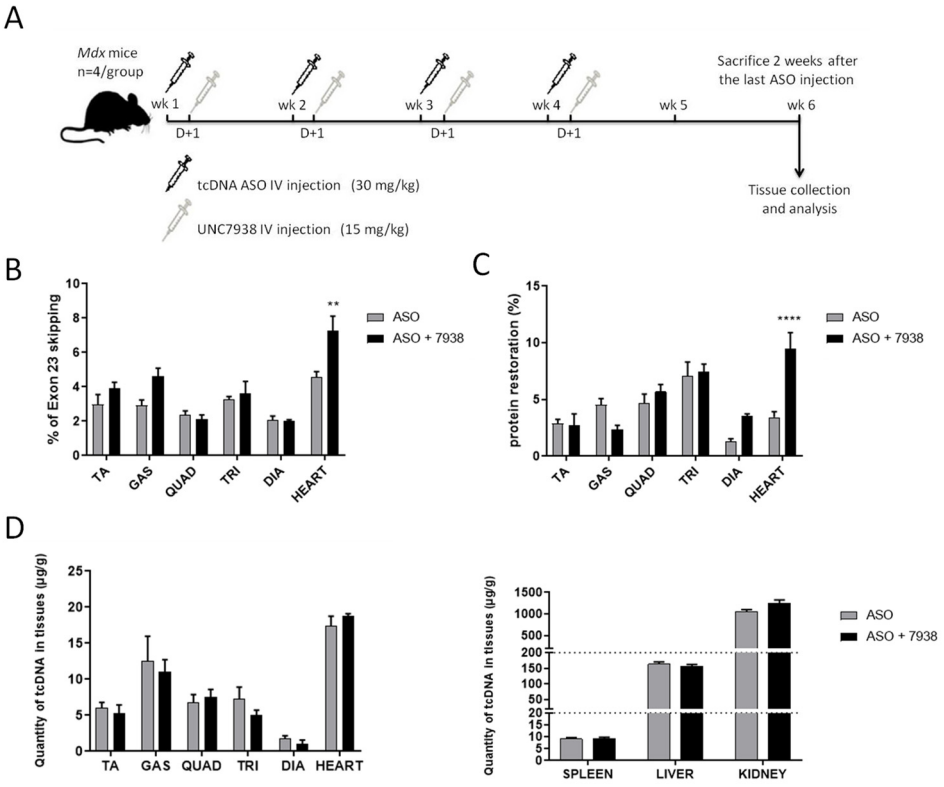

Figure 1. Short term efficacy of UNC7938 on exon skipping therapy in *mdx* mice. (**A**) Schematic representation of the injection protocol with tcDNA-ASO and the OEC UNC7938 in *mdx* mice. (**B**) Effect of UNC7938 on exon 23 skipping level. qPCR quantification of exon 23 skipping using taqman qPCR in the different muscle tissues. Tibialis anterior (TA), gastrocnemius (GAS), quadriceps (QUAD), triceps (TRI), diaphragm (DIA), and heart. $n = 4$ mice per group, ** $p < 0.01$ compared to ASO analyzed by RM two-way ANOVA. (**C**) Dystrophin restoration in treated *mdx* mice assessed by Western blotting. $n = 4$ mice per group, **** $p < 0.0001$ compared to ASO analyzed by RM two-way ANOVA. (**D**) Quantification of ASO in the different muscles tissues (left panel) and accumulation organs, such as spleen, liver, and kidney (right panel) after four weeks of treatment. Results are expressed as mean ± SEM; $n = 4$ mice per group.

3.2. Kinetics of UNC7938 Effect on Exon Skipping Therapy in Mdx Mice

To better characterize the effects of the OEC UNC7938 on ASO therapy, we treated *mdx* mice weekly with ASO + OEC during four weeks and analyzed them at different time points (72 h, one wk, three wks, and six wks) after the last injection (Figure 2A).

At very early time point (72 h), the ASO content in tissues was not impacted by UNC7938 administration in all muscles analyzed (Figures 2B and S2A). At one-wk and three-wk time points, UNC7938 treatment appears to increase the ASO concentration in muscles, especially in the triceps ($p = 0.0405$) and in the heart ($p = 0.0010$). This difference suggests a slower elimination of the ASO in mice co-treated with the OEC compared to mice treated with ASO alone. However, six weeks after the last injection, ASO content was similar for both treatments and only limited amount of ASO were detected in all muscle tissues (Figures 2B and S2A). We next measured exon skipping levels by RT-qPCR, and we found statistically higher levels of exon 23 skipping in muscles from mice treated with both ASO + OEC compared to mice treated with ASO alone. UNC7938 significantly enhanced exon skipping levels in heart ($p = 0.0002$ RM two-way ANOVA, ASO vs. ASO + 7938), with the strongest effect detected at early time points ($p < 0.0001$ at 72 h and $p = 0.0321$ at 1 wk). However, this difference decreased with time, since treatment with ASO alone induced a slower increase, though reaching similar levels as the combined therapy six weeks after the last injection (Figure 2C right). A similar effect was observed in the skeletal muscles

(diaphragm: $p = 0.0022$, triceps: $p = 0.0048$, quadriceps: $p = 0.0179$, RM two-way ANOVA, ASO vs. ASO + 7938) (Figures 2C and S2B).

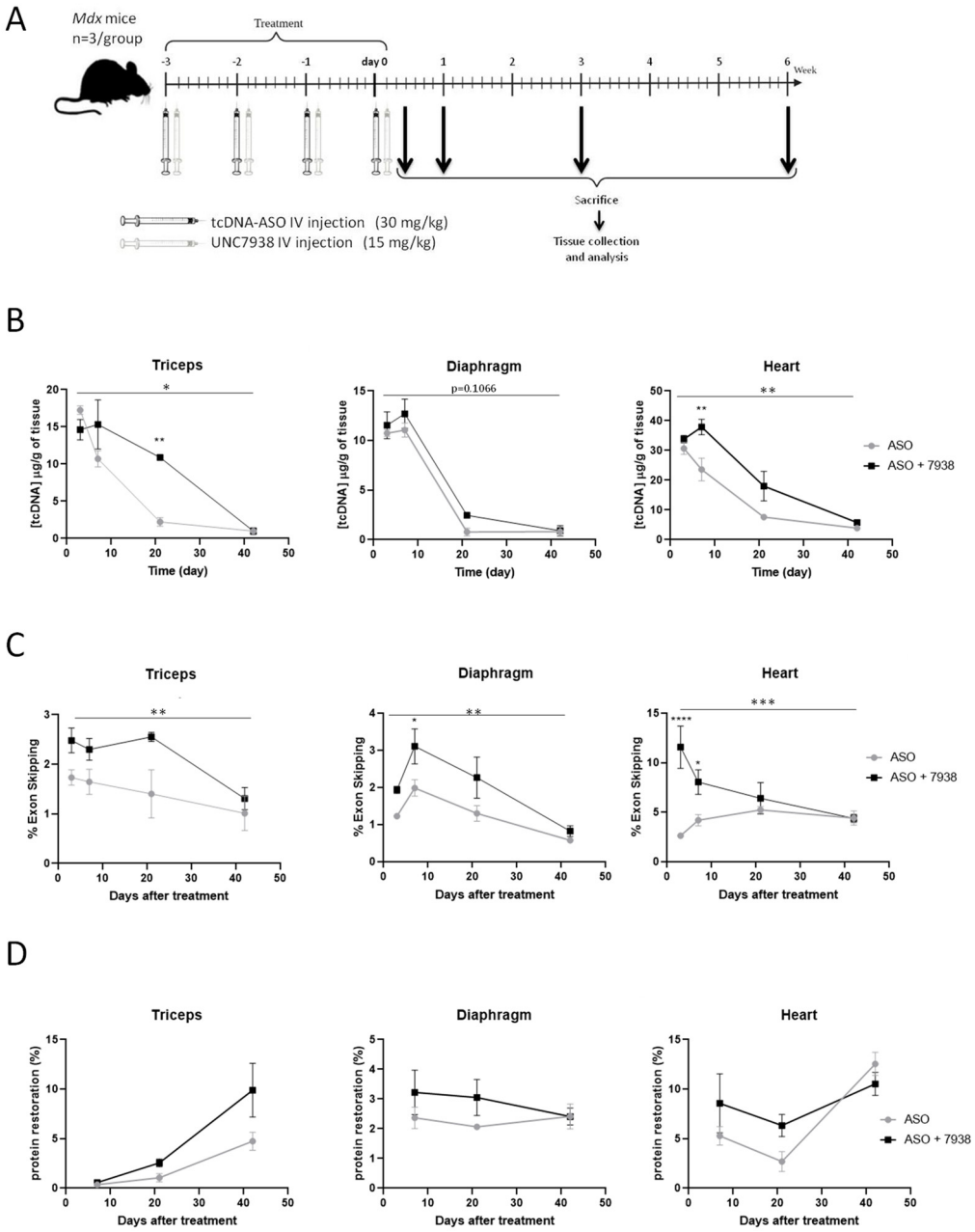

Figure 2. Kinetics of UNC7938 effect on exon skipping therapy in *mdx* mice. (**A**) Schematic representation of the injection protocol with tcDNA-ASO and the OEC UNC7938 in *mdx* mice with the different time points of analysis. (**B**) Quantification of ASO in triceps, diaphragm, and heart at different time points (72 h, one wk, three wks, and six wks) after the last ASO injection. $n = 3$ mice per group and per time point. * $p < 0.05$, ** $p < 0.01$ compared to ASO analyzed by two-way ANOVA. (**C**) Effect of UNC7938 on exon skipping level. qPCR quantification of exon 23 using taqman qPCR in the triceps, diaphragm, and heart at different time points (72 h, one wk, three wks and six wks) after last ASO injection. $n = 3$ mice per group and per time point. * $p < 0.05$, *** $p < 0.001$, **** $p < 0.0001$ compared to ASO analyzed by two-way ANOVA. (**D**) Quantification of dystrophin restoration levels by western blot in treated *mdx* mice at different time points (one wk, three wks, and six wks). Results are expressed as mean ± SEM; $n = 3$ mice per group and per time point.

We next assessed the levels of dystrophin expression in the various muscle tissues following treatment with ASO alone or ASO + 7938. At early time points (up to three weeks), UNC7938 tends to improve dystrophin restoration levels compared to ASO alone. For example, in the heart, the quantity of dystrophin produced is increased by 62% at one week and by 134% at three weeks. However, at later time points (six weeks), levels were similar in both groups of mice (Figures 2D and S2C), making the overall difference (across all time points) not statistically significant ($p = 0.5201$ RM two-way ANOVA, ASO vs. ASO + 7938) (Figure 2D).

3.3. Combination of tcDNA-ASO and UNC7938 Efficiently Restores Dystrophin Expression and Improves Cardiac Function in Mdx Mice

Based on these promising results, in particular in the cardiac muscle, we aim to investigate a longer treatment period in order to assess some functional parameters, such as cardiac function. To lower the potential toxicity of repeated administrations of UNC7938 over three months, we wanted to reduce the number of UNC7938 injections, and we thus investigated whether one monthly injection would achieve similar effects than weekly injections. For that purpose, we performed an additional four-wk study in which UNC7938 was only administered after the fourth ASO injection. Analysis of exon skipping (Figure S3A) and protein restoration levels (Figure S3B) revealed no statistical difference between the two groups (ASO combined with one or four injections of OEC) with a p value of 0.4669 and 0.7915, respectively (analyzed by RM two-way ANOVA).

We, therefore, selected a monthly injection of UNC7938 for the long-term treatment investigating the therapeutic potential of the combination UNC7938 and tcDNA-ASO. Adult *mdx* mice were injected intravenously with 30 mg/kg/week of ASO and with 15 mg/kg/four weeks of UNC7938 over a period of 12 weeks (Figure 3A). ASO tissue concentrations were measured two weeks after the end of the treatment period in muscle tissues and off target organs. As previously observed in the kinetic study, we found slightly higher ASO amounts in muscles from mice co-treated with UNC7938 ($p = 0.0142$ RM two-way ANOVA, ASO vs. ASO + 7938), while there was no difference in spleen, liver, and kidney ($p = 0.2704$ RM two-way ANOVA, ASO vs. ASO + 7938) (Figure 3B). We hypothesized that these higher ASO contents in muscle lysates from mice treated with UNC7938 may result from increased amount of ASO reaching the nucleus, being less prone to elimination/degradation than the ASO fraction trapped in the endosome/lysosome compartments. To investigate this further, we sought to determine the ASO intracellular localization. Cell fractionation was performed on freshly isolated skeletal muscles from *mdx* mice treated with ASO alone or ASO + 7938 for three months, and we validated that the early endosome protein EEA1 was properly enriched in the cytosolic fraction, whereas the H3 histone was enriched in the nuclear fraction (Figure 3C). ASO content was determined in cytosolic and nuclear fractions, and the proportion of ASO detected in the nuclear fraction was higher in mice treated with ASO + 7938 compared to mice treated with ASO alone (Figure 3D).

We next evaluated the impact of UNC7938 on exon skipping and protein restoration levels in *mdx* mice treated for three months. Treatment with UNC7938 alone did not induce any exon skipping or dystrophin restoration (Figure S4). In mice treated with ASO + OEC, we found slightly, but not significantly, increased exon skipping levels in diaphragm and heart ($p = 0.1928$ RM two-way ANOVA, ASO vs. ASO + 7938) (Figure 3E) and significantly higher levels of dystrophin restoration compared to ASO alone ($p = 0.03$ RM two-way ANOVA, ASO vs. ASO + 7938) (Figure 3F). Dystrophin restoration was increased by 31% in the heart, 58% in the diaphragm, and 82% in the triceps (Figure 3F). Dystrophin expression and correct localization were also confirmed by immunostaining performed on muscle cryosections (Figure 3G). Analyses of mean fluorescence intensity revealed a similar increase in dystrophin restoration induced by UNC7938 co-treatment of approximately 33% and 46% in heart and triceps, respectively.

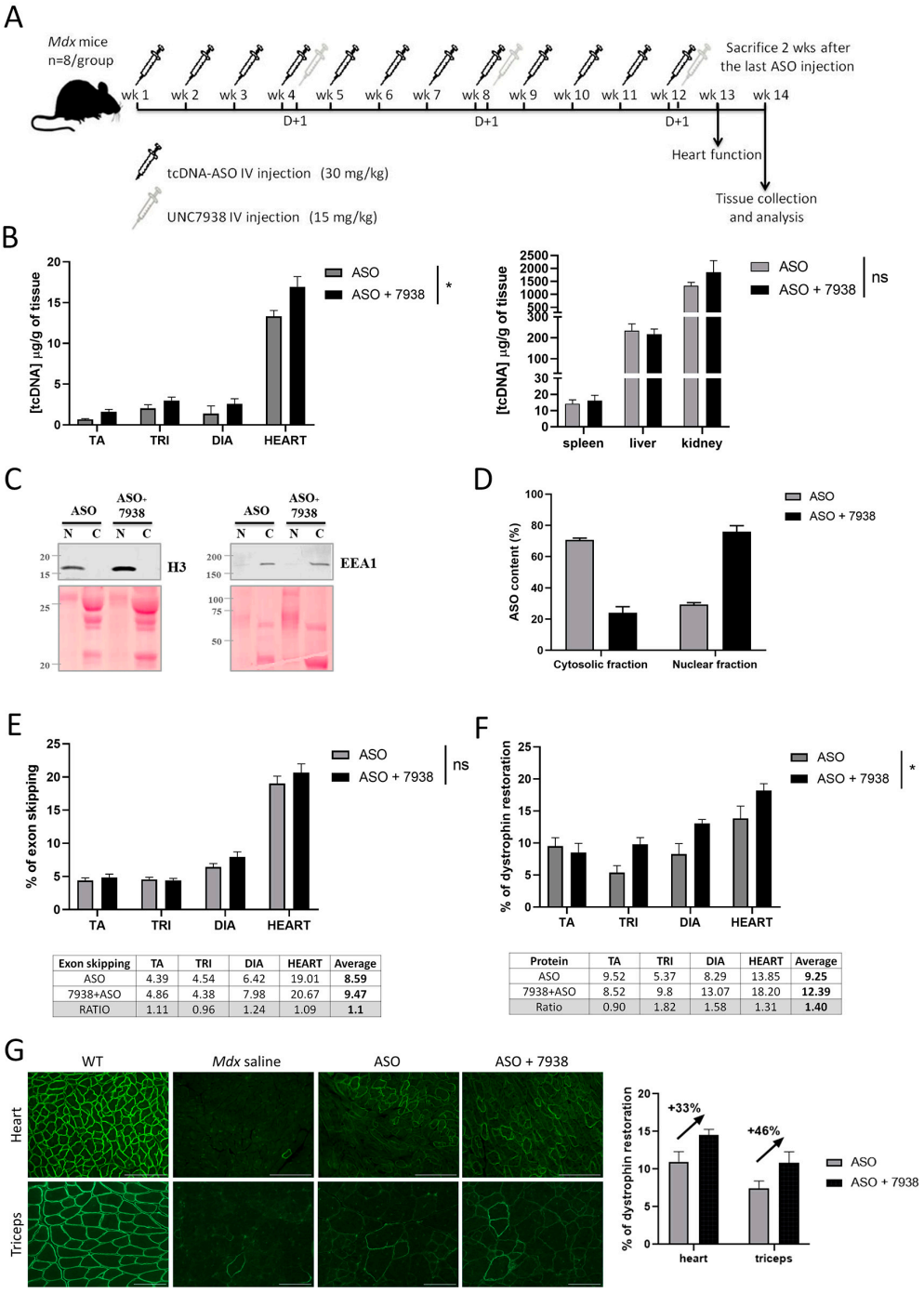

Figure 3. Efficacy of 12-wk combined UNC7938 and ASO treatment in *mdx* mice. (**A**) Schematic representation of the injection protocol with tcDNA-ASO and the OEC UNC7938 in *mdx* mice. (**B**) Quantification of ASO in the different muscles tissues (Tibialis anterior (TA), triceps (TRI), diaphragm (DIA) and heart) (left panel) and accumulation organs, such as spleen, liver and kidney (right panel) after 12 weeks of ASO treatment. $n = 7$ mice per group. (**C**) Subcellular fractionation and intracellular content of ASO following treatment with UNC7938. Western blot analysis of nuclear (*n*) and cytosolic (**C**) fractions isolated from gluteus muscles of *mdx* mice treated with ASO or ASO + 7938. The EEA1 and H3 antibodies are used to confirm cytosolic and nuclear enrichments, respectively. (**D**) Quantification of ASO in the cytosolic and nuclear fractions reveals a higher proportion of ASO in the nuclear fraction when mice have received the combined treatment ASO + 7938 compared to treatment with ASO alone. Results are expressed as means ± SEM; $n = 6$–8 mice per group, and two gluteus muscles are analyzed per mouse. (**E**) Effect of UNC7938 on exon skipping level. qPCR

quantification of exon 23 using taqman qPCR in the different muscle tissues. $n = 7$ mice per group, (**F**) Dystrophin restoration assessed by Western blotting in treated *mdx* mice. Results are expressed as mean ± SEM; $n = 7$ mice per group. (**G**) Dystrophin staining in heart (top) and triceps (bottom). Detection of dystrophin protein (green staining) by immunofluorescence on transverse sections of muscle tissues (triceps and heart) from WT and *mdx* mice treated with saline, ASO, or ASO + UNC7938. Scale bar, 100 µm. Right panel: quantification of the dystrophin intensity staining in heart and triceps, mean fluorescence intensity is normalized to the number of fiber counts. Results are expressed as mean ± SEM; $n = 4$ mice per group. * $p < 0.05$ between ASO and ASO + 7938 analyzed by two-way ANOVA.

Since cardiomyopathy is a typical feature of DMD and that the combined ASO + 7938 treatment appears to be particularly efficient in the heart, we wanted to investigate cardiac function outcomes after these three months of treatment. Echocardiography in six-month-old *mdx* mice revealed a significant reduction of the left ventricular ejection fraction (LVEF), the fractional shortening (FS), and the systolic pulse pressure (PP systole), as well as an increase in the Tei index compared with WT mice (Figure 4). Treatment of *mdx* mice with 30 mg/kg/wk of tcDNA-ASO for 12 weeks improved all parameters, although the differences did not reach statistical significance ($p > 0.05$ analyzed by one-way ANOVA). After co-treatment with UNC7938 however, LVEF, FS, and PP systole were significantly restored ($p = 0.0154$, 0.0153 and 0.0097 compared with *mdx* saline for LVEF, FS, and PP systole, respectively, one-way ANOVA) and no different from WT mice, indicating a normalization of heart function. Only the Tei index was still different between *mdx* control and ASO + 7938 treated mice ($p = 0.3161$), but it was no longer different from the WT mice (p value = 0.0951), demonstrating a promising improvement.

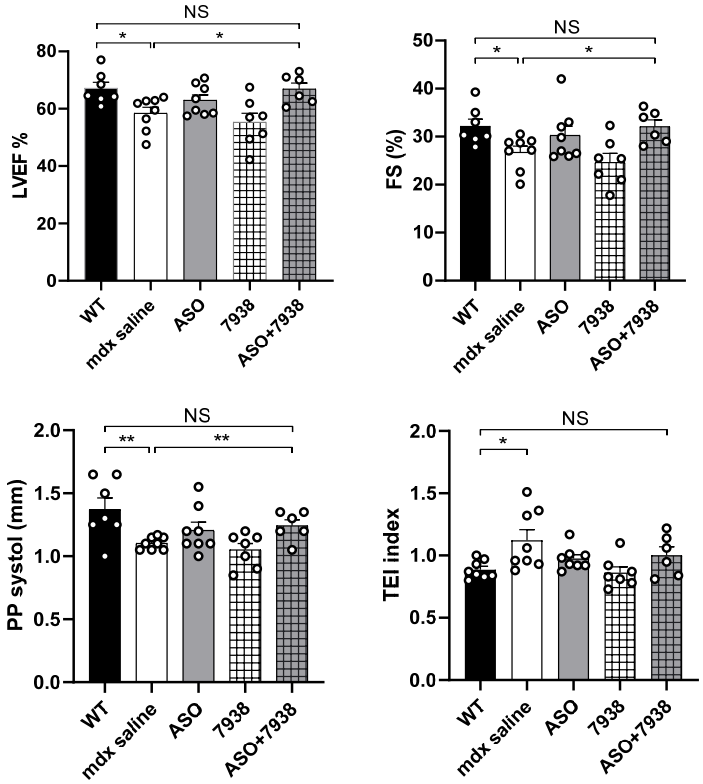

Figure 4. The combination of tcDNA-ASO and UNC7938 treatment improves cardiac function in *mdx* mice. Cardiac function was evaluated by echocardiography in six-month-old mice and the left ventricular ejection fraction (LVEF), the fractional shorting (FS), the systolic pulse pressure (PP systole), and the Tei index are represented. Results are expressed as mean ± SEM; $n = 8$ for WT, *mdx* saline and ASO, $n = 7$ for 7938 and $n = 6$ for ASO + 7938. * $p < 0.05$, ** $p < 0.01$ analyzed by one-way ANOVA.

3.4. Safety Assessment of the Combined Treatment with UNC7938 and tcDNA-ASO

To investigate whether the combination of UNC7938 and tcDNA-ASO induced any potential safety signals, we first analyzed the serum levels of various biomarkers in mice following the different treatments. Quantification of serum creatinine, urea, ALP, bilirubin, and transaminases (ALT and AST) revealed no significant increases in UNC7938 treated *mdx* mice compared to saline treated *mdx* mice (Figure 5A). Only albumin was found to be slightly increased with the combined therapy ASO + 7938. We next evaluated some urinary biomarkers, including albumin and total protein, and found no significant changes in *mdx* mice treated or co-treated with UNC7938.

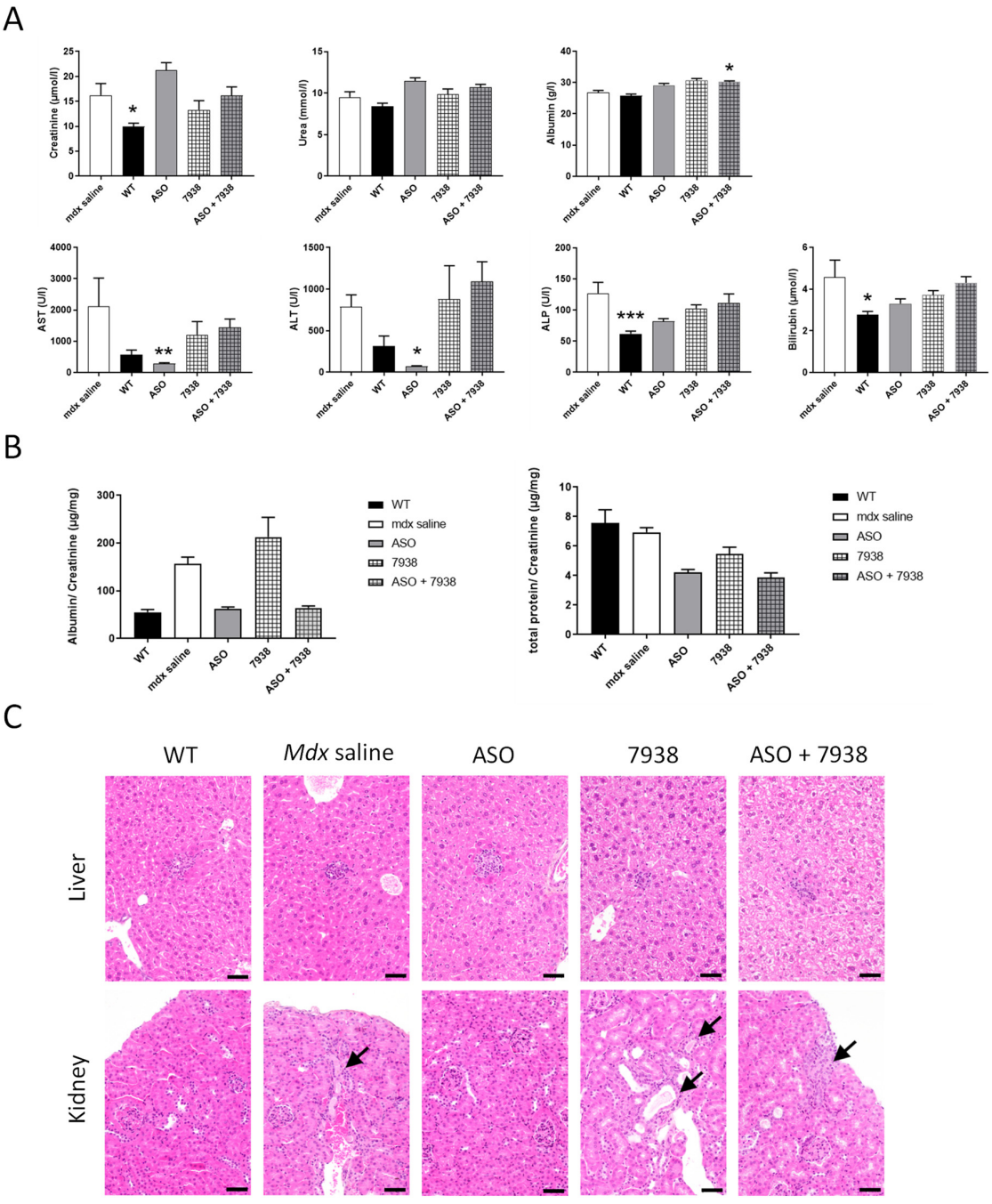

Figure 5. Safety profile of the combined UNC7938 + ASO treatment. (**A**) Quantification of general toxicity biomarkers in the serum: creatinine, urea, albumin, aspartate aminotransferase (AST), alanine aminotransferase (ALT), alkaline phosphatase (ALP), and bilirubin. Results are expressed as mean ± SEM; n = 5–8 mice per group, * $p < 0.05$, ** $p < 0.01$, *** $p < 0.001$ compared to *mdx* saline,

analyzed by Kruskal-Wallis one-way ANOVA. (**B**) Quantification of total protein and albumin levels in the urine of WT and treated *mdx* mice. Urine was collected at the end of the 12-wk treatment. Results are normalized to creatinine levels and expressed as mean ± SEM; n = 5–8 mice per group; p = ns compared to *mdx* saline (one-way ANOVA). (**C**) Histological presentation of wild-type mice and *mdx* mice treated with saline, ASO, UNC7938 or ASO + 7938 for 12 weeks. In liver (upper panel), small foci of inflammatory cell infiltration were scattered in the hepatic parenchyma of all mice in every group. In kidney (lower panel), no lesions or only sporadic changes were observed except for two animals: one UNC7938-treated mouse and one ASO + 7938-treated mouse displayed few minimal areas of tubular degeneration/regeneration (arrows) +/− associated with intraluminal proteinaceous casts and tubular ectasia. Note that one similar area was observed in one *mdx*-saline mouse. Hematoxylin-Eosin-Saffron staining. Scale bar = 50 µm.

Finally, we explored the histopathological profile of liver and kidneys (the two main sentinel organs for drug toxicity) in treated *mdx* mice and WT controls in order to evaluate potential adverse effects of UNC7938, alone or in combined therapy (Figure 5C). In the liver, all mice of every groups (WT, *mdx* saline, *mdx* ASO, *mdx* UNC7938, and *mdx* ASO + 7938) similarly displayed some small scattered foci of inflammatory cell infiltration, sometimes associated with few individual necrotizing hepatocytes. Foci of inflammatory cell infiltration is a common background lesion in the liver of mice. The only other histopathological change observed was very small amount of pigment in Kupffer cells and, less frequently, in Ito cells. This was observed in all animals treated with ASO (ASO alone and combined with 7938). Such a small degree of pigment, without associated cellular reaction or lesion, is generally considered biologically irrelevant. In the kidney, most of the mice displayed no lesion or only unspecific sporadic changes (proteinaceous casts, altered glomeruli, basophilic tubules). Only one UNC7938-treated mouse (out of 7) and one ASO + 7938-treated mouse (out of six) displayed more pronounced lesions than what observed in WT mice and *mdx*-saline-treated mice, consisting of few foci of tubular degeneration and regeneration, sometimes associated with intraluminal proteinaceous casts. Those lesions, very minimal, unspecific, and present in a very low number of animals, were not considered compound-related and significant. Thus, no hepatic or renal toxicity has been associated with UNC7938 when administrated intravenously at the dose of 15 mg/kg/4 week over a period of 12 weeks, alone or in combination with tcDNA-ASO. These findings suggest that the increased effect of ASO observed with OEC unlikely results from toxicity of UNC7938.

4. Discussion

In this study, we aimed to enhance the therapeutic potential of ASO-mediated exon skipping for DMD, which is still currently limited by several challenges. Our previous work has focused on improving the ASO compound itself, and we have optimized a tcDNA-based ASO, free of phosphorothioate linkages and conjugated to a palmitic acid, presenting a significantly higher therapeutic index [6]. Besides the optimization of the ASO compound itself, which may address some of the delivery issues, it is possible to act on cellular mechanisms to facilitate the transport of ASO to their target organelle, i.e., the nucleus in the case of splice switching ASO. The inefficiency of endosomal escape is considered one of the biggest problem preventing the widespread use of RNA therapeutics [24]. The chemical manipulation of the endosome trafficking machinery has been shown to positively impact ASO delivery and pharmacological effects [11]. However, the proof of concept has never been demonstrated for DMD and the exon skipping approach in vivo. In the present study, we therefore evaluated the potential of such a combined therapy in vivo in the *mdx* mouse model of DMD. We selected the UNC7938 compound that was discovered through high throughput screening and shown to selectively release ASO from non-productive entrapment in endosomal compartments [15–17]. UNC7938 was recently shown to potentiate the effect of a peptide conjugated PMO (PPMO) in cystic fibrosis patients cells and in vivo in mouse lung [23], but no data are available in muscle tissues.

In our preliminary four-wk treatment protocol, we showed that the combined ASO + UNC7938 therapy induced significantly higher exon skipping level (1.59 fold-changes) and dystrophin restoration levels (2.75 fold-changes) than ASO therapy alone, especially in the heart. This is in line with our hypothesis that UNC7938 treatment may help ASO to escape the endosome and diffuse to the nucleus where the pre-mRNA targets are located. However, the reasons underlying the higher effect in the heart in contrast with the other muscle tissues remain unclear and may simply be due to the fact that tcDNA is particularly efficient at targeting the heart (i.e., heart is the muscle with the highest content of ASO).

To better characterize the effects of UNC7938, we studied its impact at different time points after injection. The quantification of ASO in different tissues shows that ASO distribution is not affected by UNC7938 at the very early time point (72 h), suggesting that UNC7838 does not impact the distribution of ASO to the different tissues per se. However, ASO tissue content appeared higher between one and three weeks post-treatment in UNC7938 co-treated mice compared to mice treated with ASO alone. This suggests that ASOs are not eliminated as fast when the OEC is administrated, which would be in line with their mechanism of action. Endosomal escape would protect the ASO from a quick degradation/elimination. This was also confirmed by the pharmacological effect of ASO, which was significantly enhanced after the treatment with UNC7938. The effect was once again more important in the heart, which is the muscle tissue with the highest content of ASO, with up to a 4.4-increase in exon skipping levels at early time points. Interestingly, this 'booster' effect faded over time, and ASO content, as well as exon skipping levels, ended up being very similar six weeks after the treatment in both groups of mice (with or without UNC7938). This may be explained by the 'depot effect' occurring in mice treated with ASO alone, in which the ASO trapped in endosomes are actually slowly released over time. This phenomenon characterized by the fact that ~99% of ASO (or RNA therapeutics in general) are typically trapped inside endosomes, may indeed explain why ASO can achieve long pharmacological effects due to a constant low level of leakage into the cytoplasm over weeks or months [24]. Using an OEC, such as UNC7938, may induce a short liberation of ASO from the endosomes, but might, in counterpart, affect the depot effect, which would no longer occur. This could explain why the overall exon skipping levels end up being similar several weeks after the treatment.

We next investigated the impact of UNC7938 on exon skipping therapy over a longer period of time and treated *mdx* mice for 12 weeks, during which they received three injections of UNC7938 (every four weeks). We had previously validated that this dosing regimen induces similar effects that an injection every week. The ASO content in muscle tissues at the end of the 12-wk treatment was slightly higher in mice co-treated with UNC7938 compared to mice treated with ASO alone, as previously observed. In order to determine the ASO intracellular localization, we performed cell fractionation on freshly isolated skeletal muscles from treated *mdx* mice and quantified the ASO content in enriched nuclear and cytoplasmic fractions. Interestingly, we found a higher proportion of ASO in the nuclear fraction of mice treated with ASO + UNC7938 compared to mice treated with ASO alone, which showed a higher proportion of ASO in the cytosolic fraction. We found approximately 71% of ASO in the cytosolic fractions in mice treated with ASO alone, which is higher that the commonly assumed 99% of ASO trapped in endosomes [24]. This may be due to the repeated injections of ASO over 12 weeks, which may help accumulate more ASO in the nucleus than single injections, and also to the timing of analysis. Since muscles were analyzed two weeks after the last injection, a proportion of ASO that was trapped in the endosomal/lysosomal compartment may have already been cleared, thus lowering the quantified cytoplasmic fraction compared to the nuclear fraction. It would be interesting to perform similar fractionation analysis 24 h after a single injection as this may reveal different proportions. However, one should also keep in mind that cell fractionation protocol results in an enrichment of fractions rather that absolutely pure fractions, so it cannot be excluded that the ASO content in the nuclear fraction is slightly overestimated

because of traces of cytosolic fraction. Nonetheless, the consistent higher proportion of ASO found in the nuclear fraction after UNC7938 treatment is in line with its mechanism of action and confirms that freeing ASO from endosomes helps them reach their ultimate target organelle, the nucleus.

The exon skipping levels and restoration of dystrophin protein were also slightly improved in co-treated mice, although to a lesser extent than after the four-wk treatment. This may be explained by the depot effect that would be more noticeable after several weeks. In mice treated with ASO alone, because most of ASO are trapped in endosomes and only slowly released over time, the pharmacological effects may be delayed compared to mice co-treated with UNC7938 in which the released ASO can act more rapidly after the injection.

Considering the clear increase in the amount of ASO detected in the nuclear fraction after treatment with UNC7938, the effect reported on exon skipping levels and dystrophin rescue may appear relatively low. This may be explained by the limited amount of ASO that overall reached the target tissues. Indeed, despite improvement in the design of our tcDNA ASO, conjugated to palmitic acid in order to increase its biodistribution to muscle tissues, the proportion of ASO actually reaching skeletal muscles remains low, as shown in Figure 3B (between 0.6 and 3 µg/g of tissues). This highlights an important consideration to keep in mind—that the full potential of endosomal escape compounds can only be achieved in combination with efficient delivery of ASO to the target tissue.

Nonetheless, co-treatment of ASO + UNC7938 led to higher dystrophin restoration than treatment with ASO alone, especially in the heart (+31%), the diaphragm (+58%), and the triceps (+82%). This was also confirmed by immunostaining, which revealed a correct localization of dystrophin at the subsarcolemmal space of muscle fibers and higher intensity of staining. Given the particularly strong effect observed in the heart with UNC7938 and considering the importance of cardiac dysfunction in DMD patients, we investigated the cardiac function in treated *mdx* mice. *Mdx* mice typically show a progressive development of cardiac defects from six months of age [25,26], and electrocardiography investigations in the control *mdx* mice from this study indeed revealed significant increase in the Tei index, as well as a reduction of the systolic pulse pressure (PP systole) of the left ventricular ejection fraction (LVEF) and of the fractional shortening (FS) compared with WT mice. We found that treatment with ASO alone improved all these parameters, although the difference did not reach statistical significance. It should be noted that we demonstrated, in a previous study, that treatment with tcDNA-ASO alone can significantly improve cardiac function in *mdx* mice after 12 weeks of treatment at 50 mg/kg/wk [6]. In the current study, we selected a lower dose of 30 mg/kg/wk on purpose to be able to detect differences with the UNC7938 co-treated mice. Remarkably, *mdx* mice treated with both tcDNA-ASO and UNC7938 presented statistically significant improvement in all parameters, even reaching WT values (non-statistical difference from WT values for all parameters analyzed). This improved effect over the treatment with ASO alone at this dose likely results from higher dystrophin restoration levels in the heart of co-treated mice, but also from a possible earlier restoration. Indeed, as mentioned previously, one of the advantages of OEC molecules is their capacity to quickly release ASO from endosomes and therefore allow ASO to act more rapidly than those which would be slowly released through the depot effect. This may play an important role for cardiac function, which is more likely to be normalized when dystrophin expression has been restored for longer.

All together, our data confirm the potential of OECs, such as UNC7938, to enhance the therapeutic index of exon-skipping ASO for DMD. Yet, this may counterbalance the depot effect, which classically allows long-term effect of ASO. Ultimately, one should aim at keeping some depot effect while releasing sufficient ASO for rapid effect. Considering the high amount of ASO trapped in endosome compartments, believed to be around 99%, freeing up to 50% would suffice to maintain both rapid and long term effects.

Overall, this work establishes the proof of concept that using small molecules facilitating ASO endosomal escape enhances their efficacy in a DMD mouse model, thus opening new therapeutic avenues for combined therapies.

Supplementary Materials: The following supporting information can be downloaded at: https://www.mdpi.com/article/10.3390/cells12050702/s1, Figure S1: Representation of the tcDNA-ASO used in this study, Figure S2: kinetic efficacy of UNC7938 on exon skipping therapy in *mdx* mice, Figure S3: Comparison between 1 vs. 4 injections of UNC7938 on exon skipping efficacy, Figure S4: Treatment with UNC7938 alone has no effect on dystrophin restoration.

Author Contributions: Conceptualization, F.B. and A.G.; methodology, F.B., R.L.J. and A.G.; formal analysis, F.B., A.F., C.G., T.I., X.P., A.M., T.T. and E.B.; investigation, F.B., A.F., C.G., T.I., X.P., A.M., T.T. and E.B.; writing—original draft preparation, F.B. and A.G.; writing—review and editing, A.G.; supervision, A.G.; funding acquisition, L.G., R.L.J. and A.G. All authors have read and agreed to the published version of the manuscript.

Funding: This research was funded by the Institut National de la santé et la recherche médicale (INSERM), the Association Monegasque contre les myopathies (AMM), the Paris Ile-de-France Region and the Fondation UVSQ. F. Bizot is the recipient of a MESRI thesis fellowship.

Institutional Review Board Statement: The animal study protocol was approved by the Ethics Committee CNREEA47 and the French government (ministère de l'enseignement supérieur et de la recherche, Autorisation APAFiS #6518).

Data Availability Statement: The primary data for this study are available from the authors upon request.

Acknowledgments: We thank the personnel of the plateforme 2CARE for taking care of the animals used in this work.

Conflicts of Interest: LG is co-founder of SQY Therapeutics, which produces tricyclo-DNA oligomers. TT is employee of SQY Therapeutics.

References

1. Fortunato, F.; Rossi, R.; Falzarano, M.; Ferlini, A. Innovative Therapeutic Approaches for Duchenne Muscular Dystrophy. *J. Clin. Med.* **2021**, *10*, 820. [CrossRef]
2. Crooke, S.T.; Wang, S.; Vickers, T.A.; Shen, W.; Liang, X.-H. Cellular Uptake and Trafficking of Antisense Oligonucleotides. *Nat. Biotechnol.* **2017**, *35*, 230–237. [CrossRef]
3. Ono, D.; Asada, K.; Yui, D.; Sakaue, F.; Yoshioka, K.; Nagata, T.; Yokota, T. Separation-related rapid nuclear transport of DNA/RNA heteroduplex oligonucleotide: Unveiling distinctive intracellular trafficking. *Mol. Ther. Nucleic Acids* **2020**, *23*, 1360–1370. [CrossRef]
4. Ferlini, A.; Goyenvalle, A.; Muntoni, F. RNA-Targeted Drugs for Neuromuscular Diseases. *Science* **2021**, *371*, 29–31. [CrossRef]
5. Roberts, T.C.; Langer, R.; Wood, M.J.A. Advances in oligonucleotide drug delivery. *Nat. Rev. Drug Discov.* **2020**, *19*, 673–694. [CrossRef] [PubMed]
6. Relizani, K.; Echevarría, L.; Zarrouki, F.; Gastaldi, C.; Dambrune, C.; Aupy, P.; Haeberli, A.; Komisarski, M.; Tensorer, T.; Larcher, T.; et al. Palmitic acid conjugation enhances potency of tricyclo-DNA splice switching oligonucleotides. *Nucleic Acids Res.* **2021**, *50*, 17–34. [CrossRef] [PubMed]
7. Juliano, R.L. Intracellular Trafficking and Endosomal Release of Oligonucleotides: What We Know and What We Don't. *Nucleic Acid Ther.* **2018**, *28*, 166–177. [CrossRef] [PubMed]
8. Liang, X.-H.; Sun, H.; Shen, W.; Crooke, S.T. Identification and characterization of intracellular proteins that bind oligonucleotides with phosphorothioate linkages. *Nucleic Acids Res.* **2015**, *43*, 2927–2945. [CrossRef]
9. Liang, X.-H.; Sun, H.; Hsu, C.-W.; Nichols, J.G.; A Vickers, T.; De Hoyos, C.L.; Crooke, S.T. Golgi-endosome transport mediated by M6PR facilitates release of antisense oligonucleotides from endosomes. *Nucleic Acids Res.* **2019**, *48*, 1372–1391. [CrossRef]
10. Liang, X.-H.; Sun, H.; Nichols, J.G.; Allen, N.; Wang, S.; Vickers, T.A.; Shen, W.; Hsu, C.-W.; Crooke, S.T. COPII vesicles can affect the activity of antisense oligonucleotides by facilitating the release of oligonucleotides from endocytic pathways. *Nucleic Acids Res.* **2018**, *46*, 10225–10245. [CrossRef]
11. Juliano, R.L. Chemical Manipulation of the Endosome Trafficking Machinery: Implications for Oligonucleotide Delivery. *Biomedicines* **2021**, *9*, 512. [CrossRef] [PubMed]
12. Langel, Ü. Cell-Penetrating Peptides and Transportan. *Pharmaceutics* **2021**, *13*, 987. [CrossRef]

13. Hammond, S.M.; Aartsma-Rus, A.; Alves, S.; Borgos, S.E.; Buijsen, R.A.M.; Collin, R.W.J.; Covello, G.; Denti, M.A.; Desviat, L.R.; Echevarría, L.; et al. Delivery of oligonucleotide-based therapeutics: Challenges and opportunities. *EMBO Mol. Med.* **2021**, *13*, e13243. [CrossRef]
14. Gagliardi, M.; Ashizawa, A.T. The Challenges and Strategies of Antisense Oligonucleotide Drug Delivery. *Biomedicines* **2021**, *9*, 433. [CrossRef]
15. Juliano, R.L.; Wang, L.; Tavares, F.; Brown, E.G.; James, L.; Ariyarathna, Y.; Ming, X.; Mao, C.; Suto, M. Structure–activity relationships and cellular mechanism of action of small molecules that enhance the delivery of oligonucleotides. *Nucleic Acids Res.* **2018**, *46*, 1601–1613. [CrossRef] [PubMed]
16. Wang, L.; Ariyarathna, Y.; Ming, X.; Yang, B.; James, L.I.; Kreda, S.M.; Porter, M.; Janzen, W.; Juliano, R.L. A Novel Family of Small Molecules that Enhance the Intracellular Delivery and Pharmacological Effectiveness of Antisense and Splice Switching Oligonucleotides. *ACS Chem. Biol.* **2017**, *12*, 1999–2007. [CrossRef] [PubMed]
17. Yang, B.; Ming, X.; Cao, C.; Laing, B.; Yuan, A.; Porter, M.A.; Hull-Ryde, E.A.; Maddry, J.; Suto, M.; Janzen, W.P.; et al. High-throughput screening identifies small molecules that enhance the pharmacological effects of oligonucleotides. *Nucleic Acids Res.* **2015**, *43*, 1987–1996. [CrossRef] [PubMed]
18. Bus, T.; Traeger, A.; Schubert, U.S. The great escape: How cationic polyplexes overcome the endosomal barrier. *J. Mater. Chem. B* **2018**, *6*, 6904–6918. [CrossRef]
19. Ming, X.; Carver, K.; Fisher, M.; Noel, R.; Cintrat, J.-C.; Gillet, D.; Barbier, J.; Cao, C.; Bauman, J.; Juliano, R.L. The small molecule Retro-1 enhances the pharmacological actions of antisense and splice switching oligonucleotides. *Nucleic Acids Res.* **2013**, *41*, 3673–3687. [CrossRef]
20. Relizani, K.; Griffith, G.; Echevarría, L.; Zarrouki, F.; Facchinetti, P.; Vaillend, C.; Leumann, C.; Garcia, L.; Goyenvalle, A. Efficacy and Safety Profile of Tricyclo-DNA Antisense Oligonucleotides in Duchenne Muscular Dystrophy Mouse Model. *Mol. Ther. Nucleic Acids* **2017**, *8*, 144–157. [CrossRef]
21. Echevarria, L.; Aupy, P.; Relizani, K.; Bestetti, T.; Griffith, G.; Blandel, F.; Komisarski, M.; Haeberli, A.; Svinartchouk, F.; Garcia, L.; et al. Evaluating the Impact of Variable Phosphorothioate Content in Tricyclo-DNA Antisense Oligonucleotides in a Duchenne Muscular Dystrophy Mouse Model. *Nucleic Acid Ther.* **2019**, *29*, 148–160. [CrossRef]
22. Zhang, A.; Uaesoontrachoon, K.; Shaughnessy, C.; Das, J.R.; Rayavarapu, S.; Brown, K.J.; Ray, P.E.; Nagaraju, K.; Anker, J.N.V.D.; Hoffman, E.P.; et al. The use of urinary and kidney SILAM proteomics to monitor kidney response to high dose morpholino oligonucleotides in the mdx mouse. *Toxicol. Rep.* **2015**, *2*, 838–849. [CrossRef] [PubMed]
23. Dang, Y.; van Heusden, C.; Nickerson, V.; Chung, F.; Wang, Y.; Quinney, N.L.; Gentzsch, M.; Randell, S.H.; Moulton, H.M.; Kole, R.; et al. Enhanced delivery of peptide-morpholino oligonucleotides with a small molecule to correct splicing defects in the lung. *Nucleic Acids Res.* **2021**, *49*, 6100–6113. [CrossRef]
24. Dowdy, S.F.; Setten, R.L.; Cui, X.-S.; Jadhav, S.G. Delivery of RNA Therapeutics: The Great Endosomal Escape! *Nucleic Acid Ther.* **2022**, *32*, 361–368. [CrossRef]
25. Quinlan, J.G.; Hahn, H.S.; Wong, B.L.; Lorenz, J.N.; Wenisch, A.S.; Levin, L.S. Evolution of the mdx mouse cardiomyopathy: Physiological and morphological findings. *Neuromuscul. Disord.* **2004**, *14*, 491–496. [CrossRef] [PubMed]
26. Spurney, C.F.; Knoblach, S.; Pistilli, E.E.; Nagaraju, K.; Martin, G.R.; Hoffman, E. Dystrophin-deficient cardiomyopathy in mouse: Expression of Nox4 and Lox are associated with fibrosis and altered functional parameters in the heart. *Neuromuscul. Disord.* **2008**, *18*, 371–381. [CrossRef] [PubMed]

cells

MDPI

Supplementary material

Oligonucleotide enhancing compound increases tricyclo-DNA mediated exon-skipping efficacy in the mdx mouse model

Flavien Bizot[1], Abdallah Fayssoil[1,2], Cécile Gastaldi[3], Tabitha Irawan[1], Xaysongkhame Phongsavanh[1], Arnaud Mansart[4], Thomas Tensorer[5], Elise Brisebard[6], Luis Garcia[1], Rudolph L Juliano[7], and Aurélie Goyenvalle[1,*]

1 Université Paris-Saclay, UVSQ, Inserm, END-ICAP, 78000 Versailles, France
2 Raymond Poincaré Hospital, APHP, Garches, France.
3 Centre Scientifique de Monaco, LIA-BAHN, Monaco, Monaco
4 Université Paris-Saclay, UVSQ, INSERM U1173, 2I, Montigny-le-Bretonneux, France
5 SQY Therapeutics, UVSQ, END-ICAP, 78180 Montigny le Bretonneux, France.
6 INRAE Oniris, UMR 703 PAnTher, Nantes, France
7 Initos Pharmaceuticals LLC, UNC Eshelman School of Pharmacy, University of North Carolina, Chapel Hill, North Carolina
* Correspondence: aurelie.goyenvalle@uvsq.fr; Tel.: +33170429432

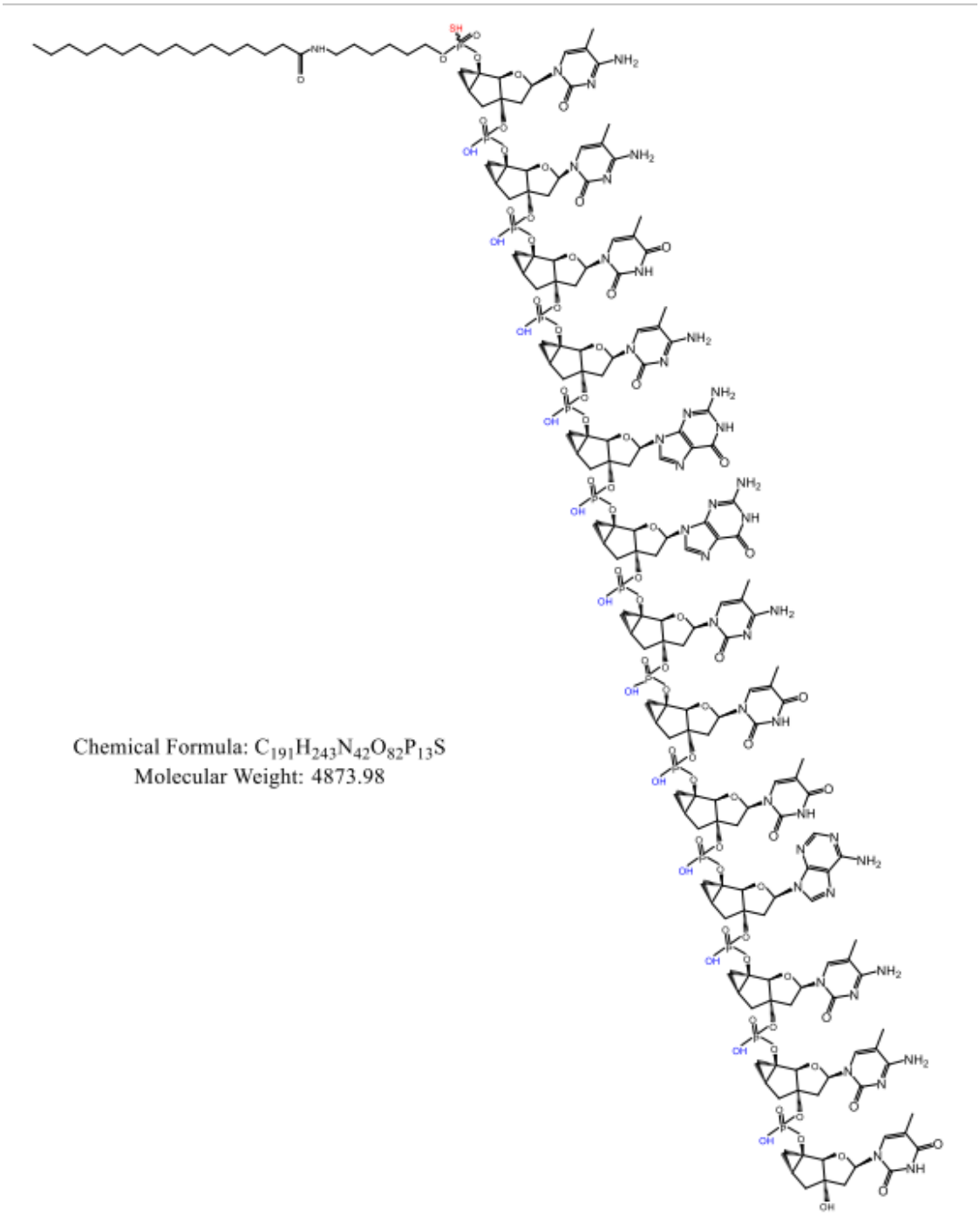

Figure S1. Representation of the tcDNA-ASO targeting the donor splice site of exon 23 of the mouse dystrophin pre-mRNA used in this study. Palmitic acid is conjugated at the 5′end of tcDNA-PO via a C6-amino linker and a phosphorothioate bond.

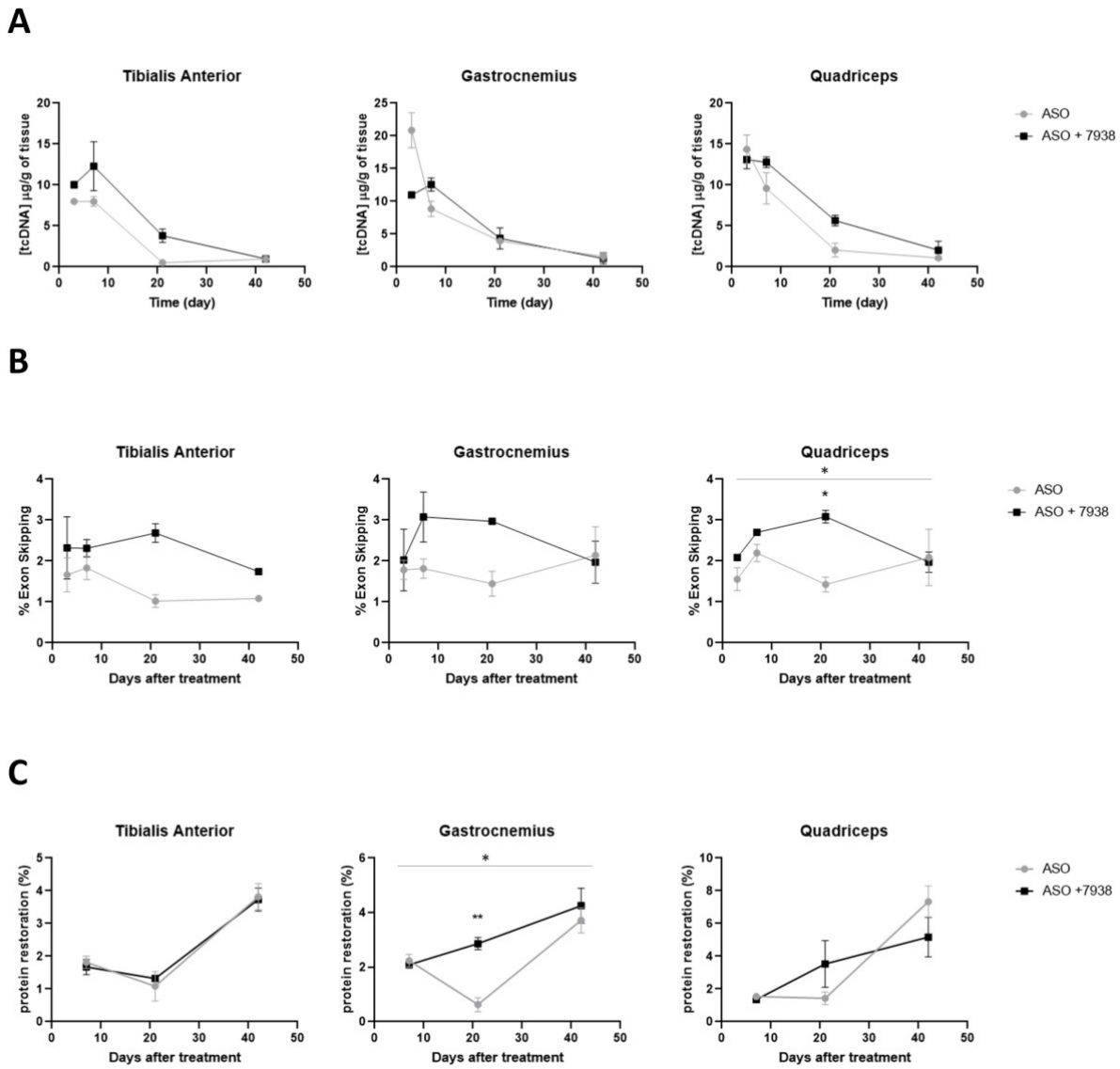

Figure S2. kinetic efficacy of UNC7938 on exon skipping therapy in *mdx* mice. (A) Quantification of ASO in tibialis anterior, gastrocnemius and quadriceps at different time points (72h, 1 week, 3 weeks and 6 weeks) after the last ASO injection. N=3 mice per group and per time point. (B) Effect of UNC7938 on exon skipping level. qPCR quantification of exon 23 skipping using taqman qPCR in the tibialis anterior, gastrocnemius and quadriceps at different time points (72h, 1 week, 3 weeks and 6 weeks) after last ASO injection. N=3 mice per group and per time point. *p<0.05, compared to ASO analyzed by two-way ANOVA. (C) Quantification of dystrophin restoration levels in treated mdx mice at different time points (1 week, 3 weeks and 6 weeks). N=3 mice per group and per time point. *p<0.05, **p<0.01 compared to ASO analyzed by two-way ANOVA.

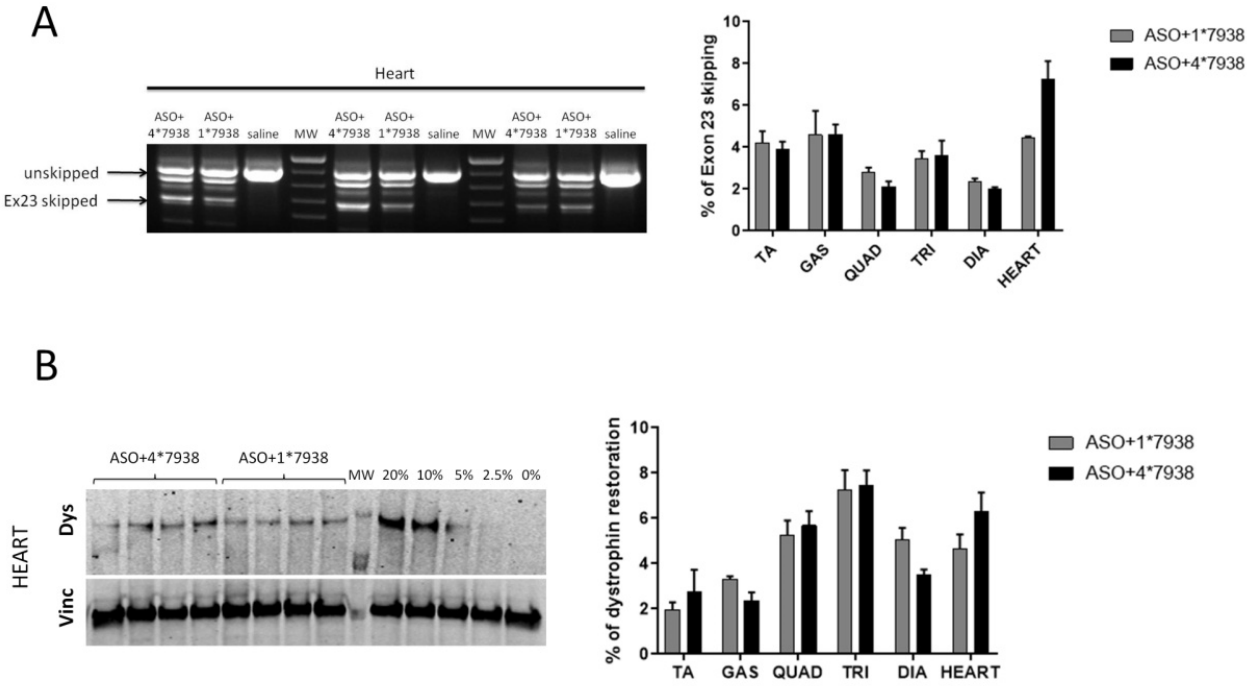

Figure S3. Comparison between 1 vs 4 injections of UNC7938 on exon skipping efficacy (A) Effect of the number of UNC7938 injections on exon skipping level. Left panel: example of the visualization of exon 23 skipping on gel in the heart of *mdx* mice treated with saline, ASO+1*7938 or ASO+4*7938. PCR amplifications between exons 20 to 26 are loaded on a 1.5% agarose gel. The top band corresponds to the unskipped transcript and the lower band to the exon 23 skipped one. Right panel: qPCR quantification of exon 23 skipping using taqman qPCR in the different muscle tissues. Tibialis anterior (TA), gastrocnemius (GAS), quadriceps (QUAD), triceps (TRI), diaphragm (DIA) and heart. Results are expressed as mean ± SEM; N=4 mice per group. P = 0.4669 between ASO+1*7938 or ASO+4*7938 analyzed by RM two-way ANOVA. (B) Quantification of dystrophin restoration level in treated *mdx* mice. A typical dystrophin western blot obtained for the heart is showed in the left panel, with vinculin used for normalization. A standard curve made from pooled lysates from C57BL10 (WT) and *mdx* control for each tissue is loaded for quantification (0%, 2.5%, 5%, 10% and 20% of WT). Right panel: quantification of dystrophin restoration using the Empiria Studio software. Results are expressed as mean ± SEM; N=3 mice per group. P = 0.7915 between ASO+1*7938 or ASO+4*7938 analyzed by RM two-way ANOVA.

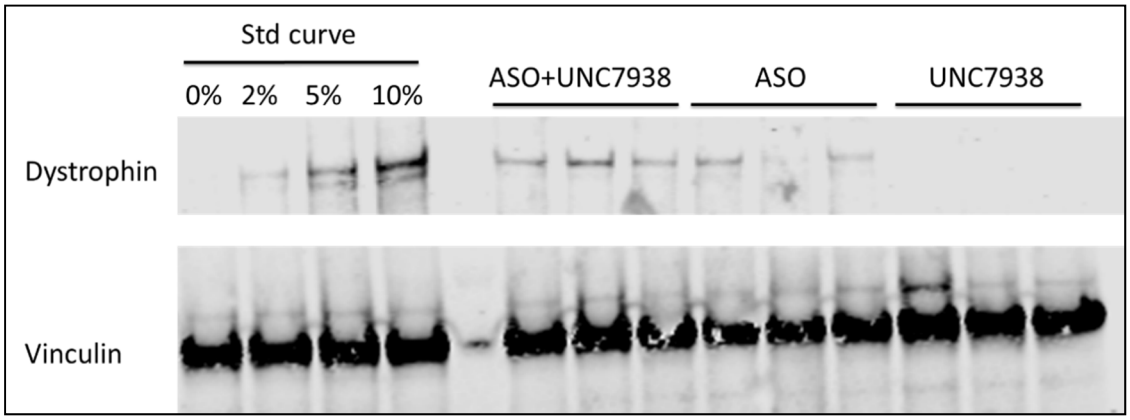

Figure S4. Treatment with UNC7938 alone has no effect on dystrophin restoration. A typical dystrophin western blot obtained for the diaphragm is showed, with vinculin used for normalization. A standard curve made from pooled lysates from C57BL10 (WT) and *mdx* control for each tissue is loaded for quantification (0%, 2%, 5% and 10% of WT).

3 INCREASE THE AMOUNT OF TARGET MRNA

Context:

As mentioned previously, the therapeutic potential of exon-skipping therapy is limited by several challenges including the biodistrubtion to target tissues and proper localization of ASO in the nucleus, limitations that we aimed to address with the studies mentioned above. Another less recognized challenge in the context of DMD is the reduced expression of the dystrophin transcript and the strong 5'-3' imbalance in mutated transcripts. We therefore hypothesized that increasing histone acetylation using histone deacetylase inhibitors (HDACi) could correct the transcript imbalance, offering more available pre-mRNA target and ultimately increase dystrophin restoration.

Methods:

Mdx mice were co-treated with TC-DNA ASO (intravenous, 30mg/kg/week) and HDACi. Three HDACi were tested: valproic acid (intraperitoneal, 500 mg/kg/day), EX527 (intraperitoneal, 2 mg/kg/day) and givinostat (gavage, 10 mg/kg/day). All HDACi were administrated 5 times per weeks.

After 4 weeks of treatment mice were sacrificed and tissues were collected to analyze the effects of HDACi on RNA production and ASO's distribution and efficacy. Some serum biomarkers were quantified to ensure that the co-treatment was not toxic. In parallel, our collaborators from the group of Annemieke Aartsma-Rus at Leiden University medical center investigated the effect of valproic acid on DMD chromatin organization and expression *in vitro*.

A long term study of 12 weeks was then performed to confirm the effects of valproic acid on ASO efficacy. (This follow-up study is not included in the published manuscript inserted below but described separately afterwards). Two weeks after the last injection of TC-DNA, muscle function was monitored by measuring tibialis anterior muscle contraction *in-situ* in response to nerve stimulation.

Main Results

Significantly higher levels of dystrophin restoration were obtained after 4 weeks of co-treatment with givinostat and valproic acid compared to mice treated with ASO alone.

An increase in H3K9 acetylation was observed in human myocytes after treatment with valproic acid.

In the long term study with valproic acid, we also found increased levels of dystrophin restoration confirming the capacity of valproic acid to improve ASO efficacy. This study also showed that the combined therapy is able to restore the muscle function in *mdx* mice.

Conclusion:

These findings indicate that HDACi can improve the therapeutic potential of exon skipping approaches offering promising perspectives for the treatment of DMD.

Molecular Therapy
Nucleic Acids
Original Article

Histone deacetylase inhibitors improve antisense-mediated exon-skipping efficacy in *mdx* mice

Flavien Bizot,[1,4] Remko Goossens,[2,4] Thomas Tensorer,[3] Sergei Dmitriev,[3] Luis Garcia,[1] Annemieke Aartsma-Rus,[2] Pietro Spitali,[2] and Aurélie Goyenvalle[1]

[1]Université Paris-Saclay, UVSQ, Inserm, END-ICAP, 78000 Versailles, France; [2]Department of Human Genetics, Leiden University Medical Center, 2333 ZA Leiden, the Netherlands; [3]SQY Therapeutics, UVSQ, END-ICAP, 78180 Montigny le Bretonneux, France

Antisense-mediated exon skipping is one of the most promising therapeutic strategies for Duchenne muscular dystrophy (DMD), and some antisense oligonucleotide (ASO) drugs have already been approved by the US FDA despite their low efficacy. The potential of this therapy is still limited by several challenges, including the reduced expression of the dystrophin transcript and the strong 5′-3′ imbalance in mutated transcripts. We therefore hypothesize that increasing histone acetylation using histone deacetylase inhibitors (HDACi) could correct the transcript imbalance, offering more available pre-mRNA target and ultimately increasing dystrophin rescue. Here, we evaluated the impact of such a combined therapy on the *Dmd* transcript imbalance phenomenon and on dystrophin restoration levels in *mdx* mice. Analysis of the *Dmd* transcript levels at different exon-exon junctions revealed a tendency to correct the 5′-3′ imbalance phenomenon following treatment with HDACi. Significantly higher levels of dystrophin restoration (up to 74% increase) were obtained with givinostat and valproic acid compared with mice treated with ASO alone. Additionally, we demonstrate an increase in H3K9 acetylation in human myocytes after treatment with valproic acid. These findings indicate that HDACi can improve the therapeutic potential of exon-skipping approaches, offering promising perspectives for the treatment of DMD.

INTRODUCTION

Duchenne muscular dystrophy (DMD) is a genetic, X-linked, muscle-wasting disease caused by different types of mutations in the *DMD* gene, which mostly disrupt the open reading frame and thus lead to an absence of functional dystrophin protein. Becker muscular dystrophy (BMD), which is also caused by mutations in the *DMD* gene, results in a variable but milder phenotype. In contrast to DMD mutations, BMD deletions do not disrupt the open reading frame, allowing translation of a partially truncated but functional dystrophin. Antisense-mediated exon skipping for DMD aims to eliminate one or several exons from the mRNA, by masking key splicing sites with antisense oligonucleotides (ASOs) during the pre-mRNA splicing process. The resulting mRNA will have a restored reading frame and therefore allow the expression of a BMD-like dystrophin. Several ASO-based exon-skipping drugs have already been approved by the US Food and Drug Administration for the treatment of DMD (eteplirsen, golodirsen, viltolarsen, and casimersen targeting exons 51, 53, 53, and 45).[1] Approval was based on safety and increased dystrophin expression in muscle biopsies of treated patients at relatively low levels (up to ∼5.9% following exon 53 skipping).[2] Recent studies suggest delayed loss of ambulation and pulmonary decline following long-term eteplirsen treatment compared with a natural history cohort,[3] and placebo-controlled clinical trials are still ongoing to assess functional outcomes for each of the compounds. However, the efficacy of exon-skipping strategies is still limited by several challenges, leaving much room for improvement.

One of the most recognized challenges of ASO-mediated exon skipping is the delivery of ASOs to the target tissues.[4,5] Many efforts are focusing on improving this delivery, notably through the development of alternative chemistries or various conjugates.[6,7,8] Among these, some of us have been working with one particular chemistry named tricyclo-DNA (tcDNA), and we recently demonstrated that conjugation of palmitic acid with tcDNA (palm-tcDNA) significantly enhances their therapeutic potential.[9] Many of these newly developed compounds are currently or soon to be evaluated in clinical trials. However, another less recognized challenge limits the effect of ASOs independently of their delivery properties: the limited amount of target mRNA. Indeed, transcriptional studies have shown that dystrophin mRNA levels are reduced in muscle when a mutation is present.[10,11] This reduction was thought to be caused by nonsense-mediated decay (NMD), which breaks down transcripts with premature termination codons (PTCs) due to nonsense mutations or

Received 4 August 2022; accepted 17 November 2022;
https://doi.org/10.1016/j.omtn.2022.11.017.

[4]These authors contributed equally

Correspondence: Pietro Spitali, PhD, Department of Human Genetics, Leiden University Medical Center, 2333 ZA Leiden, the Netherlands.
E-mail: p.spitali@lumc.nl
Correspondence: Aurélie Goyenvalle, PhD, Université Paris-Saclay, UVSQ, Inserm, END-ICAP, 78000 Versailles, France.
E-mail: aurelie.goyenvalle@uvsq.fr

frameshifts.[12] However, our recent work has shown that inhibition of NMD similarly impacts wild-type (WT) and dystrophic DMD transcript levels, suggesting that NMD does not specifically affect mutated DMD transcripts.[13] More importantly, this work confirmed previous findings describing a strong 5′-3′ transcript imbalance in mutated transcripts.[13,14] Reduced transcript accumulation toward the 3′ end was also observed in healthy controls,[15] suggesting that the locus is transcriptionally challenging. This is not surprising given that the *DMD* gene is one of the largest genes in the human genome, spanning 2.2 Mb. However, PTC-containing transcripts appear to be even more affected. The reduced transcriptional output at the DMD locus in the presence of PTC appeared to be at least partly due to a chromatin conformation less prone to transcription in *mdx* mice compared with WT mice. Indeed we previously showed an increased expression of histone methyltransferases, which are responsible for the methylation of lysine 9 on histone 3 (H3K9me3). This increase was mirrored by elevated levels of H3K9me3 in *mdx* mouse muscle compared with healthy controls and an increase of H3K9me3 modification along the *Dmd* locus.[13] H3K9 methylation is a transcriptionally repressive mark that competes with the transcriptional permissive H3K9 acetylation. Hence, promoting permissive chromatin conformation via, for example, H3K9 acetylation could counteract the effects of increased H3K9 methylation observed in the presence of PTC and increase dystrophin pre-mRNA availability. We hypothesize here that increasing histone acetylation (and therefore decreasing histone methylation) using histone deacetylase inhibitors (HDACi) could correct the transcript imbalance, offering more available pre-mRNA target for exon-skipping approaches.

HDACi have previously been studied in the context of DMD models but not for their effect on dystrophin transcript synthesis. Pharmacological blockade of histone deacetylases (HDACs) has been shown to decrease fibrosis and promote compensatory regeneration in the *mdx* skeletal muscle through follistatin upregulation.[16–18] These studies have led to the clinical evaluation of the HDACi givinostat, which is currently in a phase III clinical trial for DMD treatment (www.clinicaltrials.gov, clinical trial identifier NCT02851797). Positive topline data from this phase III trial were announced at the Annual PPMD Conference on June 25th, 2022, showing the beneficial effect of givinostat in DMD patients (https://www.businesswire.com/news/home/20220625005001/en/Italfarmaco-Group-Announces-Positive-Topline-Data-from-Phase-3-Trial-Showing-Beneficial-Effect-of-Givinostat-in-Patients-with-Duchenne-Muscular-Dystrophy). We hypothesize that on top of these beneficial effects, HDACi could significantly improve the effect of exon-skipping strategies by increasing the level of *Dmd* transcript. In this study, we have evaluated the impact of such a combined therapy on the *Dmd* transcript imbalance phenomenon and on dystrophin restoration levels both *in vivo* in *mdx* mice and *in vitro* in human myocytes. Adult *mdx* mice were treated with different HDACi: givinostat (a pan HDACi), valproic acid (VPA; inhibitor of class I/II), or EX527 (inhibitor of class III), and also received ASOs aimed at skipping exon 23. Mice receiving the combined therapy with givinostat and VPA showed significantly higher levels of dystrophin restoration compared with mice treated with ASO alone. Additionally, we demonstrate increased H3K9 acetylation along the DMD locus in human myocytes.

RESULTS

Effect of HDAC inhibitors on *Dmd* mRNA levels in *mdx* mice

We first studied *Dmd* gene expression at several exon-exon junctions in skeletal and cardiac muscles of 3-month-old *mdx* mice and their WT controls (C57/BL10 mice). The quantitative PCR (qPCR) data obtained from triceps, diaphragm, and heart revealed amounts of *Dmd* transcripts that were significantly lower in all *mdx* muscles compared with WT controls ($p = 0.0099$ for triceps, $p < 0.0001$ for diaphragm, and $p = 0.0006$ for heart) (Figure 1A). No difference was found at the exon junction 4-5, suggesting that initiation of transcription is not altered in *mdx* mice (triceps 100%, diaphragm 105%, and heart 82% compared with WT expression). However, *Dmd* expression was markedly lower in the distal part of the gene in *mdx* muscles where expression levels at the exon 65-66 junction were only 21% in triceps, 38% in diaphragm, and 31% in heart compared with WT expression. These results confirm the strong 5′-3′ transcript imbalance previously described in *mdx* mice due to the nonsense mutation in exon 23. A 5′-3′ imbalance was also detected in WT mice as shown by the absolute quantification of *Dmd* transcripts (Figure S1A), yet slopes were significantly steeper in *mdx* mice.

To investigate whether this imbalance previously linked to epigenetic effects could be counterbalanced by histone acetylation, we treated *mdx* mice with HDACi for 5 weeks. *Mdx* mice received daily administration of givinostat (10 mg/kg by oral gavage 5 days/week[13]), VPA (500 mg/kg intraperitoneally [i.p.] 5 days/week[19]), EX527 (2 mg/kg i.p. 5 days/week[20]) or saline (i.p. 5 days/week).

The quantification of *Dmd* gene expression at several exon-exon junctions by qPCR in muscles from HDACi-treated mice revealed a tendency for some HDACi to increase *Dmd* expression levels, such as EX527 in the proximal exon junctions (4-5 and 24) for all muscles or givinostat across all exon junctions in the diaphragm. However, when we compared all of the exon junctions per treatment with saline, no significant differences emerged ($p = 0.8554$ in heart, $p = 0.6694$ in triceps, and $p = 0.5552$ in diaphragm) (Figure 1B). The *Dmd* gene expression at several exon-exon junctions can also be represented by the regression line (Figure S1B), allowing better visualization of the overall expression levels.

Given that the single treatment with either HDACi (Figure 1B) or ASOs[14] did not correct the reduction at the 3′ end, we sought to investigate the potential effect of the combination treatment with HDACi and exon-skipping therapy. Therefore, we combined HDACi and palm-tcDNA ASO treatments, as this ASO could efficiently target the donor splice site of mouse Dmd exon 23.[9] After a first week of HDACi treatment, *mdx* mice were treated once weekly with 25 mg/kg ASO for a total of 4 weeks as presented in Figure 1C. Two weeks after the last ASO injection, tissues were analyzed and exon 23 skipping levels were quantified by TaqMan qRT-PCR (Figure 1D). Four injections of ASO induced exon 23 skipping levels

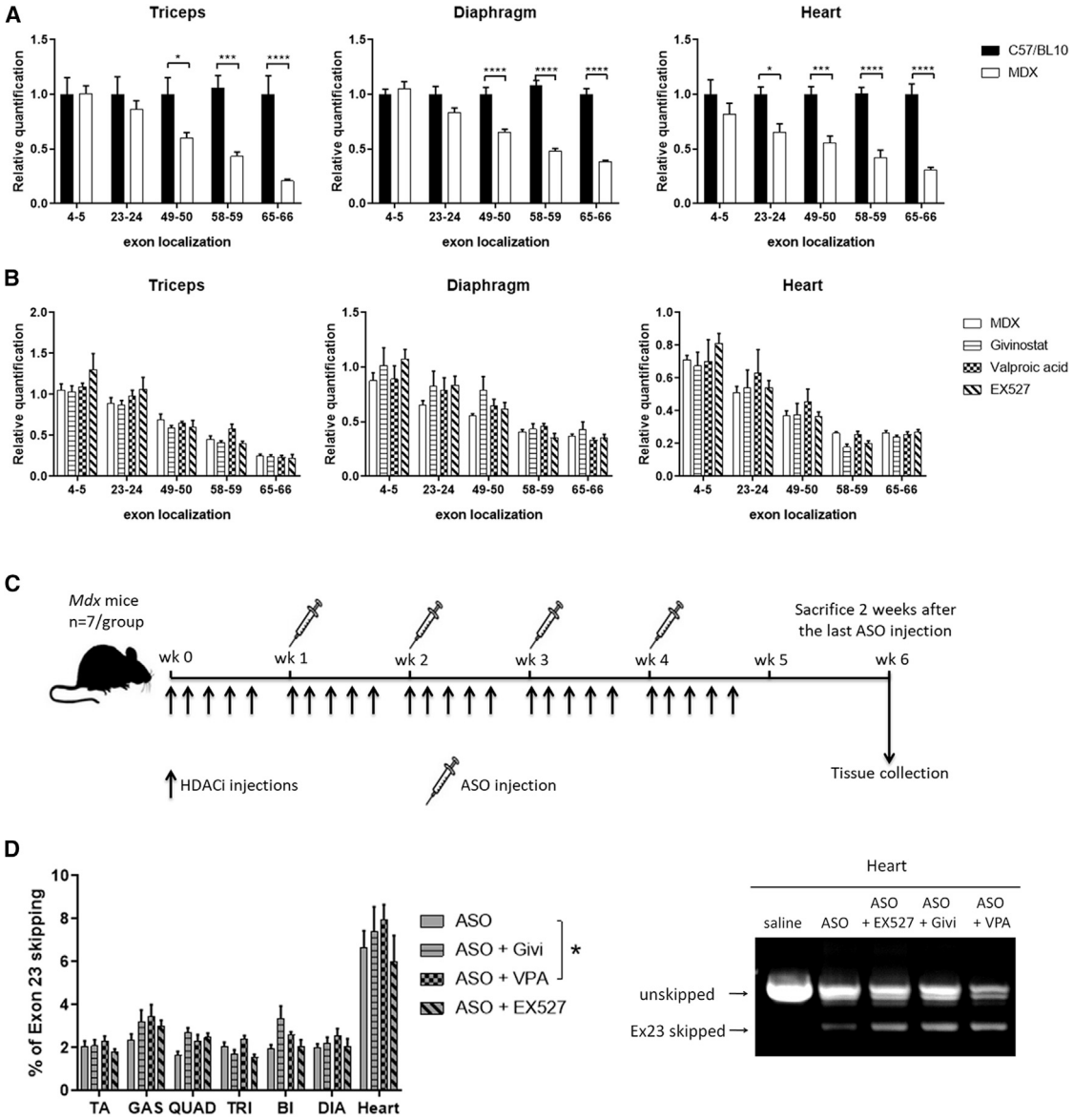

Figure 1. Effect of HDACi on *Dmd* transcript levels and exon-skipping efficacy in *mdx* mice

(A) Relative expression of *Dmd* transcript levels obtained in triceps, diaphragm, and heart for several exon-exon junctions along the *Dmd* gene in *mdx* and C57Bl10 mice (n = 6 for C57Bl10 and n = 9 for *mdx* mice) ($p = 0.0099$ in triceps, $p < 0.0001$ in diaphragm, and $p = 0.0006$ in heart between *mdx* and C57Bl10 analyzed by two-way ANOVA). (B) Effect of HDACi treatment on *Dmd* transcript imbalance in triceps, diaphragm, and heart (n = 7 mice per group). No statistical difference was detected overall between HDACi-treated mice and saline-treated mice ($p = 0.6694$ in triceps, $p = 0.5552$ in diaphragm, and $p = 0.8554$ in heart analyzed by two-way ANOVA). (C) Schematic representation of the *mdx* treatment with ASO combined with the various HDACi. (D) Effect of HDACi on exon-skipping level. Left: qPCR quantification of exon 23 using TaqMan qPCR in the different muscle tissues: tibialis anterior (TA), gastrocnemius (GAS), quadriceps (QUAD), triceps (TRI), biceps (BI), diaphragm (DIA), and heart. n = 7 mice per group, *$p < 0.05$ between ASO treatment and ASO + VPA treatment using a two-way ANOVA to compare the two groups. Right: example of the visualization of exon 23 skipping on gel in the heart with one representative mouse for each group (1/7). PCR amplifications between exons 20 and 26 are loaded in a 1.5% agarose gel. The top band corresponds to the unskipped transcript and the lower band to the exon 23 skipped transit. All data are plotted as means ± SEM.

ranging from 2% to 7% in the different muscles. However, co-treatment with VPA slightly increased the skipping levels (1.26-fold change, $p = 0.0478$, two-way analysis of variance [ANOVA], ASO versus ASO + VPA) (Table 1) as well as co-treatment with givinostat, though not statistically significant (1.21-fold change, $p = 0.1916$, two-way ANOVA, ASO versus ASO + givinostat). Exon 23 skipping levels were also visualized on gel after RT-PCR. The right panel of Figure 1D shows the gel for heart samples (n = 1/7 mouse per group on the gel) in which the bands corresponding to the exon 23 skipped transcript are clearly visible in ASO-treated samples as opposed to the

Table 1. Exon-skipping fold change following HDACi treatment in *mdx* mice

Exon-skipping fold change	TA	GAS	QUAD	TRI	DIA	HEART	Average
ASO + givistatin	1.00	1.36	1.65	0.83	1.09	1.11	1.21
ASO + VPA	1.11	1.45	1.41	1.17	1.28	1.19	1.26
ASO + EX527	0.87	1.27	1.51	0.76	1.03	0.90	1.01

Fold changes are calculated from the levels of exon 23 skipping quantified by TaqMan qPCR obtained in the muscles co-treated with ASO and HDACi compared with the same muscles treated with ASO alone. TA, tibialis anterior; GAS, gastrocnemius; QUAD, quadriceps; TRI, triceps; DIA, diaphragm.

saline-treated mice. No exon 23 skipping was detected in samples from *mdx* mice treated with HDACi only (data not shown).

Effect of HDAC inhibitors on dystrophin protein levels in *mdx* mice

We next assessed the levels of dystrophin expression in the various muscle tissues following treatment with ASO alone or ASO and HDACi. No dystrophin expression was found in samples from *mdx* mice treated with HDACi only (Figure S2A). Significant amounts of dystrophin protein (ranging from 2% to 10%) were detected by western blot in all analyzed tissues after only four administrations of ASO (Figure 2A). We found significantly more dystrophin restoration in *mdx* mice co-treated with VPA (1.74-fold change compared with ASO alone across all muscles, $p < 0.0001$, two-way ANOVA, ASO versus ASO + VPA) and givinostat (1.44-fold change, $p = 0.0076$, two-way ANOVA, ASO versus ASO + givinostat), but not with EX527 (1.10-fold change, $p = 0.7012$, two-way ANOVA, ASO versus ASO + EX527) in both skeletal muscles and heart (Figure 2A). Dystrophin restoration and correct localization were also confirmed by immunostaining performed on muscle cryosections (Figure 2B). Compared with the treatment with ASO alone, we did not detect significantly more dystrophin-positive fibers in muscles from HDACi co-treated mice (approximately 3% of dystrophin-positive fibers in all groups), but the intensity of the staining was higher (Figure S2B), which fits with the higher amounts detected on western blot. Since some HDACi have previously been shown to increase muscle fiber size in *mdx* mice, we measured the muscle fiber sizes in the triceps of all groups of mice (Figures 2C and S2C). *Mdx* muscles display a higher number of small fibers (<1,000 μm^2) compared with WT mice and ASO-treated mice, where the distribution shows a normalization toward WT muscles (fewer small fibers and more middle sized-fibers [2,000–4,000 μm^2]). Co-treatment with givinostat tends to induce very large fibers (<5,000 μm^2), as previously reported,[16] and the mean fiber area was therefore significantly improved compared with *mdx* saline (Figures 2C and 2D). Previous studies have shown that the effects of HDACi on muscle histopathology are mediated by an upregulation of follistatin, an antagonist of both myostatin and activin A.[18,21] We thus investigated the expression of follistatin in mice treated with ASO alone or in combination with HDACi and detected only a slight and not statistically significant elevation compared with the saline group ($p = 0.2769$) (Figure S2D). This suggests that the effect of HDACi on dystrophin expression and muscle fiber size are not or, at least, not completely due to increased follistatin expression.

To investigate whether the higher protein restoration obtained with the combined therapy ASO and HDACi could be due to higher mRNA levels or differences in transcript imbalance, we assessed *Dmd* gene expression at different exon junctions in co-treated mice as before. The qPCR results revealed higher levels of *Dmd* transcripts in the diaphragm (Figures 2E and S2E) of all treated groups of mice compared with saline *mdx* mice, but this was only statistically significant in *mdx* mice co-treated with VPA after multiple testing correction ($p = 0.0001$). In mice treated with HDACi alone (givinostat, VPA, or EX527), no statistical difference was detected (Figure S1B).

It has previously been demonstrated that two fragments of the myofibrillar structural protein myomesin-3 (MYOM3) are abnormally present in sera of the *mdx* mouse model and that this biomarker can be used to evaluate the efficacy of treatments.[9,22] Levels of MYOM3 in the serum following treatment with ASO alone were significantly decreased by 57% ($p < 0.0001$) after 4 weeks of treatment (Figure 2F). MYOM3 levels were also significantly reduced with HDACi co-treatment ($p < 0.0001$ for all conditions compared with the saline group) although not statistically different from ASO alone.

Effect of HDAC inhibitors on ASO biodistribution and toxicity

To verify that increased skipping and protein restoration levels are not due to higher ASO concentrations in tissues, we checked the quantity of ASO in muscle tissues (Figure 3A). ASO quantification was performed as previously described[23] and revealed similar levels of ASO in all muscle tissues ($p = 0.5122$, $p = 0.4380$, and $p = 0.5257$ for VPA, givinostat, and EX527, respectively). We calculated the ratio between protein restoration and ASO content, which reflects the therapeutic index of each treatment (Table 2). This highlights the superiority of the combined ASO + VPA therapy, since we found a nearly 2-fold increase between the two treatments (0.66 for ASO alone versus 1.26 for ASO + VPA). We also assessed the ASO content in liver, kidney, and spleen where ASOs tend to preferentially accumulate (Figure 3A, right). While we detected no difference between the different treatments in liver and spleen, we found a significant reduction (3-fold) in the kidneys of mice treated with ASO + VPA ($p = 0.0009$). This information is particularly promising for potential long-term treatment and safety, since the combined ASO + VPA therapy could lead to higher protein rescue in muscles with less ASO accumulation in kidney. Taking this result into account, we calculated the ratio between efficacy (average protein rescue across muscles) and ASO quantity in kidneys to determine the treatment with the best

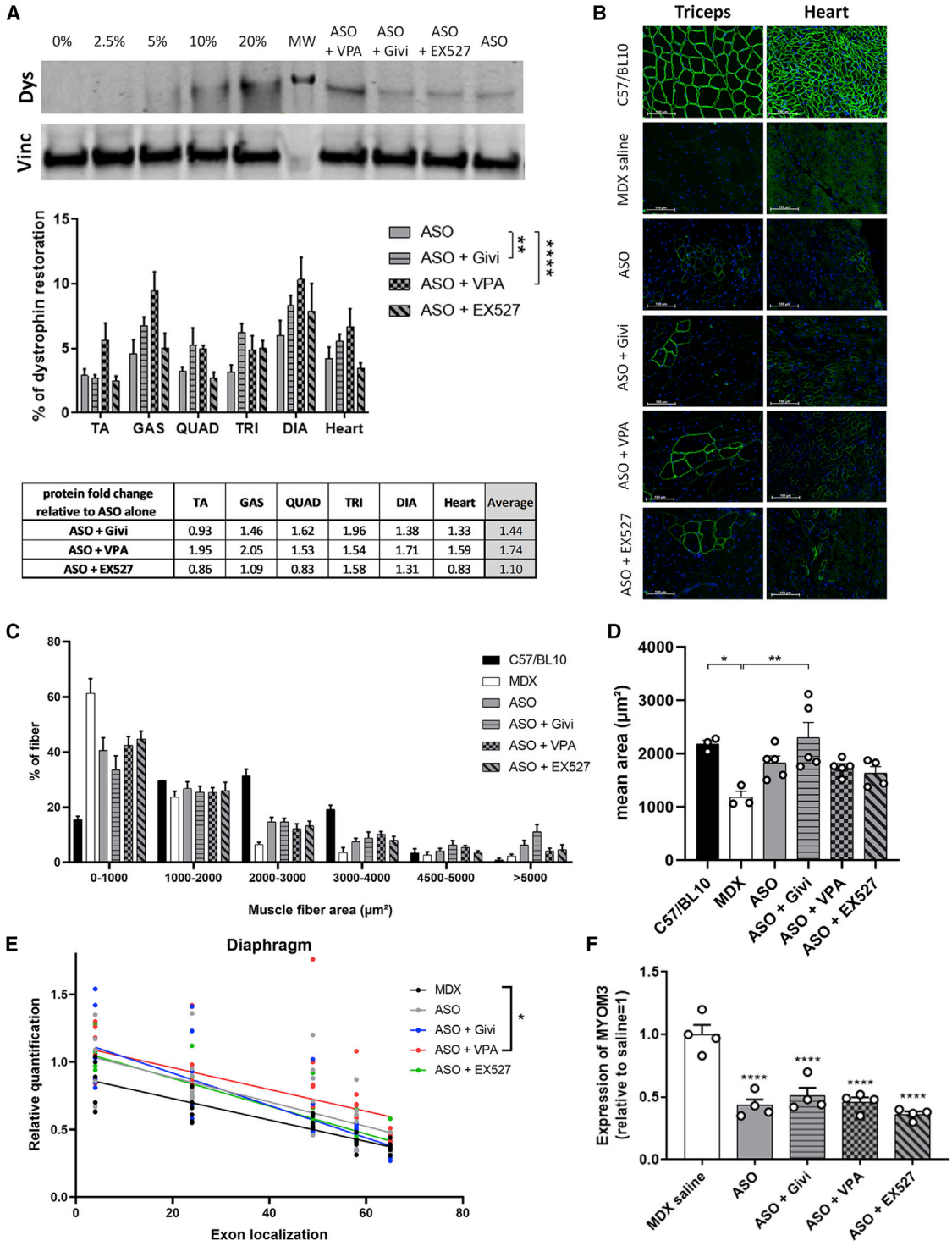

protein fold change relative to ASO alone	TA	GAS	QUAD	TRI	DIA	Heart	Average
ASO + Givi	0.93	1.46	1.62	1.96	1.38	1.33	1.44
ASO + VPA	1.95	2.05	1.53	1.54	1.71	1.59	1.74
ASO + EX527	0.86	1.09	0.83	1.58	1.31	0.83	1.10

Figure 2. Dystrophin protein expression in *mdx* mice treated with ASO and HDACi

(A) Dystrophin restoration in treated *mdx* mice. A typical dystrophin western blot obtained for the heart is shown in the top panel, with vinculin used for normalization. A standard curve made from pooled lysates from C57BL10 (WT) and *mdx* control for each tissue is loaded for quantification (0%, 2.5%, 5%, 10%, and 20% of WT). Middle panel: quantification of dystrophin restoration using Empiria Studio software. n = 7 mice per group, p = 0.0010 between treatments (two-way ANOVA), **p < 0.01 between ASO alone and ASO + givinostat groups and ****p < 0.0001 between ASO alone and ASO + VPA groups. p = 0.4496 between ASO and ASO + EX527. The fold changes

(legend continued on next page)

benefit/risk ratio. The combined therapy ASO + VPA revealed a near 4-fold improved ratio compared with ASO alone (Table 3).

We also checked ASO localization in the kidneys by *in situ* hybridization using a fluorescently labeled probe specific to the ASO. Following intravenous injections, the palm-tcDNA, like most charged ASOs, was found in the cortex area of kidneys and more specifically in proximal tubules[24] (Figure 3B). Co-treatment with HDACi did not modify ASO localization, but the staining intensity was lower in VPA-treated mice, confirming the data obtained with the ASO quantification assay. Moreover, ASO quantification in urine revealed a higher amount of ASO in the urine of VPA-treated mice compared with mice treated with ASO alone (although not statistically significant), suggesting a tendency for better kidney clearance (Figure 3C).

To ensure that the combination of HDACi with ASO did not induce any specific toxicity, we analyzed the serum levels of various general biomarkers in mice following the different treatments (Figure 4). Quantification of serum creatinine, urea, albumin, alkaline phosphatase (ALP), bilirubin, alanine aminotransferase (ALT), and aspartate aminotransferase (AST) revealed no significant changes in HDACi-treated *mdx* mice compared with saline-treated *mdx* mice. The slight elevation in AST and ALT levels observed in ASO + givinostat-treated mice was mostly due to a single individual and was not statistically significant, as was the effect of givinostat alone (Figure S3).

Effect of valproic acid on chromatin organization

To further investigate the impact of VPA and the possible mechanisms underlying the higher dystrophin rescue induced by the combined ASO + VPA therapy, we next studied the effect of the combined treatment on *DMD* transcripts in cultured human myocytes. We first assessed whether changes in the chromatin landscape could be detected after treatment with ASOs and/or VPA. For this purpose, we treated immortalized myocytes derived from a healthy control (HC) or a DMD patient carrying a deletion of exons 48 through 50 with: a control ASO (not targeting DMD), an ASO targeting *DMD* exon 41 (generating an in-frame exon 41-skipped transcript in HC cells), or an ASO targeting *DMD* exon 51 (restoring the reading frame in these DMD cells); ASOs were tested alone as well as in combination with VPA treatment. As expected by blocking HDACs, treatment with VPA (alone and in combination with the ASO) increased the level of observed permissive histone mark H3K9Ac over the gene body of the *DMD* locus in HC cells, indicating that the *DMD* chromatin is indeed regulated through HDAC activity in the absence of pathogenic mutations (Figure 5A). No additional difference in H3K9Ac levels was observed for co-treatment of VPA with ASOs. Similarly, H3K9Ac levels were elevated in DMD patient cells treated with VPA, although the increase was only significant in DMD cells treated with ASO + VPA. Levels of the repressive histone mark H3K9me3 were not altered by treatment with VPA (Figure S4). None of the other histone marks that we investigated (H3K4me3, H3K27me3, and H3K36me3) showed any reproducible changes over the *DMD* locus caused by the treatment of cells with VPA and/or ASO (Figure S4).

Exon-skipping efficiency in the different *in vitro* samples was measured by RT-PCR followed by analysis of PCR product ratios using an Agilent Femto Pulse system (Figure 5B). Exon-skipping levels were comparable across VPA and ASO + VPA combination treatment for *DMD* exon 41 skipping in HC cells (∼64%) as well as for exon 51 skipping in DMD cells (∼81%), meaning that VPA did not induce changes in skipping efficiency in either cell type.

To assess whether VPA treatment affects production of dystrophin protein, we compared dystrophin recovery in samples treated with ASOs and ASO + VPA combination treatment using western blot that allows the detection of full-length dystrophin (Dp427) (Figure 5C). In HC cells, ASOs or ASO + VPA treatments had no significant impact on Dp427 expression ($p > 0.9999$) (Figure 5D). In DMD cells, ASO-mediated exon 51 skipping induces a distinct recovery of full-length dystrophin (Dp427) ($p = 0.0407$ and $p = 0.0483$ for ASO and ASO + VPA compared with control ASO, respectively), but no difference was observed between ASO alone or ASO + VPA (Figure 5D). The mRNA levels of Dp427 showed no significant alterations compared with the control ASO sample resulting from the described treatments (Figure 5E), although we observed a slight decrease (not statistically significant) in samples transfected with DMD-targeting ASOs (in both HC and DMD cells). Since DMD is primarily expressed in mature muscle cells, we looked at the expression levels of *MYOG* (Figure S5A) and *MYH3* (Figure S5B) as markers of myogenesis progression. We noted a loss of myogenic potential, as determined by *MYH3* levels in cells transfected with DMD-targeting ASOs (Figure S5B), which may explain the reduced levels of *DMD* transcripts in these samples.

Analysis of various exon-exon junctions of the *DMD* gene confirmed lower expression of *DMD* transcripts in DMD cells when compared with HC cells (Figure S5C), with a clear 5′-3′ imbalance, especially in the samples derived from the DMD patient (Figure S5C). The exon 3-4 junction seems equally abundant in HC and DMD cells, again suggesting that the ratio of transcription initiation is similar in either cell type, but the 5′-3′ transcript imbalance is clearer in DMD cells.

between protein restoration detected in ASO-treated mice and ASO + HDACi-treated mice is shown in the bottom panel. (B) Detection of dystrophin protein (green staining) by immunostaining on transverse sections of muscle tissues (triceps and heart) from WT and *mdx* mice treated with saline, ASO, or ASO + HDACi. Nuclei are labeled with DAPI (blue staining). Scale bars, 100 μm. (C and D) Graphs representing the distribution (C) and the mean (D) of muscle fiber area in triceps muscles from *mdx* mice treated with ASO or ASO + HDACi and compared with WT (C57/BL10) or saline control *mdx* mice. *$p < 0.05$ and **$p < 0.01$ compared with treatment with *mdx* saline. (E) Effect of the combination HDACi + ASO on *Dmd* transcript imbalance in the diaphragm, analyzed by TaqMan qPCR at different exon junctions. n = 7 mice per group; asterisk indicates an adjusted $p = 0.0001$ between *mdx* and ASO + VPA after multiple testing comparison using Tukey's method for p-value correction. (F) MYOM3 quantification by western blot in serum of *mdx* mice treated with ASO or ASO + HDACi and compared with saline control *mdx* mice. n = 4 mice/group, ****$p < 0.0001$ compared with saline control *mdx* mice. All data are plotted as means ± SEM.

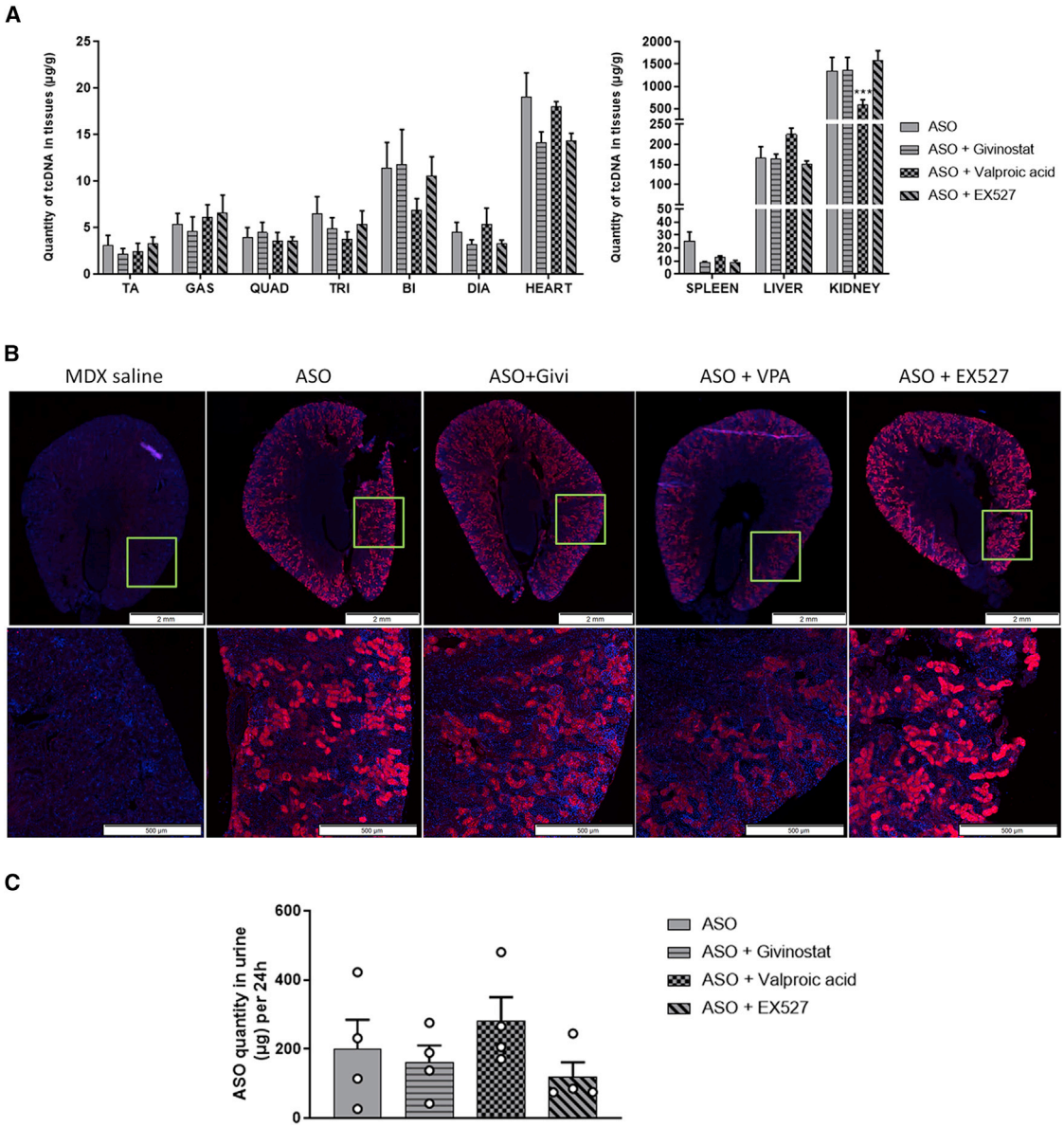

Figure 3. Impact of HDAC inhibitors on ASO biodistribution

(A) Quantification of ASO in the different muscle tissues tibialis anterior (TA), gastrocnemius (GAS), quadriceps (QUAD), triceps (TRI), biceps (BI), diaphragm (DIA) and heart (left), and accumulation organs such as spleen, liver, and kidney (right) after 4 weeks of ASO treatment. n = 7 mice per group, ***$p < 0.001$ compared with ASO analyzed by two-way ANOVA. (B) Detection of ASO (red staining) by *in situ* hybridization on transverse sections of kidneys from *mdx* mice treated with saline, ASO, or ASO + HDACi. Nuclei are labeled in blue (DAPI). Scale bars, 2,000 µm for the entire kidney sections (top panels) and 500 µm for the zoomed-in cortex regions (lower panels). The green squares indicate the location of the zoomed-in region. (C) ASO quantification in urine collected during 24 h after the last ASO injection (n = 4 mice per group). All data are plotted as means ± SEM.

However, we could not detect any significant changes in the imbalance following ASO or VPA treatment in DMD cells (Figure S5D).

DISCUSSION

In this study, we used three different HDACi: givinostat (a pan HDACi), VPA (inhibitor of HDAC class I and II), and EX527 (an inhibitor of sirtulin: HDAC class III) and combined them with an exon-skipping approach using tcDNA-based ASOs. We have previously demonstrated that palm-tcDNA ASOs represent promising drugs for the systemic treatment of DMD based on a 12-week treatment.[9] In the present proof-of-concept study evaluating combined therapies, we deliberately used a short-term 4-week treatment, resulting in lower levels of dystrophin expression (approximately 3% of WT levels) in order to leave space for improvement.

Table 2. Ratio between protein rescue and ASO content in muscle tissues and fold change compared with treatment with ASO alone

Protein rescue/ASO quantification	TA	GAS	QUAD	TRI	DIA	HEART	Average	Fold change
ASO	0.93	0.86	0.82	0.49	1.33	0.22	0.66	1.00
ASO + GIVI	1.27	1.45	1.17	1.26	2.60	0.39	1.16	1.75
ASO + VPA	2.32	1.55	1.38	1.29	1.92	0.37	1.26	1.90
ASO + EX527	0.76	0.77	0.76	0.93	2.43	0.24	0.84	1.27

The combined ASO + givinostat and ASO + VPA treatments induced significantly higher dystrophin restoration levels than ASO therapy alone (1.7- and 1.4-fold, respectively) as detected by western blot. Restoration of dystrophin was also confirmed by immunohistochemistry which did not reveal more dystrophin-positive fibers in muscles from HDACi co-treated mice, suggesting that the increase in dystrophin recovery is a consequence of higher intracellular levels of dystrophin rather than a higher number of cells expressing dystrophin. This would be in line with our hypothesis according to which HDACi treatment may increase available mRNA (leading to increased dystrophin production in each targeted nucleus) rather than have an impact on ASO biodistribution, which may have led to more dystrophin-positive fibers.

To investigate whether higher dystrophin restoration could have been due to unexpected higher uptake of ASO in muscle tissues, we checked ASO biodistribution after combined therapies. ASO amount in target muscle tissues was not altered by any of the HDACi, but VPA treatment surprisingly reduced the amount of ASO accumulated in kidneys. This may be due to higher kidney clearance given that more ASOs were found in the urine of VPA-treated mice, although this does not necessarily mean that the initial biodistribution to kidney was affected (perhaps only the clearance rate). While further work will be required to determine the underlying mechanisms, this represents an interesting advantage for the combined ASO + VPA therapy, which shows a 4-fold increase in the benefit/risk ratio.

HDACi have previously been studied in the context of DMD models but not directly for their effect on dystrophin transcript synthesis. Previous published work has shown how HDACs play a role in DMD pathophysiology and how they can mediate the connection between the dystrophin-associated glycoprotein complex (DAPC) and nuclear gene/microRNA (miRNA) expression. For example, expression of miRNA-1 in healthy muscle fibers occurs as a consequence of HDAC2 nitrosylation by nitric oxide synthase (NOS), which happens when NOS is bound to dystrophin at the DAPC. Nitrosylated HDAC2 is then released by the miRNA-1 locus with consequent gene expression.[25] A similar connection has also been established for follistatin, which is controlled by class I HDACs, specifically HDAC2 (even though some evidence connecting follistatin expression with class II HDAC4 activity is also present). Inhibition of HDAC2 as well as reconstitution of the dystrophin-NOS signaling has been shown to result in derepression of follistatin. Pharmacological blockade of HDACs has been shown to decrease fibrosis and promote compensatory regeneration in the *mdx* skeletal muscle through this follistatin upregulation.[16–18]

In our study, we only detected a slight and not statistically significant upregulation of follistatin gene expression following HDACi treatment, suggesting that increased dystrophin expression was not directly linked. We further measured muscle fiber cross-sectional area (CSA) and demonstrated that givinostat indeed significantly increased fiber size area but not VPA. Givinostat treatment was previously shown to ameliorate morphology and muscular function in *mdx* mice by significantly reducing fibrosis in muscle tissue and promoting the increase of CSA of the muscles.[16] It is possible that the increased level of dystrophin detected in ASO + givinostat-treated mice is due to the overall improvement of muscle histopathology and the increase in fiber size. However, CSA was not significantly impacted by the VPA treatment, suggesting a different underlying mechanism. When investigating whether combined therapies with HDACi had impacted the levels of dystrophin mRNA, we detected a significantly increased level of transcripts in VPA co-treated muscles. This may explain the higher dystrophin expression in ASO + VPA-treated mice and would be in line with our hypothesis which assumed that HDACi could increase the level of *Dmd* transcript and ultimately improve the efficacy of the exon-skipping approach.

While we observed a significant increase in VPA-induced dystrophin protein recovery *in vivo* in *mdx* mice treated with ASO + VPA, this effect was not recapitulated in the *in vitro* human myocyte model. This may be explained by the difference in treatment regimen between the two models, as the murine samples were treated with VPA for 5 weeks, as opposed to 24 h for human *in vitro* samples. Exon-skipping efficiency is also significantly higher in cultured cells than in muscles *in vivo*, likely due to the direct delivery of ASO to the cells. This high *in vitro* exon-skipping efficiency could potentially obscure subtle positive effects of VPA, which are observable *in vivo* where dystrophin recovery only reaches a fraction of WT levels. We also noted a loss of myogenic potential, as determined by *MYH3* levels in cells transfected with DMD-targeting ASOs, suggesting that the *in vitro* model may not be the most appropriate model to analyze subtle dystrophin expression changes.

HDACi have previously been shown to alter the myogenesis of various cultured myocytes models,[16,26,27] but this was not readily observed in the ASO-treated cell lines treated with VPA in our study. However, most reports claiming increased myogenesis have used pan-HDAC inhibitors such as givinostat or trichostatin A.[16,27] Given that VPA is an HDAC class I and IIa inhibitor, it may not inhibit the HDACs that cause the reported increase in myogenic potential.

Table 3. Ratio between the average protein rescue across muscles and ASO content in kidneys, representing the benefit/risk of each combined therapy

	Average protein restoration (%)	ASO content in kidney (mg/g)	Benefit/risk ratio	Fold change compared with ASO
ASO	4.03	1.35	2.99	1.00
ASO + GIVI	5.80	1.37	4.24	1.42
ASO + VPA	6.99	0.59	11.81	3.95
ASO + EX527	4.44	1.58	2.81	0.94

The fold change is expressed in comparison with treatment with ASO alone.

Despite the lack of detectable increase in dystrophin levels, we observed increased H3K9Ac levels at the *DMD* gene upon treatment with VPA and combination of targeting ASO and VPA of human myocytes as assessed by chromatin immunoprecipitation followed by qPCR (ChIP-qPCR). This result confirms our hypothesis that predicted an impact of HDACi *DMD* transcript levels.

Of note, increased histone acetylation levels have been reported to cause spontaneous exon skipping in neuronal cells (in the neural cell adhesion molecule gene),[28] presumably by the kinetic coupling of transcription and splicing.[29] As such, it is possible that HDACi could facilitate ASO-mediated exon skipping (although this is not observed in our *in vitro* model). However, it is unclear as to what the threshold is for H3K9Ac to induce increased exon skipping, and whether our VPA-treated samples reach such levels.

Interestingly, Marasco et al. recently reported that co-treatment of VPA and ASOs could improve exon 7 inclusion in SMN2 transcripts.[30] They showed that SMN2 exon 7 belongs to the class of type 2 exons where acetylation of H3K9 improves RNA polymerase II speed and inclusion and H3K9me2 results in slower RNA polymerase II and exon 7 skipping. They also observed that ASO treatment resulted in increased dimethylation in SMN2 intron 7. Thus, while the net effect of ASO treatment was more exon 7 inclusion, the dimethylation decreased exon 7 inclusion. Co-treatment with VPA reduced dimethylation and increased ASO-induced exon 7 inclusion. We did not assess local chromatin changes in the targeted regions. Furthermore, we target exonic regions in our study while Marasco et al. targeted an intronic region. In either case, we did not observe a clear effect of VPA treatment on exon-skipping levels but rather on dystrophin protein levels. This suggests that an effect like the one described for SMN2 intron 7 did not occur and that our positive effects are rather due to increased expression of dystrophin transcripts.

It has recently been reported that HDACi have an influence on the activity of other cell types present in the muscle tissue, such as fibro-adipogenic progenitors and muscle stem cells.[31] The altered microenvironment influenced by HDACi might improve general muscle tissue health and, concomitantly, result in improved delivery of the ASO and/or recovery of ASO-induced dystrophin protein. This potential positive effect of HDACi + VPA is not properly mimicked in the homogeneous *in vitro* myocyte cultures, potentially explaining why this model does not benefit from HDACi in similar fashion to our *in vivo* model system.

In conclusion, our results show a clear beneficial effect of VPA on the recovery of dystrophin protein in *mdx* mice after exon skipping and confirm that even short treatments with VPA have a noticeable effect on the chromatin marks present at the *DMD* locus. However, whether these two observations are causative or correlative is currently unclear and warrants further research into the epigenetic status of the *Dmd* locus in muscle tissue of VPA-treated *mdx* mice. Moreover, it would be useful to evaluate the functional outcomes of this increased dystrophin expression in future studies.

Considering that the HDACi used in this study have either been approved in the clinic (VPA) or are being evaluated in late-stage clinical trials (givinostat), this work provides encouraging data supporting a future combined therapy which could be rapidly translated to the clinic.

MATERIALS AND METHODS

Antisense oligonucleotides and animal experiments

Animal procedures were performed in accordance with national and European legislation, approved by the French government (Ministère de l'Enseignement Supérieur et de la Recherche, Autorisation APAFiS #6518). *Mdx* (C57BL/10ScSc-Dmdmdx/J) mice were bred in our animal facility at the Plateforme 2Care, UFR des Sciences de la Santé, Université de Versailles Saint Quentin, and were maintained in a standard 12:12-h light/dark cycle with free access to food and water. Mice were weaned at weeks 4–5 postnatal, and 2–5 individuals were housed per cage.

tcDNA-ASO targeting the donor splice site of exon 23 of the mouse dystrophin pre-mRNA[32] were synthesized by SQY Therapeutics (Montigny le Bretonneux, France). Palmitic acid was conjugated at the 5′ end of tcDNA-PO via a C6-amino linker and a phosphorothioate bond as previously described.[9]

Groups of 8- to 10-week-old *mdx* mice were treated with HDAC inhibitors or saline (n = 7 mice per group) for 5 weeks as follows: VPA (Santa Cruz, dissolved in PBS and used at a final concentration of 500 mg/kg/day) and EX527, also known as Selisistat or SEN0014196 (ADOOQ Bioscience, dissolved in PBS 2% dimethyl sulfoxide [DMSO] and used at a final concentration of 2 mg/kg/day) were injected i.p. five times per week as previously described;[19,20] givinostat (ADOOQ Bioscience. dissolved in H_2O 2% DMSO and used at a final concentration of 10 mg/kg/day) was administered by oral gavage as previously described.[13] After the first week of HDACi treatment,

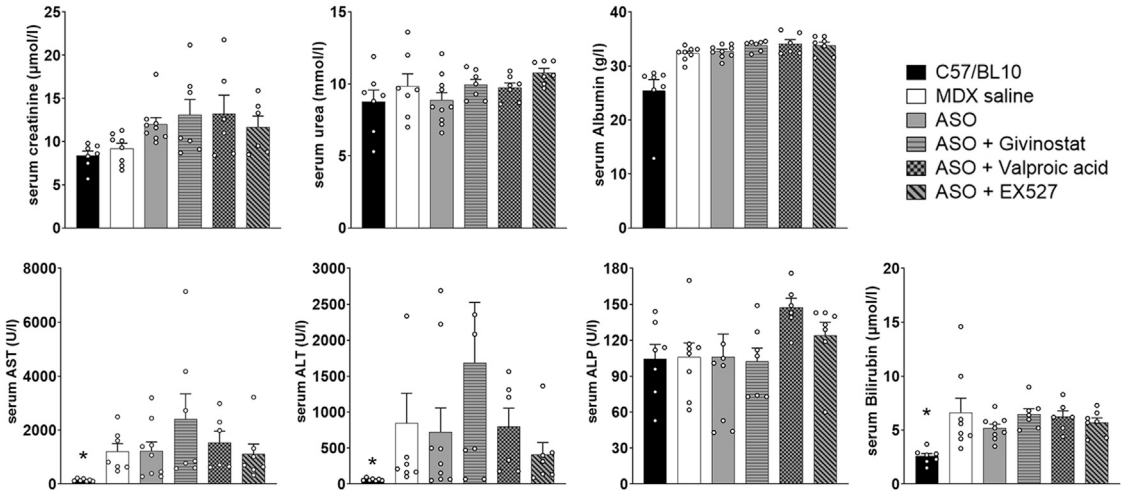

Figure 4. Serum biochemistry following HDACi treatment

Quantification of general toxicity biomarkers in the serum: creatinine, urea, albumin, aspartate aminotransferase (AST), alanine aminotransferase (ALT), alkaline phosphatase (ALP), and bilirubin. n = 7 mice per group, *p < 0.05 compared with *mdx* saline, analyzed by Kruskal-Wallis test. All data are plotted as means ± SEM.

mice were treated with ASO (one intravenous injection per week at 25 mg/kg/week under general anesthesia using 2% isoflurane). Age-matched *mdx* groups receiving an equivalent volume of sterile saline were included as controls, and C57BL/10 mice were included as WT controls.

Animals were euthanized 2 weeks after the last ASO injection; thereafter, muscles and tissues were harvested and snap-frozen in liquid-nitrogen-cooled isopentane and stored at −80°C before further analysis. To assess the biodistribution of the ASO treatment, kidneys were sampled at the end of the protocol, fixed in 10% neutral buffered formalin, and embedded in paraffin wax. Blood samples were also collected at the end of the treatment for MYOM-3 and biochemistry analysis. Analyses of serum ALT, AST, ALP, bilirubin, creatinine, urea, and albumin levels were performed by the pathology laboratory at the Mary Lyon Centre, Medical Research Council, Harwell, Oxfordshire, UK.

ASO quantification by fluorescent hybridization assay

Tissues were homogenized using the Precellys 24 (Bertin Instruments, France) in lysis buffer (100 mmol/L Tris-HCl [pH 8.5], 200 mmol/L NaCl, 5 mmol/L EDTA, 0.2% SDS) containing 2 mg/mL of proteinase K (Invitrogen) (50 mg tissue/mL of buffer), followed by incubation overnight at 55°C in a hybridization oven. After centrifugation at 7,000 × *g* (Sorval ST 8R centrifuge, 75005719 rotor) for 15 min, the supernatant was used in the assay. Quantification of ASO was performed using a hybridization assay with a molecular beacon probe, as previously described.[23] In brief, 10 µL of tissue lysates or serum was incubated with a 5′ Cy3-DNA complementary probe conjugated with HBQ quencher at 3′ in black non-binding 96-well plates (Thermo Fisher Scientific, USA). PBS was added to a final volume of 100 µL per well, and fluorescence was measured on a spectrophotometer (excitation 544 nm/emission 590 nm using FluoStar Omega). The amount of tcDNA in tissues was determined using a standard curve built on the measurement of known tcDNA quantities dissolved in the respective tissue lysates of mock-injected animals.

RNA analysis

Total RNA was isolated from snap-frozen muscle tissues using TRIzol reagent according to the manufacturer's instructions (Thermo Fisher Scientific).

To visualize exon-skipping levels, aliquots of 500 ng of total RNA were used for RT-PCR analysis using the Access RT-PCR System (Promega, USA) in a 25-µL reaction using the external primers Ex 20Fo (5′-CAG AAT TCT GCC AAT TGC TGA G-3′) and Ex 26Ro (5′-TTC TTC AGC TTG TGT CAT CC-3′). The cDNA synthesis was carried out at 45°C for 45 min, directly followed by the primary PCR of 29 cycles of 95°C (30 s), 55°C (1 min), and 72°C (2 min). 1.5 µL of these reactions was then reamplified in nested PCRs by 24 cycles of 95°C (30 s), 55°C (1 min), and 72°C (2 min) using the internal primers Ex 20Fi (5′-CCC AGT CTA CCA CCC TAT CAG AGC-3′) and Ex 26Ri (5′-CCT GCC TTT AAG GCT TCC TT-3′). PCR products were analyzed on 1.5% agarose gels with ethidium bromide.

Exon 23 skipping levels were quantified using real-time qPCR using TaqMan assays designed against the exon 23–24 junction and exon 22–24 junction as previously described.[9] Seventy nanograms of cDNA was used as input per reaction, and all assays were carried out in triplicate. Assays were performed under fast cycling conditions on a Bio-Rad CFX384 Touch Real-Time PCR Detection System, and all data were analyzed using the absolute copy number method. For a given sample the copy number of skipped product (exon 22–24 assay) and unskipped product (exon 23–24 assay) were determined using the standards Ex20-26 and Ex20-26Delta23 respectively (gBlocks gene fragments from Integrated DNA Technologies). Exon 23

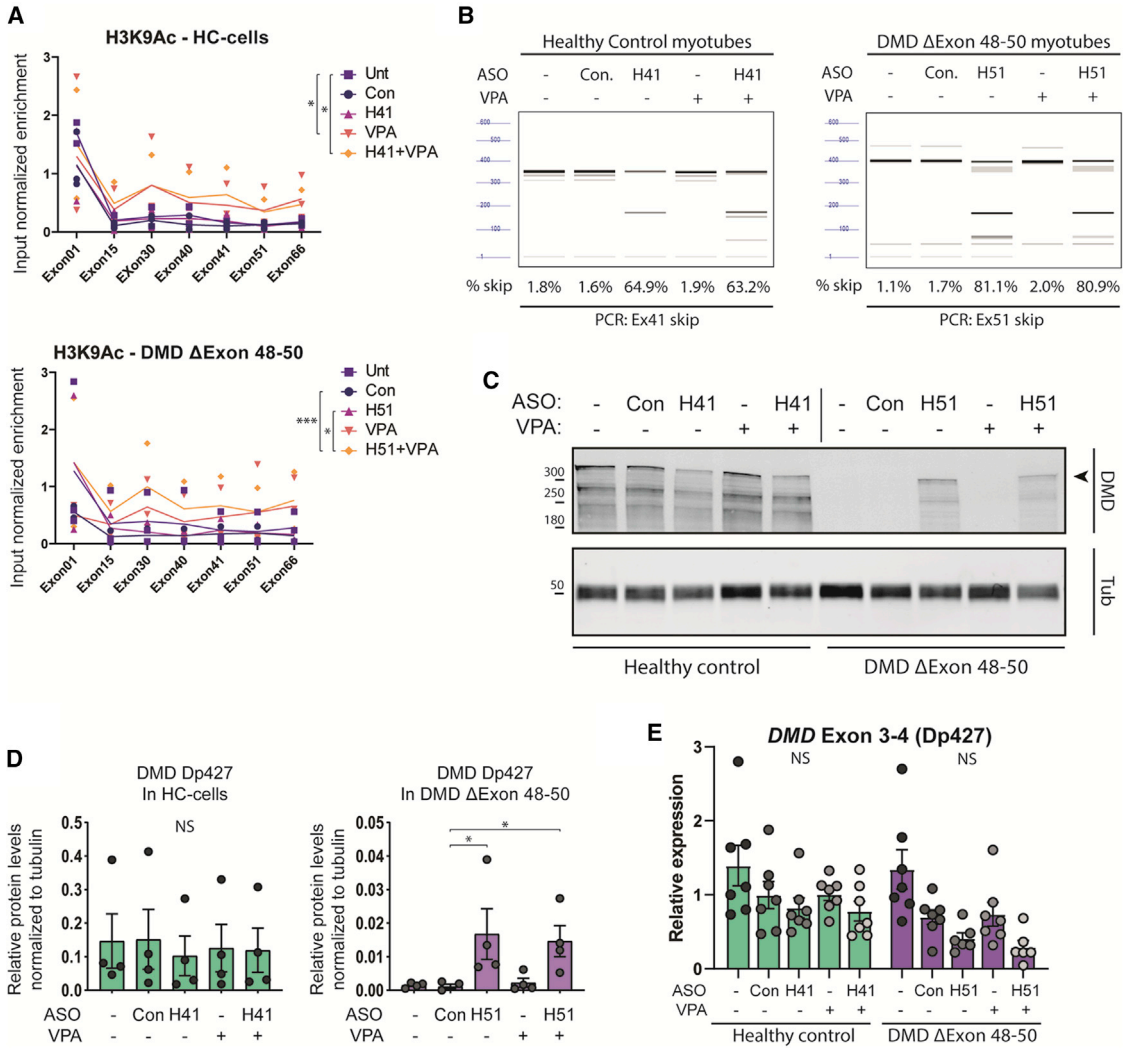

Figure 5. Effect of valproic acid on *DMD* chromatin organization and expression *in vitro*

(A) ChIP-qPCR analysis of the histone mark H3K9Ac at various locations in the *DMD* locus in immortalized myocytes derived from a healthy control (HC) or a DMD patient. Cells were untreated (Unt), treated with a control ASO (targeting NOTCH3 [Con]), ASOs inducing exon skipping of *DMD* exon 41 (H41), *DMD* exon 51 (H51), valproic acid (VPA), or a combination of ASOs and VPA as indicated. Enrichment of H3K9Ac was normalized to input chromatin. n = 3 replicates, *p < 0.05, ***p < 0.001, RM-ANOVA between two groups as indicated. (B) Quantification of exon skipping induced in a representative sample set corresponding to (A), as determined by analysis with Femto pulse. PCR around exon 41 in HC cells and PCR around exon 51 in DMD patient cells are shown; percentages below each lane indicate exon-skipping efficiency over the WT PCR product. Expected PCR product sizes for unskipped and skipped transcripts are 357 bp and 174 bp for exon 41 skipping, and 401 bp and 168 bp for exon 51, respectively. (C) Western blot analysis of DMD protein expression after combinatorial treatment with ASOs and VPA. HC or DMD immortal myocytes were treated with ASOs and/or VPA as indicated. Arrowhead indicates expected size of the DMD Dp427 protein. Tubulin was probed as a loading control for normalization purposes. (D) Quantification of n = 4 western blots, as presented in (C). Band intensity of DMD Dp427 was normalized to tubulin expression. Arbitrary units, n = 4 experiments, *p < 0.05, NS denotes non-significant; Kruskal-Wallis test. (E) qRT-PCR analysis of the expression of *DMD* Dp427 in myotube samples corresponding to the samples presented in (A) and (C) using isoform-specific primer sets. Gene expression was normalized to housekeeping genes *GUSB* and *GAPDH*. NS, not significant; Kruskal-Wallis test. All data are plotted as means ± SEM.

skipping was then expressed as a percentage of total dystrophin (calculated by the addition of exon 22–23 and exon 22–24 copy numbers). Quantification of Dmd transcripts at different exon-exon junctions was performed similarly, with probes targeting ex4-5 junction (Mm.PT.58.41636025), ex49-50 junction (Mm.PT.58.6233636), ex58-59 junction (Mm.PT.58.43613256), ex65-66 junction (Mm.PT.58.42993407), and GAPDH (Mm.PT.39a.1) (Integrated DNA Technologies). Absolute quantification was determined for each probe using the corresponding standards (gBlocks gene fragments from Integrated DNA Technologies).

Exon-skipping levels of samples derived from *in vitro* cultures were determined using RT-PCR with exon-specific primers (Table S1) followed by analysis of skipping ratios using an Agilent Femto Pulse.

Peaks were called, and molarity of each PCR product was determined using the corresponding ProSize data analysis software (Agilent). Further data analysis and visualization was performed using GraphPad Prism version 9.

Follistatin quantification was performed using real-time qPCR using TaqMan assays (Mm.PT.58.11399784 from IDT). ΔΔCt analysis was performed with GAPDH as normalization.

Western blot analysis

Protein lysates were obtained from intervening muscle sections collected during cryosection using the Precellys 24 (Bertin Instruments) in RIPA buffer (Thermo Fisher Scientific) complemented with SDS powder (5% final) (Bio-Rad, France) and protease inhibitor cocktail (Thermo Fisher Scientific). Protein extracts were denatured at 100°C for 3 min and centrifuged at 13,000 rpm for 10 min at 10°C. Supernatants were collected, and the total protein concentration was determined with the BCA Protein Assay Kit (Thermo Fisher Scientific). Twenty-five micrograms of protein was loaded onto NuPAGE 3%–8% Tris-acetate protein gels (Invitrogen), following the manufacturer's instructions. Dystrophin protein was stained using iBind Flax Western Device (Thermo Fisher Scientific), and the membrane was labeled with NCL-DYS1 primary monoclonal antibody (NCL-DYS1, dilution 1:200; Novocastra, Newcastle, UK) and hVin-1 primary antibody (dilution 1:4,000; Sigma), followed by incubation with a goat anti-mouse secondary antibody (IRDye 800CW Goat anti-mouse immunoglobulin G [IgG], dilution 1:2,000; Li-Cor, Germany). Bands were visualized using the Odyssey CLx system (Li-Cor), and quantification was carried out using the Empiria Studio software (Li-Cor) based on a standard curve made from pooled lysates from C57BL10 (WT) and *mdx* control for each tissue.

For myomesin-3 detection, mouse sera were diluted at 1:20 before loading onto 3%–8% Criterion XT Tris-Acetate Protein Gel, following the manufacturer's instructions (Bio-Rad). Myomesin-3 protein was detected by probing the nitrocellulose membrane with MYOM3 primary rabbit polyclonal antibody (MYOM3; Proteintech, Manchester, UK), followed by incubation with a goat anti-rabbit secondary antibody (IRDye 800CW Goat anti-rabbit IgG; Li-Cor). Bands were visualized using the Odyssey Imaging System (Biosciences, Lincoln, NE, USA). Signal intensities in treated samples were quantified and normalized to PBS control mouse signals using Image Studio software (Li-Cor).

For protein samples derived from i*n vitro* cell cultures, cells were lysed in 1× Laemmli sample buffer (2% SDS, 10% glycerol, 60 mM Tris [pH 6.8]) and denatured at 95°C. After normalization of protein concentration determined by the BCA Protein Assay Kit, samples were supplemented with 2% β-mercaptoethanol and 0.01% bromophenol blue prior to PAGE. The Immobulon-FL PVDF membrane (Merck-Millipore) was probed for dystrophin using ab154168 (Abcam) and tubulin T6199 (Sigma-Aldrich) in Takara immunobooster (Takara), followed by secondary antibodies donkey-α-Rabbit IRDye-800CW and donkey-α-Mouse IRDye-680RD (926-68072). The membrane was visualized using an Odyssey CLx infrared imaging system (Li-Cor) and analyzed using the accompanying Image Studio software v5.2 (Li-Cor).

Immunohistochemistry analysis

Sections of 10 μm were cut from triceps and heart and examined for dystrophin expression using the rabbit polyclonal antibody dystrophin (dilution 1:500; Thermo Fisher Scientific, cat. no. RB-9024-P), which was then detected by donkey anti-rabbit IgG Alexa 594 (dilution 1:400; Jackson ImmunoResearch). Controls prepared by omitting primary antibody showed no specific staining. Images were taken at equivalent locations and exposure times using a Zeiss Axio Imager with an Orkan camera (Hamamatsu) and AxioVision software, and analyzed with ImageJ software.

To visualize ASO in kidney, 5-μm sections were cut from paraffin blocks, dewaxed (3× 5 min in xylene and 3× 3 min in ethanol 100) and stained with a complementary DNA probe fluorescently labeled with Alexa 594. Controls prepared by omitting the probe showed no specific staining. Scans were taken at equivalent exposure times using an IX83 inverted microscope (Olympus) with an Orca-R2 camera (Hamamatsu) and cellSens Dimension software.

For measurement of muscle fiber size, sections of 10 μm were cut from triceps and stained with the rabbit polyclonal antibody laminin (dilution 1:200; Sigma, ref. L9393-2ML), which was then detected by donkey anti-rabbit IgG Alexa 488 (dilution 1:400; Thermo Fisher Scientific, ref. A11008). Images were taken using a Zeiss Axio Imager with an Orkan camera (Hamamatsu) and AxioVision software, and analyzed with ImageJ software.

Cell culture

Immortalized HC and DMD patient cell lines were kindly provided by Prof. Vincent Mouly (Institute of Myology, Paris).[33,34] Cells were cultured in skeletal muscle growth medium (SMGM; Promokine), supplemented with 15% heat-inactivated fetal bovine serum (HI-FBS) and gentamycin. To induce differentiation of proliferating myoblasts to myotubes, SMGM medium was replaced with fusion medium consisting of Dulbecco's modified Eagle's medium (DMEM)-Glutamax, high-glucose (Gibco), supplemented with 2% HI-FBS and 1% penicillin-streptomycin (Gibco). Cells were maintained at 37°C and 5% CO_2 in humidified incubators and were routinely tested for mycoplasma infection by the use of the Mycoalert Kit (Lonza). For transfection of myocytes with ASO, a 200-nM end concentration of ASO was transfected at day 3 of myogenic differentiation for 3 h, after which cells were left to further differentiate for 48 h as indicated. In brief, 200 nM end concentration of ASO (2′ O-methyl RNA; phosphorothioate backbone) (H41, cuccucuuucuucuucugc; H51, ucaaggaagauggcauuucu; Control-NOTCH3 (h4c12), agcagaggaagcguccauc, which is very inefficient at skipping NOTCH3 exon 4 by itself and known to not induce motif-related events such as an inflammatory response[35]) was mixed with a 1:4 ratio of Lipofectamine 2000 (Thermo Fisher Scientific), incubated at room temperature for 20 min, and added to culture dishes. After 3 h of incubation, transfection medium was replaced with fusion

medium for further differentiation of myocytes. For VPA treatment, fusion medium was supplemented with 3 mM VPA (Sigma-Aldrich, ref. P4543-25G) freshly dissolved in Milli-Q® water for 24 h before harvesting as indicated.

Chromatin immunoprecipitation

ChIP-qPCR was performed as previously described.[36] In brief, after described treatments cells were crosslinked for 10 min by addition of formaldehyde to 1% final concentration. Fixation was quenched by addition of 125 mM glycine, after which cells were washed in cold PBS and collected. Nuclei were liberated from cells by resuspension in NP-ChIP buffer (150 mM NaCl, 5 mm EDTA, 0.5% Igepal CA-630, 1% Triton X-100 in 50 mM Tris-HCl [pH 7.5]), which were sheared for 25 cycles (30 s on, 30 s off) using a Bioruptor Pico (Diagenode). For each histone mark described, 3 μg of chromatin was precleared and incubated with antibodies (Table S2) overnight. Chromatin-antibody immunocomplexes were captured for 2 h using 20 μL of a mix of protein A and protein G Dynabeads (Life Technologies) at a 3:1 ratio. Beads were washed in a series of wash buffers: low salt buffer (0.1% SDS, 1% Triton X-100, 2 mM EDTA, 150 mM NaCl in 20 mM Tris-HCl [pH 8]), high salt buffer (0.1% SDS, 1% Triton X-100, 2 mM EDTA, 300 mM NaCl in 20 mM Tris-HCl [pH 8]), lithium chloride wash buffer (0.25 M LiCl, 1% Igepal CA-630, 1% sodium deoxycholate, 1 mM EDTA in 10 mM Tris-HCl [pH 8]), and twice with TE-wash buffer (1 mM EDTA in 10 mM Tris-HCl [pH 8]). DNA was eluted from the beads by boiling at 95°C for 10 min in the presence of 10% Chelex-100 resin (Bio-Rad). Corresponding input samples were phenol-chloroform isolated from 10% of input material used for each chromatin sample. Samples were analyzed using locus-specific primer sets (Table S1) and SensiMix Sybr HI-ROX (Bioline), run in a CFX-384 Real-Time PCR system (Bio-Rad). Values from histone ChIP samples were normalized to corresponding input samples using ΔCt calculations.

Statistical analysis

All *in vivo* data were analyzed with GraphPad Prism8 software (GraphPad, San Diego, CA, USA) and expressed as means ± SEM. "n" refers to the number of mice per group.

Group comparisons were performed using one- and two-way ANOVA with repeated-measures comparisons when needed (e.g., effects at different exon junctions or in different muscle tissues), followed by post hoc Dunnett's or Sidak's multiple comparisons when appropriate. To compare the overall effect of two treatments across the different tissues or different exon junctions, the two groups were directly compared using a two-way ANOVA, and the p value of the treatment effect is indicated in the figure legends. The Kruskal-Wallis test was used to compare groups that did not follow a normal distribution (assessed with the Shapiro-Wilk test).

The statistical analysis of gene expression and transcript imbalance assessed by qPCR at various exon-exon junctions was also performed using a linear model, in which exons were included as a covariate (continuous) and group was included as a factor. Pairwise contrasts were assessed using the *emmeans* R package, and multiple testing correction was performed with the Tukey method.

Statistical analysis of all *in vitro* data was performed using GraphPad Prism version 9. Kruskal-Wallis test followed by Dunn's multiple correction was performed as indicated. Repeated-measures (RM)-ANOVA was used as indicated. Data are plotted as means ± SEM. "n" refers to independently acquired and processed samples (biological replicates) as indicated. Biological replicates consist of technical triplicates in the case of qRT-PCR and ChIP-qPCR measurements. Significance levels were set at $*p < 0.05$, $**p < 0.01$, $***p < 0.001$, and $****p < 0.0001$.

DATA AVAILABILITY

The primary data for this study are available from the authors upon request.

SUPPLEMENTAL INFORMATION

Supplemental information can be found online at https://doi.org/10.1016/j.omtn.2022.11.017.

ACKNOWLEDGMENTS

We thank the personnel of the platform 2CARE for taking care of the animals used in this work. We thank Dr. Vincent Mouly (Institute of Myology, Paris, France) for providing the myogenic cell lines used in the study. The authors are part of the European BIND consortium and the COST Action DARTER. Several authors of this publication are members of the Netherlands Neuromuscular Center, the Duchenne Centrum Netherlands (funded by Spieren voor Spieren), and the European Reference Network for Rare Neuromuscular Diseases EURO-NMD. This work was supported by the Institut National de la Santé et de la Recherche Médicale (INSERM), the Association Monegasque contre les Myopathies (AMM), the Paris Ile-de-France Region, and the Fondation UVSQ. F.B. is the recipient of a MESRI thesis fellowship. The salary of R.G. is paid by an unrestricted grant from Sarepta Therapeutics and the Ammodo Organization.

AUTHOR CONTRIBUTIONS

Conceptualization, A.G. and P.S.; methodology, F.B., R.G., P.S., A.A.-R., and A.G.; investigation, F.B., R.G., T.T., and S.D.; writing – original draft, F.B., R.G., P.S., and A.G.; writing – review & editing, P.S., A.A.-R., and A.G.; funding acquisition, P.S., A.A.-R., L.G., and A.G.; resources, L.G., P.S., A.A.-R., and A.G.; supervision, P.S., A.A.-R., and A.G.

DECLARATION OF INTERESTS

L.G. is co-founder of SQY Therapeutics, which produces tcDNA oligomers. T.T. and S.D. are employees of SQY Therapeutics. A.A.-R. discloses being employed by LUMC, which has patents on exon-skipping technology, some of which has been licensed to BioMarin and subsequently sublicensed to Sarepta. As co-inventor of some of these patents, A.A.-R. is entitled to a share of royalties. A.A.-R. further discloses being ad hoc consultant for PTC Therapeutics, Sarepta Therapeutics, Regenxbio, Alpha Anomeric, BioMarin Pharmaceuticals Inc.,

Eisai, Entrada, Takeda, Splicesense, Galapagos, and Astra Zeneca. Past ad hoc consulting has occurred for CRISPR Therapeutics, Summit PLC, Audentes Santhera, Bridge Bio, Global Guidepoint, GLG consultancy, Grunenthal, Wave, and BioClinica. A.A.-R. also reports having been a member of the Duchenne Network Steering Committee (BioMarin) and being a member of the scientific advisory boards of Eisai, Hybridize Therapeutics, Silence Therapeutics, and Sarepta Therapeutics. Past SAB memberships: ProQR, Philae Pharmaceuticals. Remuneration for these activities is paid to LUMC. LUMC also received speaker honoraria from PTC Therapeutics and BioMarin Pharmaceuticals and funding for contract research from Italfarmaco, Sapreme, Eisai, Galapagos, Synnaffix, and Alpha Anomeric. Project funding is received from Sarepta Therapeutics.

REFERENCES

1. Fortunato, F., Rossi, R., Falzarano, M.S., and Ferlini, A. (2021). Innovative therapeutic approaches for duchenne muscular dystrophy. J. Clin. Med. *10*, 820. https://doi.org/10.3390/jcm10040820.
2. Clemens, P.R., Rao, V.K., Connolly, A.M., Harper, A.D., Mah, J.K., Smith, E.C., McDonald, C.M., Zaidman, C.M., Morgenroth, L.P., Osaki, H., et al. (2020). Safety, tolerability, and efficacy of viltolarsen in boys with duchenne muscular dystrophy amenable to exon 53 skipping: a phase 2 randomized clinical trial. JAMA Neurol. *77*, 982–991. https://doi.org/10.1001/jamaneurol.2020.1264.
3. Mitelman, O., Abdel-Hamid, H.Z., Byrne, B.J., Connolly, A.M., Heydemann, P., Proud, C., Shieh, P.B., Wagner, K.R., Dugar, A., Santra, S., et al. (2022). A combined prospective and retrospective comparison of long-term functional outcomes suggests delayed loss of ambulation and pulmonary decline with long-term eteplirsen treatment. J. Neuromuscul. Dis. *9*, 39–52. https://doi.org/10.3233/JND-210665.
4. Godfrey, C., Desviat, L.R., Smedsrød, B., Piétri-Rouxel, F., Denti, M.A., Disterer, P., Lorain, S., Nogales-Gadea, G., Sardone, V., Anwar, R., et al. (2017). Delivery is key: lessons learnt from developing splice-switching antisense therapies. EMBO Mol. Med. *9*, 545–557. https://doi.org/10.15252/emmm.201607199.
5. Hammond, S.M., Aartsma-Rus, A., Alves, S., Borgos, S.E., Buijsen, R.A.M., Collin, R.W.J., Covello, G., Denti, M.A., Desviat, L.R., Echevarría, L., et al. (2021). Delivery of oligonucleotide-based therapeutics: challenges and opportunities. EMBO Mol. Med. *13*, e13243. https://doi.org/10.15252/emmm.202013243.
6. Ferlini, A., Goyenvalle, A., and Muntoni, F. (2021). RNA-targeted drugs for neuromuscular diseases. Science *371*, 29–31. https://doi.org/10.1126/science.aba4515.
7. Roberts, T.C., Langer, R., and Wood, M.J.A. (2020). Advances in oligonucleotide drug delivery. Nat. Rev. Drug Discov. *19*, 673–694. https://doi.org/10.1038/s41573-020-0075-7.
8. Hammond, S.M., Hazell, G., Shabanpoor, F., Saleh, A.F., Bowerman, M., Sleigh, J.N., Meijboom, K.E., Zhou, H., Muntoni, F., Talbot, K., et al. (2016). Systemic peptide-mediated oligonucleotide therapy improves long-term survival in spinal muscular atrophy. Proc. Natl. Acad. Sci. USA *113*, 10962–10967. https://doi.org/10.1073/pnas.1605731113.
9. Relizani, K., Echevarría, L., Zarrouki, F., Gastaldi, C., Dambrune, C., Aupy, P., Haeberli, A., Komisarski, M., Tensorer, T., Larcher, T., et al. (2022). Palmitic acid conjugation enhances potency of tricyclo-DNA splice switching oligonucleotides. Nucleic Acids Res. *50*, 17–34. https://doi.org/10.1093/nar/gkab1199.
10. Chamberlain, J.S., Pearlman, J.A., Muzny, D.M., Gibbs, R.A., Ranier, J.E., Caskey, C.T., and Reeves, A.A. (1988). Expression of the murine Duchenne muscular dystrophy gene in muscle and brain. Science *239*, 1416–1418. https://doi.org/10.1126/science.3347839.
11. Haslett, J.N., Sanoudou, D., Kho, A.T., Bennett, R.R., Greenberg, S.A., Kohane, I.S., Beggs, A.H., and Kunkel, L.M. (2002). Gene expression comparison of biopsies from Duchenne muscular dystrophy (DMD) and normal skeletal muscle. Proc. Natl. Acad. Sci. USA *99*, 15000–15005. https://doi.org/10.1073/pnas.192571199.
12. Gehring, N.H., Kunz, J.B., Neu-Yilik, G., Breit, S., Viegas, M.H., Hentze, M.W., and Kulozik, A.E. (2005). Exon-junction complex components specify distinct routes of nonsense-mediated mRNA decay with differential cofactor requirements. Mol. Cell *20*, 65–75. https://doi.org/10.1016/j.molcel.2005.08.012.
13. García-Rodríguez, R., Hiller, M., Jiménez-Gracia, L., van der Pal, Z., Balog, J., Adamzek, K., Aartsma-Rus, A., and Spitali, P. (2020). Premature termination codons in the DMD gene cause reduced local mRNA synthesis. Proc. Natl. Acad. Sci. USA *117*, 16456–16464. https://doi.org/10.1073/pnas.1910456117.
14. Spitali, P., van den Bergen, J.C., Verhaart, I.E.C., Wokke, B., Janson, A.A.M., van den Eijnde, R., den Dunnen, J.T., Laros, J.F.J., Verschuuren, J.J.G.M., 't Hoen, P.A.C., and Aartsma-Rus, A. (2013). DMD transcript imbalance determines dystrophin levels. FASEB J *27*, 4909–4916. https://doi.org/10.1096/fj.13-232025.
15. Tennyson, C.N., Shi, Q., and Worton, R.G. (1996). Stability of the human dystrophin transcript in muscle. Nucleic Acids Res. *24*, 3059–3064. https://doi.org/10.1093/nar/24.15.3059.
16. Consalvi, S., Mozzetta, C., Bettica, P., Germani, M., Fiorentini, F., Del Bene, F., Rocchetti, M., Leoni, F., Monzani, V., Mascagni, P., et al. (2013). Preclinical studies in the mdx mouse model of duchenne muscular dystrophy with the histone deacetylase inhibitor givinostat. Mol. Med. *19*, 79–87. https://doi.org/10.2119/molmed.2013.00011.
17. Licandro, S.A., Crippa, L., Pomarico, R., Perego, R., Fossati, G., Leoni, F., and Steinkühler, C. (2021). The pan HDAC inhibitor Givinostat improves muscle function and histological parameters in two Duchenne muscular dystrophy murine models expressing different haplotypes of the LTBP4 gene. Skelet. Muscle *11*, 19. https://doi.org/10.1186/s13395-021-00273-6.
18. Minetti, G.C., Colussi, C., Adami, R., Serra, C., Mozzetta, C., Parente, V., Fortuni, S., Straino, S., Sampaolesi, M., Di Padova, M., et al. (2006). Functional and morphological recovery of dystrophic muscles in mice treated with deacetylase inhibitors. Nat. Med. *12*, 1147–1150. https://doi.org/10.1038/nm1479.
19. Gurpur, P.B., Liu, J., Burkin, D.J., and Kaufman, S.J. (2009). Valproic acid activates the PI3K/Akt/mTOR pathway in muscle and ameliorates pathology in a mouse model of Duchenne muscular dystrophy. Am. J. Pathol. *174*, 999–1008. https://doi.org/10.2353/ajpath.2009.080537.
20. Daenthanasanmak, A., Iamsawat, S., Chakraborty, P., Nguyen, H.D., Bastian, D., Liu, C., Mehrotra, S., and Yu, X.-Z. (2019). Targeting Sirt-1 controls GVHD by inhibiting T-cell allo-response and promoting Treg stability in mice. Blood *133*, 266–279. https://doi.org/10.1182/blood-2018-07-863233.
21. Iskenderian, A., Liu, N., Deng, Q., Huang, Y., Shen, C., Palmieri, K., Crooker, R., Lundberg, D., Kastrapeli, N., Pescatore, B., et al. (2018). Myostatin and activin blockade by engineered follistatin results in hypertrophy and improves dystrophic pathology in mdx mouse more than myostatin blockade alone. Skelet. Muscle *8*, 34. https://doi.org/10.1186/s13395-018-0180-z.
22. Rouillon, J., Poupiot, J., Zocevic, A., Amor, F., Léger, T., Garcia, C., Camadro, J.M., Wong, B., Pinilla, R., Cosette, J., et al. (2015). Serum proteomic profiling reveals fragments of MYOM3 as potential biomarkers for monitoring the outcome of therapeutic interventions in muscular dystrophies. Hum. Mol. Genet. *24*, 4916–4932. https://doi.org/10.1093/hmg/ddv214.
23. Echevarría, L., Aupy, P., Relizani, K., Bestetti, T., Griffith, G., Blandel, F., Komisarski, M., Haeberli, A., Svinartchouk, F., Garcia, L., and Goyenvalle, A. (2019). Evaluating the impact of variable phosphorothioate content in tricyclo-DNA antisense oligonucleotides in a duchenne muscular dystrophy mouse model. Nucleic Acid Ther. *29*, 148–160. https://doi.org/10.1089/nat.2018.0773.
24. Hung, G., Xiao, X., Peralta, R., Bhattacharjee, G., Murray, S., Norris, D., Guo, S., and Monia, B.P. (2013). Characterization of target mRNA reduction through in situ RNA hybridization in multiple organ systems following systemic antisense treatment in animals. Nucleic Acid Ther. *23*, 369–378. https://doi.org/10.1089/nat.2013.0443.
25. Cacchiarelli, D., Martone, J., Girardi, E., Cesana, M., Incitti, T., Morlando, M., Nicoletti, C., Santini, T., Sthandier, O., Barberi, L., et al. (2010). MicroRNAs involved in molecular circuitries relevant for the Duchenne muscular dystrophy pathogenesis are controlled by the dystrophin/nNOS pathway. Cell Metab. *12*, 341–351. https://doi.org/10.1016/j.cmet.2010.07.008.
26. Breuls, N., Giarratana, N., Yedigaryan, L., Garrido, G.M., Carai, P., Heymans, S., Ranga, A., Deroose, C., and Sampaolesi, M. (2021). Valproic acid stimulates myogenesis in pluripotent stem cell-derived mesodermal progenitors in a NOTCH-dependent manner. Cell Death Dis. *12*, 677. https://doi.org/10.1038/s41419-021-03936-w.

27. Iezzi, S., Di Padova, M., Serra, C., Caretti, G., Simone, C., Maklan, E., Minetti, G., Zhao, P., Hoffman, E.P., Puri, P.L., and Sartorelli, V. (2004). Deacetylase inhibitors increase muscle cell size by promoting myoblast recruitment and fusion through induction of follistatin. Dev. Cell *6*, 673–684. https://doi.org/10.1016/s1534-5807(04)00107-8.

28. Schor, I.E., Rascovan, N., Pelisch, F., Alló, M., and Kornblihtt, A.R. (2009). Neuronal cell depolarization induces intragenic chromatin modifications affecting NCAM alternative splicing. Proc. Natl. Acad. Sci. USA *106*, 4325–4330. https://doi.org/10.1073/pnas.0810666106.

29. Saldi, T., Cortazar, M.A., Sheridan, R.M., and Bentley, D.L. (2016). Coupling of RNA polymerase II transcription elongation with pre-mRNA splicing. J. Mol. Biol. *428*, 2623–2635. https://doi.org/10.1016/j.jmb.2016.04.017.

30. Marasco, L.E., Dujardin, G., Sousa-Luís, R., Liu, Y.H., Stigliano, J.N., Nomakuchi, T., Proudfoot, N.J., Krainer, A.R., and Kornblihtt, A.R. (2022). Counteracting chromatin effects of a splicing-correcting antisense oligonucleotide improves its therapeutic efficacy in spinal muscular atrophy. Cell *185*, 2057–2070.e15. https://doi.org/10.1016/j.cell.2022.04.031.

31. Consalvi, S., Tucciarone, L., Macrì, E., De Bardi, M., Picozza, M., Salvatori, I., Renzini, A., Valente, S., Mai, A., Moresi, V., and Puri, P.L. (2022). Determinants of epigenetic resistance to HDAC inhibitors in dystrophic fibro-adipogenic progenitors. EMBO Rep. *23*, e54721. https://doi.org/10.15252/embr.202254721.

32. Relizani, K., Griffith, G., Echevarría, L., Zarrouki, F., Facchinetti, P., Vaillend, C., Leumann, C., Garcia, L., and Goyenvalle, A. (2017). Efficacy and safety profile of tricyclo-DNA antisense oligonucleotides in duchenne muscular dystrophy mouse model. Mol. Ther. Nucleic Acids *8*, 144–157. https://doi.org/10.1016/j.omtn.2017.06.013.

33. Echigoya, Y., Lim, K.R.Q., Trieu, N., Bao, B., Miskew Nichols, B., Vila, M.C., Novak, J.S., Hara, Y., Lee, J., Touznik, A., et al. (2017). Quantitative antisense screening and optimization for exon 51 skipping in duchenne muscular dystrophy. Mol. Ther. *25*, 2561–2572. https://doi.org/10.1016/j.ymthe.2017.07.014.

34. Mamchaoui, K., Trollet, C., Bigot, A., Negroni, E., Chaouch, S., Wolff, A., Kandalla, P.K., Marie, S., Di Santo, J., St Guily, J.L., et al. (2011). Immortalized pathological human myoblasts: towards a universal tool for the study of neuromuscular disorders. Skelet. Muscle *1*, 34. https://doi.org/10.1186/2044-5040-1-34.

35. Rutten, J.W., Dauwerse, H.G., Peters, D.J.M., Goldfarb, A., Venselaar, H., Haffner, C., van Ommen, G.-J.B., Aartsma-Rus, A.M., and Lesnik Oberstein, S.A.J. (2016). Therapeutic NOTCH3 cysteine correction in CADASIL using exon skipping: in vitro proof of concept. Brain *139*, 1123–1135. https://doi.org/10.1093/brain/aww011.

36. Nelson, J.D., Denisenko, O., and Bomsztyk, K. (2006). Protocol for the fast chromatin immunoprecipitation (ChIP) method. Nat. Protoc. *1*, 179–185. https://doi.org/10.1038/nprot.2006.27.

OMTN, Volume *30*

Supplemental information

Histone deacetylase inhibitors improve antisense-mediated exon-skipping efficacy in *mdx* mice

Flavien Bizot, Remko Goossens, Thomas Tensorer, Sergei Dmitriev, Luis Garcia, Annemieke Aartsma-Rus, Pietro Spitali, and Aurélie Goyenvalle

Supplemental Information

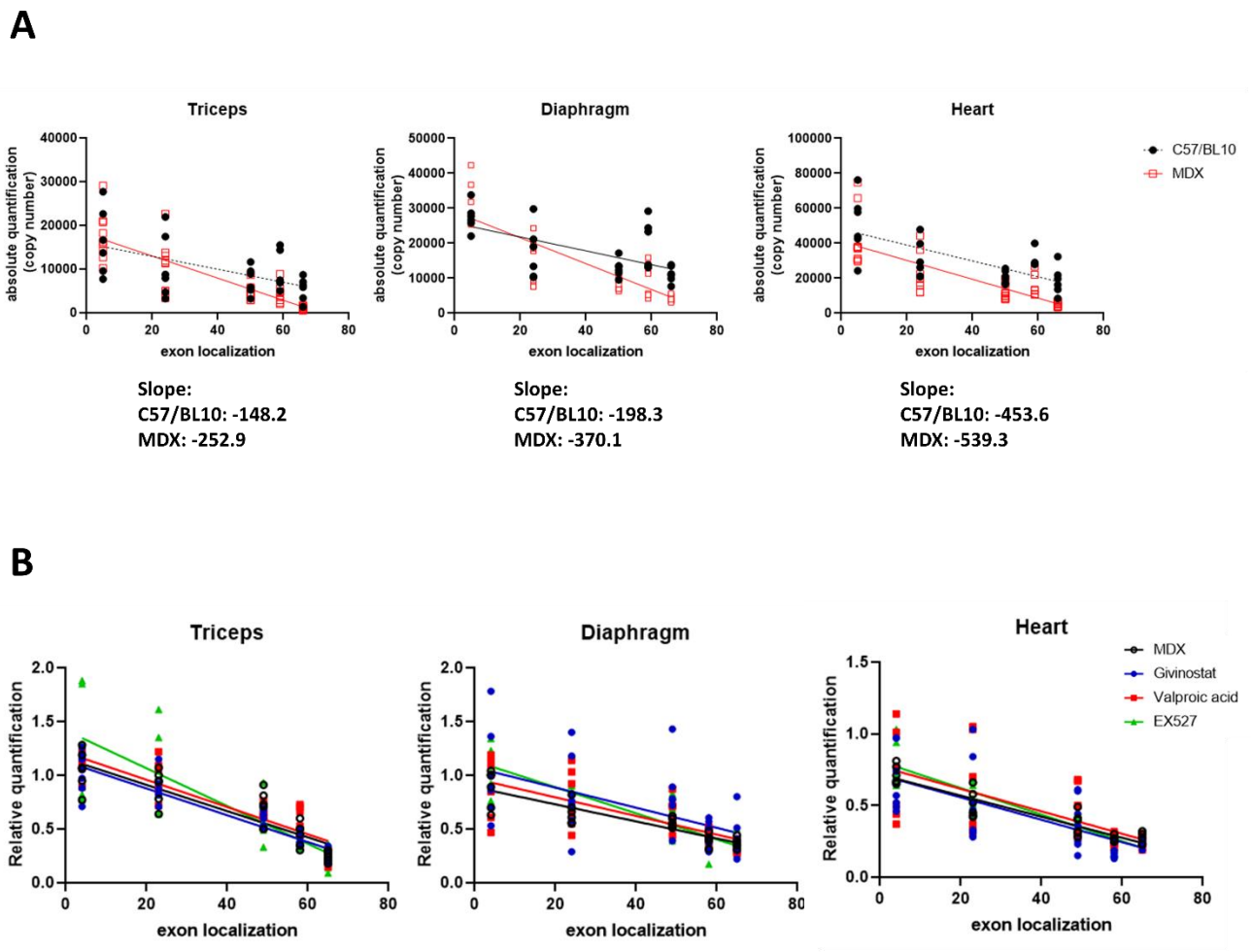

Figure S1: *Dmd* transcript levels in *mdx* and wt mice

(A) Absolute quantification of *Dmd* transcript levels obtained in triceps, diaphragm and heart for several exon−exon junctions along the *Dmd* gene in *mdx* and C57Bl10 mice (N=6 for C57Bl10 and 9 for *mdx* mice), normalized to GAPDH expression. (B) Relative quantification of *Dmd* transcript levels obtained in triceps, diaphragm and heart for several exon−exon junctions along the *Dmd* gene (N=6 mice per group), normalized to C57Bl10 mice.

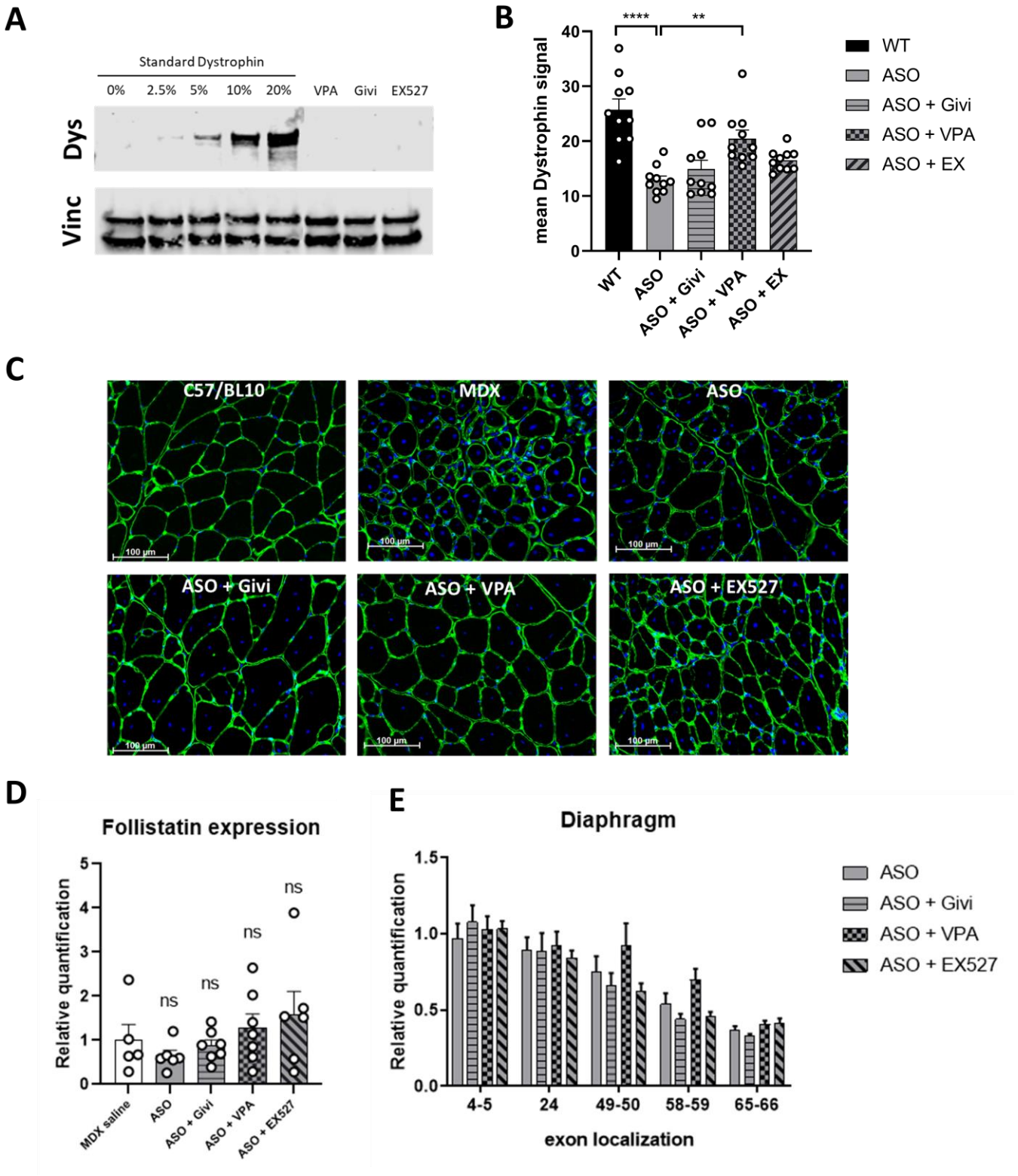

Figure S2: Histological and molecular characterization of muscles treated with ASO+HDACi.

(A) Western blot showing no dystrophin restoration in triceps from *mdx* mice treated with HDACi only. Vinculin is used for normalization (bottom panel). A standard curve made from pooled lysates from C57BL10 (WT) and *mdx* control was loaded as control (0%, 2.5%, 5%, 10% and 20% of WT). (B) Quantification of the dystrophin staining intensity in the triceps (illustrated in the Figure 2B), $p>0.05$ between treatments (one-way ANOVA). (C)

Detection of laminin protein (green staining) by immunostaining on transverse sections of triceps from WT and *mdx* mice treated with saline, ASO or ASO+HDACi. Nuclei are labelled with dapi (blue staining). Scale bar, 100µm. (D) Relative expression of follistatin quantified by RT-qPCR in diaphragm of mdx mice treated with ASO+HDACi (Givinostat, valproic acid or EX527). N=7 mice per group, $p>0.05$ between treatments (one-way ANOVA). (E) Relative quantification of *Dmd* transcript levels obtained in diaphragm of mdx mice treated with ASO+HDACi (Givinostat, valproic acid or EX527) for several exon−exon junctions along the *Dmd* gene normalized to C57Bl10 mice, N=6 mice per group (two-way ANOVA).

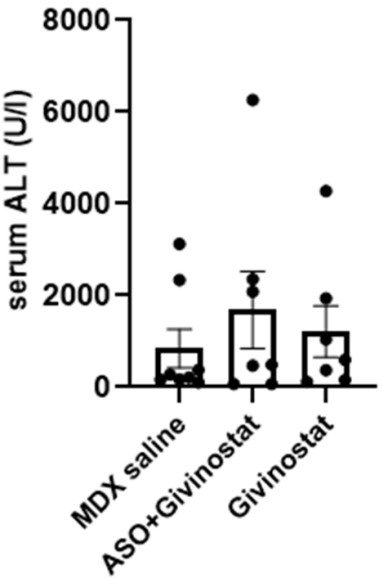

One way Anova (Kruskal-Wallis)	P=0.8047
Mann-Whitney saline vs ASO+Givi	P=0.6126
Mann-Whitney saline vs Givi	P=0.6126

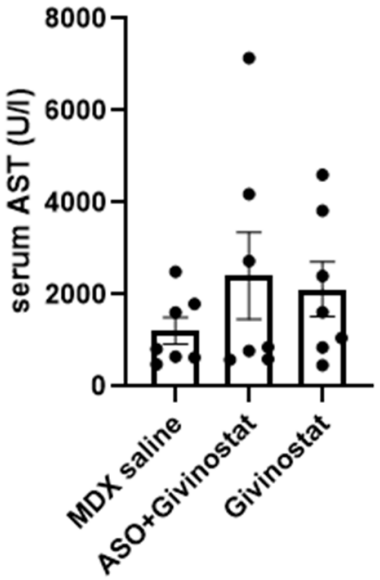

One way Anova (Kruskal-Wallis)	P=0.5809
Mann-Whitney saline vs ASO+Givi	P=0.5350
Mann-Whitney saline vs Givi	P=0.3176

Figure S3: Effect of Givinostat on serum transaminases level

Quantification of transaminases in the serum of *mdx* mice treated with PBS (Saline), ASO+Givinostat or Givinostat alone: alanine aminotransferase (ALT), aspartate aminotransferase (AST), N=7 mice per group. Statistical analysis was performed using two different tests as reported in the tables: One-way Anova and Mann-Whitney test for the comparison two per two.

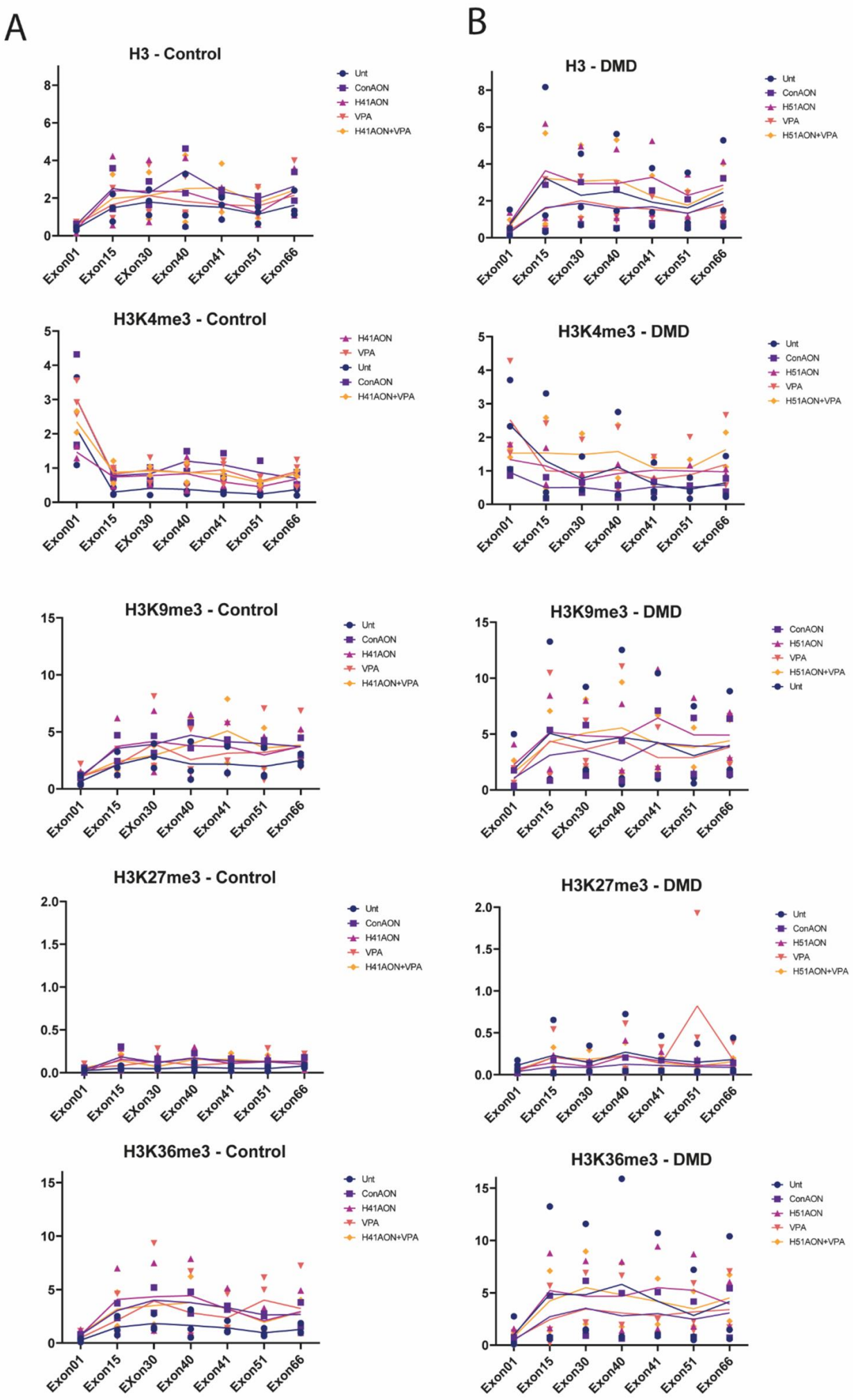
A
B
H3 - Control
H3 - DMD
H3K4me3 - Control
H3K4me3 - DMD
H3K9me3 - Control
H3K9me3 - DMD
H3K27me3 - Control
H3K27me3 - DMD
H3K36me3 - Control
H3K36me3 - DMD
Unt
ConAON
H41AON
H51AON
VPA
H41AON+VPA
H51AON+VPA
Exon01
Exon15
EXon30
Exon40
Exon41
Exon51
Exon66

Figure S4: Effect of valproic acid on chromatin organization

Additional ChIP-qPCR data of healthy control cells (A) or DMD-patient cells (B). ChIP-qPCR analysis of the histone marks H3, H3K4me3, H3K9me3, H3K27me3 and H3K36me3 at various locations in the *DMD* locus in immortalised myocytes are shown as indicated. Cells were untreated (Unt), treated with a control ASO (targeting NOTCH3 (Con)), ASOs inducing exon skipping of *DMD* exon 41 (H41), *DMD* exon 51 (H51), valproic acid (VPA), or a combination of ASOs and VPA as indicated. Enrichment of histone marks was normalized to input chromatin. N= 3 experiments.

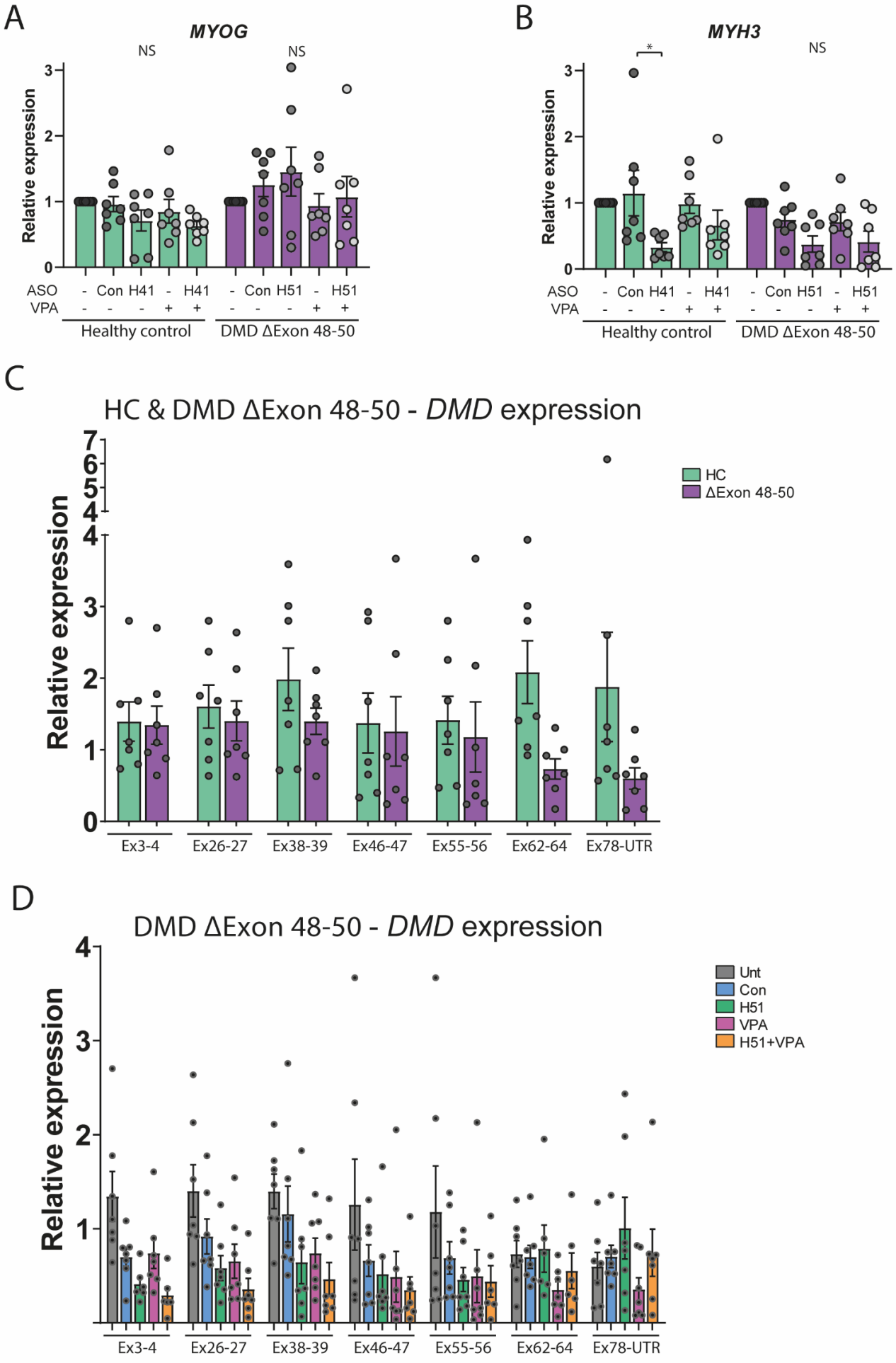
A
MYOG
NS
NS
Relative expression
ASO - Con H41 - H41 - Con H51 - H51
VPA - - - + + - - - + +
Healthy control
DMD ΔExon 48-50
B
MYH3
*
NS
Relative expression
ASO - Con H41 - H41 - Con H51 - H51
VPA - - - + + - - - + +
Healthy control
DMD ΔExon 48-50
C
HC & DMD ΔExon 48-50 - DMD expression
Relative expression
HC
ΔExon 48-50
Ex3-4
Ex26-27
Ex38-39
Ex46-47
Ex55-56
Ex62-64
Ex78-UTR
D
DMD ΔExon 48-50 - DMD expression
Relative expression
Unt
Con
H51
VPA
H51+VPA
Ex3-4
Ex26-27
Ex38-39
Ex46-47
Ex55-56
Ex62-64
Ex78-UTR

Figure S5: Myogenic potential and dystrophin RNA expression in DMD cells

(A) RT-qPCR analysis of the expression of *MYOG* (A) or *MYH3* (B) in myotube samples corresponding to the samples presented in figures 5A and 5C. Gene expression was normalized to housekeeping genes *GUSB* and *GAPDH*. *: P<0.05, NS: Not-significant – Kruskal-Wallis test. (C) RT-qPCR data for various *DMD* exon junctions as indicated in healthy control and DMD patient cells. Gene expression was normalized to housekeeping genes *GUSB* and *GAPDH*. (D) RT-qPCR data for various *DMD* exon junctions as indicated in DMD-patient cells. Gene expression was normalized to housekeeping genes *GUSB* and *GAPDH*.

Table S1: primers used (RT-qPCR, RT-PCR and ChIP-qPCR)

Name:	Forward 5'-->3' Sequence:	Reverse 5'-->3' Sequence:	Gene symbol
RT-qPCR_cDNA-GUSB	CCGAGTGAAGATCCCCTTTTTA	CTCATTTGGAATTTTGCCGATT	GUSB
RT-qPCR_cDNA-GAPDH	CTCTGCTCCTCCTGTTCGAC	ACGACCAAATCCGTTGACTC	GAPDH
RT-qPCR_cDNA-MYOG	GCCAGACTATCCCCTTCCTC	GGGGATGCCCTCTCCTCTAA	MYOG
RT-qPCR_cDNA-MYH3	CCTGCTGGAGGTGAAGTCTC	GATTGCAGGATCTGGTGGAT	MYH3
RT-qPCR_cDNA DMD exon 03-04	gggaagcagcatattgagaac	gggcatgaactcttgtggat	DMD
RT-qPCR_cDNA DMD exon 26-27	aagatctatcagagatgcacg	gttgggcctcttctttagctct	DMD
RT-qPCR_cDNA DMD exon 38-39	attgcttgaaccactggagg	TTTACAGTACCCTCATTGTCTTCAT	DMD
RT-qPCR_cDNA DMD exon 46-47	gttttatggttggaggaagcagat	gagcacttacaagcacggg	DMD
RT-qPCR_cDNA DMD exon 55-56	caggatgctacccgtaagga	cgtctttgtaacaggactgc	DMD
RT-qPCR_cDNA DMD exon 62-64	gccaaacaaagtgccctacta	ctgagaatctgacattattcagg	DMD
RT-qPCR_cDNA DMD exon 78-UTR	cctggaaagccaatgagaga	gcgggaatcaggagttgtaa	DMD
RT-PCR - DMD Exon40-42	GGCTCTAGAAATTTCTCATCAGTG	ggcatgtcttcagtcatcac	
RT-PCR - DMD Exon47-52	cccataagcccagaagagc	tctagcctcttgattgctgg	
ChIP-qPCR - DMD_Exon1	AAGCTGCTGAAGTTTGTTGG	TCTTCCCACCAAAGCATTTT	
ChIP-qPCR - DMD_Exon15	ccttttagtgcatggctttc	GGCCAGTTTTTGAAGACTTGAT	
ChIP-qPCR - DMD_Exon30	AGTCTGCCCAGGAGACTGAA	CGTCCACCTTGTCTGCAATA	
ChIP-qPCR - DMD_Exon40	GGCTCTAGAAATTTCTCATCAGTG	ATTTTCCTTTCATCTCTGGGC	
ChIP-qPCR - DMD_Exon41	GATCGGGAATTGCAGAAGAA	ATCTGAGTTGGCTCCACTGC	
ChIP-qPCR - DMD_Exon51	ggcttggacagaacttaccg	cttctgcttgatgatcatctc	
ChIP-qPCR - DMD_Exon66	gaggatccgtgtcctgtctt	tttacacagggaaatgatgcc	

Table S2: Antibodies used

Antibody:	Supplier (Cat. Nr.)	Dil. WB	Dil. ChIP
Histone H3	Abcam - Ab1791	N/A	2.5 µl for 3 µg Chromatin
H3K4me3	Millipore - 17-614	N/A	3 µl for 3 µg Chromatin
H3K9me3	Abcam - Ab8898	N/A	1.5 µl for 3 µg Chromatin
H3K9Ac	Abcam - Ab4441	N/A	2 µg for 3 µg Chromatin
H3K27me3	Millipore - 17-622	N/A	4 µl for 3 µg Chromatin
H3K36me3	Diagenode - C15410058	N/A	2.2 µl for 3 µg Chromatin
IgG control	Cell signaling - 2729S	N/A	1.5 µl for 3 µg Chromatin
Rabbit anti Dystrophin	Abcam - Ab154168	1:2000	N/A
Mouse anti Tubulin	Sigma-Aldrich - T6199	1:5000	N/A
N/A: Not applied for technique.			

To confirm data obtained during the 4-week study performed in *mdx* mice, a long term study was performed. During this protocol, mice were weekly injected with TC-DNA ASO during 12 weeks and were treated with VPA 5 times per week during 1 month, followed by 3 times per week during the second month and 1 time per week the last month (**Figure 13**A). The number of VPA injections was decreased over time because of its accumulation and to avoid potential toxicities. VPA's half-life is estimated between 11 and 20 hours in tissues (Bentué-Ferrer et al. 2010), so the drug is eliminated at 99% after 3.2 to 5.8 days.

Two weeks after the last injection of TC-DNA, mice were sacrificed and tissues were collected. The ASO biodistribution study performed in muscles and off target organs confirmed the data obtained in the 4 weeks study with a decreased accumulation in the kidney but we also found here higher amount of ASO in the heart compared to treatment with ASO alone (**Figure 13**B). The quantification of exon skipping revealed higher levels in all muscles examined appart from the diaphragm after treatment with ASO+VPA as compared to treatment with ASO alone (**Figure 13**C). This effect on RNA was confirmed with the quantification of dystrophin restored in the tissues (global *P-value*<0.0001 ASO+VPA *vs* ASO) (**Figure 13**D). The heart had the highest level of dystrophin restoration (2-fold increase compared to ASO alone) and no difference was found between the 2 treatments in the diaphragm. We then investigated the effect of VPA on the imbalance phenomena and quantified the level of dmd RNA at the various exon junctions (**Figure 13**E). In contrast with the results obtained in the 4-week study, no significant differences emerged in diaphragm, triceps or heart. We could only detect slightly higher levels of transcripts in the heart of ASO+VPA compared to *mdx* or ASO alone, but the trend was not statistically significant.

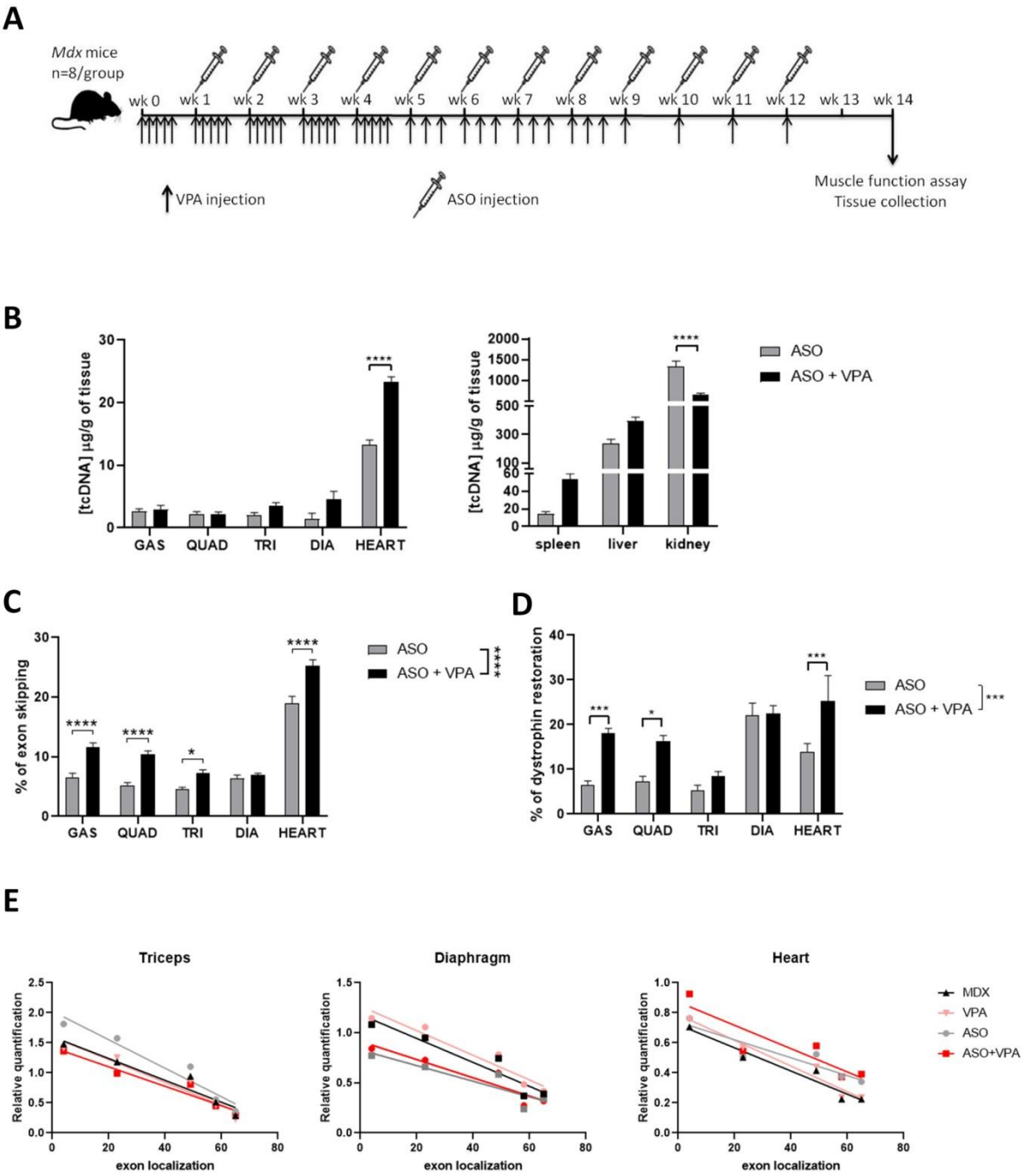

Figure 13. Long term treatment with VPA increases exon skipping efficacy

(A) Schematic representation of the *mdx* treatment with ASO combined with valproic acid (VPA). (B) Effect of VPA on the TC-DNA distribution in various organs. (C) Effect of VPA on exon skipping level. (D) Dystrophin restoration in *mdx* mice treated with ASO or ASO+VPA. (E) Effect of the combination VPA+ASO on Dmd transcript imbalance in the triceps, diaphragm, and heart analyzed by taqman qPCR at different exon junctions.

Tibialis anterior (TA), gastrocnemius (GAS), quadriceps (QUAD), triceps (TRI), diaphragm (DIA). N=7 mice per group, Two-way ANOVA analyzes. *p<0.05, **p<0.01, ***p<0.001, ****p<0.0001.

Dystrophin restoration and correct localization were also confirmed by immunostaining performed on muscles cryosections (**Figure 14**A). Compared to the treatment with ASO alone, the intensity of the dystrophin staining was higher in heart and triceps from VPA co-treated mice compared to ASO treated mice (+177% and +12% respectively).

It has been previously demonstrated that the serum level of two fragments of the myofibrillar structural protein myomesin-3 (MYOM3) can be used to evaluate the efficacy of a treatment (Relizani et al. 2022). We therefore evaluated the level of MYOM3 in serum of treated and control mice after the treatment. Levels of MYOM3 in the serum was significantly decreased by 90% following ASO treatment (*P-value* < 0.0001) and by 94.2% following ASO+VPA combined therapy (*P-value* < 0.0001) compared to the untreated mice (**Figure 14**B). There was no difference between the mice treated with ASO+VPA and the ones treated with ASO only (*P-value* =0.2287), which may be explained by the already maximal effect of the ASO treatment (leaving not much space for further improvement).

To evaluate the functionality of the dystrophin restored in muscles, the maximal specific force and resistance to eccentric contraction were measured. Tibialis anterior muscles from control *mdx* mice showed a decrease of 40% in maximal specific force compared to the wild type muscle (**Figure 14**C left). Treatment with ASO combined with VPA improved the maximal specific force compared to control *mdx* mice (*P-value* = 0.0197).

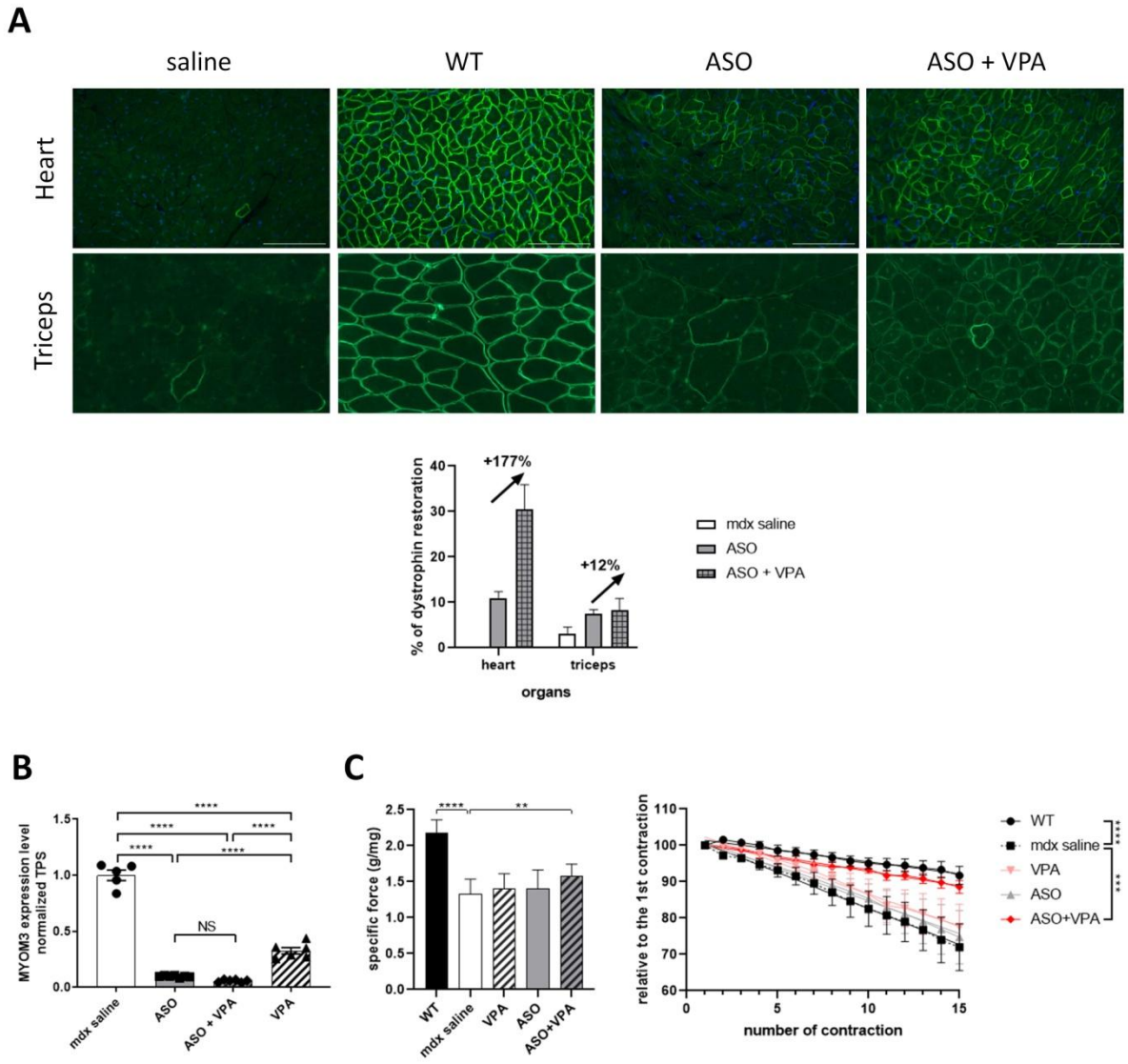

Figure 14: Functional recovery following the combined therapy VPA + ASO

(A) Dystrophin staining in triceps and heart. Top: Detection of dystrophin protein (green staining) by immunostaining on transverse sections of muscle tissues (triceps and heart) from WT and *mdx* mice treated with saline, ASO, VPA or ASO+VPA. Nuclei are labelled with DA PI (blue staining). Scale bar, 100µm. Bottom: Quantification of the dystrophin intensity staining in heart and triceps N=4 mice per group. (B) Myomesin level in serum of mice. Quantification performed by western blot. N=7 mice per group. (C) Maximal specific force (left panel) and percentage of force drop following a series of eccentric contractions (right panel) measured on semi-isolated tibialis anterior muscles from treated *mdx* mice. N=7 mice per group, Two-way ANOVA analyzes. *p<0.05, **p<0.01, ***p<0.001, ****p<0.0001.

Moreover, TA muscles from control *mdx* mice were unable to sustain tetanic tension, falling to 72% of their initial force after fifteen eccentric contractions (**Figure 14**C right). The bi-therapy significantly improved the resistance to tetanic contractions since treated TA muscles maintained 89% of their force following the eccentric contractions (*P-value* = 0.0005).

Safety pharmacological evaluation is a crucial aspect in the development of a new drug or new medical practice. We used this long term study to perform a preliminary assessment of the safety profile of the bi-therapy, in particular focussing on hepatotoxicity and nephrotoxicity which are most frequently found. The serum levels of various general biomarkers in mice were analyzed. The serum levels of transaminases (ALT and AST, biomarkers of liver toxicity) were lower in ASO treated mice, which is a consequence of the efficacy of the treatment. Apart from these positive effects resulting from the improved dystrophic pathology of treated *mdx* mice, we observed no significant difference in bilirubin, alkaline phosphatase (ALP), albumin, creatinine and urea of treated mice compared to *mdx* control mice (**Figure 15**A). The only toxicity we found was an elevation of the serum creatine kinase (CK) in VPA treated mice, a side effect already described in human patients treated with VPA (Gokcay, Kirlioglu, and Balcioglu 2020) and which may be due to a too high dose exposure of the drug.

In order to investigate further the potential renal toxicity of the bi-therapy, several biomarkers were examined in the urine of the treated mice. Urine were collected during the 24h following the last injection and levels of total protein and albumin were measured and normalized to creatinine levels (**Figure 15**B). No changes in normalized total protein levels were found after treatment. Urinary albumin levels appeared elevated in *mdx* mice compared to the WT ones. The levels were normalized by the TC-DNA ASO treatment (P-value 1=0.0350) but slightly increased by VPA (although not significantly, P-value= 0.0583).

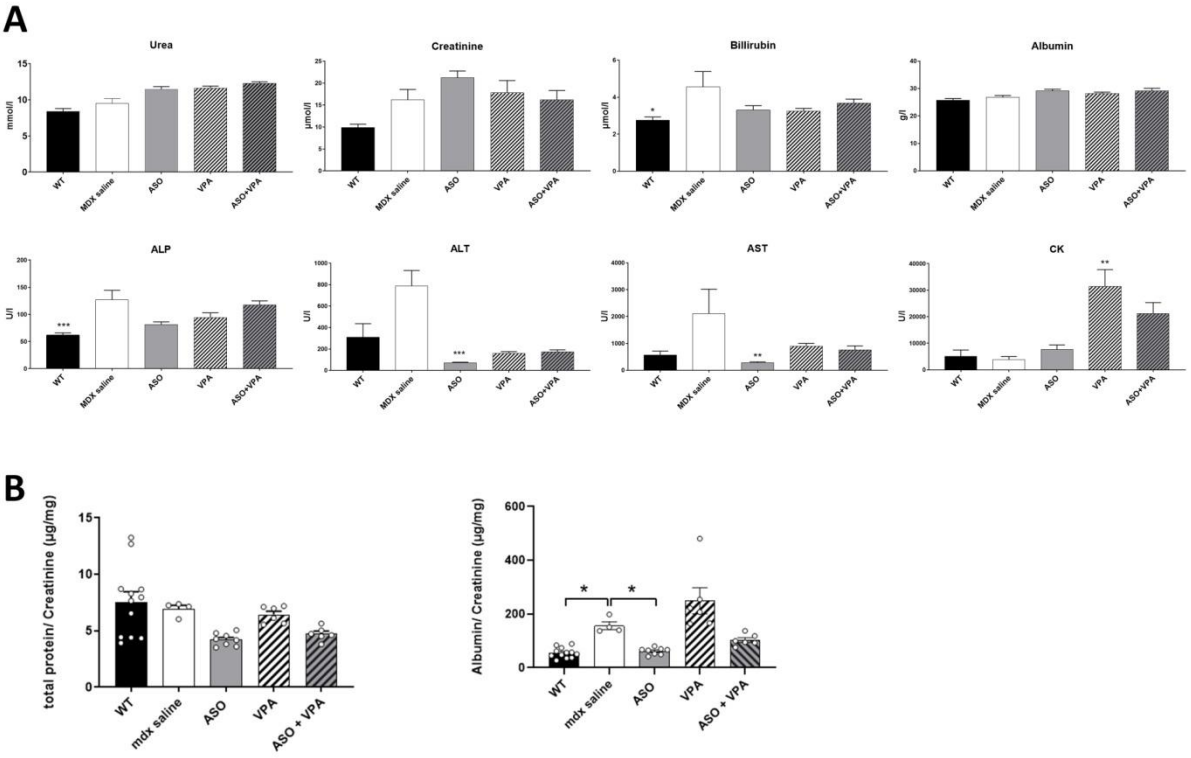

Figure 15: Toxicity evaluation of the combination VPA + ASO

(A) Quantification of general toxicity biomarkers in the serum: creatinine, urea, albumin, aspartate aminotransferase (AST), Alanine aminotransferase (ALT), alkaline phosphatase (ALP) and bilirubin. N=7 mice per group, *P<0.05**, p<0.01, ***p<0.001 compared to *mdx* saline, analyzed by Kruskal-Wallis. (B) Quantification of general toxicity biomarkers in the urine N=7 mice per group, Two-way ANOVA analyze. *p<0.05.

DISCUSSION

The overall objective of my thesis was to improve exon skipping therapy for the treatment of Duchenne muscular dystrophy. To this end, I focused my research on combined therapies and evaluated molecules with three different mechanisms. The first one aimed to improve the distribution of the ASO in the target tissus by inhibiting its renal clearance, the second one used an endosomal escape activator to modulate the ASO's intracellular trafficking and increase the quantity of ASO in the nucleus and the last mechanism aimed at correcting the imbalance phenomena and produce more dystrophin RNA in the target cells.

The discussion of the results obtained with all these methods will be divided in two sections:

- the first will recall the context and objectives of each of the studies and will discuss the mains results obtained
- the second will discuss the more general aspects of my thesis projetcs and will put the results into perspective.

Inhibition of organic anion transporter to increase tricyclo-DNA mediated exon-skipping efficacy in the *mdx* mouse model

ASO-mediated exon skipping therapy has made a lot of progress in the treatment of DMD and has led to the approval of four drugs by the FDA and the Japanese health authority but not by the European authority due their poor efficacy. One of the hypothesis that could explain the low benefit of these drugs may be their fast renal clearance. Indeed, approved ASO are fastly excreted in urine as unmodified drug, with the largest amount excreted during the first 4 hours after a patient's infusion is started (Wagner et al. 2021). In this study we sought to delay this elimination in order to allow time for the ASOs to diffuse into the target organs.

One method used to delay the ASO's elimination is to bind ASO with peptides. Vesleteplirsen developped by Sarepta Therapeutics uses this method and is currently tested in clinic. Unfortunately, the peptides used to improve the ASO distribution are charged; therefore they

can not be link to charged ASO (like TC-DNA). The second family of molecules that we may use to delay the elimination of ASOs and to improve their distribution in the target tissues are the fatty acids. To this end, palmitic acid has already been conjugated to TC-DNA and shown to improve the therapeutic index (Relizani et al. 2022). Still, 20% of the palm conjugated TC-DNA ASO are eliminated in the urine during the first 40 hours post injection. To understand how the TC-DNA ASO linked to the plamitic acid are eliminated in the urine, we investigated its localization in the kidney. Histological stainings performed with a fluorescent complementary probe showed that the ASO is especially found in the proximal convoluted tubules of the kidney. This localization is in line with the renal elimination process of the ASO because most of organics anions are transfered from the blood to the urine in the convoluted tubules (Dresser, Leabman, and Giacomini 2001). This tubular secretion of the anion molecules is mainly performed by the OATs which are localized at the basolateral membrane of renal epithelial cells (the membrane in contact with the blood). The co-localization obtained between the TC-DNA ASOs and the OAT channel (OAT1) in the kidney seems to confirm this way of elimination. Therefore, we hypothesized that inhibition of OATs may enhance biodistribution and delay renal elimination of TC-DNA ASOs. To test this hypothesis, we have treated mice with a combination of palm-TC-DNA ASO and probenecid (a competitive inhibitor of all OAT channels).

Unfortunaltely, the analysis of ASO biodistribution performed at both early time point (24h post 1 injection) and mid time point (2 weeks post 4 injections) as well as the exon skipping efficacy analyzed at mid time point showed that probenecid did not significantly improve TC-DNA ASO mediated exon skipping therapy. In parralel, immunostaining of TC-DNA ASO in the kidney showed more ASO accumulated in the Bowman's capsule. Bowman's capsule is involved in almost 10% of the renal anion molecule elimination process (Dresser, Leabman, and Giacomini 2001). An increasing level of TC-DNA ASO in this localization may be a compensation process of the OAT inhibition (normal one or toxic one). The failure of blocking OAT to improve ASO therapy might be caused by this process. Furthermore, a renal toxicity study should be performed to investigate the possibility of a nephrotoxicity process as underlying cause of the TC-DNA accumulation in the Bowman's capsule. The accumulation of TC-DNA ASO in the Bowman's capsule observed with the bi-therapy shows that TC-DNA ASO

are not eliminated by passive transfer from the blood to the urine in the glomerulus before their reabsorption in the proximal convoluted tubules (as first generation PS-ASO may be (Engelhardt 2016)). Indeed, if the ASO were eliminated in the glomerulus, probenecid would have increased their eliminination by bloking the OAT channels involved in the reabsoption of the anion in the kidney. It is by this mechanism of action that probenecid increases uric acid elimination in the kidney and treats gout (Pui, Gow, and Dalbeth 2013).

The general biodistribution of TC-DNA shows that the liver is the second off target organ where the ASO are accumulated. In this study, we did not investigate the localization of the ASO in this organ because we did not aim to modify it but the histological results obtained in the kidney and the fact that OAT3 transporter is also present in the liver make this analysis relevant. Indeed, OAT3 is with OAT1 one of the main transporter involved in the kidney tubular secretion of the anion's molecule but it also plays a central role in the movement of bile acid through the "intestinal-liver-kidney" axis and is involved in the absorption, metabolism, and excretion of bile acids (Li et al. 2019). The inhibition of OAT3 by the probenecid may have impacted the ASO distribution in the liver tissue with an accumulation in other cells type (like in hepatocytes).

In conclusion, OAT inhibition failed to improve exon skipping therapy in the muscle but changed the ASO distribution in the kidney (and maybe in the liver too). Other investigations are needed to elucidate whether its new localization is linked to toxicity or not and whether this combined therapy may be used to improve the treatment of renal or liver diseases.

Oligonucleotide enhancing compound increases tricyclo-DNA mediated exon-skipping efficacy in the *mdx* mouse model

During our first study, we tried to improve ASO biodistribution to tissues, which is one of the first causes for the low efficiency of ASOs in clinic. To reach this objective in liver, some ASOs have been conjugated to an N-Acetylgalactosamine, a sugar wich binds to trimeric asialoglycoprotein receptors in the liver. By this method, a large number of ASO manage to

enter the hepatocytes. Unfortunately, cell penetration occurs through the endosomal pathway and less than 0.01% of ASOs manage to escape from endosomes to reach their targets (Dowdy 2017). In this study, we therefore focused on this second limitation of ASO efficacy and we tried to improve the endosomal escape of the molecules with an endosomal escape promotor: UNC7938.

UNC7938 is a 3-deazapteridine analog developped at the university of North Carolina (Yang et al. 2015). In contradistinction to the 'proton sponge' effect, which physically disrupts lysosomes and late endosomes due to pH changes and swelling, UNC7938 acts on a specific target in the endomembrane system (Yang et al. 2015). Indeed, UNC7938 preferentially destabilizes the membrane of late endosomes by binding to lysobisphosphatidic acid (Allen et al. 2019; Juliano 2021), a lipid found predominately in late endosome membrane and involved in the endosomal escape of molecules like cholesterol (Chevallier et al. 2008).

After 4 weeks of treatment, the combined ASO+UNC7938 induced significantly higher exon skipping level (1.59 fold-change) and dystrophin restoration levels (2.75 fold-change) in the heart compared to ASO therapy alone. Moreover, the quantification of cellular (which combined endosomal and cytoplasmic fraction) and nuclear amount of ASO performed on skeletal muscle has shown a higher quantity of TC-DNA ASO in the nucleus of mice treated with the combined therapy. These results may be in line with our hypothesis that UNC7938 treatment may decrease the quantity of ASO trapped in the endosome (almost 99% of the ASO as previously discussed). Indeed, by increasing the ASO quantity in the cellular cytoplasm, UNC7938 may statistically increase the quantity of ASO which diffuse to the nucleus where their target is located. To investigate the effects of UNC7938 on ASO intracellular distribution, muscles of treated mice have been stained with a complementary fluorescent probe. Unfortunatelly, the amount of ASO localised in muscle cells were under the detection level of our microscope and we did not manage to see the effect of the combined therapy on the cellular trafficking of the ASO at the histological level.

To investigate whether higher dystrophin restoration was stable with time, we performed a kinetics study and euthanized mice from 72h to 6 weeks post treatment. The quantification of ASO in different tissues showed that ASO distribution is not affected by UNC7938 at the very early time point (72h). Between 1 and 3 weeks post treatment, ASOs seem to be less degraded / eliminated when the oligonucleotide enhancing compound is administered. This data may be linked to a higher quantity of ASO released in the cytoplasm before their degradation in the lysosomes. To confirm this hypothesis, we have monitored ASO activity by qPCR. The quantification of exon-skipping levels shows that UNC7938 has a strong booster effect on ASO therapy especially in the early time points. Indeed, the amount of corrected mRNA is significantly increased at the early time point (4.40 fold change in the heart at 72h post treatment) but not at 6 weeks post treatment. Quantification of dystrophin restoration level has shown the same trend than exon skipping level with an improvement of the treatment at the early time point and no effect after 6 weeks. This result may be explained by the ''depot effect'' which takes place during ASO therapy (Dowdy et al. 2022). This phenomenon is characterized by a slow release of the ASO accumulated in the endosomes. That way, a small quantity of ASO diffuses in the cytoplasm and goes in the nucleus of the cell several weeks or months after the injections. This phenomenon is believed to contribute to the maintenance of ASO therapeutic effect over time. By increasing the endosomal escape, we boosted the early effect of the ASO (as shown during the first time points of the kinetic) but we have reduced the "endosomal stock" of ASO. By consequence, the ''depot effect'' was reduced/suppressed and the maintenance of effects on RNA (exon skipping level) was lost with time.

During our preliminary study of 4 weeks of treatment, we saw a significant effect of UNC7938 to improve the ASO efficacy in the heart. To investigate the consequences of this improvement in the heart and to ensure that the benefit of the combined therapy still exists after a longer time of treatment (even if we lost the ''depot effect''), we performed a 12 weeks study. This study was performed on older mice to allow the functional analysis of the heart, since cardiac symptoms only start at six months of age in *mdx* mice). One week after the end of the treatment, heart function was monitored and two week after the end of the treatment tissues were harvested to perform molecular analysis.

In contrast with results observed during the preliminary study, exon skipping levels analysed at the end of the long term study were similar between the two groups of mice (mice injected with TC-DNA alone or in combination with UNC7938). This result may be explained by a higher level of corrected mRNA (so less place to improve it) and by a suboptimal time point for RNA analysis. Indeed, during the kinetics, we saw that the highest effects on exon skipping level were obtained during the earliest time points and were lost after few days. The time point we chose was optimized to measure the protein restoration level but not the exon skipping one.

Analysis of dystrophin restoration showed an effect of UNC7938 especially in the heart (+31%), the diaphragm (58%) and the triceps (+82%). This effect of high dystrophin restoration level in the heart, although not statistically significant, was very promising. To evaluate the localization of the expressed protein, we performed an immunostaining in the triceps muscle and heart. The dystrophin localisation was correct in both groups of mice (treated with ASO alone or in combination with UNC7938) and the mean intensity was higher with the combined therapy; which confirms the effects observed by western blot.

Finally, we investigated the heart function by electrocardiography which revealed that the untreated *mdx* mice (saline group) had alterations of Tei index, systolic pulse pressure, left ventricular ejection fraction and fractional shortening. Mice treated with the combined therapy presented a significant improvement of the heart function with almost no detectable symptoms (no statistical differences were found with the WT group for all parameters). Mice treated with TC-DNA ASO alone had less severe symptoms but the differences with the saline group were not significant. Mice treated with UNC7938 only were as sick as the saline *mdx* which proves that effects obtained with the combined therapy was not caused by intrinsic effect of UNC7938 in the heart but by the improvement of the ASO mediated therapy.

Molecular and functional effects obtained with the combined therapy UNC7938 and TC-DNA ASO are very interesting and should be put into perspective with the main cause of death of

DMD patients, which is cardiac dysfunction (cardiomyopathy). Being able to restore heart function may truly increase their life expectancy but, to achieve this objective we should ensure that this new combined therapy does not increase the toxicity as well. By consequence a toxicity study of each compound and of their combination should be performed before entering in clinic. Indeed, the main limitations of endosomal escape enhancers are their toxicity. The first molecules used to increase endosomal escape were not specific to the endosomes and led to the disruption of lysosomes which is known to cause activation of the inflammasome and generation of inflammatory mediators and cell death (Dowling and O'Neill 2012). To avoid this toxicity, some molecules that do not disrupt lysosomes (or less) were tested like melittin which forms a pore through the cell membrane or dynamic polyconjugate polymers which lyses the entire endosomes by modifying their pH. Both molecules have shown high cytotoxicity and their development stopped (Dowdy et al. 2022). To ensure that our combined therapy is not as toxic as the other endosomal escape enhancers, we performed a preliminary toxicity study. Various biomarkers were measured in both serum and urine and the histopathological profile of the liver and kidneys was studied in mice treated for 12 weeks. No toxicity was found during this study, which is a good sign for future clinical development of a combined therapy: ASO with endosomal escape promotor.

As we saw during the kinetic study, UNC7938 boosts the efficacy of our ASO during the early time point but reduces/cancels the ''depot effect'' of the ASOs. In order to decrease the toxicity mediated by a combined therapy and to preserve the ''depot effect'' of the ASO; effect which may be important for the long term efficacy of the ASO or to delay the time between two injections, an additional study would be useful. In this study we should analyse when the maximal level of skipped RNA is obtained (after how many injections) in order to stop the UNC7938 co-treatment after this point and use the ''depot effect'' to maintain the effect as long as possible. That way, patients will have a maximum level of protein restoration as fast as possible; which is important to stop the evolution of the disease; and a longer period of time between injections (with the "depot effect") so less toxicity and side effects induced by repeated injections.

Histone deacetylase inhibitors improve antisense-mediated exon skipping efficacy in *mdx* mice

During our first studies, we tried to improve the *in-vivo* distribution of ASOs (in the target organs or in cells with endosomal escape promotor), which is one of the first cause of the low efficiency of ASOs in clinic. In this study we did not focus on ASO distribution but we tried to modulate the expression of the *DMD* gene to increase the protein restoration level. For that purpose, three histone deacetylase inhibitors have been tested: givinostat (a pan HDACi), valproic acid (class I/IIa HDACi) and EX527 (class III HDACi).

The analysis of DMD transcript profile in muscle biopsies of 11 BMD patients carrying heterogeneous mutations within the DMD gene has shown a significant reduction in DMD transcript levels toward the end of the gene in three patients (Hamed et al. 2005). This phenomenon is called imbalance and is characterized by a reduced dystrophin RNA quantity produced from the 5′ to the 3′ end of the sequence. The causes of the imbalance phenomenon are unclear but it seems to be independent of the mutation in the *DMD* gene (BMD patients have no premature stop codon in the mRNA sequence and the 3 patients of the study had different mutations). In the same time, the three patients showed a reduced production of dystrophin protein, which may be linked to the reduced production of full-length dystrophin RNA (Hamed et al. 2005). The transcript imbalance phenomenon has been characterized in skeletal muscle and heart of WT and *mdx* mice and has been shown to be more severe in *mdx* mice (Spitali et al. 2013). In another study performed on *mdx* mice, it has been shown that this phenomenon increases with age (with a more severe imbalance phenomenon in mice of 10 months compared to the ones of 2 months of age) and is linked to a modification in histone conformation on the dystrophin gene (García-Rodríguez et al. 2020). Moreover, this study was the first to show a beneficial effect of HDACi for the correction of the imbalance phenomenon.

During our *in-vitro* study performed on human myocytes, we observed an increase in H3K9 acetylation levels of the DMD gene upon treatment with a combination of ASO and VPA as

assessed by ChIP-qPCR. During the 4-week study performed in *mdx* mice, the quantification of dystrophin mRNA level confirmed the data obtained in vitro and showed an increased level of transcripts in VPA co-treated muscles. These results are in line with our hypothesis that HDACi could increase the level of *Dmd* transcript and ultimately improve the exon-skipping approach efficacy. Surprisingly, the effects of VPA on the imbalance phenomenon were not found in the long term study. This result may be the consequence of the reduction of the dose of VPA injected over time and/or of the short half-life of the DMD mRNA. Indeed, compared to its transcription which takes 16 hours, the half-life of the dystrophin mRNA is very short in muscles of *mdx* mice: only few hours (Hildyard et al. 2020). The objectives of our *in-vivo* studies were to investigate the effects of HDACi on ASO mediated exon skipping efficacy, on protein restoration level and (for the long term study) on muscle function. For these reasons, the time point of "2 weeks after the end of the treatment" was selected. However, to specifically study the impact of VPA on dystrophin mRNA production, a subsequent study with mice analyzed just after the last injection of VPA would be needed.

The combined ASO+givinostat and ASO+VPA treatment induced significantly higher dystrophin restoration levels than ASO therapy alone (1.7 and 1.4 fold respectively after 4 weeks of treatment) as detected by western blot. Restoration of dystrophin was also confirmed by immuno-histochemistry which did not reveal more dystrophin positive fibers in muscles from HDACi co-treated mice but rather higher intensity of staining. This result suggests that the increase in dystrophin recovery is a consequence of higher intracellular levels of dystrophin rather than higher number of cells expressing dystrophin. This is in line with our hypothesis that HDACi treatment may increase available mRNA (leading to increased dystrophin production in each targeted nucleus) rather than having an impact on ASO biodistribution which would have led to more dystrophin positive fibers.

To investigate whether higher dystrophin restoration could have been due to unexpected higher uptake of ASO in muscle tissues, we examined ASO biodistribution after combined therapies. After 4 weeks of treatment, ASO amount in target muscle tissues was not altered by any of the HDACi. Unexpectedly, a higher level of ASO was found in heart of mice treated with VPA + ASO during 12 weeks. This phenomenon might be linked to the high restoration

level of dystrophin obtained with the combined therapy. The production of dystrophin may indeed decrease the local inflammation caused by the muscle fibrosis and decrease the recruitment of inflammatory cells. Inflammatory cells may degrade the ASO before penetration into the heart cells. Further studies will be required to determine the underlying mechanisms.

VPA treatment reduced the amount of ASO accumulated in kidneys too. Since more ASO were found in the urine of VPA treated mice, we hypothesize that this decrease in ASO accumulation in the kidney maybe caused by higher renal clearance. While further work will be required to determine the underlying mechanisms, this represents an interesting advantage for the combined ASO+VPA therapy that shows a 4-fold increase in the benefit/risk ratio.

To investigate whether higher dystrophin restoration obtained with VPA may improve muscle function, we performed an extension study of 12 weeks. During this protocol, the improvement of dystrophin restoration with VPA was confirmed by both western blot and immunohistochemistry but with high variability between muscles. For example, dystrophin was improved by +22% in tibialis anterior and by +175% in gastrocnemius muscles. Tibialis anterior muscle of mice treated with the combination VPA and TC-DNA showed a higher maximal specific force and a higher resistance to eccentric contraction compared to untreated mice. This confirmed the functionality of the restored protein and validated the potential of HDACi to improve ASO therapy. However the low difference in protein recovery obtained between mice treated with ASO or with ASO+VPA cannot explain by itself the difference in functional recovery. We speculate that VPA activates other pathways which help to improve muscle function and decrease muscle damage (like follistatin up-regulation). This would also explain the reduction of myomesine in serum of mice treated with VPA alone, which suggest an beficial effect of VPA treatment on its own.

Inhibition of HDAC2 as well as reconstitution of the dystrophin-NOS signalling has been shown to result in de-repression of follistatin (Colussi et al. 2008). HDACi have also been

shown to decrease fibrosis and promote compensatory regeneration in the *mdx* skeletal muscle through this follistatin up-regulation (Iezzi et al. 2004). In our 4-week study, we only detected a slight and not statistically significant up-regulation of dystrophin RNA production following HDACi treatment, suggesting that increased dystrophin protein expression was not directly linked to its RNA production. We further measured muscle fiber cross sectional area and demonstrated that givinostat indeed significantly increased fiber size area but not VPA. It is possible that the increased level of dystrophin detected in ASO + givinostat treated mice is due to its anti-inflamatory (corticoid like) effects which induce an overall improvement of muscle histopathology and the increase in fiber size. However cross sectional area was not significantly impacted by the VPA treatment suggesting a different underlying mechanism. For that reason, follistatin expression may be monitored in the tissus of mice treated with VPA.

It has recently been reported that HDAC6 is involved in microtubule organization. Its inhibition with HDACi may stabilize the microtubule cytoskeleton network which will protect the muscle against contraction induced injury (Osseni et al. 2022). Since VPA is an inhibitor of HDAC6 (Sixto-López, Bello, and Correa-Basurto 2020), its effect on microtubule cytoskeleton combined with the effect on dystrophin restoration level may also contribute to the muscle function recovery.

Another recent study has shown that HDACi have an influence on the activity of other cell types that are present in muscle tissue, such as fibro-adipogenic progenitors and muscle stem cells. The altered microenvironment influenced by HDACi might improve muscle regeneration, decrease local inflammation, and induce extra cellular matrix remodeling (Consalvi et al. 2022). This effect may result in improved recovery of ASO-induced dystrophin protein and/or muscle function.

Valproic acid has its own intrinsic effect on the muscle which are independent of its HDACi effects (like givinostat and its corticoid-like effects). It has been shown on *mdx; utr*$^{-/-}$ mice that VPA activate Akt pathway which plays a central role in inhibiting muscle apoptosis.

Futhermore, VPA increases myofiber integrity that leads to less damage and thus less inflammation (less CD8-positive inflammatory cells) in muscle and this eventually results in decreased fibrosis (Gurpur et al. 2009). This effect of VPA may explain the decrease level of MOYM3 observed in serum of mice treated with VPA alone.

Our results showed a clear beneficial effect of VPA on the recovery of functional dystrophin protein in *mdx* mice after exon skipping, and confirmed that treatments with VPA have a noticeable effect on the chromatin marks present at the DMD locus. This improvement was associated with some toxicity too: an elevation of the serum creatine kinase was found in the serum of mice treated with VPA. This side effect has already been found in human patients treated with VPA and may be due to a too high dose exposure of the drug. Yet this was not associated with pathological liver or kidney function (Gokcay, Kirlioglu, and Balcioglu 2020). The quantification of albumin, creatinine and total protein in urine showed no kidney toxicity. The histopathological profile of liver and kidney in treated *mdx* mice are ongoing to determine and evaluate the potential toxic response within the tissues.

Considering that VPA used in these studies has been approved in clinic, this work provides encouraging data supporting a future combined therapy which could be rapidly translated to the clinic.

General outlook

In this thesis I have tested different strategies to improve ASO based therapy. One of them failed to achieve our objectives (probenecid), but other ones showed more promising results (valproic acid and UNC7938). This work provides encouraging data for the development of a combined therapy for the treatment of DMD especially since TC-DNA ASOs are entering clinical trials. However, further investigations on pharmacokinetic and on toxicity are necessary. For example, the timing of UNC7938 administration after ASO injection should be optimised. It would be interesting to see if it is possible to mix it with ASO in the same syringe to decrease the number of injections for the patients.

In this work, we have shown that VPA improves the efficiency of exon 23 skipping mediated by ASO in *mdx* mice. Indeed, the combined therapy is able to restore more dystrophin in the muscles of *mdx* mice. These molecular effects have led to a partial correction of the muscle phenotype with a significant improvement of the resistance to tetanic contractions. However another therapeutic pathway of VPA has not been investigated in this thesis: the neurological one. Indeed, VPA is an antiepileptic drug that is able to cross the blood brain barrier. Like DMD patients, *mdx* mice have neurological symptoms. Intracerebroventricular injection of ASO combined with VPA therapy may be tested to investigate the effect of VPA in the brain and to detect a potential benefit of the combined therapy for the treatment of the neurological deficits.

Considering that VPA and UNC7938 have two different mechanisms of action, it would be interesting to test the efficacy of the tri-therapy (ASO+VPA+UNC) to further increase ASO treatment efficacy. It is also possible to imagine that ASO may be conjugated with a peptide or a small molecule to increase its biodistribution and cellular trafficking, and at the same time, use an HDACi to increase the production of dystrophin RNA by the cells. All the molecules we tested use different pathways so a combination of two or three molecules is possible. The only limitation may be the toxicity. By consequence toxicity studies should be performed with all drugs (used alone and in combination with ASO) to ensure the safety of the treatment.

Toxicity is one of the most constraining limitations for the development of combination therapy. Indeed, increasing the number of molecules injected leads to enhanced effects of the treatment but increase in toxicity too. This limit is all the more important to take into account when the products have similar toxicological profiles. Indeed, the combined therapy we tested may have increased the toxicity of our ASO by modulating its pharmacokinetic and pharmacodynamic properties. The toxicity of ASO may be divided in three pathways (Andersson 2022):

1. Sequence and hybridization dependent
2. Sequence and hybridization independent
3. Sequence dependent, but hybridization independent

These pathways may be impacted by the co-administration of compounds wich modify the pharmacological activity of the ASOs. The on-target and off-target toxicity which are sequence and hybridization dependents may be increased by endosomal escape promoters or by strategies which increase the quantity of ASO in cells. Indeed, some chemical modifications used to slow the tissue elimination and extended the effect duration of ASOs increased this toxicity (Andersson 2022).

With probenecid, we have tried to decrease the elimination of ASOs and therefore increase the time and the amount of ASOs in circulation. The prolongation of coagulation time and the activation of the alternative complement system are sequence and hybridization independent toxicities of ASO which are dependant of ASO plasma concentration (Andersson 2022). By consequence, increasing circulation time of ASOs may increase the toxicity of ASOs and patients may experience significant drops in blood pressure and vascular inflammation.

With the endosomal escape promoter, we tried to increase the productive fraction of ASO by increasing its quantity into the cells. This cellular accumulation of ASO may also lead to toxicity. Indeed, in the case of gapmer ASO that work via RNase H recruitment, the use of endosomal escape compound increasing the intracellular amount of gapmer ASO may induce an exaggerated RNase H activity resulting from non-selective hybridization (Andersson 2022).

In addition to increasing the toxicity of ASOs, the molecules used in the bi-therapy may be toxic by themselves. During the 12 weeks study experience, we observed an increase level of CK in mice treated with VPA. This effect did not seem to be related to the administration of ASO but was a unique consequence of doses of VPA that were likely too high. Consequently, a combined VPA+ASO therapy should be evaluated with lower doses of VPA.

No specific toxicity was found with UNC7938 (used alone or in combination) during our studies but additional toxicity studies with at least two animal models would be mandatory to

ensure the safety of the combination. Same studies may be done for VPA to investigate the long term toxicity and to ensure that there are no specie dependant toxicities.

In conclusion, all our data showed that chemical modifications of ASO are not the only way to improve exon skipping therapy efficacy. The work of this thesis is in continuity with the current development of ASO technology. The molecules and strategies tested here are currently in full development, with pharmaceutical companies specialized in endosomal escape for example. The development of new generations of ASO by Entrada Therapeutics using this combined approach is only an example among dozens (entrada 2022), but it illustrates the possibilities offered by these optimization strategies; possibilities which will ultimately lead to the developement of more efficient drugs.

REFERENCES

Aartsma-Rus, A, and D Corey
2020 The 10th Oligonucleotide Therapy Approved: Golodirsen for Duchenne Muscular Dystrophy. Nucleic Acid Therapeutics 30(2). Nucleic Acid Ther. https://pubmed.ncbi.nlm.nih.gov/32043902/, accessed January 9, 2023.

Aartsma-Rus, Annemieke, and Arthur M. Krieg
2017 FDA Approves Eteplirsen for Duchenne Muscular Dystrophy: The Next Chapter in the Eteplirsen Saga. Nucleic Acid Therapeutics 27(1): 1–3.

Aartsma-Rus, Annemieke, Maaike van Putten, Paola Mantuano, and Annamaria De Luca
2023 On the Use of D2.B10-Dmdmdx/J (D2.Mdx) Versus C57BL/10ScSn-Dmdmdx/J (Mdx) Mouse Models for Preclinical Studies on Duchenne Muscular Dystrophy: A Cautionary Note from Members of the TREAT-NMD Advisory Committee on Therapeutics. Journal of Neuromuscular Diseases 10(1): 155–158.

Action Duchenne
2022 Results from Italfarmaco's EPIDYS Trial. Action Duchenne. https://www.actionduchenne.org/results-from-italfarmacos-epidys-trial/, accessed December 8, 2022.

Allen, David G., Nicholas P. Whitehead, and Stanley C. Froehner
2016 Absence of Dystrophin Disrupts Skeletal Muscle Signaling: Roles of Ca2+, Reactive Oxygen Species, and Nitric Oxide in the Development of Muscular Dystrophy. Physiological Reviews 96(1): 253–305.

Allen, Jason, Kristina Najjar, Alfredo Erazo-Oliveras, et al.
2019 Cytosolic Delivery of Macromolecules in Live Human Cells Using the Combined Endosomal Escape Activities of a Small Molecule and Cell Penetrating Peptides. ACS Chemical Biology 14(12): 2641–2651.

Alter, Julia, Fang Lou, Adam Rabinowitz, et al.
2006 Systemic Delivery of Morpholino Oligonucleotide Restores Dystrophin Expression Bodywide and Improves Dystrophic Pathology. Nature Medicine 12(2): 175–177.

Ambrósio, C. E., M. C. Valadares, E. Zucconi, et al.
2008 Ringo, a Golden Retriever Muscular Dystrophy (GRMD) Dog with Absent Dystrophin but Normal Strength. Neuromuscular Disorders: NMD 18(11): 892–893.

Amoasii, Leonela, John C. W. Hildyard, Hui Li, et al.
2018 Gene Editing Restores Dystrophin Expression in a Canine Model of Duchenne Muscular Dystrophy. Science (New York, N.Y.) 362(6410): 86–91.

Amoasii, Leonela, Chengzu Long, Hui Li, et al.
2017 Single-Cut Genome Editing Restores Dystrophin Expression in a New Mouse Model of Muscular Dystrophy. Science Translational Medicine 9(418): eaan8081.

Andersson, Patrik
2022 Preclinical Safety Assessment of Therapeutic Oligonucleotides. Methods in Molecular Biology (Clifton, N.J.) 2434: 355–370.

Araki, E., K. Nakamura, K. Nakao, et al.
1997 Targeted Disruption of Exon 52 in the Mouse Dystrophin Gene Induced Muscle Degeneration Similar to That Observed in Duchenne Muscular Dystrophy. Biochemical and Biophysical Research Communications 238(2): 492–497.

Aslesh, Tejal, Esra Erkut, and Toshifumi Yokota
2021 Restoration of Dystrophin Expression and Correction of Duchenne Muscular Dystrophy by Genome Editing. Expert Opinion on Biological Therapy 21(8): 1049–1061.

Avidity Biosciences
2022 Avidity Biosciences Announces Phase 1/2 EXPLORE44™ Trial of AOC 1044 for Duchenne Muscular Dystrophy Mutations Amenable to Exon 44 Skipping. https://www.prnewswire.com/news-releases/avidity-biosciences-announces-phase-12-explore44-trial-of-aoc-1044-for-duchenne-muscular-dystrophy-mutations-amenable-to-exon-44-skipping-301646531.html, accessed January 9, 2023.

Banihani, Rudaina, Sharon Smile, Grace Yoon, et al.
2015 Cognitive and Neurobehavioral Profile in Boys With Duchenne Muscular Dystrophy. Journal of Child Neurology 30(11): 1472–1482.

Barton-Davis, E. R., L. Cordier, D. I. Shoturma, S. E. Leland, and H. L. Sweeney
1999 Aminoglycoside Antibiotics Restore Dystrophin Function to Skeletal Muscles of Mdx Mice. The Journal of Clinical Investigation 104(4): 375–381.

Bengtsson, Niclas E., John K. Hall, Guy L. Odom, et al.
2017 Muscle-Specific CRISPR/Cas9 Dystrophin Gene Editing Ameliorates Pathophysiology in a Mouse Model for Duchenne Muscular Dystrophy. Nature Communications 8: 14454.

Bentué-Ferrer, Danièle, Olivier Tribut, Marie-Clémence Verdier, and pour le groupe Suivi Thérapeutique Pharmacologique de la Société Française de Pharmacologie et de Thérapeutique
2010 Suivi thérapeutique pharmacologique du valproate. Therapie 65(3): 233–240.

Bergsma, Atze J., Erik van der Wal, Mike Broeders, Ans T. van der Ploeg, and W. W. M. Pim Pijnappel
2018 Alternative Splicing in Genetic Diseases: Improved Diagnosis and Novel Treatment Options. International Review of Cell and Molecular Biology 335: 85–141.

Bettica, Paolo, Stefania Petrini, Valentina D'Oria, et al.
2016 Histological Effects of Givinostat in Boys with Duchenne Muscular Dystrophy. Neuromuscular Disorders: NMD 26(10): 643–649.

Betts, Corinne A., Amer F. Saleh, Carolyn A. Carr, et al.
2015 Prevention of Exercised Induced Cardiomyopathy Following Pip-PMO Treatment in Dystrophic Mdx Mice. Scientific Reports 5: 8986.

Betts, Corinne, Amer F. Saleh, Andrey A. Arzumanov, et al.
2012 Pip6-PMO, A New Generation of Peptide-Oligonucleotide Conjugates With Improved Cardiac Exon Skipping Activity for DMD Treatment. Molecular Therapy. Nucleic Acids 1(8): e38.

Biressi, Stefano, Antonio Filareto, and Thomas A. Rando
2020 Stem Cell Therapy for Muscular Dystrophies. The Journal of Clinical Investigation 130(11): 5652–5664.

Bizot, Flavien, Adeline Vulin, and Aurélie Goyenvalle
2020 Current Status of Antisense Oligonucleotide-Based Therapy in Neuromuscular Disorders. Drugs 80(14): 1397–1415.

Bladen, Catherine L., David Salgado, Soledad Monges, et al.
2015 The TREAT-NMD DMD Global Database: Analysis of More than 7,000 Duchenne Muscular Dystrophy Mutations. Human Mutation 36(4): 395–402.

Bourke, John P., Gillian Watson, Francesco Muntoni, et al.
2018 Randomised Placebo-Controlled Trial of Combination ACE Inhibitor and Beta-Blocker Therapy to Prevent Cardiomyopathy in Children with Duchenne Muscular Dystrophy? (DMD Heart Protection Study): A Protocol Study. BMJ Open 8(12): e022572.

Brandsema, John F., and Basil T. Darras
2015 Dystrophinopathies. Seminars in Neurology 35(4): 369–384.

Bremmer-Bout, Mattie, Annemieke Aartsma-Rus, Emile J. de Meijer, et al.
2004 Targeted Exon Skipping in Transgenic HDMD Mice: A Model for Direct Preclinical Screening of Human-Specific Antisense Oligonucleotides. Molecular Therapy: The Journal of the American Society of Gene Therapy 10(2): 232–240.

Brumbaugh, David, Laura Watne, Frederic Gottrand, et al.
2018 Nutritional and Gastrointestinal Management of the Patient With Duchenne Muscular Dystrophy. Pediatrics 142(Suppl 2): S53–S61.

Brun, C., D. Suter, C. Pauli, et al.
2003 U7 SnRNAs Induce Correction of Mutated Dystrophin Pre-MRNA by Exon Skipping. Cellular and Molecular Life Sciences: CMLS 60(3): 557–566.

Buddhe, Sujatha, Linda Cripe, Joshua Friedland-Little, et al.
2018 Cardiac Management of the Patient With Duchenne Muscular Dystrophy. Pediatrics 142(Suppl 2): S72–S81.

Bulfield, G., W. G. Siller, P. A. Wight, and K. J. Moore
1984 X Chromosome-Linked Muscular Dystrophy (Mdx) in the Mouse. Proceedings of the National Academy of Sciences of the United States of America 81(4): 1189–1192.

Bushby, Katharine, Richard Finkel, Brenda Wong, et al.
2014 Ataluren Treatment of Patients with Nonsense Mutation Dystrophinopathy. Muscle & Nerve 50(4): 477–487.

Byers, T. J., H. G. Lidov, and L. M. Kunkel
1993 An Alternative Dystrophin Transcript Specific to Peripheral Nerve. Nature Genetics 4(1): 77–81.

Cai, Aojie, and Xiangdong Kong
2019 Development of CRISPR-Mediated Systems in the Study of Duchenne Muscular Dystrophy. Human Gene Therapy Methods 30(3): 71–80.

Carroll, Kate, Eppie M. Yiu, Monique M. Ryan, Rachel A. Kennedy, and Katy de Valle
2021 The Effects of Calf Massage in Boys with Duchenne Muscular Dystrophy: A Prospective Interventional Study. Disability and Rehabilitation 43(26): 3803–3809.

Chabot, Benoit, and Lulzim Shkreta
2016 Defective Control of Pre-Messenger RNA Splicing in Human Disease. The Journal of Cell Biology 212(1): 13–27.

Chamberlain, J. S., J. A. Pearlman, D. M. Muzny, et al.
1988 Expression of the Murine Duchenne Muscular Dystrophy Gene in Muscle and Brain. Science (New York, N.Y.) 239(4846): 1416–1418.

Chamberlain, Jeffrey S.
2002 Gene Therapy of Muscular Dystrophy. Human Molecular Genetics 11(20): 2355–2362.

Chamberlain, Jeffrey S., Joseph Metzger, Morayma Reyes, DeWayne Townsend, and John A. Faulkner
2007 Dystrophin-Deficient Mdx Mice Display a Reduced Life Span and Are Susceptible to Spontaneous Rhabdomyosarcoma. FASEB Journal: Official Publication of the Federation of American Societies for Experimental Biology 21(9): 2195–2204.

Chapman, V. M., D. R. Miller, D. Armstrong, and C. T. Caskey
1989 Recovery of Induced Mutations for X Chromosome-Linked Muscular Dystrophy in Mice. Proceedings of the National Academy of Sciences of the United States of America 86(4): 1292–1296.

Chevallier, Julien, Zeina Chamoun, Guowei Jiang, et al.
2008 Lysobisphosphatidic Acid Controls Endosomal Cholesterol Levels*. Journal of Biological Chemistry 283(41): 27871–27880.

Cirak, Sebahattin, Virginia Arechavala-Gomeza, Michela Guglieri, et al.
2011 Exon Skipping and Dystrophin Restoration in Patients with Duchenne Muscular Dystrophy after Systemic Phosphorodiamidate Morpholino Oligomer Treatment: An Open-Label, Phase 2, Dose-Escalation Study. Lancet (London, England) 378(9791): 595–605.

Clemens, Paula R., Vamshi K. Rao, Anne M. Connolly, et al.
2020 Safety, Tolerability, and Efficacy of Viltolarsen in Boys With Duchenne Muscular Dystrophy Amenable to Exon 53 Skipping: A Phase 2 Randomized Clinical Trial. JAMA Neurology 77(8): 982–991.
2022 Long-Term Functional Efficacy and Safety of Viltolarsen in Patients with Duchenne Muscular Dystrophy. Journal of Neuromuscular Diseases 9(4): 493–501.

Clerk, A., G. E. Morris, V. Dubowitz, K. E. Davies, and C. A. Sewry
1993 Dystrophin-Related Protein, Utrophin, in Normal and Dystrophic Human Fetal Skeletal Muscle. The Histochemical Journal 25(8): 554–561.

Colussi, Claudia, Chiara Mozzetta, Aymone Gurtner, et al.
2008 HDAC2 Blockade by Nitric Oxide and Histone Deacetylase Inhibitors Reveals a Common Target in Duchenne Muscular Dystrophy Treatment. Proceedings of the National Academy of Sciences of the United States of America 105(49): 19183–19187.

Connuck, David M., Lynn A. Sleeper, Steven D. Colan, et al.
2008 Characteristics and Outcomes of Cardiomyopathy in Children with Duchenne or Becker Muscular Dystrophy: A Comparative Study from the Pediatric Cardiomyopathy Registry. American Heart Journal 155(6): 998–1005.

Consalvi, Silvia, Chiara Mozzetta, Paolo Bettica, et al.
2013 Preclinical Studies in the Mdx Mouse Model of Duchenne Muscular Dystrophy with the Histone Deacetylase Inhibitor Givinostat. Molecular Medicine (Cambridge, Mass.) 19(1): 79–87.

Consalvi, Silvia, Luca Tucciarone, Elisa Macrì, et al.
2022 Determinants of Epigenetic Resistance to HDAC Inhibitors in Dystrophic Fibro-Adipogenic Progenitors. EMBO Reports 23(6): e54721.

Cossu, Giulio, Stefano C. Previtali, Sara Napolitano, et al.
2015 Intra-Arterial Transplantation of HLA-Matched Donor Mesoangioblasts in Duchenne Muscular Dystrophy. EMBO Molecular Medicine 7(12): 1513–1528.

Crisafulli, Salvatore, Janet Sultana, Andrea Fontana, et al.
2020 Global Epidemiology of Duchenne Muscular Dystrophy: An Updated Systematic Review and Meta-Analysis. Orphanet Journal of Rare Diseases 15(1): 141.

Crooke, Stanley T., Shiyu Wang, Timothy A. Vickers, Wen Shen, and Xue-Hai Liang
2017 Cellular Uptake and Trafficking of Antisense Oligonucleotides. Nature Biotechnology 35(3): 230–237.

Cure Rare Disease
2022 Cure Rare Disease An Update to the CRD Community. https://www.cureraredisease.org/blog-posts/update-to-crd-community, accessed December 8, 2022.

Dai, Alper, Osman Baspinar, Ahmet Yeşilyurt, et al.
2018 Efficacy of Stem Cell Therapy in Ambulatory and Nonambulatory Children with Duchenne Muscular Dystrophy - Phase I-II. Degenerative Neurological and Neuromuscular Disease 8: 63–77.

Daiichi Sankyo
2021 Daiichi Sankyo Announces the Results Summary of Phase 1/2 Clinical Trial in Japan for DS-5141 - Press Releases - Media - Daiichi Sankyo.
https://www.daiichisankyo.com/media/press_release/detail/index_4112.html, accessed December 8, 2022.

Daniels, Tracy R., Tracie Delgado, Gustavo Helguera, and Manuel L. Penichet
2006 The Transferrin Receptor Part II: Targeted Delivery of Therapeutic Agents into Cancer Cells. Clinical Immunology (Orlando, Fla.) 121(2): 159–176.

Davidson, Z. E., M. M. Ryan, A. J. Kornberg, et al.
2014 Observations of Body Mass Index in Duchenne Muscular Dystrophy: A Longitudinal Study. European Journal of Clinical Nutrition 68(8): 892–897.

De Angelis, Fernanda Gabriella, Olga Sthandier, Barbara Berarducci, et al.
2002 Chimeric SnRNA Molecules Carrying Antisense Sequences against the Splice Junctions of Exon 51 of the Dystrophin Pre-MRNA Induce Exon Skipping and Restoration of a Dystrophin Synthesis in Delta 48-50 DMD Cells. Proceedings of the National Academy of Sciences of the United States of America 99(14): 9456–9461.

Deconinck, A. E., J. A. Rafael, J. A. Skinner, et al.
1997 Utrophin-Dystrophin-Deficient Mice as a Model for Duchenne Muscular Dystrophy. Cell 90(4): 717–727.

Del Rio-Pertuz, Gaspar, Cristina Morataya, Kanak Parmar, Sarah Dubay, and Erwin Argueta-Sosa
2022 Dilated Cardiomyopathy as the Initial Presentation of Becker Muscular Dystrophy: A Systematic Review of Published Cases. Orphanet Journal of Rare Diseases 17(1): 194.

Den Dunnen, J. T., P. M. Grootscholten, E. Bakker, et al.
1989 Topography of the Duchenne Muscular Dystrophy (DMD) Gene: FIGE and CDNA Analysis of 194 Cases Reveals 115 Deletions and 13 Duplications. American Journal of Human Genetics 45(6): 835–847.

Deng, Jiexin, Junshi Zhang, Keli Shi, and Zhigang Liu
2022 Drug Development Progress in Duchenne Muscular Dystrophy. Frontiers in Pharmacology 13: 950651.

Desjardins, Cody A., Monica Yao, John Hall, et al.
2022 Enhanced Exon Skipping and Prolonged Dystrophin Restoration Achieved by TfR1-Targeted Delivery of Antisense Oligonucleotide Using FORCE Conjugation in Mdx Mice. Nucleic Acids Research 50(20): 11401–11414.

van Deutekom, Judith C., Anneke A. Janson, Ieke B. Ginjaar, et al.
2007 Local Dystrophin Restoration with Antisense Oligonucleotide PRO051. The New England Journal of Medicine 357(26): 2677–2686.

Doorenweerd, Nathalie, Ahmed Mahfouz, Maaike van Putten, et al.
2017 Timing and Localization of Human Dystrophin Isoform Expression Provide Insights into the Cognitive Phenotype of Duchenne Muscular Dystrophy. Scientific Reports 7(1): 12575.

Douglas, Andrew G. L., and Matthew J. A. Wood
2013 Splicing Therapy for Neuromuscular Disease. Molecular and Cellular Neurosciences 56: 169–185.

Dowdy, Steven F.
2017 Overcoming Cellular Barriers for RNA Therapeutics. Nature Biotechnology 35(3). Nature Publishing Group: 222–229.

Dowdy, Steven F., Ryan L. Setten, Xian-Shu Cui, and Satish G. Jadhav
2022 Delivery of RNA Therapeutics: The Great Endosomal Escape! Nucleic Acid Therapeutics 32(5): 361–368.

Dowling, Jennifer K., and Luke A. J. O'Neill
2012 Biochemical Regulation of the Inflammasome. Critical Reviews in Biochemistry and Molecular Biology 47(5): 424–443.

Drachman, D. B., K. V. Toyka, and E. Myer
1974 Prednisone in Duchenne Muscular Dystrophy. Lancet (London, England) 2(7894): 1409–1412.

Dresser, M. J., M. K. Leabman, and K. M. Giacomini
2001 Transporters Involved in the Elimination of Drugs in the Kidney: Organic Anion Transporters and Organic Cation Transporters. Journal of Pharmaceutical Sciences 90(4): 397–421.

D'Souza, V. N., T. M. Nguyen, G. E. Morris, et al.
1995 A Novel Dystrophin Isoform Is Required for Normal Retinal Electrophysiology. Human Molecular Genetics 4(5): 837–842.

Duan, Dongsheng
2018 Systemic AAV Micro-Dystrophin Gene Therapy for Duchenne Muscular Dystrophy. Molecular Therapy: The Journal of the American Society of Gene Therapy 26(10): 2337–2356.

Duan, Dongsheng, Nathalie Goemans, Shin'ichi Takeda, Eugenio Mercuri, and Annemieke Aartsma-Rus
2021 Duchenne Muscular Dystrophy. Nature Reviews. Disease Primers 7(1): 13.

Duboc, Denis, Christophe Meune, Bertrand Pierre, et al.
2007 Perindopril Preventive Treatment on Mortality in Duchenne Muscular Dystrophy: 10 Years' Follow-Up. American Heart Journal 154(3): 596–602.

Duchêne, Benjamin L., Khadija Cherif, Jean-Paul Iyombe-Engembe, et al.
2018 CRISPR-Induced Deletion with SaCas9 Restores Dystrophin Expression in Dystrophic Models In Vitro and In Vivo. Molecular Therapy: The Journal of the American Society of Gene Therapy 26(11): 2604–2616.

Duchenne
1868 De La Paralysie Musculaire Pseudo-Hypertrophique Ou Paralysie Myo-Sclérosique / Par Le Dr Duchenne (de Boulogne). Wellcome Collection. https://wellcomecollection.org/works/fkv5yrjv/items, accessed December 8, 2022.

Dumont, Nicolas A., Yu Xin Wang, Julia von Maltzahn, et al.
2015 Dystrophin Expression in Muscle Stem Cells Regulates Their Polarity and Asymmetric Division. Nature Medicine 21(12): 1455–1463.

Eagle, Michelle, John Bourke, Robert Bullock, et al.
2007 Managing Duchenne Muscular Dystrophy--the Additive Effect of Spinal Surgery and Home Nocturnal Ventilation in Improving Survival. Neuromuscular Disorders: NMD 17(6): 470–475.

Echevarría, Lucía, Philippine Aupy, and Aurélie Goyenvalle
2018 Exon-Skipping Advances for Duchenne Muscular Dystrophy. Human Molecular Genetics 27(R2): R163–R172.

Echevarría, Lucía, Philippine Aupy, Karima Relizani, et al.
2019 Evaluating the Impact of Variable Phosphorothioate Content in Tricyclo-DNA Antisense Oligonucleotides in a Duchenne Muscular Dystrophy Mouse Model. Nucleic Acid Therapeutics 29(3): 148–160.

Eckstein, Fritz
2014 Phosphorothioates, Essential Components of Therapeutic Oligonucleotides. Nucleic Acid Therapeutics 24(6): 374–387.

Engelhardt, Jeffery A.
2016 Comparative Renal Toxicopathology of Antisense Oligonucleotides. Nucleic Acid Therapeutics 26(4): 199–209.

England, S. B., L. V. Nicholson, M. A. Johnson, et al.
1990 Very Mild Muscular Dystrophy Associated with the Deletion of 46% of Dystrophin. Nature 343(6254): 180–182.

entrada
2022 Entrada Therapeutics | Entrada Therapeutics Reports Second Quarter 2022 Financial Results. https://ir.entradatx.com/news-releases/news-release-details/entrada-therapeutics-reports-second-quarter-2022-financial/, accessed January 25, 2023.

Erkut, Esra, and Toshifumi Yokota
2022 CRISPR Therapeutics for Duchenne Muscular Dystrophy. International Journal of Molecular Sciences 23(3): 1832.

Ervasti, James M., and Kevin J. Sonnemann
2008 Biology of the Striated Muscle Dystrophin-Glycoprotein Complex. International Review of Cytology 265: 191–225.

Fee, Robert J., and Veronica J. Hinton
2011 Resilience in Children Diagnosed with a Chronic Neuromuscular Disorder. Journal of Developmental and Behavioral Pediatrics: JDBP 32(9): 644–650.

Ferrero, Amanda, and Marta Rossi
2022 Cognitive Profile and Neuropsychiatric Disorders in Becker Muscular Dystrophy: A Systematic Review of Literature. Neuroscience and Biobehavioral Reviews 137: 104648.

Frank, Diane E., Frederick J. Schnell, Cody Akana, et al.
2020 Increased Dystrophin Production with Golodirsen in Patients with Duchenne Muscular Dystrophy. Neurology 94(21): e2270–e2282.

Fukada, So-ichiro, Daisuke Morikawa, Yukiko Yamamoto, et al.
2010 Genetic Background Affects Properties of Satellite Cells and Mdx Phenotypes. The American Journal of Pathology 176(5): 2414–2424.

Gagliardi, Delia, Mafalda Rizzuti, Roberta Brusa, et al.
2022 MicroRNAs as Serum Biomarkers in Becker Muscular Dystrophy. Journal of Cellular and Molecular Medicine 26(17): 4678–4685.

Gait, Michael J., Andrey A. Arzumanov, Graham McClorey, et al.
2019 Cell-Penetrating Peptide Conjugates of Steric Blocking Oligonucleotides as Therapeutics for Neuromuscular Diseases from a Historical Perspective to Current Prospects of Treatment. Nucleic Acid Therapeutics 29(1): 1–12.

García-Cruz, César, Candelaria Merino-Jiménez, Jorge Aragón, et al.
2022 Overexpression of the Dystrophins Dp40 and Dp40L170P Modifies Neurite Outgrowth and the Protein Expression Profile of PC12 Cells. Scientific Reports 12(1): 1410.

García-Rodríguez, Raquel, Monika Hiller, Laura Jiménez-Gracia, et al.
2020 Premature Termination Codons in the DMD Gene Cause Reduced Local MRNA Synthesis. Proceedings of the National Academy of Sciences of the United States of America 117(28): 16456–16464.

Gaschen, F. P., E. P. Hoffman, J. R. Gorospe, et al.
1992 Dystrophin Deficiency Causes Lethal Muscle Hypertrophy in Cats. Journal of the Neurological Sciences 110(1–2): 149–159.

Gaschen, L., J. Lang, S. Lin, et al.
1999 Cardiomyopathy in Dystrophin-Deficient Hypertrophic Feline Muscular Dystrophy. Journal of Veterinary Internal Medicine 13(4): 346–356.

Gaus, Hans J., Ruchi Gupta, Alfred E. Chappell, et al.
2019 Characterization of the Interactions of Chemically-Modified Therapeutic Nucleic Acids with Plasma Proteins Using a Fluorescence Polarization Assay. Nucleic Acids Research 47(3): 1110–1122.

Gayraud, Jerome, Stefan Matecki, Karim Hnia, et al.
2007 Ventilation during Air Breathing and in Response to Hypercapnia in 5 and 16 Month-Old Mdx and C57 Mice. Journal of Muscle Research and Cell Motility 28(1): 29–37.

genethon
2021 Genethon Announces First Patient Dosed in Clinical Trial of Investigational Gene Therapy GNT 0004 for Duchenne Muscular Dystrophy. Généthon. https://www.genethon.com/genethon-announces-first-patient-dosed-in-clinical-trial-of-investigational-gene-therapy-gnt-0004-for-duchenne-muscular-dystrophy/, accessed December 8, 2022.
2022 From 2021, a Seminal Year for Genethon, to 2022, a Year of Challenges. Généthon. https://www.genethon.com/perspectives-2022-gene-therapy/, accessed December 8, 2022.

Georgiadou, Michaella, Melina Christou, Kleitos Sokratous, et al.
2021 Intramuscular Evaluation of Chimeric Locked Nucleic Acid/2'OMethyl-Modified Antisense Oligonucleotides for Targeted Exon 23 Skipping in Mdx Mice. Pharmaceuticals (Basel, Switzerland) 14(11): 1113.

Gilar, M., A. Belenky, D. L. Smisek, A. Bourque, and A. S. Cohen
1997 Kinetics of Phosphorothioate Oligonucleotide Metabolism in Biological Fluids. Nucleic Acids Research 25(18): 3615–3620.

Gloss, David, Richard T. Moxley, Stephen Ashwal, and Maryam Oskoui
2016 Practice Guideline Update Summary: Corticosteroid Treatment of Duchenne Muscular Dystrophy: Report of the Guideline Development Subcommittee of the American Academy of Neurology. Neurology 86(5): 465–472.

Goemans, Nathalie M., Mar Tulinius, Johanna T. van den Akker, et al.
2011 Systemic Administration of PRO051 in Duchenne's Muscular Dystrophy. The New England Journal of Medicine 364(16): 1513–1522.

Goemans, Nathalie M., Már Tulinius, Marleen van den Hauwe, et al.
2016 Long-Term Efficacy, Safety, and Pharmacokinetics of Drisapersen in Duchenne Muscular Dystrophy: Results from an Open-Label Extension Study. PloS One 11(9): e0161955.

Goemans, Nathalie, Eugenio Mercuri, Elena Belousova, et al.
2018 A Randomized Placebo-Controlled Phase 3 Trial of an Antisense Oligonucleotide, Drisapersen, in Duchenne Muscular Dystrophy. Neuromuscular Disorders: NMD 28(1): 4–15.

Gokcay, Hasan, Simge Seren Kirlioglu, and Yasin Hasan Balcioglu
2020 Valproate-Associated Isolated Serum Creatine Kinase Elevation. American Journal of Therapeutics.

Goonasekera, Sanjeewa A., Jennifer Davis, Jennifer Q. Kwong, et al.
2014 Enhanced Ca^{2+} Influx from STIM1-Orai1 Induces Muscle Pathology in Mouse Models of Muscular Dystrophy. Human Molecular Genetics 23(14): 3706–3715.

Górecki, D. C., A. P. Monaco, J. M. Derry, et al.
1992 Expression of Four Alternative Dystrophin Transcripts in Brain Regions Regulated by Different Promoters. Human Molecular Genetics 1(7): 505–510.

Gorman, L., D. Suter, V. Emerick, D. Schümperli, and R. Kole
1998 Stable Alteration of Pre-MRNA Splicing Patterns by Modified U7 Small Nuclear RNAs. Proceedings of the National Academy of Sciences of the United States of America 95(9): 4929–4934.

Goyenvalle, Aurélie, Graziella Griffith, Arran Babbs, et al.
2015 Functional Correction in Mouse Models of Muscular Dystrophy Using Exon-Skipping Tricyclo-DNA Oligomers. Nature Medicine 21(3): 270–275.

Goyenvalle, Aurélie, Adeline Vulin, Françoise Fougerousse, et al.
2004 Rescue of Dystrophic Muscle through U7 SnRNA-Mediated Exon Skipping. Science (New York, N.Y.) 306(5702): 1796–1799.

Grady, R. M., R. W. Grange, K. S. Lau, et al.
1999 Role for Alpha-Dystrobrevin in the Pathogenesis of Dystrophin-Dependent Muscular Dystrophies. Nature Cell Biology 1(4): 215–220.

Grady, R. M., H. Teng, M. C. Nichol, et al.
1997 Skeletal and Cardiac Myopathies in Mice Lacking Utrophin and Dystrophin: A Model for Duchenne Muscular Dystrophy. Cell 90(4): 729–738.

Greenstein, R. M., M. P. Reardon, and T. S. Chan
1977 An X/Autosome Translocation in a Girl with Duchenne Muscular Dystrophy (Dmd): Evidence for Dmd Gene Localization. Pediatric Research 11(4). Nature Publishing Group: 457–457.

Gregorevic, Paul, Michael J. Blankinship, James M. Allen, et al.
2004 Systemic Delivery of Genes to Striated Muscles Using Adeno-Associated Viral Vectors. Nature Medicine 10(8): 828–834.

Griepenburg, J. C., T. L. Rapp, P. J. Carroll, J. Eberwine, and I. J. Dmochowski
2015 Ruthenium-Caged Antisense Morpholinos for Regulating Gene Expression in Zebrafish Embryos. Chemical Science 6(4): 2342–2346.

Guglieri, Michela, Kate Bushby, Michael P. McDermott, et al.
2022 Effect of Different Corticosteroid Dosing Regimens on Clinical Outcomes in Boys With Duchenne Muscular Dystrophy: A Randomized Clinical Trial. JAMA 327(15): 1456–1468.

Gupta, Rajat M., and Kiran Musunuru
2014 Expanding the Genetic Editing Tool Kit: ZFNs, TALENs, and CRISPR-Cas9. The Journal of Clinical Investigation 124(10): 4154–4161.

Gurpur, Praveen B., Jianming Liu, Dean J. Burkin, and Stephen J. Kaufman
2009 Valproic Acid Activates the PI3K/Akt/MTOR Pathway in Muscle and Ameliorates Pathology in a Mouse Model of Duchenne Muscular Dystrophy. The American Journal of Pathology 174(3): 999–1008.

Gushchina, Liubov V., Emma C. Frair, Natalie Rohan, et al.
2021 Lack of Toxicity in Nonhuman Primates Receiving Clinically Relevant Doses of an AAV9.U7snRNA Vector Designed to Induce DMD Exon 2 Skipping. Human Gene Therapy 32(17–18): 882–894.

Hagedorn, Peter H., Robert Persson, Erik D. Funder, et al.
2018 Locked Nucleic Acid: Modality, Diversity, and Drug Discovery. Drug Discovery Today 23(1): 101–114.

Hamed, Sa, Aj Sutherland-Smith, Jrm Gorospe, J Kendrick-Jones, and Ep Hoffman
2005 DNA Sequence Analysis for Structure/Function and Mutation Studies in Becker Muscular Dystrophy. Clinical Genetics 68(1): 69–79.

Hammond, Suzan M., Annemieke Aartsma-Rus, Sandra Alves, et al.
2021 Delivery of Oligonucleotide-Based Therapeutics: Challenges and Opportunities. EMBO Molecular Medicine 13(4): e13243.

Hammond, Suzan M., Gareth Hazell, Fazel Shabanpoor, et al.
2016 Systemic Peptide-Mediated Oligonucleotide Therapy Improves Long-Term Survival in Spinal Muscular Atrophy. Proceedings of the National Academy of Sciences of the United States of America 113(39): 10962–10967.

Harper, Scott Q., Michael A. Hauser, Christiana DelloRusso, et al.
2002 Modular Flexibility of Dystrophin: Implications for Gene Therapy of Duchenne Muscular Dystrophy. Nature Medicine 8(3): 253–261.

HAS
2019 Protocole National de Diagnostic et de Soins (PNDS) Dystrophie Musculaire de Duchenne. https://www.has-sante.fr/upload/docs/application/pdf/2019-11/pnds_duchenne_vlongue_final_20_nov_2019_.pdf, accessed January 10, 2023.

Haslett, Judith N., Despina Sanoudou, Alvin T. Kho, et al.
2002 Gene Expression Comparison of Biopsies from Duchenne Muscular Dystrophy (DMD) and Normal Skeletal Muscle. Proceedings of the National Academy of Sciences of the United States of America 99(23): 15000–15005.

Hendriksen, Jos G. M., James T. Poysky, Debby G. M. Schrans, et al.
2009 Psychosocial Adjustment in Males with Duchenne Muscular Dystrophy: Psychometric Properties and Clinical Utility of a Parent-Report Questionnaire. Journal of Pediatric Psychology 34(1): 69–78.

Henry, S., K. Stecker, D. Brooks, et al.
2000 Chemically Modified Oligonucleotides Exhibit Decreased Immune Stimulation in Mice. The Journal of Pharmacology and Experimental Therapeutics 292(2): 468–479.

Henry, Scott P., Greg Beattie, Grace Yeh, et al.
2002 Complement Activation Is Responsible for Acute Toxicities in Rhesus Monkeys Treated with a Phosphorothioate Oligodeoxynucleotide. International Immunopharmacology 2(12): 1657–1666.

Hildyard, John C. W., Faye Rawson, Dominic J. Wells, and Richard J. Piercy
2020 Multiplex in Situ Hybridization within a Single Transcript: RNAscope Reveals Dystrophin MRNA Dynamics. PloS One 15(9): e0239467.

Hirawat, Samit, Ellen M. Welch, Gary L. Elfring, et al.
2007 Safety, Tolerability, and Pharmacokinetics of PTC124, a Nonaminoglycoside Nonsense Mutation Suppressor, Following Single- and Multiple-Dose Administration to Healthy Male and Female Adult Volunteers. Journal of Clinical Pharmacology 47(4): 430–444.

't Hoen, Peter A. C., Emile J. de Meijer, Judith M. Boer, et al.
2008 Generation and Characterization of Transgenic Mice with the Full-Length Human DMD Gene. The Journal of Biological Chemistry 283(9): 5899–5907.

Hoffman, E. P., R. H. Brown, and L. M. Kunkel
1987 Dystrophin: The Protein Product of the Duchenne Muscular Dystrophy Locus. Cell 51(6): 919–928.

Hoffman, E. P., C. M. Knudson, K. P. Campbell, and L. M. Kunkel
1987 Subcellular Fractionation of Dystrophin to the Triads of Skeletal Muscle. Nature 330(6150): 754–758.

Holder, E., M. Maeda, and R. D. Bies
1996 Expression and Regulation of the Dystrophin Purkinje Promoter in Human Skeletal Muscle, Heart, and Brain. Human Genetics 97(2): 232–239.

Holland, Dr Ashling, Dr Smita Gunnoo, Sam Ching, et al.
2021 A Novel Enhanced Delivery Oligonucleotide (EDO) Therapeutic Demonstrates Considerable Potential in Treating Duchenne Muscular Dystrophy: 1.

Horton, Rebecca H., Dimah Saade, Theodora Markati, et al.
2022 A Systematic Review of Adeno-Associated Virus Gene Therapies in Neurology: The Need for Consistent Safety Monitoring of a Promising Treatment. Journal of Neurology, Neurosurgery, and Psychiatry 93(12): 1276–1288.

Howard, P. L., G. Y. Dally, M. H. Wong, et al.
1998 Localization of Dystrophin Isoform Dp71 to the Inner Limiting Membrane of the Retina Suggests a Unique Functional Contribution of Dp71 in the Retina. Human Molecular Genetics 7(9): 1385–1391.

Hsu, John D., and Ros Quinlivan
2013 Scoliosis in Duchenne Muscular Dystrophy (DMD). Neuromuscular Disorders: NMD 23(8): 611–617.

Hudziak, R. M., E. Barofsky, D. F. Barofsky, et al.
1996 Resistance of Morpholino Phosphorodiamidate Oligomers to Enzymatic Degradation. Antisense & Nucleic Acid Drug Development 6(4): 267–272.

Iannaccone, S., H. Phan, V. Straub, et al.
2022 P.132 Casimersen in Patients with Duchenne Muscular Dystrophy Amenable to Exon 45 Skipping: Interim Results from the Phase 3 ESSENCE Trial. Neuromuscular Disorders 32: S102.

Iannitti, Tommaso, Julio Cesar Morales-Medina, and Beniamino Palmieri
2014 Phosphorothioate Oligonucleotides: Effectiveness and Toxicity. Current Drug Targets 15(7): 663–673.

Ibrahim, Ahmed Gamal-Eldin, Ke Cheng, and Eduardo Marbán
2014 Exosomes as Critical Agents of Cardiac Regeneration Triggered by Cell Therapy. Stem Cell Reports 2(5): 606–619.

Iezzi, Simona, Monica Di Padova, Carlo Serra, et al.
2004 Deacetylase Inhibitors Increase Muscle Cell Size by Promoting Myoblast Recruitment and Fusion through Induction of Follistatin. Developmental Cell 6(5): 673–684.

Iff, Joel, Nicolae Done, Ed Tuttle, et al.
2022 Survival in Eteplirsen-Treated vs Duchenne Muscular Dystrophy (DMD) Natural History Controls: An Indirect Treatment Comparison Using Real-World Data. Wms: 2.

Ivanova, Gabriela D., Andrey Arzumanov, Rachida Abes, et al.
2008 Improved Cell-Penetrating Peptide-PNA Conjugates for Splicing Redirection in HeLa Cells and Exon Skipping in Mdx Mouse Muscle. Nucleic Acids Research 36(20): 6418–6428.

Iwamoto, Naoki, David C. D. Butler, Nenad Svrzikapa, et al.
2017 Control of Phosphorothioate Stereochemistry Substantially Increases the Efficacy of Antisense Oligonucleotides. Nature Biotechnology 35(9): 845–851.

Janghra, Narinder, Jennifer E. Morgan, Caroline A. Sewry, et al.
2016 Correlation of Utrophin Levels with the Dystrophin Protein Complex and Muscle Fibre Regeneration in Duchenne and Becker Muscular Dystrophy Muscle Biopsies. PloS One 11(3): e0150818.

Jearawiriyapaisarn, Natee, Hong M. Moulton, Brian Buckley, et al.
2008 Sustained Dystrophin Expression Induced by Peptide-Conjugated Morpholino Oligomers in the Muscles of Mdx Mice. Molecular Therapy: The Journal of the American Society of Gene Therapy 16(9): 1624–1629.

Jinek, Martin, Krzysztof Chylinski, Ines Fonfara, et al.
2012 A Programmable Dual-RNA-Guided DNA Endonuclease in Adaptive Bacterial Immunity. Science (New York, N.Y.) 337(6096): 816–821.

Juliano, Rudolph L.
2021 Chemical Manipulation of the Endosome Trafficking Machinery: Implications for Oligonucleotide Delivery. Biomedicines 9(5): 512.

Jung, D., D. Filliol, M. H. Metz-Boutigue, and A. Rendon
1993 Characterization and Subcellular Localization of the Dystrophin-Protein 71 (Dp71) from Brain. Neuromuscular Disorders: NMD 3(5–6): 515–518.

Kandasamy, Pachamuthu, Graham McClorey, Mamoru Shimizu, et al.
2022 Control of Backbone Chemistry and Chirality Boost Oligonucleotide Splice Switching Activity. Nucleic Acids Research 50(10): 5443–5466.

Karamanlidis, Georgios, Usue Etxaniz, Maria Azzurra Missinato, et al.
2022 AOC 1044 Mediated Exon 44 Skipping and Restoration of Dystrophin Protein in Cynomolgus Monkeys and DMD Patient Derived Myotubes.

Kariyawasam, Didu, Arlene D'Silva, David Mowat, et al.
2022 Incidence of Duchenne Muscular Dystrophy in the Modern Era; an Australian Study. European Journal of Human Genetics: EJHG 30(12): 1398–1404.

Kaur, Harleen, Jesper Wengel, and Souvik Maiti
2007 LNA-Modified Oligonucleotides Effectively Drive Intramolecular-Stable Hairpin to Intermolecular-Duplex State. Biochemical and Biophysical Research Communications 352(1): 118–122.

Khairallah, Ramzi J., Guoli Shi, Francesca Sbrana, et al.
2012 Microtubules Underlie Dysfunction in Duchenne Muscular Dystrophy. Science Signaling 5(236): ra56.

Khvorova, Anastasia, and Jonathan K. Watts
2017 The Chemical Evolution of Oligonucleotide Therapies of Clinical Utility. Nature Biotechnology 35(3): 238–248.

Kim, Sunkyung, Yong Zhu, Paul A. Romitti, et al.
2017 Associations between Timing of Corticosteroid Treatment Initiation and Clinical Outcomes in Duchenne Muscular Dystrophy. Neuromuscular Disorders: NMD 27(8): 730–737.

Kinali, Maria, Virginia Arechavala-Gomeza, Lucy Feng, et al.
2009 Local Restoration of Dystrophin Expression with the Morpholino Oligomer AVI-4658 in Duchenne Muscular Dystrophy: A Single-Blind, Placebo-Controlled, Dose-Escalation, Proof-of-Concept Study. The Lancet. Neurology 8(10): 918–928.

Klamut, H. J., S. B. Gangopadhyay, R. G. Worton, and P. N. Ray
1990 Molecular and Functional Analysis of the Muscle-Specific Promoter Region of the Duchenne Muscular Dystrophy Gene. Molecular and Cellular Biology 10(1): 193–205.

Klymiuk, Nikolai, Andreas Blutke, Alexander Graf, et al.
2013 Dystrophin-Deficient Pigs Provide New Insights into the Hierarchy of Physiological Derangements of Dystrophic Muscle. Human Molecular Genetics 22(21): 4368–4382.

Koenig, M., E. P. Hoffman, C. J. Bertelson, et al.
1987 Complete Cloning of the Duchenne Muscular Dystrophy (DMD) CDNA and Preliminary Genomic Organization of the DMD Gene in Normal and Affected Individuals. Cell 50(3): 509–517.

Koizumi, Makoto
2004 2′-O,4′-C-Ethylene-Bridged Nucleic Acids (ENA) as next-Generation Antisense and Antigene Agents. Biological & Pharmaceutical Bulletin 27(4): 453–456.

Komaki, H., E. Takeshita, K. Kunitake, et al.
2022 P.123 A Phase I/II Study of NS-089/NCNP-02, Exon 44 Skipping Drug, in Patients with Duchenne Muscular Dystrophy. Neuromuscular Disorders 32: S99–S100.

Komaki, Hirofumi, Tetsuya Nagata, Takashi Saito, et al.
2018 Systemic Administration of the Antisense Oligonucleotide NS-065/NCNP-01 for Skipping of Exon 53 in Patients with Duchenne Muscular Dystrophy. Science Translational Medicine 10(437): eaan0713.

Komaki, Hirofumi, Yasuhiro Takeshima, Tsuyoshi Matsumura, et al.
2020 Viltolarsen in Japanese Duchenne Muscular Dystrophy Patients: A Phase 1/2 Study. Annals of Clinical and Translational Neurology 7(12): 2393–2408.

Kumamoto, T., H. Ueyama, S. Watanabe, et al.
1995 Immunohistochemical Study of Calpain and Its Endogenous Inhibitor in the Skeletal Muscle of Muscular Dystrophy. Acta Neuropathologica 89(5): 399–403.

Kunkel, L. M., J. F. Hejtmancik, C. T. Caskey, et al.
1986 Analysis of Deletions in DNA from Patients with Becker and Duchenne Muscular Dystrophy. Nature 322(6074): 73–77.

Kunkel, L. M., A. P. Monaco, W. Middlesworth, H. D. Ochs, and S. A. Latt
1985 Specific Cloning of DNA Fragments Absent from the DNA of a Male Patient with an X Chromosome Deletion. Proceedings of the National Academy of Sciences of the United States of America 82(14): 4778–4782.

Lai, Yi, Gail D. Thomas, Yongping Yue, et al.
2009 Dystrophins Carrying Spectrin-like Repeats 16 and 17 Anchor NNOS to the Sarcolemma and Enhance Exercise Performance in a Mouse Model of Muscular Dystrophy. The Journal of Clinical Investigation 119(3): 624–635.

Larcher, Thibaut, Aude Lafoux, Laurent Tesson, et al.
2014 Characterization of Dystrophin Deficient Rats: A New Model for Duchenne Muscular Dystrophy. PloS One 9(10): e110371.

Le, Bao T., Abbie M. Adams, Susan Fletcher, Stephen D. Wilton, and Rakesh N. Veedu
2017 Rational Design of Short Locked Nucleic Acid-Modified 2′-O-Methyl Antisense Oligonucleotides for Efficient Exon-Skipping In Vitro. Molecular Therapy. Nucleic Acids 9: 155–161.

Le Hir, Maëva, Aurélie Goyenvalle, Cécile Peccate, et al.
2013 AAV Genome Loss from Dystrophic Mouse Muscles during AAV-U7 SnRNA-Mediated Exon-Skipping Therapy. Molecular Therapy: The Journal of the American Society of Gene Therapy 21(8): 1551–1558.

Lee, Tomoko, Hiroyuki Awano, Mariko Yagi, et al.
2017 2′-O-Methyl RNA/Ethylene-Bridged Nucleic Acid Chimera Antisense Oligonucleotides to Induce Dystrophin Exon 45 Skipping. Genes 8(2): 67.

Leung, Doris G., Daniel A. Herzka, W. Reid Thompson, et al.
2014 Sildenafil Does Not Improve Cardiomyopathy in Duchenne/Becker Muscular Dystrophy. Annals of Neurology 76(4): 541–549.

Li, Hongmei Lisa, Naoko Fujimoto, Noriko Sasakawa, et al.
2015 Precise Correction of the Dystrophin Gene in Duchenne Muscular Dystrophy Patient Induced Pluripotent Stem Cells by TALEN and CRISPR-Cas9. Stem Cell Reports 4(1): 143–154.

Li, Ting-Ting, Jia-Xing An, Jing-Yu Xu, and Bi-Guang Tuo
2019 Overview of Organic Anion Transporters and Organic Anion Transporter Polypeptides and Their Roles in the Liver. World Journal of Clinical Cases 7(23): 3915–3933.

Lidov, H. G., and L. M. Kunkel
1997 Dp140: Alternatively Spliced Isoforms in Brain and Kidney. Genomics 45(1): 132–139.

Lipovsek, D.
2011 Adnectins: Engineered Target-Binding Protein Therapeutics. Protein Engineering, Design & Selection: PEDS 24(1–2): 3–9.

Long, Chengzu, Leonela Amoasii, Alex A. Mireault, et al.
2016 Postnatal Genome Editing Partially Restores Dystrophin Expression in a Mouse Model of Muscular Dystrophy. Science (New York, N.Y.) 351(6271): 400–403.

Lorain, Stéphanie, David-Alexandre Gross, Aurélie Goyenvalle, et al.
2008 Transient Immunomodulation Allows Repeated Injections of AAV1 and Correction of Muscular Dystrophy in Multiple Muscles. Molecular Therapy: The Journal of the American Society of Gene Therapy 16(3): 541–547.

Love, D. R., D. F. Hill, G. Dickson, et al.
1989 An Autosomal Transcript in Skeletal Muscle with Homology to Dystrophin. Nature 339(6219): 55–58.

Lu, Qi Long, Christopher J. Mann, Fang Lou, et al.
2003 Functional Amounts of Dystrophin Produced by Skipping the Mutated Exon in the Mdx Dystrophic Mouse. Nature Medicine 9(8): 1009–1014.

Magri, Francesca, Alessandra Govoni, Maria Grazia D'Angelo, et al.
2011 Genotype and Phenotype Characterization in a Large Dystrophinopathic Cohort with Extended Follow-Up. Journal of Neurology 258(9): 1610–1623.

Mah, Jean K., Lawrence Korngut, Jonathan Dykeman, et al.
2014 A Systematic Review and Meta-Analysis on the Epidemiology of Duchenne and Becker Muscular Dystrophy. Neuromuscular Disorders: NMD 24(6): 482–491.

Manini, Arianna, Elena Abati, Andi Nuredini, Stefania Corti, and Giacomo Pietro Comi
2021 Adeno-Associated Virus (AAV)-Mediated Gene Therapy for Duchenne Muscular Dystrophy: The Issue of Transgene Persistence. Frontiers in Neurology 12: 814174.

Matthews, Emma, Ruth Brassington, Thierry Kuntzer, Fatima Jichi, and Adnan Y. Manzur
2016 Corticosteroids for the Treatment of Duchenne Muscular Dystrophy. The Cochrane Database of Systematic Reviews 2016(5): CD003725.

Mayer, U., G. Saher, R. Fässler, et al.
1997 Absence of Integrin Alpha 7 Causes a Novel Form of Muscular Dystrophy. Nature Genetics 17(3): 318–323.

McCombs, Jessica R., and Shawn C. Owen
2015 Antibody Drug Conjugates: Design and Selection of Linker, Payload and Conjugation Chemistry. The AAPS Journal 17(2): 339–351.

McDonald, Craig M., Perry B. Shieh, Hoda Z. Abdel-Hamid, et al.
2021 Open-Label Evaluation of Eteplirsen in Patients with Duchenne Muscular Dystrophy Amenable to Exon 51 Skipping: PROMOVI Trial. Journal of Neuromuscular Diseases 8(6): 989–1001.

Mellion, M., J. McArthur, A. Holland, et al.
2022 P.120 Unlocking the Potential of Oligonucleotide Therapeutics for Duchenne Muscular Dystrophy through Enhanced Delivery. Neuromuscular Disorders 32: S99.

Mendell, J. R., R. T. Moxley, R. C. Griggs, et al.
1989 Randomized, Double-Blind Six-Month Trial of Prednisone in Duchenne's Muscular Dystrophy. The New England Journal of Medicine 320(24): 1592–1597.

Mendell, Jerry R., Nathalie Goemans, Linda P. Lowes, et al.
2016 Longitudinal Effect of Eteplirsen versus Historical Control on Ambulation in Duchenne Muscular Dystrophy. Annals of Neurology 79(2): 257–271.

Mendell, Jerry R., Louise R. Rodino-Klapac, Zarife Sahenk, et al.
2013 Eteplirsen for the Treatment of Duchenne Muscular Dystrophy. Annals of Neurology 74(5): 637–647.

Mendell, Jerry R., Louise Rodino-Klapac, Zarife Sahenk, et al.
2012 Gene Therapy for Muscular Dystrophy: Lessons Learned and Path Forward. Neuroscience Letters 527(2): 90–99.

Mendell, Jerry R., Zarife Sahenk, Kelly Lehman, et al.
2020 Assessment of Systemic Delivery of RAAVrh74.MHCK7.Micro-Dystrophin in Children With Duchenne Muscular Dystrophy: A Nonrandomized Controlled Trial. JAMA Neurology 77(9): 1122–1131.

Mercuri, Eugenio, Francesco Muntoni, Andrés Nascimento Osorio, et al.
2020 Safety and Effectiveness of Ataluren: Comparison of Results from the STRIDE Registry and CINRG DMD Natural History Study. Journal of Comparative Effectiveness Research 9(5): 341–360.

Min, Yi-Li, Hui Li, Cristina Rodriguez-Caycedo, et al.
2019 CRISPR-Cas9 Corrects Duchenne Muscular Dystrophy Exon 44 Deletion Mutations in Mice and Human Cells. Science Advances 5(3): eaav4324.

Mitelman, Olga, Hoda Z. Abdel-Hamid, Barry J. Byrne, et al.
2022 A Combined Prospective and Retrospective Comparison of Long-Term Functional Outcomes Suggests Delayed Loss of Ambulation and Pulmonary Decline with Long-Term Eteplirsen Treatment. Journal of Neuromuscular Diseases 9(1): 39–52.

Moise, N. S., B. A. Valentine, C. A. Brown, et al.
1991 Duchenne's Cardiomyopathy in a Canine Model: Electrocardiographic and Echocardiographic Studies. Journal of the American College of Cardiology 17(3): 812–820.

Moizard, M. P., A. Toutain, D. Fournier, et al.
2000 Severe Cognitive Impairment in DMD: Obvious Clinical Indication for Dp71 Isoform Point Mutation Screening. European Journal of Human Genetics: EJHG 8(7): 552–556.

Monaco, A. P., R. L. Neve, C. Colletti-Feener, et al.
1986 Isolation of Candidate CDNAs for Portions of the Duchenne Muscular Dystrophy Gene. Nature 323(6089): 646–650.

Moretti, A., L. Fonteyne, F. Giesert, et al.
2020 Somatic Gene Editing Ameliorates Skeletal and Cardiac Muscle Failure in Pig and Human Models of Duchenne Muscular Dystrophy. Nature Medicine 26(2): 207–214.

Moulton, Hong M., and Jon D. Moulton
2010 Morpholinos and Their Peptide Conjugates: Therapeutic Promise and Challenge for Duchenne Muscular Dystrophy. Biochimica Et Biophysica Acta 1798(12): 2296–2303.

Moulton, Jon D., and Shan Jiang
2009 Gene Knockdowns in Adult Animals: PPMOs and Vivo-Morpholinos. Molecules (Basel, Switzerland) 14(3): 1304–1323.

Murphy, Kate T., James G. Ryall, Sarah M. Snell, et al.
2010 Antibody-Directed Myostatin Inhibition Improves Diaphragm Pathology in Young but Not Adult Dystrophic Mdx Mice. The American Journal of Pathology 176(5): 2425–2434.

Murray, Sue, Damian Ittig, Erich Koller, et al.
2012 TricycloDNA-Modified Oligo-2′-Deoxyribonucleotides Reduce Scavenger Receptor B1 MRNA in Hepatic and Extra-Hepatic Tissues--a Comparative Study of Oligonucleotide Length, Design and Chemistry. Nucleic Acids Research 40(13): 6135–6143.

Nakamura, Katsuyuki, Wataru Fujii, Masaya Tsuboi, et al.
2014 Generation of Muscular Dystrophy Model Rats with a CRISPR/Cas System. Scientific Reports 4: 5635.

Nationwide Children's Hospital
2022 Nationwide Children's Announces Restoration of Full-Length Dystrophin Using Dup 2 Gene Therapy Approach. Parent Project Muscular Dystrophy. https://www.parentprojectmd.org/nationwide-childrens-hospital-announces-restoration-of-full-length-dystrophin-using-duplication-2-gene-therapy-approach/, accessed January 17, 2023.

Nelson, Christopher E., Yaoying Wu, Matthew P. Gemberling, et al.
2019 Long-Term Evaluation of AAV-CRISPR Genome Editing for Duchenne Muscular Dystrophy. Nature Medicine 25(3): 427–432.

Nichols, Bailey, Shin'ichi Takeda, and Toshifumi Yokota
2015 Nonmechanical Roles of Dystrophin and Associated Proteins in Exercise, Neuromuscular Junctions, and Brains. Brain Sciences 5(3): 275–298.

Nudel, U., D. Zuk, P. Einat, et al.
1989 Duchenne Muscular Dystrophy Gene Product Is Not Identical in Muscle and Brain. Nature 337(6202): 76–78.

Osseni, Alexis, Aymeric Ravel-Chapuis, Edwige Belotti, et al.
2022 Pharmacological Inhibition of HDAC6 Improves Muscle Phenotypes in Dystrophin-Deficient Mice by Downregulating TGF-β via Smad3 Acetylation. Nature Communications 13(1): 7108.

Pasternak, C., S. Wong, and E. L. Elson
1995 Mechanical Function of Dystrophin in Muscle Cells. The Journal of Cell Biology 128(3): 355–361.

PepGen
2022a PepGen Reports Positive Data from Phase 1 Trial of PGN-EDO51 for the Treatment of Duchenne Muscular Dystrophy | PepGen. https://investors.pepgen.com/news-releases/news-release-details/pepgen-reports-positive-data-phase-1-trial-pgn-edo51-treatment/, accessed December 8, 2022.
2022b PepGen Announces Positive Preclinical Data for PGN-EDO53, PGN-EDO45 and PGN-EDO44, Three Novel Duchenne Muscular Dystrophy Candidates | PepGen. https://investors.pepgen.com/news-releases/news-release-details/pepgen-announces-positive-preclinical-data-pgn-edo53-pgn-edo45/, accessed January 4, 2023.

Pfizer
2020 Pfizer's New Phase 1b Results of Gene Therapy in Ambulatory Boys with Duchenne Muscular Dystrophy (DMD) Support Advancement into Pivotal Phase 3 Study | Pfizer. https://www.pfizer.com/news/press-release/press-release-detail/pfizers-new-phase-1b-results-gene-therapy-ambulatory-boys, accessed December 8, 2022.
2021a Pfizer 2021a. http://join.parentprojectmd.org/site/DocServer/A_Message_from_Pfizer_on_our_DMD_Clinical_Program_-_Sept.pdf, accessed December 8, 2022.
2021b Pfizer 2021b. https://www.parentprojectmd.org/wp-content/uploads/2021/12/DMD-Study-1001-Update_Letter-to-the-Community.pdf, accessed December 8, 2022.

Philippidis, Alex
2022 Food and Drug Administration Lifts Clinical Hold on Pfizer Duchenne Muscular Dystrophy Gene Therapy Linked to Patient Death. Human Gene Therapy 33(11–12): 573–576.

Pires, Vanessa Borges, Ricardo Simões, Kamel Mamchaoui, Célia Carvalho, and Maria Carmo-Fonseca
2017 Short (16-Mer) Locked Nucleic Acid Splice-Switching Oligonucleotides Restore Dystrophin Production in Duchenne Muscular Dystrophy Myotubes. PloS One 12(7): e0181065.

Pivonello, Rosario, Andrea M. Isidori, Maria Cristina De Martino, et al.
2016 Complications of Cushing's Syndrome: State of the Art. The Lancet. Diabetes & Endocrinology 4(7): 611–629.

Politano, L., G. Nigro, V. Nigro, et al.
2003 Gentamicin Administration in Duchenne Patients with Premature Stop Codon. Preliminary Results. Acta Myologica: Myopathies and Cardiomyopathies: Official Journal of the Mediterranean Society of Myology 22(1): 15–21.

Pons, F., L. V. Nicholson, A. Robert, T. Voit, and J. J. Leger
1993 Dystrophin and Dystrophin-Related Protein (Utrophin) Distribution in Normal and Dystrophin-Deficient Skeletal Muscles. Neuromuscular Disorders: NMD 3(5–6): 507–514.

Prosser, Benjamin L., Christopher W. Ward, and W. J. Lederer
2011 X-ROS Signaling: Rapid Mechano-Chemo Transduction in Heart. Science (New York, N.Y.) 333(6048): 1440–1445.

Pui, Karen, Peter J. Gow, and Nicola Dalbeth
2013 Efficacy and Tolerability of Probenecid as Urate-Lowering Therapy in Gout; Clinical Experience in High-Prevalence Population. The Journal of Rheumatology 40(6): 872–876.

van Putten, Maaike, Kayleigh Putker, Maurice Overzier, et al.
2019 Natural Disease History of the D2-Mdx Mouse Model for Duchenne Muscular Dystrophy. FASEB Journal: Official Publication of the Federation of American Societies for Experimental Biology 33(7): 8110–8124.

Quinlan, John G., Harvey S. Hahn, Brenda L. Wong, et al.
2004 Evolution of the Mdx Mouse Cardiomyopathy: Physiological and Morphological Findings. Neuromuscular Disorders: NMD 14(8–9): 491–496.

Relizani, Karima, Lucía Echevarría, Faouzi Zarrouki, et al.
2022 Palmitic Acid Conjugation Enhances Potency of Tricyclo-DNA Splice Switching Oligonucleotides. Nucleic Acids Research 50(1): 17–34.

Relizani, Karima, Graziella Griffith, Lucía Echevarría, et al.
2017 Efficacy and Safety Profile of Tricyclo-DNA Antisense Oligonucleotides in Duchenne Muscular Dystrophy Mouse Model. Molecular Therapy. Nucleic Acids 8: 144–157.

Renneberg, Dorte, Emilie Bouliong, Ulrich Reber, Daniel Schümperli, and Christian J. Leumann
2002 Antisense Properties of Tricyclo-DNA. Nucleic Acids Research 30(13): 2751–2757.

Ricotti, Valeria, William P. L. Mandy, Mariacristina Scoto, et al.
2016 Neurodevelopmental, Emotional, and Behavioural Problems in Duchenne Muscular Dystrophy in Relation to Underlying Dystrophin Gene Mutations. Developmental Medicine and Child Neurology 58(1): 77–84.

Roberts, R. G., A. J. Coffey, M. Bobrow, and D. R. Bentley
1993 Exon Structure of the Human Dystrophin Gene. Genomics 16(2): 536–538.

Robinson-Hamm, Jacqueline N., and Charles A. Gersbach
2016 Gene Therapies That Restore Dystrophin Expression for the Treatment of Duchenne Muscular Dystrophy. Human Genetics 135(9): 1029–1040.

Roche
2019 Roche Genentech Releases Letter to DMD Community Announcing Discontinuation of Clinical Trials Program for DMD. Muscular Dystrophy Association. https://strongly.mda.org/roche-genentech-releases-letter-to-dmd-community-announcing-discontinuation-of-clinical-trials-program-for-dmd/, accessed December 8, 2022.

Romero, Norma B., Serge Braun, Olivier Benveniste, et al.
2004 Phase I Study of Dystrophin Plasmid-Based Gene Therapy in Duchenne/Becker Muscular Dystrophy. Human Gene Therapy 15(11): 1065–1076.

Ruggiero, Lucia, Rosa Iodice, Marcello Esposito, et al.
2018 One-Year Follow up of Three Italian Patients with Duchenne Muscular Dystrophy Treated with Ataluren: Is Earlier Better? Therapeutic Advances in Neurological Disorders 11: 1756286418809588.

Rugowska, Anna, Alicja Starosta, and Patryk Konieczny
2021 Epigenetic Modifications in Muscle Regeneration and Progression of Duchenne Muscular Dystrophy. Clinical Epigenetics 13(1): 13.

Ryder, S., R. M. Leadley, N. Armstrong, et al.
2017 The Burden, Epidemiology, Costs and Treatment for Duchenne Muscular Dystrophy: An Evidence Review. Orphanet Journal of Rare Diseases 12: 79.

Salari, Nader, Behnaz Fatahi, Elahe Valipour, et al.
2022 Global Prevalence of Duchenne and Becker Muscular Dystrophy: A Systematic Review and Meta-Analysis. Journal of Orthopaedic Surgery and Research 17(1): 96.

Sander, M., B. Chavoshan, S. A. Harris, et al.
2000 Functional Muscle Ischemia in Neuronal Nitric Oxide Synthase-Deficient Skeletal Muscle of Children with Duchenne Muscular Dystrophy. Proceedings of the National Academy of Sciences of the United States of America 97(25): 13818–13823.

Santhera
2021 Santhera 2021. https://www.santhera.com/assets/files/press-releases/2021-04-28_Vamorolone-2.5yr-e-final.pdf, accessed December 8, 2022.
2022 Santhera 2022. https://www.santhera.com/assets/files/press-releases/2022-10-31_MAAvalidated_e_final.pdf, accessed December 8, 2022.

Sarepta
2021a Sarepta Therapeutics' Investigational Gene Therapy for the Treatment of Duchenne Muscular Dystrophy, SRP-9001, Demonstrates Robust Expression and Consistent Safety Profile Using Sarepta's Commercial Process Material | Sarepta Therapeutics, Inc. https://investorrelations.sarepta.com/news-releases/news-release-details/sarepta-therapeutics-investigational-gene-therapy-treatment, accessed December 8, 2022.
2021b Sarepta Therapeutics Announces Top-Line Results for Part 1 of Study 102 Evaluating SRP-9001, Its Investigational Gene Therapy for the Treatment of Duchenne Muscular Dystrophy | Sarepta Therapeutics, Inc. https://investorrelations.sarepta.com/news-releases/news-release-details/sarepta-therapeutics-announces-top-line-results-part-1-study-102, accessed December 8, 2022.

Sarepta Therapeutics
2020 Sarepta Therapeutics Announces Positive Clinical Results from MOMENTUM, a Phase 2 Clinical Trial of SRP-5051 in Patients with Duchenne Muscular Dystrophy Amenable to Skipping Exon 51 | Sarepta Therapeutics, Inc. https://investorrelations.sarepta.com/news-releases/news-release-details/sarepta-therapeutics-announces-positive-clinical-results, accessed December 8, 2022.
2021C Sarepta Therapeutics Reports Positive Clinical Results from Phase 2 MOMENTUM Study of SRP-5051 in Patients with Duchenne Muscular Dystrophy Amenable to Skipping Exon 51 | Sarepta Therapeutics, Inc. https://investorrelations.sarepta.com/news-releases/news-release-details/sarepta-therapeutics-reports-positive-clinical-results-phase-2, accessed December 8, 2022.
2022A Sarepta Therapeutics Provides Update on SRP-5051 for the Treatment of Duchenne Muscular Dystrophy | Sarepta Therapeutics, Inc. https://investorrelations.sarepta.com/news-releases/news-release-details/sarepta-therapeutics-provides-update-srp-5051-treatment-duchenne, accessed December 8, 2022.
2022B Sarepta Therapeutics Announces That FDA Has Lifted Its Clinical Hold on SRP-5051 for the Treatment of Duchenne Muscular Dystrophy | Sarepta Therapeutics, Inc. https://investorrelations.sarepta.com/news-releases/news-release-details/sarepta-therapeutics-announces-fda-has-lifted-its-clinical-hold, accessed December 8, 2022.

Sawnani, Hemant, Paul S. Horn, Brenda Wong, et al.
2019 Comparison of Pulmonary Function Decline in Steroid-Treated and Steroid-Naïve Patients with Duchenne Muscular Dystrophy. The Journal of Pediatrics 210: 194-200.e2.

Senn, Joseph J., Sebastien Burel, and Scott P. Henry
2005 Non-CpG-Containing Antisense 2′-Methoxyethyl Oligonucleotides Activate a Proinflammatory Response Independent of Toll-like Receptor 9 or Myeloid Differentiation Factor 88. The Journal of Pharmacology and Experimental Therapeutics 314(3): 972–979.

Servais, Laurent, Eugenio Mercuri, Volker Straub, et al.
2022 Long-Term Safety and Efficacy Data of Golodirsen in Ambulatory Patients with Duchenne Muscular Dystrophy Amenable to Exon 53 Skipping: A First-in-Human, Multicenter, Two-Part, Open-Label, Phase 1/2 Trial. Nucleic Acid Therapeutics 32(1): 29–39.

Sharp, N. J., J. N. Kornegay, S. D. Van Camp, et al.
1992 An Error in Dystrophin MRNA Processing in Golden Retriever Muscular Dystrophy, an Animal Homologue of Duchenne Muscular Dystrophy. Genomics 13(1): 115–121.

Sheehan, Daniel W., David J. Birnkrant, Joshua O. Benditt, et al.
2018 Respiratory Management of the Patient With Duchenne Muscular Dystrophy. Pediatrics 142(Suppl 2): S62–S71.

Sheehan, J. P., and T. M. Phan
2001 Phosphorothioate Oligonucleotides Inhibit the Intrinsic Tenase Complex by an Allosteric Mechanism. Biochemistry 40(16): 4980–4989.

Sheikh, Omar, and Toshifumi Yokota
2022 Pharmacology and Toxicology of Eteplirsen and SRP-5051 for DMD Exon 51 Skipping: An Update. Archives of Toxicology 96(1): 1–9.

Shimatsu, Yoshiki, Kouichi Katagiri, Toshio Furuta, et al.
2003 Canine X-Linked Muscular Dystrophy in Japan (CXMDJ). Experimental Animals 52(2): 93–97.

Simmons, Tabatha R., Tatyana A. Vetter, Nianyuan Huang, et al.
2021 Pre-Clinical Dose-Escalation Studies Establish a Therapeutic Range for U7snRNA-Mediated DMD Exon 2 Skipping. Molecular Therapy. Methods & Clinical Development 21: 325–340.

Sixto-López, Yudibeth, Martiniano Bello, and José Correa-Basurto
2020 Exploring the Inhibitory Activity of Valproic Acid against the HDAC Family Using an MMGBSA Approach. Journal of Computer-Aided Molecular Design 34(8): 857–878.

Skuk, Daniel, and Jacques P. Tremblay
2014 First Study of Intra-Arterial Delivery of Myogenic Mononuclear Cells to Skeletal Muscles in Primates. Cell Transplantation 23 Suppl 1: S141-150.

Solid Biosciences
2021 Solid Biosciences Provides First Quarter 2021 Business Update and Financial Results. Text. Solid Biosciences. https://www.solidbio.com/about/media/press-releases/solid-biosciences-provides-first-quarter-2021-business-update-and-financial-results, accessed December 8, 2022.
2018a Solid Biosciences Announces Clinical Hold On SGT-001 Phase I/II Clinical Trial For Duchenne Muscular Dystrophy. Text. Solid Biosciences. https://www.solidbio.com/about/media/press-releases/solid-biosciences-announces-clinical-hold-on-sgt-001-phase-i-ii-clinical-trial-for-duchenne-muscular-dystrophy, accessed December 8, 2022.
2019a Solid Biosciences Announces Preliminary SGT-001 Data and Intention to Dose Escalate in IGNITE DMD Clinical Trial for Duchenne Muscular Dystrophy. Text. Solid Biosciences. https://www.solidbio.com/about/media/press-releases/solid-biosciences-announces-preliminary-sgt-

001-data-and-intention-to-dose-escalate-in-ignite-dmd-clinical-trial-for-duchenne-muscular-dystrophy-1, accessed December 8, 2022.
2019b Solid Biosciences Provides SGT-001 Program Update. Text. Solid Biosciences. https://www.solidbio.com/about/media/press-releases/solid-biosciences-provides-sgt-001-program-update, accessed December 8, 2022.
2022a Solid Biosciences Reports Fourth Quarter and Full-Year 2021 Financial Results and 2-Year Efficacy and Safety Data from the Ongoing Phase I/II IGNITE DMD Clinical Trial of SGT-001. Text. Solid Biosciences. https://www.solidbio.com/about/media/press-releases/solid-biosciences-reports-fourth-quarter-and-full-year-2021-financial-results-and-2-year-efficacy-and-safety-data-from-the-ongoing-phase-i-ii-ignite-dmd-clinical-trial-of-sgt-001, accessed January 9, 2023.
2022b Solid Biosciences Announces Updated Corporate Strategy to Develop SGT-001 and SGT-003 Pipeline Programs for Patients with Duchenne Muscular Dystrophy. Text. Solid Biosciences. https://www.solidbio.com/about/media/press-releases/solid-biosciences-announces-updated-corporate-strategy-to-develop-sgt-001-and-sgt-003-pipeline-programs-for-patients-with-duchenne-muscular-dystrophy, accessed January 9, 2023.
2022c Solid Biosciences Reports Additional Preclinical Data Demonstrating That Its Novel Capsid, AAV-SLB101, Provides Superior Transduction Efficiency and Enhanced Distribution to Skeletal Muscle. Text. Solid Biosciences. https://www.solidbio.com/about/media/press-releases/solid-biosciences-reports-additional-preclinical-data-demonstrating-that-its-novel-capsid-aav-slb101-provides-superior-transduction-efficiency-and-enhanced-distribution-to-skeletal-muscle, accessed January 9, 2023.

Spitali, Pietro, Janneke C. van den Bergen, Ingrid E. C. Verhaart, et al.
2013 DMD Transcript Imbalance Determines Dystrophin Levels. The FASEB Journal 27(12): 4909–4916.

Stedman, H. H., H. L. Sweeney, J. B. Shrager, et al.
1991 The Mdx Mouse Diaphragm Reproduces the Degenerative Changes of Duchenne Muscular Dystrophy. Nature 352(6335): 536–539.

Sui, Tingting, Yeh Siang Lau, Di Liu, et al.
2018 A Novel Rabbit Model of Duchenne Muscular Dystrophy Generated by CRISPR/Cas9. Disease Models & Mechanisms 11(6): dmm032201.

Summerton, J.
1999 Morpholino Antisense Oligomers: The Case for an RNase H-Independent Structural Type. Biochimica Et Biophysica Acta 1489(1): 141–158.

Summit Therapeutics
2018 Summit Therapeutics Discontinues Ezutromid for DMD after Disappointing Phase 2 Trial Results. Muscular Dystrophy Association. https://strongly.mda.org/summit-therapeutics-discontinues-ezutromid-dmd-disappointing-trial-results/, accessed December 8, 2022.

Sun, Congshan, Carlo Serra, Gabsang Lee, and Kathryn R. Wagner
2020 Stem Cell-Based Therapies for Duchenne Muscular Dystrophy. Experimental Neurology 323: 113086.

Takeda, S.
2001 [Development of new therapy on muscular dystrophy]. Rinsho Shinkeigaku = Clinical Neurology 41(12): 1154–1156.

Takeshima, Yasuhiro, Mariko Yagi, Hiroko Wada, et al.
2006 Intravenous Infusion of an Antisense Oligonucleotide Results in Exon Skipping in Muscle Dystrophin MRNA of Duchenne Muscular Dystrophy. Pediatric Research 59(5): 690–694.

Taylor, Michael, John Jefferies, Barry Byrne, et al.
2019 Cardiac and Skeletal Muscle Effects in the Randomized HOPE-Duchenne Trial. Neurology 92(8): e866–e878.

Tinsley, J., N. Deconinck, R. Fisher, et al.
1998 Expression of Full-Length Utrophin Prevents Muscular Dystrophy in Mdx Mice. Nature Medicine 4(12): 1441–1444.

Tinsley, J. M., D. J. Blake, and K. E. Davies
1993 Apo-Dystrophin-3: A 2.2kb Transcript from the DMD Locus Encoding the Dystrophin Glycoprotein Binding Site. Human Molecular Genetics 2(5): 521–524.

Tinsley, Jon, Neil Robinson, and Kay E. Davies
2015 Safety, Tolerability, and Pharmacokinetics of SMT C1100, a 2-Arylbenzoxazole Utrophin Modulator, Following Single- and Multiple-Dose Administration to Healthy Male Adult Volunteers. Journal of Clinical Pharmacology 55(6): 698–707.

Tinsley, Jonathon M., Rebecca J. Fairclough, Richard Storer, et al.
2011 Daily Treatment with SMTC1100, a Novel Small Molecule Utrophin Upregulator, Dramatically Reduces the Dystrophic Symptoms in the Mdx Mouse. PloS One 6(5): e19189.

Toussaint, Michel, Zoe Davidson, Veronique Bouvoie, et al.
2016 Dysphagia in Duchenne Muscular Dystrophy: Practical Recommendations to Guide Management. Disability and Rehabilitation 38(20). Taylor & Francis: 2052.

Tsoumpra, Maria K., Seiji Fukumoto, Toshio Matsumoto, et al.
2019 Peptide-Conjugate Antisense Based Splice-Correction for Duchenne Muscular Dystrophy and Other Neuromuscular Diseases. EBioMedicine 45: 630–645.

Turner, P. R., T. Westwood, C. M. Regen, and R. A. Steinhardt
1988 Increased Protein Degradation Results from Elevated Free Calcium Levels Found in Muscle from Mdx Mice. Nature 335(6192): 735–738.

Valera, Isela C., Amanda L. Wacker, Hyun Seok Hwang, et al.
2021 Essential Roles of the Dystrophin-Glycoprotein Complex in Different Cardiac Pathologies. Advances in Medical Sciences 66(1): 52–71.

Veltrop, Marcel, Laura van Vliet, Margriet Hulsker, et al.
2018 A Dystrophic Duchenne Mouse Model for Testing Human Antisense Oligonucleotides. PloS One 13(2): e0193289.

Verma, Sumit, Stella N. Nwosu, Raj Razdan, et al.
2022 Seroprevalence of AAV Neutralizing Antibodies in Males with Duchenne Muscular Dystrophy. Human Gene Therapy.

Victor, Ronald G., H. Lee Sweeney, Richard Finkel, et al.
2017 A Phase 3 Randomized Placebo-Controlled Trial of Tadalafil for Duchenne Muscular Dystrophy. Neurology 89(17): 1811–1820.

Vulin, Adeline, Inès Barthélémy, Aurélie Goyenvalle, et al.
2012 Muscle Function Recovery in Golden Retriever Muscular Dystrophy after AAV1-U7 Exon Skipping. Molecular Therapy: The Journal of the American Society of Gene Therapy 20(11): 2120–2133.

Wagner, J. A., T. Reynolds, M. L. Moran, et al.
1998 Efficient and Persistent Gene Transfer of AAV-CFTR in Maxillary Sinus. Lancet (London, England) 351(9117): 1702–1703.

Wagner, K., H. Phan, L. Servais, et al.
2019 O.28Safety and Tolerability of Suvodirsen (WVE-210201) in Patients with Duchenne Muscular Dystrophy: Results from a Phase 1 Clinical Trial. Neuromuscular Disorders 29. Elsevier: S124.

Wagner, Kathryn R., Hoda Z. Abdel-Hamid, Jean K. Mah, et al.
2020 Randomized Phase 2 Trial and Open-Label Extension of Domagrozumab in Duchenne Muscular Dystrophy. Neuromuscular Disorders: NMD 30(6): 492–502.

Wagner, Kathryn R., Nancy L. Kuntz, Erica Koenig, et al.
2021 Safety, Tolerability, and Pharmacokinetics of Casimersen in Patients with Duchenne Muscular Dystrophy Amenable to Exon 45 Skipping: A Randomized, Double-Blind, Placebo-Controlled, Dose-Titration Trial. Muscle & Nerve 64(3): 285–292.

Waldrop, Dr Megan, Dr Michael Lawlor, Tatyana Meyers Vetter, et al.
2020 LATE BREAKING NEWS ORAL PRESENTATION: LBO 3 Expression of Apparent Full-Length Dystrophin in Skeletal Muscle in a First-in-Human Gene Therapy Trial Using the ScAAV9.U7-ACCA Vector. Neuromuscular Disorders 30. Elsevier: S166–S167.

Waldrop, Megan A., and Kevin M. Flanigan
2019 Update in Duchenne and Becker Muscular Dystrophy. Current Opinion in Neurology 32(5): 722–727.

Wallace, G. B., and R. W. Newton
1989 Gowers' Sign Revisited. Archives of Disease in Childhood 64(9): 1317–1319.

Walmsley, Gemma L., Virginia Arechavala-Gomeza, Marta Fernandez-Fuente, et al.
2010 A Duchenne Muscular Dystrophy Gene Hot Spot Mutation in Dystrophin-Deficient Cavalier King Charles Spaniels Is Amenable to Exon 51 Skipping. PloS One 5(1): e8647.

Wang, B., J. Li, and X. Xiao
2000 Adeno-Associated Virus Vector Carrying Human Minidystrophin Genes Effectively Ameliorates Muscular Dystrophy in Mdx Mouse Model. Proceedings of the National Academy of Sciences of the United States of America 97(25): 13714–13719.

Wang, Zhong, Tong Zhu, Chunping Qiao, et al.
2005 Adeno-Associated Virus Serotype 8 Efficiently Delivers Genes to Muscle and Heart. Nature Biotechnology 23(3): 321–328.

Wave Life Sciences
2019 Wave Life Sciences Announces Discontinuation of Suvodirsen Development for Duchenne Muscular Dystrophy - Wave Life Sciences. https://ir.wavelifesciences.com/news-releases/news-release-details/wave-life-sciences-announces-discontinuation-suvodirsen, accessed December 8, 2022.
2022A Wave Life Sciences Reports Third Quarter 2022 Financial Results and Provides Business Update - Wave Life Sciences. https://ir.wavelifesciences.com/news-releases/news-release-details/wave-life-sciences-reports-third-quarter-2022-financial-results, accessed December 8, 2022.
2022b Wave Life Sciences Provides Positive Update on Proof-of-Concept Study for WVE-N531 in Duchenne Muscular Dystrophy - Wave Life Sciences. https://ir.wavelifesciences.com/news-releases/news-release-details/wave-life-sciences-provides-positive-update-proof-concept-study, accessed January 9, 2023.

Welch, Ellen M., Elisabeth R. Barton, Jin Zhuo, et al.
2007 PTC124 Targets Genetic Disorders Caused by Nonsense Mutations. Nature 447(7140): 87–91.

Wickstrom, E.
1986 Oligodeoxynucleotide Stability in Subcellular Extracts and Culture Media. Journal of Biochemical and Biophysical Methods 13(2): 97–102.

Willmann, Raffaella, Stefanie Possekel, Judith Dubach-Powell, Thomas Meier, and Markus A. Ruegg
2009 Mammalian Animal Models for Duchenne Muscular Dystrophy. Neuromuscular Disorders: NMD 19(4): 241–249.

Xu, Li, Ki Ho Park, Lixia Zhao, et al.
2016 CRISPR-Mediated Genome Editing Restores Dystrophin Expression and Function in Mdx Mice. Molecular Therapy: The Journal of the American Society of Gene Therapy 24(3): 564–569.

Yang, B., X. Ming, C. Cao, et al.
2015 High-Throughput Screening Identifies Small Molecules That Enhance the Pharmacological Effects of Oligonucleotides. Nucleic Acids Research 43(4): 1987–1996.

Yavas, Alper, Rudie Weij, Maaike van Putten, et al.
2020 Detailed Genetic and Functional Analysis of the HDMDdel52/Mdx Mouse Model. PloS One 15(12): e0244215.

Yazaki, M., K. Yoshida, A. Nakamura, et al.
1999 Clinical Characteristics of Aged Becker Muscular Dystrophy Patients with Onset after 30 Years. European Neurology 42(3): 145–149.

Yin, HaiFang, Amer F. Saleh, Corinne Betts, et al.
2011 Pip5 Transduction Peptides Direct High Efficiency Oligonucleotide-Mediated Dystrophin Exon Skipping in Heart and Phenotypic Correction in Mdx Mice. Molecular Therapy: The Journal of the American Society of Gene Therapy 19(7): 1295–1303.

Yoon, Mee-Sup
2017 MTOR as a Key Regulator in Maintaining Skeletal Muscle Mass. Frontiers in Physiology 8: 788.

Young, Courtney S., Ekaterina Mokhonova, Marbella Quinonez, April D. Pyle, and Melissa J. Spencer
2017 Creation of a Novel Humanized Dystrophic Mouse Model of Duchenne Muscular Dystrophy and Application of a CRISPR/Cas9 Gene Editing Therapy. Journal of Neuromuscular Diseases 4(2): 139–145.

Yuasa, K., A. Ishii, Y. Miyagoe, and S. Takeda
1997 [Introduction of rod-deleted dystrophin cDNA, delta DysM3, into mdx skeletal muscle using adenovirus vector]. Nihon Rinsho. Japanese Journal of Clinical Medicine 55(12): 3148–3153.

Yucel, Nora, Alex C. Chang, John W. Day, Nadia Rosenthal, and Helen M. Blau
2018 Humanizing the Mdx Mouse Model of DMD: The Long and the Short of It. NPJ Regenerative Medicine 3: 4.

Yue, Yongping, Arkasubhra Ghosh, Chun Long, et al.
2008 A Single Intravenous Injection of Adeno-Associated Virus Serotype-9 Leads to Whole Body Skeletal Muscle Transduction in Dogs. Molecular Therapy: The Journal of the American Society of Gene Therapy 16(12): 1944–1952.

Zamecnik, P. C., and M. L. Stephenson
1978 Inhibition of Rous Sarcoma Virus Replication and Cell Transformation by a Specific Oligodeoxynucleotide. Proceedings of the National Academy of Sciences of the United States of America 75(1): 280–284.

Zarrouki, Faouzi, Karima Relizani, Flavien Bizot, et al.
2022 Partial Restoration of Brain Dystrophin and Behavioral Deficits by Exon Skipping in the Muscular Dystrophy X-Linked (Mdx) Mouse. Annals of Neurology 92(2): 213–229.

Zaynitdinova, M. I., A. V. Lavrov, and S. A. Smirnikhina
2021 Animal Models for Researching Approaches to Therapy of Duchenne Muscular Dystrophy. Transgenic Research 30(6): 709–725.

Zhang, Goufeng, James J. Ludtke, Christine Thioudellet, et al.
2004 Intraarterial Delivery of Naked Plasmid DNA Expressing Full-Length Mouse Dystrophin in the Mdx Mouse Model of Duchenne Muscular Dystrophy. Human Gene Therapy 15(8): 770–782.

Zhang, Yu, Chengzu Long, Rhonda Bassel-Duby, and Eric N. Olson
2018 Myoediting: Toward Prevention of Muscular Dystrophy by Therapeutic Genome Editing. Physiological Reviews 98(3): 1205–1240.

Zou, Xiaodong, Hongsheng Ouyang, Daxin Pang, Renzhi Han, and Xiaochun Tang
2021 Pathological Alterations in the Gastrointestinal Tract of a Porcine Model of DMD. Cell & Bioscience 11(1): 131.

ANNEXES

Current status of antisense oligonucleotide-based therapy in neuromuscular disorders

Flavien Bizot[1], Adeline Vulin[1,2] and Aurélie Goyenvalle[1,3§]

[1] Université Paris-Saclay, UVSQ, Inserm, END-ICAP, 78000 Versailles, France.

[2] SQY Therapeutics, Université de Versailles St-Quentin, Montigny le bretonneux, France.

[3]LIA BAHN, Centre scientifique de Monaco, Monaco.

[§]Correspondence to: aurelie.goyenvalle@uvsq.fr

Short title: Antisense oligonucleotide-based therapies

Key points:

ASO hold great promise as a therapeutic platform for the treatment of neuromuscular disorders.

The clinical benefit of ASO-therapy still highly depends on the target tissue and route of administration.

Development of more potent chemistries or novel delivery systems is still required to improve targeted delivery to muscles.

This is a pre-print of an article published in Drugs. The final authenticated version is available online at: https://doi.org/10.1007/s40265-020-01363-3

ABSTRACT

Neuromuscular disorders include a wide-range of diseases affecting the peripheral nervous system, which are primarily characterized by progressive muscle weakness and wasting. While there were no effective therapies until recently, several therapeutic approaches have advanced to clinical trials in the past few years. Among these, the antisense technology aiming at modifying RNA processing and function has remarkably progressed and a few antisense oligonucleotides (ASO) have now been approved. Despite these recent clinical successes, several ASO have also failed and clinical programs have been suspended, in most cases when the route of administration was systemic, highlighting the existing challenges notably with respect to effective ASO delivery.

In this review we will summarize the recent advances and current status of antisense based-therapies for neuromuscular disorders, using successful as well as unsuccessful examples to highlight the variability of outcomes depending on the target tissue and route of administration. We will describe the different ASO-mediated therapeutic approaches, including splice switching applications, steric blocking strategies and targeted gene knock-down mediated by ribonuclease H recruitment. Throughout this overview, we will discuss the merits and challenges of the current ASO technology, and discuss the future of ASO development.

1. INTRODUCTION

Antisense oligonucleotide (ASO)-based therapeutics have made tremendous progress in the last 20 years and the recent approval of several drugs have increased the interest in the field even more.

ASOs are typically synthetic single stranded oligonucleotides of 12 to 30 nucleotides long[1–3], designed to bind to a messenger RNA (mRNA) or non-coding RNA through Watson-Crick base pairing in order to modulate their function/expression. ASOs were first used in 1978 by Zamecnik and Stephenson as a gene silencing approach[4], but the technology has rapidly evolved since then with numerous other possible applications making them a valuable tool for genetic-based therapeutics[5]. While the first unmodified ASOs composed of a phosphodiester backbone and sugar rings were rapidly degraded within cells and bloodstream[6], various modifications have progressively been introduced in their chemical structure in order to protect them from nuclease activity and increase their stability and affinity to target RNA[7]. One of the first modifications introduced was the replacement of one of non-bridging oxygen atoms in the phosphate group with a sulfur atom resulting in phosphorothioate (PS) ASO. This substitution increases the resistance to nuclease degradation and still supports ribonuclease H (RNase H) activity to degrade the target mRNA or mutant toxic mRNA. In addition to their endogenous nuclease resistance, PS modifications offer a significant advantage in terms of pharmacokinetics. Their enhanced affinity for numerous proteins, including plasma, cell surface and intracellular proteins[8,9] facilitates distribution and cellular uptake of PS-ASOs compared to their phosphodiester (PO) counterparts. However, PS modifications are also known to cause undesirable effects due to plasma protein binding[10], raising questions for their safety in humans[11]. Acute reactions of PS backbones may include immune-cell activation[12], complement activation[13] or prolongation of coagulation times[14,15]; known to be transient and normalize when ASOs are cleared from the bloodstream. Despite these safety concerns, PS backbones remain one of the most largely used chemical modifications to protect ASOs from nuclease activity and increase their stability[16].

To further improve nuclease resistance and RNA binding affinity, second generation ASOs were developed with introduction of a chemical modification in the 2'-position of the sugar moiety such as

2'O-methyl (2'OMe), 2'O-methoxyethyl (2'MOE), 2'-fluorinated (2'F) and 2'-O-aminopropyl analogs[17]. Interestingly 2'-modified ASOs were reported to reduce immune stimulation side effects compared to PS-modified ASOs[18]. Chemical ASO modifications have kept evolving with substantial changes in the sugar and have led to a wide variety of designs such as morpholinos[19], locked nucleic acids (LNAs)[20], 2'-4'-constrained ethyl (cEt)[21] or peptide nucleic acids (PNAs)[22].

ASOs can interfere and modulate RNA function via multiple mechanisms which will impact their design and chemical modifications. Several reviews have previously detailed the various molecular mechanisms through which an ASO can impact gene expression[23–25]. Briefly, ASOs can be used to promote RNA degradation via the recruitment of RNase H1 which will cleave the mRNA-ASO hetero-duplex while leaving the ASO intact (figure 1, left panel). It is important to note that most sugar modified ASOs became unable to elicit RNase H1-mediated RNA degradation, hence ASOs must be designed as "gapmers" with a central core of 8 to 10 consecutive DNA nucleotides to support binding and cleavage by RNase H1. Alternatively, ASOs can be fully modified and work through steric hindrance mechanisms either to modulate splicing (in which case they may be called splice switching oligomer - SSO), inhibit RNA toxicity through the disruption of RNA structure, impact polyadenylation selection site, inhibit translation, or bind to microRNAs to block their interaction with mRNA (figure 1, right panel). The variety of mechanisms through which ASO can act and the subsequent therapeutic applications truly represent unique opportunities for the treatment of many conditions. Steady progress in chemistry and design over the years have led to several approved ASO and numerous others currently being tested in clinical trials, in particular for neuromuscular diseases. These recent successes elicit optimism and hope for the development of future therapeutics using the antisense technology. However, the clinical benefit of ASO therapy still very much depends on the target tissue and route of administration. The therapeutic potential of systemically delivered ASOs remains far behind since it is assumed that only about 1% of ASO reach the correct cellular compartment after intravenous or subcutaneous administration[26]. In this review, we will discuss the

recent advances and current status of ASO therapies for several neuromuscular disorders including Duchenne muscular dystrophy (DMD), spinal muscular atrophy (SMA), myotonic dystrophy (DM1), amyotrophic lateral sclerosis (ALS) and Huntington disease (HD). Through these examples, we will cover the broad range of neuromuscular disorders from the muscle to the more neurodegenerative end of the spectrum, like ALS and HD, to reflect the variation in clinical benefit depending on the target tissue/route of administration, but also with respect to the diversity of chemistries and mechanisms of action.

2. Duchenne muscular dystrophy

With an incidence of one per 5,000 boys on average[27], Duchenne muscular dystrophy is the most common muscular dystrophy. DMD is caused by mutations, typically large deletions (approximately 65%) in the DMD gene, disrupting the open reading frame and leading to non-functional or absent dystrophin protein. As dystrophin plays a major mechanical and signalling link between the actin cytoskeleton and the extracellular matrix, its absence leads to progressive muscle wasting and premature death of patients. In contrast to the frame shifting mutations observed in DMD, mutations maintaining an open reading frame allow the production of a partially deleted but, in most cases, functional dystrophin. This is observed in the milder phenotype, Becker muscular dystrophy (BMD), which results in a later age of onset and milder clinical involvement (ranging from intermediate to asymptomatic). Moreover, about 50% of DMD patients have individual dystrophin-positive muscle fibers [28], called revertant fibers, with protein correctly localized at the membrane. It has been shown that they come from a spontaneous skipping of several exons allowing to restore an in-frame transcript[29]. Altogether these observations led to the emergence of a novel therapeutic approach named exon-skipping using ASO to modulate the pre-mRNA splicing (figure 1, right panel). The principle to restore an opening reading frame by exon-skipping therapy for DMD has first been demonstrated more than twenty years ago in culture cells[29]. Since, numerous *in vivo* studies performed in several animal models have provided pre-clinical evidence for the therapeutic potential

of antisense strategy. Although the exon-skipping approach appears to be able to restore the reading frame in a large proportion of patients (possibly up to 83% of all DMD patients[32]), this strategy will not offer a definite cure but an improvement towards a BMD-like phenotype depending on the functionality of the restored dystrophin, as not all protein domains are dispensable. Favorably, the majority of deletions clusters into hotspot regions between exons 43 and 53, suggesting that skipping of the same group of exons is applicable to large groups of patients. Notably, exon 51 skipping (applicable to 13% of all patients) was the primary choice for numerous phase 1 clinical trials, which evaluated various chemistries of antisense oligonucleotides as detailed below.

2.1. 2'-O-Methyl-PS RNA.

While most of the preclinical work using 2'OMe-PS ASO for DMD was produced by the LUMC (Leiden University Medical Center)-based research groups, first clinical data were actually published by a Japanese group in 2006 using a PS DNA ASO (Table 1). A single patient, with an exon 20 deletion, was injected with a 31-mer ASO targeting the exon 19 of the DMD gene (named AO19) in the peripheral vein at 0.5 mg/kg four times at one-week intervals[33]. The treatment was well tolerated and resulted in the detection of skipped transcript in lymphocytes (despite this target being questionable), and traces in biopsied biceps muscle. Nevertheless, the novel transcript did not allow the restoration of quantifiable dystrophin expression and no follow-up studies were ever conducted.

In parallel in Europe, a 20-mer 2'OMe-PS ASO targeting exon 51 was developed and shown to restore significant levels of dystrophin in mouse models of DMD[34]. Based on these encouraging preclinical data, the Dutch group in collaboration with Prosensa evaluated the intramuscular injection of this ASO named drisapersen in four DMD patients eligible for exon 51 skipping[35]. The treatment was well tolerated and confirmed the proof of principle of the ASO-mediated exon skipping approach for DMD since some dystrophin expression was detected, supporting the development of further clinical investigations. Results of the phase 1/2a trial evaluating the systemic administration of drisapersen were published in 2011[36]. Four groups of 3 DMD boys received abdominal subcutaneous injection at

doses of 0.5, 2, 4 and 6 mg/kg/week of 2'OMe-PS ASO for 5 weeks followed by a 6 to 15 months off-treatment and a 12-week extension phase at 6 mg/kg/week. While no serious adverse effects were reported, a total of 120 mild or moderate adverse events occurred, notably proteinuria and several types of reactions at the injection site. Tibialis anterior muscle biopsy samples were analyzed at 2 weeks and 7 weeks after the end of the dose-escalation phase. Exon 51 skipping was observed in all patients receiving 2, 4 or 6 mg/kg/week at both time points but with variable extent. Quantification of western blot shows that dystrophin signal intensity was 1.5 to 8.2 times greater than the baseline condition (taken from 0.5 mg/kg group of patients) in the groups receiving 4 and 6 mg/kg/week, 2 weeks after the end of the treatment. Following 12 weeks of treatment, no increase in specific muscle force was observed but there was average improvement of 35.2 ±28.7m in the distance walked in 6 minutes (6MWD). Those 12 patients entered a long-term 188-week extension study with subcutaneous injection of 6 mg/kg/week initially[37]. Similar adverse effects were reported, including injection-site reactions (erythema, hematoma, and induration), increased urinary α1-microglobulin, and proteinuria. Biopsies were taken from the tibialis anterior muscle at week 24 for all subjects and at either week 68 or 72 for volunteering subjects. Although exon-skipping and dystrophin were detected at both time-points, no formal conclusion could be drawn on potential increase from baseline because no material from pre-treatment biopsies was available. At the end of the treatment, 2 patients were non-ambulant and 2 were unable to complete the 6MWD at later visits. Nevertheless, on the 8 remaining subjects, the 6MWD appeared improved by a median increase of 64 meters (mean=33) and the cardiac function showed stability but on the other hand, muscle strength decreased during the study. Interestingly though, despite the heterogeneity of subjects, some of them who were in a decline stage of the disease maintained ambulation throughout the study. Based on these relatively encouraging data, an open-label extension phase 3 study was launched with 186 ambulant subjects[38]. Unfortunately, the slight difference observed in the 6MWD from baseline was found non-significant, which was thought to be largely due to subgroup heterogeneity. A post-hoc analysis, performed on a subgroup of 80 subjects with a baseline 6MWD

between 300 and 400 meters, revealed a treatment benefit in 6MWD of 35.4 meters (95% CI: 1.8, 69.0), supporting early intervention. The inability to meet the primary efficacy endpoint (improvement in 6MWD) together with the significant adverse effects (injection-site reactions and renal issues) led to the rejection of drisapersen's application by the US Food and drugs Administration (FDA). By mid-2016, Biomarin announced the withdrawal of drisapersen market authorization application in Europe and the discontinuation of all their ASO programs for DMD which included exons 44, 45 and 53 to invest in research of next generation ASOs.

2.2. Phosphorodiamidate Morpholino Oligomer (PMO)

In parallel to the 2'OMe-PS ASO development, another chemistry of ASO was developed for DMD: Phosphorodiamidate Morpholino Oligomers also called PMO. Following numerous preclinical studies showing encouraging results[39], the UK MDEX consortium conducted a phase 1/2 trial with a 30-mer PMO targeting exon 51, named eteplirsen, in seven patients. Intramuscular injection of eteplirsen was well tolerated by all patients and intensity of dystrophin staining increased to 42% of normal levels in dystrophin positive fibers of patients treated with the higher dose[40]. While intramuscular injection was a valuable proof-of-concept, the main challenge in DMD is to target cardiac and respiratory muscles therefore systemic delivery was next assessed. Sarepta started a dose escalation study from 0.5 to 20 mg/kg with multiple injections[41]. Adverse events were generally mild to moderate and a dose-dependent significant increase in dystrophin expression was observed and associated with α-sarcoglycan and neuronal nitric oxide (nNOS) restoration at the sarcolemma. Following these encouraging results, phase 2 studies with higher doses (30 and 50 mg/kg) were launched[42]. Eteplirsen injections resulted in increased dystrophin production in all patients following at least 24 weeks of treatment with a statistically significant difference in the 6MWD in some patients, depending on the age-related disease progression[43]. Based on detection of dystrophin protein (although minor) and the absence of adverse events, eteplirsen was approved by the FDA in 2016, under the accelerated approval pathway, despite no measures of muscle function. Although its

approval was shrouded in controversy, eteplirsen became the first approved drug for DMD in the US, as well as the first approved splice-switching ASO[44]. Sarepta was asked to perform confirmatory studies to establish a clinical benefit which had not been demonstrated. In 2019, they started to recruit patients for a phase 3 study with intravenous (IV) injections of two different high doses (>30 mg/kg). In the meantime, they reported functional data from two non-ambulatory patients compared to 10 patients who remained ambulatory[45] and showed that despite the loss of ambulation, their cardiac, pulmonary and upper limb functions remained relatively stable and the increase in dystrophin production (less than 2%) was similar to those of ambulatory patients. As eteplirsen was well tolerated over 3.2 years, Sarepta performed a phase 3 study with 7 to 16 years old patients and a phase 2 study on younger child (4-6 years old), but no results have been published yet.

Regardless of eteplirsen's approval by the FDA in 2016, two years later the European Medicines Agency (EMA) gave a negative opinion for this treatment[44]. In their public report, the Committee for Medicinal Products for Human Use (CHMP) considered that the safety profile of eteplirsen had not been thoroughly characterized and they mentioned that a sufficient number of patients compared to placebo would be needed to conclude. They concluded that the current benefit-risk balance was not positive since the efficacy was not sufficiently demonstrated. This difference between the two agencies highlights their dissimilar views on the role of dystrophin as a surrogate endpoint. Despite this setback in Europe, Sarepta continued the clinical development of their PMO-ASOs notably targeting exons 45 and 53. Toxicology results in non-human primates suggested an encouraging safety profile of these two PMOs, SRP-4045 (Casimersen) and SRP-4053 (Golodirsen), similar to eteplirsen[46]. Findings were mostly limited to the kidneys, which presented minor microscopic changes that were non-adverse after 12 weeks of infusion with SRP-4045 and SRP-4053, or 39 weeks of infusion with eteplirsen at various doses (5, 40 and 320 mg/kg/week)[46]. Based on positive results from a phase 1/2 clinical trial [47], golodirsen received in December 2019 its first global approval in the USA for the treatment of DMD patients amenable to exon 53 skipping[48].

Another company, NS-Pharma, in collaboration with Japanese groups, used another optimized sequence named Viltolarsen (NS-065/NCNP-01) to target exon 53 but with much higher doses (up to 80 mg/kg). In a phase 1 dose-escalation trial, the increase of dystrophin was negligible, except for one patient with a dystrophin/spectrin ratio increased by 8.1%, correlated to a significant skipping in the higher dose group[49]. No serious adverse events were reported and the observed drug reactions were common for ASOs such as proteinuria, albuminuria or increase in N-acetyl-β-D-glucosaminidase but also anemia. Following this phase 1, parallel trials in USA/Canada and in Japan have been completed. During the Japanese phase 1/2 study with the higher doses of 40 and 80 mg/kg/week for 24 weeks, the increase of dystrophin expression was between 0.13 and 2.78% respectively. In parallel, the North American phase 2 study with the same doses showed that the average increase in dystrophin protein was about 5% from baseline[50]. However, it is important to note that there are no standardized methodologies for dystrophin quantification between those studies, despite the recent emergence of alternative methods to quantify dystrophin, such as mass spectrometry, capillary western immunoassay or immune-affinity liquid chromatography [51]. Based on the presence of dystrophin restoration (without measurement of muscle function), and the absence of serious adverse effects Viltolarsen was approved in March 2020 and thus became the first ASO to be approved by the Japanese agency.

In spite of these recent approvals suggesting some success, the levels of restored dystrophin in biopsies from DMD patients treated with these compounds remain extremely low. It is therefore unclear at the moment whether these drugs can truly achieve clinically relevant outcomes. To improve the delivery of ASOs to targeted tissues[26], alternative chemistries are being developed, as well as novel generations of conjugated ASOs.

2.3. Alternative chemistries and next generations of compounds

Wave Life Sciences recently developed an investigational stereopure ASO (suvodirsen), designed for exon 51 skipping, which was shown to induce enhanced exon skipping and dystrophin protein restoration in cell cultures compared with other exon-skipping compounds such as eteplirsen or drisapersen (52% dystrophin protein restoration in cells versus 1% with other exon skipping ASOs). A phase 1 clinical trial was initiated in November 2017 to assess the safety and tolerability of suvodirsen with 5 ascending doses, from 0.5 to 10 mg/kg/week. They reported infusion-associated reactions consisting of pyrexia, headache, vomiting and tachycardia, essentially for the doses equal or higher than 5 mg/kg. As patients who received 7 or 10 mg/kg met the predefined stopping criteria, the remained patients moved directly into the open label extension at the 5 mg/kg dose level[52]. In December 2019, Wave announced that interim results showed no change from baseline in dystrophin expression with either the 3.5 or 5 mg/kg doses of suvodirsen. Both the extension trial and the phase 2/3 trial were discontinued and further development of exon 53 compounds was suspended.

Among advancing chemistries, a Japanese group developed a 2'-OMe RNA/ENA (2'-O,4'-C-ethylene-bridged nucleic acid) chimera ASO to induce dystrophin exon 45 skipping[54]. During the congress Myology in 2016, the group presented results from one clinical study with a 7-year old boy. After 4 weeks IV infusion at 0.5 mg/kg/week, they showed partial exon skipping and reported an increase of the 6MWD. A phase 1/2 clinical trial is ongoing in Japan to evaluate the safety, tolerability, effectiveness, and pharmacokinetics of the drug (DS-5141). DMD patients are given subcutaneous injections of DS-5141 at different doses (0.1, 0.5, 2 and 6 mg/kg) for up to 12 weeks and then enrolled in an extension protocol of 48 weeks with doses at 2 and 6 mg/kg. Results announced in April 2018 by the company revealed no serious adverse events but efficacy data were unclear with detection of exon 45 skipping in all participants while dystrophin protein was only partially

identified[55]. The study has been updated on the US Clinical Trials website and announced a study completion date in December 2020.

Conjugation of ASO to cell penetrating peptides (CPP) has also been investigated to improve delivery to the muscle and peptide conjugated-PMO (PPMO) have shown encouraging preclinical data[56]. Despite the toxicity issues arisen in non-human primates treated with the first PPMO developed against exon 50 [57], newer generations of CPP with better safety profile have since been developed. Sarepta has recently completed a phase 1 trial with a PPMO targeting exon 51 and is now recruiting for a phase 1/2. No results have been posted or published yet.

Development of other alternative chemistries led to the identification of tricyclo-DNA (tcDNA) as a promising ASO for therapeutic splice-switching applications. TcDNA have demonstrated unique pharmaceutical properties and widespread uptake in many tissues after systemic delivery; including the capacity to cross the blood brain barrier (BBB) at low level after systemic delivery[58,59]. A phase 1/2 clinical trial is programmed for mid-2021.

Another alternative to overcome the delivery and potential toxicity challenges of ASO is the use of viral vectors encoding small nuclear RNAs engineered to shuttle antisense sequences into cells. This type of vectorization in adeno-associated virus (AAV) vector has demonstrated promising preclinical data in mouse and dog models of DMD, allowing appropriate subcellular localization with pre-mRNAs and long term correction[60–62]. Based on these encouraging findings, a phase 1/2 clinical trial is currently being planned by Audentes therapeutics in collaboration with the Nationwide Children's Hospital to develop a first product candidate, AT702 targeting exon 2. Exon duplications account for 11% of DMD mutations and exon 2 is the most common duplication in patients. Targeting duplications aims to create a full-length dystrophin (i.e. fully functional) in contrast with internally deleted dystrophin resulting from the correction of frameshift or nonsense mutations.

3. Spinal muscular atrophy

Spinal muscular atrophy (SMA) is a group of autosomal-recessive inherited disease characterized by progressive muscle atrophy due to the degeneration of α-motor neurons of the anterior horn of spinal cord. In most cases SMA is caused by homozygous deletions of the gene *SMN1* (survival motor neuron 1) encoding the SMN protein and its clinical phenotype is heterogeneous, ranging from a severe to a mild phenotype (SMA type 1 to 4). A prevalence of approximately 1–2 per 100,000 persons and incidence around 1 in 10,000 live births have been estimated with SMA type 1 accounting for around 60% of all cases[63]. Loss of SMN leads to a progressive proximal muscle weakness and deleterious effects on respiratory function. In humans, the severity of the disease is mostly counterbalanced by the presence of the *SMN2* gene and inversely proportional to its copy number but discrepant SMA cases support the role of other phenotype modifiers[64]. *SMN2* differs from *SMN1* by one nucleotide in the coding sequence: a C-T substitution at position 6 of exon 7 which results in its exclusion during the splicing of the pre-mRNA in about 90% of the transcripts, but with cells and tissues variation. This alternative spliced product lacking exon 7 is translated into a truncated protein that is degraded shortly after while the 10% correct transcript translates for a full-length functional SMN protein.

Considering that *SMN2* gene is similar in all SMA patients and that they usually have several copies of *SMN2*, modulating its splicing has become an attractive therapeutic option. The mechanism of splicing regulation is complex and involves more than 40 regulatory protein factors. Splicing of *SMN2* exon 7 requires many different elements, including a suboptimal intron 6 branch point[65], an extended inhibitory context, a conserved tract domain, an inhibitory 3'-cluster, an intronic silencer element in intron 7 (ISS-N1) and a terminal stem-loop (TSL) structure on the 5' splice site of exon 7[66]. Once the genomic organization of *SMN2* was better characterized, research groups started using the antisense platform in order to force the inclusion of exon 7 (figure 1, right panel).

Various classes of ASOs have been developed to modulate *SMN2* mRNA splicing, including 2'OMe-PS, PMO and 2'MOE-PS. The most promising candidate identified was an 18-mer 2'MOE-PS ASO targeting the ISS-N1 sequence which was reported to regulate *SMN2* exon 7 inclusion[67]. Initial studies using this ISS-N1 ASO in a mild SMA mouse model (type 3) demonstrated rescue of tail and ear necrosis following intracerebroventricular (ICV) infusion[68]. A year later, the same group demonstrated increased survival of type 1 SMA mice after subcutaneous injections at postnatal day P0 and P3[69]. Clinical trials were initiated in 2012 with this oligonucleotide, named nusinersen (originally IONIS-SMNRx) by Ionis Pharmaceuticals. The first phase 1 clinical trial was conducted in patients with type 2 and 3 SMA[70] and was aimed at evaluating safety, tolerability and pharmacokinetics of a single intrathecal injection at different doses (1, 3, 6 and 9 mg). In this study, nusinersen was not only well tolerated but an improvement of motor function was observed with the 9 mg dose. Moreover, with a half-life in cerebrospinal fluid (CSF) of 4 to 6 months, nusinersen allows large intervals between injections. Several clinical studies quickly followed these encouraging results. First, a phase 2 evaluating multi intrathecal doses of 6 to 12 mg over 32 months of treatment was launched in infants with early onset[71]. The treatment was well tolerated and patients in the 12 mg group showed improvement in motor function and an increase in electrically excitable muscle. Moreover, these patients surpassed median age of death, compared to natural history cohorts. Following these favorable results, a phase 3 study was also initiated with more injections in the first months. Since a greater improvement was seen in patient with a shorter disease progression during treatment initiation, the crucial question of a better clinical response with a pre-symptomatic treatment has been examined in a phase 2 study. Interim efficacy and safety results were recently published[72] and reported that all injected patients past the age of symptom onset were alive, without permanent ventilation. They achieved motor milestones and are continuing to make progress, highlighting the need to start treatment before symptomatic period.

In parallel to these trials on type 1 and 2 patients, studies were conducted on patients with later-onset SMA, including a phase 3 study in children over the course of 15 months[73] and a phase 1b/2a followed by a 3-year extension study[74]. They both confirmed the improvement of motor function and reported that none of the adverse effect was considered drug related therefore validating the effectiveness of nusinersen. In the extension study, electrophysiological outcome measures were reported stable suggesting that the benefit of treatment on distal innervation capacity may be less robust than the overall benefit on motor function. The authors suggested that this may be influenced by different factors such as age, severity of denervation at the time of enrollment, duration of exposure, and nerve muscle group tested.

Nusinersen was approved by the FDA in late December 2016 and by the EMA in June 2017. Commercialized by Biogen under the name spinraza®, this drug probably represents the biggest success of the ASO-based therapy. However, many challenges remain and need to be addressed in the near future. Even if nusinersen leads to global improvement, the response varies from a patient to another and improvement in type 2 patients is less significant than in those with SMA type 1 and there is insufficient evidence of efficacy in SMA types 3 and 4 [75]. Ongoing studies show that presymptomatic treatment may be an important consideration; nevertheless, in patients with active disease, combination of nusinersen with other drugs, including those targeting peripheral tissues may also prove useful and require additional investigations. The involvement of additional peripheral organs, such as cardiac dysfunctions and distal digits necrosis has indeed been reported in the pathogenesis of the disease progression, especially in the most severe cases[76]. The current mode of administration using intrathecal injections does not address these peripheral issues and can be a risk of tissue damage or infection after multiple administrations. Several groups have successfully worked on alternative, albeit still lumbar, route of injection in patients with severe scoliosis or with metal implantation[77–79]. To date, intrathecal administration is used because most PS-ASOs are not able to cross the BBB despite an effective uptake by brain tissues. Promising alternatives are currently being

explored at the preclinical level, with PPMO[80] or tcDNA[81] chemistries which have been shown to cross the BBB after systemic delivery. Besides ASOs, other promising candidates administered systemically are in clinical trials including gene therapy with AAV9 (IV and intrathecal administration), risdiplam, acting as a splicing modifier (oral administration), anti-myostatin antibody and reldesemtiv, a muscle troponin activator (oral administration) (approaches reviewed in [82]). Amongst these, only *SMN1* gene replacement mediated by the AAV vector AVXS-101 has been approved by the FDA so far and offers the advantage of a single administration in contrast with the repeated injections required for nusinersen.

4. **Myotonic dystrophy**

Another example of inherited neuromuscular disorder which can be targeted by ASO is Myotonic dystrophy type 1 (DM1), which is the most common form of muscular dystrophy in adults with an estimated incidence of 1 per 8,000 individuals worldwide[83]. DM1 is a multisystemic disease characterised by myotonia, muscle weakness, cardiac arrhythmias, insulin resistance and cognitive dysfunction. DM1 is caused by an abnormal expansion of a CTG trinucleotide repeat in the 3'-untranslated region of the human dystrophia myotonica protein kinase (*DMPK*) gene.

Transcription of the *DMPK* CTG repeats into a highly structured *DMPK* CUG^{exp} RNA leads to RNA aggregates, referred to as foci in which the muscle blind-like 1 protein (MBNL1) is found sequestered. Limiting the availability of MBLN1 splicing regulator results in the missplicing of several important muscle-expressed genes including *CLCN1*, *INSR*, *BIN1*, *DMD*, and *SCN5A* that have been associated respectively with myotonia, insulin resistance, muscle weakness, dystrophic process, and cardiac conduction defects, all symptoms of DM1[84]. Restoring the abnormal splicing of some of these targets using ASOs has been explored and the correction of *CLCN1* transcripts was achieved using a PMO for example, leading to reduced myotonia in mouse models of DM1[85]. However, targeting the downstream effects may not address all the symptoms of the disease given the large number of misspliced mRNAs in DM1. Alternatively, therapeutic ASOs targeting directly the *DMPK* RNA have

been developed over the years, aiming at either degrading the CUG^{exp} transcripts using gapmer ASOs recruiting RNase H (figure 1, left panel) or at releasing sequestered MBNL1 from CUG^{exp}-containing RNAs by direct competition using steric blocker (fully modified, figure 1 right panel) ASOs. A PMO CAG25 binding to CUG^{exp} RNA was shown to block its interaction with MBNL1, disperse the nuclear foci and therefore reduce the overall burden of this toxic RNA[86]. Interestingly studies using steric blocker ASOs (PMO as well as 2'OMe modified) found a reduction in CUG repeat transcripts when these ASO should only "block" and not degrade the transcripts, therefore suggesting degradation by another pathway once released from binding with MBNL proteins. Reduction of the CUG^{exp} RNA and subsequent reduction in myotonia were also induced more directly using gapmer ASO targeted either to the CUG repeats[87], to the 3'UTR or to the coding region of the human skeletal actin (*HAS*) gene in the HSA^{LR} mouse model, a transgenic mouse carrying 250 CTG repeats in the 3'UTR of the HSA transgene[88]. Following these encouraging results, Ionis Pharmaceuticals designed higher affinity ASOs containing 2'-4'-constrained ethyl (cEt) modifications, which were described with significantly enhanced *in vivo* potency compared with 2'-MOE–modified ASO[89]. The cEt-modified DMPK ASO demonstrated potent activity in the skeletal and cardiac muscles of normal mice, as well as cynomolgus monkeys[90]. Moreover the same gapmer was shown to improve body weight, muscle strength and muscle histology in the DMSXL mouse model, which harbors a mutant form of the human DMPK gene (carrying >1,000 CTG repeats)[91].

Together with a favourable safety profile, these encouraging preclinical results led to the clinical evaluation of this approach in a human clinical trial (NCT02312011). While the primary objective of the study was safety and tolerability, the results of the trial also revealed insufficient concentration of the therapeutic ASO in muscle tissues following systemic administration and the development of this drug was therefore discontinued[84]. These disappointing results confirmed that delivery remains one of the main challenge of the ASO-therapy for neuromuscular disorders and even more so for DM1. Since the membrane integrity of muscles from patients with DM1 was found no more

permeable than in healthy patients[92], in contrast to patients with DMD for example, DM1 drugs must overcome the barrier of a fully functional membrane. Therefore, more potent chemistries or improved delivery systems must be developed. Ionis Pharmaceuticals has recently focused on ligand conjugated-ASO and published the enhanced potency of fatty acid conjugated ASO in mouse muscles[93]. In particular, palmitic acid conjugation was shown to increase ASO peak plasma concentration (Cmax) and improve delivery to interstitial space of mouse muscle. However, the same group also reported that the promising palmitate conjugate was found less effective in monkeys, therefore limiting its therapeutic potential in humans[94].

Among strategies to improve delivery of ASOs in DM1 muscles, CPP conjugates also offer an attractive option. A recent study from Klein and colleagues demonstrated that a low-dose treatment with a Pip6a-conjugated PMO directed against pathogenic CUG^{exp} repeats was sufficient to achieve an effective concentration of ASOs in muscle fibers and induce an efficient and long-lasting correction of myotonic dystrophy features in DM1 mice as well as in patient-derived cells[95]. Amelioration of the DM1 phenotype included normalization of the transcriptome and reduction in the prevalence of foci-positive fibers. These encouraging results support the clinical development of peptide conjugates for systemic corrective therapy in DM1 but the promise of such compounds still crucially depends on how well they will be tolerated in humans.

5. Amyotrophic lateral sclerosis

Amyotrophic lateral sclerosis (ALS) is a progressive neurodegenerative disease affecting motor neurons in the cortex and spinal cord. With a prevalence of approximately 6 cases per 100 000 individuals, ALS is the most common motor neuron disease in adults[96]. Symptoms in ALS depend on the neurons affected by the disease, most patients have onset in one limb or two upper or lower limbs in an asymmetric fashion and one-third have bulbar onset. Voluntary muscle action is gradually

affected and patients may become completely paralyzed in the later stages of the disease. In general the death of patients occurs due to a respiratory paralysis generally 3 to 5 years following diagnosis[97]. ALS is considered as a complex genetic disorder without discernible family history in the majority of cases. However, ≥30 genes have been reported to confer a major risk of ALS and evidence suggests roles of oligogenic inheritance and of genetic pleiotropy[98]. In the populations with a family history, four genes account for up to 70% of all cases, namely, *SOD1, C9orf72*, *TARDBP* and *FUS*[98]. The antisense technology is an attractive option for ALS and different ASOs are currently being developed preclinically and clinically; the most promising approaches targeting these genes are reviewed below.

5.1. *SOD1* mutations

12–20% of familial cases of ALS are due to mutations in the *SOD1* gene. More than 100 different mutations in the *SOD1* gene confer a toxic gain of function of the SOD1 protein that may impact neuronal function and survival[99]. Reduction of the mutant SOD1 protein concentration can slow progression of SOD1-linked ALS[100] and ASOs have therefore been developed in this aim. During the preclinical studies performed in rats and nonhuman primates models, ASOs were shown to effectively target the central nervous system (CNS) after intrathecal administrations, decrease SOD1 concentration and increase survival[101]. Following these encouraging preclinical data, ISIS333611, a 2'MOE-PS gapmer ASO targeting the exon 1 of *SOD1* mRNA was further developed and became the first experimental ASO delivered intrathecally into patients for the treatment of a neurodegenerative disease[102]. This clinical study confirmed that intrathecal administration of ASOs into the CNS of patients was well tolerated without dose-limiting toxic effects or safety concerns[102]. Moreover, SOD1 concentrations in brain tissue were found to correlate with SOD1 concentrations in the CSF, which allowed the use of CSF SOD1 protein concentrations as a pharmacodynamic marker for ASO activity in the next clinical trials. Despite being encouraging, ISIS333611 effects were modest and advances in ASO technology in particular for other neuromuscular disorders like SMA identified more effective delivery methods to the CNS as well as more potent ASO designs. Further research highlighted a six fold more effective 2'MOE gapmer (named BIIB067) targeting a different region of the *SOD1* mRNA

(the 3' UTR part) and resulting in increased survival of transgenic rodents compared to the previous ISI333611[103]. Preliminary results from the phase 1b/2a clinical study with this ASO (NCT02623699) revealed that intrathecal administration of the highest dose tested of BIIB067 reduced SOD1 concentrations in patients CSF without toxicity, although results must be confirmed on higher number of patients. Currently, two phase 3 clinical trials are ongoing with BIIB067: one to confirm the efficacy, safety, tolerability, pharmacokinetics, and pharmacodynamics of the ASO (NCT02623699) and another to evaluate the long-term safety and tolerability (NCT03070119). The first results of these studies are expected in 2021.

5.2. *C9orf72*

40% of familial cases of ALS are due to an hexanucleotide expansion (GGGGCC) in the noncoding region of the *C9orf72* gene[104]. Several potential mechanisms have been suggested to explain the neurodegeneration caused by this expansion[105]. Amongst them, a toxic gain of function of the RNA, depleting RNA-binding protein similar to the mechanisms of DM1, or a decreased production of the C9orf72 have been proposed. However, the loss of C9orf72 protein alone is not sufficient to create the disease since deletion of the *C9orf72* gene in mice did not result in detectable neurodegeneration[106]. Alternatively, it was reported that the *C9orf72* mutations lead to the transcription of RNAs containing sense GGGGCC (G4C2) and antisense CCCCGG (C4G2) repeats which can exert toxic gain of function and drive neurodegeneration through the production of different poly-dipeptides[107]. These repeats induce an increase in 5 species of dipeptide repeat proteins: poly(GP), poly(GA), poly(PR), poly(GR), and poly(PA), each shown to aggregate in CNS tissues of individuals with ALS[108]. The most important one being the poly(GP) because it is C9orf72 specific and its levels are consistent over time, supporting its continued use as a pharmacodynamics biomarker for expansion-targeted therapeutics[108]. Several studies have reported the use of RNase H1-recruiting ASO and shown reduction of RNA foci and dipeptides in cellular as well as mouse models of C9orf72 ALS[105,109]. In particular, Jiang and colleagues demonstrated that an ASO targeting the region between

exon 1a and 1b leads to a 60-80% decrease of repeat-containing *C9orf72* RNA levels (with exon 1a) in the cortex and spinal cord and preserves C9orf72 protein encoding RNAs (with exon 1b). Four weeks after a single injection of this ASO, a 55-60% decrease of sense foci number was observed and both poly(GP) and poly(GA) were decreased to almost undetectable levels[109]. These results suggest that ASO therapy can mitigate the toxicity from repeat RNAs without exacerbating the disease with a potential loss of C9orf72 function. Based on these findings, clinical studies have been initiated to evaluate the safety, tolerability and pharmacokinetics of BIIB078 (an ASO targeting the same region of *C9orf72* gene)[110] administered intrathecally to ALS patients with C9orf72 hexanucleotide expansion (NCT03626012 and NCT04288856).

5.3. Other targets for ALS

The field has rapidly advanced over the past 5 years and other targets related to TDP-43, ATXN2, FUS or stress pathways are also being investigated as potential therapeutics for ALS[111]. FUS protein is involved in RNA metabolism, including transcription, alternative splicing, and mRNA transport, as well as DNA damage regulation[112] and FUS mutations account for ~5% of familial cases of ALS[113]. FUS-related ALS pathology is characterized by mislocalization of FUS to the cytoplasm and a concomitant reduction in nuclear expression in affected neurons. Loss of nuclear FUS leads to neuronal cell death and accumulation of FUS leads to the formation of toxic stress granules[112]. In their preliminary studies, Zhou and colleagues have demonstrated that FUS is a repressor of its exon 7 and that the exon 7-skipped splice variants of FUS are subjected to nonsense-mediated decay[114]. A 2'OMe-PS ASO was therefore developed to skip exon 7 and ex-vivo studies demonstrated decrease in FUS protein synthesis and restoration of the deficient FUS autoregulation[114].

Ataxin-2 is an additional target which has been investigated as a therapeutic approach for ALS. Ataxin-2 is an RNA-binding protein involved in RNA metabolism. Presence of high number of CAG trinucleotide repeats in this gene is associated with the severe neurodegenerative disease

spinocerebellar ataxia 2 (SCA2) (more than 33 repeats) but also with an increased risk of ALS (29 to 33 repeat expansions)[115]. Reducing expression of ataxin-2 was shown to decrease neurodegeneration in several models, thus opening ASO-mediated therapeutic options to treat these diseases. 2'MOE gapmer ASOs targeting human *ATXN2* were recently screened and shown to decrease *ATXN2* mRNA in cerebella without astroglial and microglial cells activation following ICV injection[116]. A single treatment markedly extended survival of TDP-43 transgenic mice[117], suggesting the therapeutic potential of this approach. Importantly, ASO-mediated reduction of ataxin2 could represent an effective therapeutic strategy for two neurodegenerative diseases, SCA2 and ALS[118]. It is also important to highlight that it may be beneficial for most forms of ALS since TDP-43 aggregation is a common pathological feature for both sporadic and familial forms of ALS[119]. However, evidence suggest that ALS related to SOD1-mutations is independent of TDP-43 cascade, implying there would be no benefit with ataxin-2 inhibition[120].

6. Huntington's disease

Huntington's disease (HD) is an autosomal dominant neurodegenerative disease characterized by progressive movement dysfunction, cognitive impairment and brain atrophy[121]. HD is caused by CAG expansions in the exon 1 of *HTT* gene, encoding an elongated polyglutamine tract in the huntingtin protein (HTT). HTT is critical for nerve cells viability and plays a role in orientation of the mitotic spindle, trafficking of autophagosomes in neurons, and in regulating autophagy[122]. While the pathogenesis of HD is still unclear, most published studies suggest a toxic gain of function for the mutant HTT protein which particularly aggregates and has toxic effects on neurons. Gene silencing approaches including the use of ASOs has been investigated to lower the levels of HTT. ASO therapies for HD offer two main options: the allele specific silencing which aims at knocking down specifically the mutant allele or the non-specific silencing which will lower both alleles and therefore all HTT proteins.

6.1. Non-allele specific approaches

The non-allele specific approach aiming at decreasing the total *HTT* mRNA and protein can be achieved using gapmer ASOs targeting a sequence common to both alleles. Preclinical studies have demonstrated that the ICV infusion of a 2'MOE gapmer ASO during 2 weeks induced efficient and sustainable reduction of HTT in the CNS of YAC128 mice which express the mutant human *HTT* transgene[121]. This inhibition of human HTT in mouse models of HD reversed existing behavioral phenotypes and prevented progressive loss of brain mass[123]. Similar results were also obtained in Rhesus monkeys after intrathecal infusions[121]. Based on these encouraging results, a clinical phase 1b/2a study was initiated with this 2'MOE gapmer (HTTRx later renamed RG6042) targeting an exonic sequence in the *HTT* RNA. RG6042 was delivered by bolus intrathecal injection every 3 months in 46 patients with early stage of HD and five doses were investigated from 10 to 120 mg[124]. The treatment was well-tolerated and a dose-dependent reduction of mutant HTT (mHTT) concentration, which appeared to plateau at higher doses was detected in the CSF[125]. An open-label extension study was started (NCT03342053) as well as a pivotal phase 3 (NCT03761849) at the dose of 120 mg monthly or bimonthly during 25 months to evaluate the long term efficacy and safety of RG6042[126].

6.2. Allele specific approaches

As previously mentioned and given that HTT is involved in nerve cells viability, there is a concern that non-allele specific approach aiming at lowering total HTT may be detrimental for normal neural function. To circumvent this potential risk, some ASOs have been developed to inhibit specifically the mHTT. One way to preferentially silence the mutant allele is to directly target the CAG repeats which are more represented on the mutant allele. This was achieved in preclinical studies using a steric blocker ASO, fully modified 2'OMe-PS named (CUG)7. The first result obtained with this ASO *in vitro* confirmed a difference between the inhibition of WT HTT and mHTT with a higher effect with the mutant gene in HD fibroblasts[127]. This difference was confirmed *in vivo* in HD mouse models with a 15-60% reduction of both soluble and aggregated mutant HTT protein observed in striatum, hippocampus and cortex of treated mice[128]. In the same study, the authors also investigated the

effect of the CUG7 ASO on several endogenous genes with shorter non-expanded CAG repeats and reported no change in expression levels of any of these genes (5 to 20 CAG repeats) suggesting the importance of CAG repeat length for CUG7-mediating silencing[128].

While these encouraging results may suggest an interesting alternative HTT-lowering strategy for HD, this approach has not yet moved to the clinic and the use of CAG targeting ASO is still debated because CAG repeats are also present on the normal allele. Since most patients have a number of CAG repeats relatively close between both alleles, the allele specificity may become more challenging in the clinic. Thus, unambiguous allele-specific approaches have been developed and in particular ASO targeting single-nucleotide polymorphisms (SNP) that are linked to the expanded CAG repeat. 91 SNP were found across the *HTT* gene region but the development of only 3 ASOs may enable selective treatment of a maximum of 80% of HD patients[129]. Several preclinical studies using ASO targeting SNPs have demonstrated robust mHTT suppression and the subsequent reduction of cognitive and behavioral impairment in HD mouse models[130–132]. Wave Live Sciences has been running parallel trials (NCT03225846 and NCT03225833) with two new ASOs, which could theoretically target two-thirds of the HD population; one specific to the region rs362331 (WVE-120101) and the other to rs362307 (WVE-120102). Preliminary results suggest that WVE-120102 induced a reduction of 12% of mHTT protein in the CSF of patients treated intrathecally with the highest dose, i.e. 16 mg[133]. While this figure may appear lower than the previously reported 40-60% reduction of total HTT obtained with RG6042, it is important to note the significant difference in the doses of drug used (16 mg for WVE-120102 vs 120 mg of RG6042). Based on their results showing their drug was safe at lower doses, Wave has also announced it will now add an extra dosing arms to the *PRECISION-HD* trials to test higher doses (32 mg per injection)[133].

Altogether these results highlight that both allele specific and non-allele specific ASO approaches are moving forward for the treatment for HD and the long term results of these trials will definitely shed some light on the debated role of huntingtin in adults and the safety of a non-allele specific approach.

7. CONCLUDING REMARKS

The different examples presented above highlight the variable therapeutic outcomes of the ASO therapies for neuromuscular and neurodegenerative diseases. While some of these drugs have truly demonstrated a significant impact on patient lives, such as the profound clinical benefit observed in SMA patients treated with nusinersen, others have failed to do so. Some of the main reasons for these differences are the target tissue and the route of administration which depend on the disease itself. Indeed the therapeutic outcomes appear much better for diseases where local delivery is possible, as exemplified with SMA, ALS and HD. On the other hand, when the entire musculature must be reached and systemic delivery is the only possible route of administration, things get a bit more complicated, as illustrated by the unsuccessful trial for DM1 and the still limited clinical benefit reported in DMD patients (despite the approval of 3 ASO drugs). Paradoxically the CNS or motor neurons may have been considered more difficult targets to reach than skeletal muscles, but it turns out that ASOs present a relatively good uptake in brain tissues after intrathecal injection.

Overall this illustrates more than ever that delivery is key in the success of ASO therapies and that further efforts are needed to improve it. The development of improved targeted delivery is not only required for muscular dystrophies for which systemic administration is needed but would also be advantageous for the diseases currently treated via intrathecal injection. Antisense treatment is administered via intrathecal route because ASO do not cross the BBB, but this way of administration remains an invasive procedure. Besides the obvious clinical challenges, especially when repeated injections are required, it limits the range of applications to severe and rapidly progressive diseases based on the benefit-risk concept. Moreover it neglects the issue of delivering ASOs to the periphery, which could be crucial for some of these diseases like HD or SMA for example[76,134]. In this context, the development of new ASOs or delivery systems which could deal with the issue of both peripheral and central tissue penetration is also an important milestone.

Development of more potent chemistries or novel delivery systems has become a very active line of research in the past few years [26]. Amongst these potentially interesting technological advances was the advent of stereopure ASO chemistry developed by Wave Life sciences, permitting chirally controlled ASO synthesis, with improvements in both potency and safety. However, in spite of having raised hopes in the DMD community, the recent clinical results did not confirm such improved potency and Wave announced the discontinuation of their DMD ASO program. This highlights the caution that is needed in interpreting *in vitro* data, since the apparent 52% of dystrophin restoration measured in human cells in vitro vs 1% with the PMO clearly did not translate into the same results in the clinic.

There are many opportunities to further improve the ASO platform and a plethora of delivery technologies are emerging to overcome the very poor intracellular bioavailability of nucleic acid drugs. The recent development (and approval) of ASO incorporating GalNAc (N-Acetylgalactosamine) conjugates showing 20- to 30-fold increases in potency has proven the possibility of creating better antisense drugs. These improvements have impacts on many different levels since increasing potency not only reduces the doses of drug to be used, which may impact the cost, but also reduces or eliminates some of the adverse events often associated with high doses of ASOs.

Inspired by the success of the GalNAc conjugates, the conjugation of ASO to various ligands such as peptides or lipids has been explored. In this context, PPMO have shown very promising results in preclinical studies for DMD[56], SMA[80] and DM1[95]. Similarly, lipid-conjugated cEt-ASO have also demonstrated enhanced potency in muscles[93]. Recently, conjugation of ASOs to antibodies has also gained increasing interest and several groups and companies such as Avidity biosciences have started exploring their potential. However, the promise of all these novel compounds still crucially depends on how well they will be tolerated in humans.

Other promising therapeutic approaches have been developed for most of the diseases mentioned in this review and in particular gene replacement therapies mediated by AAV vectors which are particularly useful tools to overcome the delivery challenges in NMDs. AVXS-101, an AAV9 vector designed for *SMN1* replacement was approved by the FDA in 2019 for the treatment of SMA pediatric patients. Given the ability of AAV9 vectors to cross the BBB and the persistence of AAV genomes in tissues, AVXS-101 (commercialized as Zolgensma®) offers the advantage of being a single, one-time intravenous (IV) infusion in contrast with nusinersen which is administered intrathecally several times/year.

Zolgensma® was the first (and only so far) gene therapy drug for SMA and is currently the world's most expensive drug with a price of $2.1M announced by Novartis. In comparison, spinraza® (nusinersen) medication is estimated to cost $750,000 during the first year of treatment and then $375,000 annually thereafter [135]. Gene and ASO therapies are therefore extremely expensive therapies with record high prices, which require a careful consideration of reimbursement and insurance company coverage of medication costs. Nonetheless, it is important to put the costs and benefits of these therapies into perspective, since they offer substantial health gains compared to less expensive conventional treatments and thus may have comparable value in terms of cost-effectiveness [136].

AAV gene therapy programs are also being developed for the treatment of DMD using AAV vectors carrying a microdystrophin transgene. Several clinical trials have been launched to evaluate this strategy in DMD patients and preliminary data have revealed encouraging results with significant restoration of dystrophin expression [138] . The AAV-microdystrophin approach for DMD offers the advantage of being applicable to most DMD patients as opposed to the personalised ASO therapy targeting specific exons. Yet, the limited packaging capacity of AAV vectors imposes a much shorter dystrophin (microdystrophin) which may turn out less functional than the potential dystrophin resulting from exon skipping. As for the SMA gene therapy, the medication would only require a

single IV administration which also compares favourably to the lifelong treatment required with ASO. However, the gene therapy's effectiveness durability still remains to be assessed over long period of time in patients because preclinical studies using AAV vectors in animal models of DMD have suggested a progressive loss of AAV genomes in muscles [61,139]. This is of significant importance considering the immunological challenges (such as neutralizing antibodies) faced by the AAV-gene therapy, currently impairing re-administration. In that regard, ASO do not trigger neutralizing antibodies and can therefore be advantageously re-administered. It is thus not excluded to consider future combination therapies of AAV and ASO as it has already been explored in SMA Type 1 patients treated with both Nusinersen and AVXS-101 [137].

In conclusion, ASO therapies have made tremendous progress in the past 15 years as illustrated by the numerous approvals of ASOs for the treatment of neuromuscular disorders as well as additional diseases not discussed in this review. Even though many challenges remain, notably with respect to targeted delivery, these first successes have paved the way for future disease modifying-therapies based on the ASO technology.

FIGURE LEGENDS

Figure 1: ASOs mechanisms of action. ASOs may exert different effects depending on their structure and design. To induce mRNA degradation via RNase H, ASO must be designed as gapmers (I) with a central core of 8 to 10 consecutive DNA nucleotides to support binding and cleavage by RNase H1 (in blue), flanked by modified nucleotides for nuclease resistance (in red). Fully modified ASO (II) are not able to elicit RNase H activity and they are commonly used as splice switchers (A) to manipulate alternative splicing (exon skipping or exon inclusion); or as steric blockers (B) to either block protein translation or inhibit RNA mediated toxicity by competing with protein binding. ASO: antisense oligonucleotide.

TABLES

Table 1. List of clinical trials for DMD, SMA, DM1, ALS and HD. Abbreviations: 2'OMe-PS: 2'O-methyl with phosphorothioate link; 2'OMe/ENA: 2'OMe-PS and 2'-O,4'-C-ethylene-bridged nucleic acid chimera ASO; 2'MOE-PS: 2'O-methoxyethyl with phosphorothioate link; ALS : Amyotrophic lateral sclerosis; cET: 2'-4'-constrained ethyl; DM1: Myotonic dystrophy type 1; DMD: Duchenne muscular dystrophy; Ex: exon; HD : Huntington's disease; HTT : Huntington's gene; IM: intramuscular; IV: intravenous; PMO: Phosphorodiamidate Morpholino Oligomer; PPMO: peptide conjugated PMO; SMA: Spinal muscular atrophy; Subcut.: Subcutaneous

Figure 1

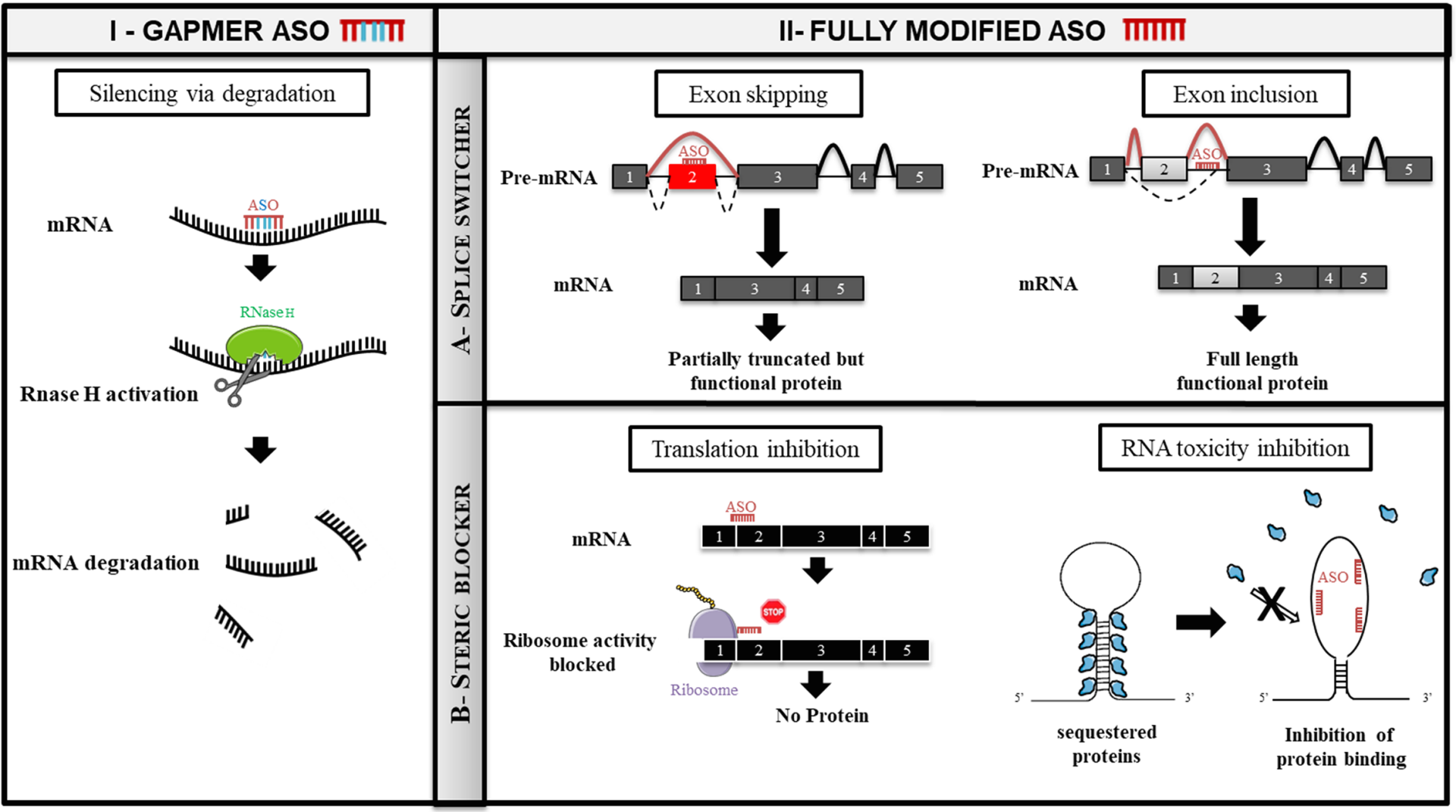
I - GAPMER ASO
II- FULLY MODIFIED ASO
Silencing via degradation
mRNA
ASO
RNaseH
Rnase H activation
mRNA degradation
A- SPLICE SWITCHER
Exon skipping
Pre-mRNA
ASO
1
2
3
4
5
mRNA
Partially truncated but functional protein
Exon inclusion
Pre-mRNA
ASO
mRNA
Full length functional protein
B- STERIC BLOCKER
Translation inhibition
mRNA
ASO
Ribosome activity blocked
STOP
Ribosome
No Protein
RNA toxicity inhibition
5'
3'
sequestered proteins
ASO
Inhibition of protein binding

Disease (target gene)	Drug name	Chemistry and mecanism	Phase	Administration Route	Clinical status	registration number and age of patients	Sponsor
DMD (Ex20)	AO19	2'OMePS exon skipping	1/2	IV (0.5mg/kg)	completed		Kobe university, Japan
DMD (Ex51)	PRO051 (Drisapersen®)	2'OMePS exon skipping	1	IM (0.8mg)	completed		Prosensa
			1/2	Subcut. (escalating doses) and IV	Terminated (2008-2016)	NCT01910649 (5 to 16 years)	Biomarin
			3	Subcut. and IV (6mg/kg and 3mg/kg)	Terminated (2013-2016)	NCT01803412 (5 years and older)	
				Subcut. (6mg/kg)	Terminated (2011-2014)	NCT01480245 (5 years and older)	GSK
	Exondys 51® (AVI-4658 / Eteplirsen) Approved by FDA (2016)– rejected by EMA (2018)	PMO exon skipping	1/2	IM (0.09 to 0.9mg)	Completed (2007-2009)	NCT00159250 (10 to 17 years)	Imperial College of London / AVI biopharma
			1/2	IV (0.5, 1, 2, 4, 10 and 20mg/kg)	Completed (2009-2010)	NCT00844597 (5 to 15 years)	Sarepta
			2	IV (30 and 50mg/kg)	Completed (2011-2012, 2012-2017, 2014-2018 and 2015-2018)	NCT01396239 and NCT01540409 (7 to 13 years) NCT02286947 (7 to 21 years) NCT02420379 (4 to 6 years)	
			3	IV (30mg/kg)	Completed (2014-2019)	NCT02255552 (7 to 16 years)	
			3	IV (2 high doses)	Recruiting (2019-2024)	NCT03992430 (7 to 13 years)	
			2	IV (2, 4, 10, 20, and 30 mg/kg)	Active, not recruiting (2017-2021)	NCT03218995 (6 to 48Mo babies)	
	WVE-210201 (Suvodirsen®)	Stereopure exon skipping	1	IV (0.5, 1, 2, 5 and 10 mg/kg)	Completed (2018-2019)	NCT03508947 (5 to 18 years)	Wave Life Sciences
			2/3	IV (2 doses)	Terminated (2019-2020)	NCT03907072 (5 to 12 years)	
	SRP-5051	PPMO exon skipping	1	IV (escalating doses)	Completed (2018-2019)	NCT03375255 (12 years and older)	Sarepta
			1/2		Recruting (2018-2024)	NCT03675126 (7 years and older)	
			2	IV (12 or 24 week)	Recruting (2019-2021)	NCT04004065 (4 to 21 years)	

DMD (Ex44)	PRO044	2'OMePS exon skipping	1/2	Subcut. (0.5, 1.5, 5, 8, 10 and 12 mg/kg) and IV (1.5, 5 and 8 mg/kg)	Completed (2009-2013)	NCT01037309 (5 to 16 years)	Biomarin
			2	Subcut. (6 mg/kg) and IV (6 and 9 mg/kg)	Terminated (2014-2016)	NCT02329769 (9 to 20 years) NCT02958202 (5 years and older)	
DMD (Ex45)	PRO045	2'OMePS exon skipping	1/2	Subcut. (0.15 to 9mg/kg)	Terminated (2013-2016)	NCT01826474 (5 to 18 years)	Biomarin
	SRP-4045 (casimersen®)	PMO exon skipping	1	IV (4 dose levels)	Completed (2015-2018)	NCT02530905 (7 to 21 years)	Sarepta
			3	IV (30mg/kg)	Recruiting (2016-2023)	NCT02500381 (7 to 13 years)	
	DS-5141b	2'OMe/ENA exon skipping	1/2	Subcut. (0.1, 0.5, 2 and 6 mg/kg)	Active, not recruiting (2015-2020)	NCT02667483 (5 to 10 years)	Daiichi Sankyo Co.
DMD (Ex53)	PRO053	2'OMePS exon skipping	2	Subcut. (1, 3, 6 and 9mg/kg) and IV	Terminated (2013-2016)	NCT01957059 (5 to 18 years)	Biomarin
	NS-065/NCNP-01 (Viltolarsen®) Approved in Japan (2020)	PMO exon skipping	1	IV (1.25, 5 and 20 mg/kg)	Completed (2013-2015)	NCT02081625 (5 to 18 years)	National Center of Neurology and Psychiatry, Japan
			2	IV (40 and 80 mg/kg)	Completed (2016-2018)	NCT02740972 (4 to 9 years)	NS Pharma, Inc.
			3	IV (80 mg/kg)	Recruiting (2019-2024)	NCT04060199 (4 to 7 years)	
			2	IV (40 and 80 mg/kg) Child (4 to 10 years old)	Active, not recruiting (2017-2021)	NCT03167255 (4 to 10 years)	
	SRP-4053 (Golodirsen® Vyondys 53®) Approved by FDA (2019)	PMO exon skipping	1/2	IV (4,10,20 and 30 mg/kg)	Completed (2015-2019)	NCT02310906 (6 to 15 years)	Sarepta
			3	IV (30 mg/kg)	Recruiting (2016-2023)	NCT02500381 (7 to 13 years)	
SMA	ISIS396443 (Nusinersen®= Spinraza®) Approved by FDA (2016) and EMA (2017)	2'-MOE-PS Exon inclusion	1	Intrathecal (1, 3, 6 and 9mg)	Completed (2011-2013 and 2013-2014)	NCT01494701 NCT01780246 (2-14 years)	Biogen
			1/2	Intrathecal (3, 6, 9 and 12 mg)	Completed (2012-2015)	NCT01703988 (2-15 years)	
			1	Intrathecal (12 mg)	Completed (2014-2017)	NCT02052791 (extension of NCT01703988)	
			2	Intrathecal (6 and 12 mg)	Completed (2013-2017)	NCT01839656 (3 weeks-7 months)	

			2	Intrathecal (9.6 to 12 mg)	Terminated (2015-2018)	NCT02462759 (≤18 months)	
			3	Intrathecal (9.6 to 12 mg)	Active (2015-)	NCT02594124 (extension of NCT02462759)	
			2	Intrathecal (12 mg)	Active (2015-)	NCT02386553 (≤ 6 weeks)	
			3	Intrathecal (2.4 mg)	Terminated (2014-2016)	NCT02193074 (<7 months old babies)	
			3	Intrathecal (12 mg)	Completed (2014-2017)	NCT02292537 (2-12 years)	
			2	Intrathecal	Recruiting (2018-2022)	NCT03709784 (18 to 70 years)	Washington University School of Medicine
DM1	ISIS-DMPKRx	cET gapmer	1/2	Subcut.	Completed (2014-2016)	NCT02312011	Ionis Pharma.
ALS (SOD1)	BIIB067 (Tofersen®)	2'MOE-PS Gapmer	1	Intrathecal (0.15, 0.5, 1.5 and 3 mg)	Completed (2010-2012)	NCT01041222	Ionis Pharma.
			3	Intrathecal (20, 40, 60, or 100 mg)	Recruiting (2016-2021 and 2017-2023)	NCT02623699 NCT03070119	Biogen
ALS (C9orf72)	BIIB078 (IONIS-C9Rx®)	2'MOE-PS Gapmer	1	Intrathecal	Active, not recruiting (2018-2021 and 2020-2023)	NCT03626012 NCT04288856	Biogen
HD (HTT)	RO7234292 = RG6042 = ISIS 443139 = IONIS-HTTRx® (Tominersen®)	2'MOE-PS Gapmer	3	Intrathecal (120mg)	Recruiting (2019 2022)	NCT03761849	Hoffmann-La Roche
			1/2	Intrathecal (10, 30, 60, 90 and 120mg)	Completed (2015-2017)	NCT02519036	Ionis Pharma.
	WVE-120101	stereopure Gapmer	1/2	Intrathecal (2, 4, 8, 16 and 32mg)	Recruiting (2017-2020)	NCT03225846	Wave Life Sciences
	WVE-120102					NCT03225833	

COMPLIANCE WITH ETHICAL STANDARDS

CONFLICT OF INTEREST

AV is an employee of SQY therapeutics, developing tcDNA-ASOs. AG and FB declare no conflict of interest.

FUNDING

Authors are supported by the Institut National de la santé et la recherche médicale (INSERM), the Association Monegasque contre les myopathies (AMM), the Duchenne Parent project France (DPPF) and the Fondation UVSQ. AV is an employee of SQY therapeutics.

ACKNOLEDGEMENT

This is a pre-print of an article published in Drugs. The final authenticated version is available online at: https://doi.org/10.1007/s40265-020-01363-

REFERENCES

1. Kaur, H, Wengel, J and Maiti, S (2007). LNA-modified oligonucleotides effectively drive intramolecular-stable hairpin to intermolecular-duplex state. *Biochem. Biophys. Res. Commun.* **352**: 118–122.
2. Griepenburg, JC, Rapp, TL, Carroll, PJ, Eberwine, J and Dmochowski, IJ (2015). Ruthenium-Caged Antisense Morpholinos for Regulating Gene Expression in Zebrafish Embryos. *Chem Sci* **6**: 2342–2346.
3. Gilar, M, Belenky, A, Smisek, DL, Bourque, A and Cohen, AS (1997). Kinetics of phosphorothioate oligonucleotide metabolism in biological fluids. *Nucleic Acids Res.* **25**: 3615–3620.
4. Zamecnik, PC and Stephenson, ML (1978). Inhibition of Rous sarcoma virus replication and cell transformation by a specific oligodeoxynucleotide. *Proc. Natl. Acad. Sci. U.S.A.* **75**: 280–284.
5. Schoch, KM and Miller, TM (2017). Antisense Oligonucleotides: Translation from Mouse Models to Human Neurodegenerative Diseases. *Neuron* **94**: 1056–1070.
6. Wickstrom, E (1986). Oligodeoxynucleotide stability in subcellular extracts and culture media. *J. Biochem. Biophys. Methods* **13**: 97–102.
7. Wickstrom, E (1986). Oligodeoxynucleotide stability in subcellular extracts and culture media. *J. Biochem. Biophys. Methods* **13**: 97–102.
8. Gaus, HJ, Gupta, R, Chappell, AE, Østergaard, ME, Swayze, EE and Seth, PP (2019). Characterization of the interactions of chemically-modified therapeutic nucleic acids with plasma proteins using a fluorescence polarization assay. *Nucleic Acids Res.* **47**: 1110–1122.
9. Crooke, ST, Wang, S, Vickers, TA, Shen, W and Liang, X-H (2017). Cellular uptake and trafficking of antisense oligonucleotides. *Nat. Biotechnol.* **35**: 230–237.

10. Iannitti, T, Morales-Medina, JC and Palmieri, B (2014). Phosphorothioate oligonucleotides: effectiveness and toxicity. *Curr Drug Targets* **15**: 663–673.
11. Crooke, ST, Baker, BF, Witztum, JL, Kwoh, TJ, Pham, NC, Salgado, N, *et al.* (2017). The Effects of 2'-O-Methoxyethyl Containing Antisense Oligonucleotides on Platelets in Human Clinical Trials. *Nucleic Acid Ther* **27**: 121–129.
12. Senn, JJ, Burel, S and Henry, SP (2005). Non-CpG-containing antisense 2'-methoxyethyl oligonucleotides activate a proinflammatory response independent of Toll-like receptor 9 or myeloid differentiation factor 88. *J. Pharmacol. Exp. Ther.* **314**: 972–979.
13. Henry, SP, Beattie, G, Yeh, G, Chappel, A, Giclas, P, Mortari, A, *et al.* (2002). Complement activation is responsible for acute toxicities in rhesus monkeys treated with a phosphorothioate oligodeoxynucleotide. *Int. Immunopharmacol.* **2**: 1657–1666.
14. Iannitti, T, Morales-Medina, JC and Palmieri, B (2014). Phosphorothioate oligonucleotides: effectiveness and toxicity. *Curr Drug Targets* **15**: 663–673.
15. Sheehan, JP and Phan, TM (2001). Phosphorothioate oligonucleotides inhibit the intrinsic tenase complex by an allosteric mechanism. *Biochemistry* **40**: 4980–4989.
16. Eckstein, F (2014). Phosphorothioates, essential components of therapeutic oligonucleotides. *Nucleic Acid Ther* **24**: 374–387.
17. Goyenvalle, A, Leumann, C and Garcia, L (2016). Therapeutic Potential of Tricyclo-DNA antisense oligonucleotides. *J Neuromuscul Dis* **3**: 157–167.
18. Henry, S, Stecker, K, Brooks, D, Monteith, D, Conklin, B and Bennett, CF (2000). Chemically modified oligonucleotides exhibit decreased immune stimulation in mice. *J. Pharmacol. Exp. Ther.* **292**: 468–479.
19. Summerton, J and Weller, D (1997). Morpholino antisense oligomers: design, preparation, and properties. *Antisense Nucleic Acid Drug Dev.* **7**: 187–195.
20. Hagedorn, PH, Persson, R, Funder, ED, Albæk, N, Diemer, SL, Hansen, DJ, *et al.* (2017). Locked nucleic acid: modality, diversity, and drug discovery. *Drug Discov. Today*doi:10.1016/j.drudis.2017.09.018.
21. Seth, PP, Siwkowski, A, Allerson, CR, Vasquez, G, Lee, S, Prakash, TP, *et al.* (2008). Design, synthesis and evaluation of constrained methoxyethyl (cMOE) and constrained ethyl (cEt) nucleoside analogs. *Nucleic Acids Symp Ser (Oxf)*: 553–554doi:10.1093/nass/nrn280.
22. Gupta, A, Mishra, A and Puri, N (2017). Peptide nucleic acids: Advanced tools for biomedical applications. *J. Biotechnol.* **259**: 148–159.
23. Crooke, ST, Witztum, JL, Bennett, CF and Baker, BF (2019). RNA-Targeted Therapeutics. *Cell Metab.* **29**: 501.
24. Bennett, CF (2019). Therapeutic Antisense Oligonucleotides Are Coming of Age. *Annu. Rev. Med.* **70**: 307–321.
25. Crooke, ST (2017). Molecular Mechanisms of Antisense Oligonucleotides. *Nucleic Acid Therapeutics* **27**: 70–77.
26. Godfrey, C, Desviat, LR, Smedsrød, B, Piétri-Rouxel, F, Denti, MA, Disterer, P, *et al.* (2017). Delivery is key: lessons learnt from developing splice-switching antisense therapies. *EMBO Mol Med* **9**: 545–557.
27. Mah, JK, Korngut, L, Dykeman, J, Day, L, Pringsheim, T and Jette, N (2014). A systematic review and meta-analysis on the epidemiology of Duchenne and Becker muscular dystrophy. *Neuromuscul. Disord.* **24**: 482–491.
28. Arechavala-Gomeza, V, Kinali, M, Feng, L, Guglieri, M, Edge, G, Main, M, *et al.* (2010). Revertant fibres and dystrophin traces in Duchenne muscular dystrophy: implication for clinical trials. *Neuromuscul. Disord.* **20**: 295–301.
29. Lu, QL, Morris, GE, Wilton, SD, Ly, T, Artem'yeva, OV, Strong, P, *et al.* (2000). Massive idiosyncratic exon skipping corrects the nonsense mutation in dystrophic mouse muscle and produces functional revertant fibers by clonal expansion. *J Cell Biol* **148**: 985–96.

32. Aartsma-Rus, A, Fokkema, I, Verschuuren, J, Ginjaar, I, van Deutekom, J, van Ommen, GJ, *et al.* (2009). Theoretic applicability of antisense-mediated exon skipping for Duchenne muscular dystrophy mutations. *Hum Mutat* **30**: 293–9.
33. Takeshima, Y, Yagi, M, Wada, H, Ishibashi, K, Nishiyama, A, Kakumoto, M, *et al.* (2006). Intravenous infusion of an antisense oligonucleotide results in exon skipping in muscle dystrophin mRNA of Duchenne muscular dystrophy. *Pediatr Res* **59**: 690–4.
34. Lu, QL, Mann, CJ, Lou, F, Bou-Gharios, G, Morris, GE, Xue, SA, *et al.* (2003). Functional amounts of dystrophin produced by skipping the mutated exon in the mdx dystrophic mouse. *Nat Med* **9**: 1009–14.
35. Van Deutekom, JC, Janson, AA, Ginjaar, IB, Frankhuizen, WS, Aartsma-Rus, A, Bremmer-Bout, M, *et al.* (2007). Local dystrophin restoration with antisense oligonucleotide PRO051. *New England Journal of Medicine* **357**: 2677–2686.
36. Goemans, NM, Tulinius, M, van den Akker, JT, Burm, BE, Ekhart, PF, Heuvelmans, N, *et al.* (2011). Systemic administration of PRO051 in Duchenne's muscular dystrophy. *New England Journal of Medicine* **364**: 1513–1522.
37. Goemans, NM, Tulinius, M, van den Hauwe, M, Kroksmark, A-K, Buyse, G, Wilson, RJ, *et al.* (2016). Long-Term Efficacy, Safety, and Pharmacokinetics of Drisapersen in Duchenne Muscular Dystrophy: Results from an Open-Label Extension Study. *PloS one* **11**: e0161955.
38. Goemans, N, Mercuri, E, Belousova, E, Komaki, H, Dubrovsky, A, McDonald, CM, *et al.* (2018). A randomized placebo-controlled phase 3 trial of an antisense oligonucleotide, drisapersen, in Duchenne muscular dystrophy. *Neuromuscul. Disord.* **28**: 4–15.
39. Alter, J, Lou, F, Rabinowitz, A, Yin, H, Rosenfeld, J, Wilton, SD, *et al.* (2006). Systemic delivery of morpholino oligonucleotide restores dystrophin expression bodywide and improves dystrophic pathology. *Nat Med* **12**: 175–7.
40. Kinali, M, Arechavala-Gomeza, V, Feng, L, Cirak, S, Hunt, D, Adkin, C, *et al.* (2009). Local restoration of dystrophin expression with the morpholino oligomer AVI-4658 in Duchenne muscular dystrophy: a single-blind, placebo-controlled, dose-escalation, proof-of-concept study. *Lancet Neurol* **8**: 918–28.
41. Cirak, S, Arechavala-Gomeza, V, Guglieri, M, Feng, L, Torelli, S, Anthony, K, *et al.* (2011). Exon skipping and dystrophin restoration in patients with Duchenne muscular dystrophy after systemic phosphorodiamidate morpholino oligomer treatment: an open-label, phase 2, dose-escalation study. *Lancet* **378**: 595–605.
42. Mendell, JR, Rodino-Klapac, LR, Sahenk, Z, Roush, K, Bird, L, Lowes, LP, *et al.* (2013). Eteplirsen for the treatment of Duchenne muscular dystrophy: Eteplirsen for DMD. *Annals of Neurology* **74**: 637–647.
43. Mendell, JR, Goemans, N, Lowes, LP, Alfano, LN, Berry, K, Shao, J, *et al.* (2016). Longitudinal effect of eteplirsen versus historical control on ambulation in Duchenne muscular dystrophy: Eteplirsen in DMD. *Annals of Neurology* **79**: 257–271.
44. Aartsma-Rus, A and Goemans, N (2019). A Sequel to the Eteplirsen Saga: Eteplirsen Is Approved in the United States but Was Not Approved in Europe. *Nucleic Acid Ther* **29**: 13–15.
45. Alfano, LN, Charleston, JS, Connolly, AM, Cripe, L, Donoghue, C, Dracker, R, *et al.* (2019). Long-term treatment with eteplirsen in nonambulatory patients with Duchenne muscular dystrophy. *Medicine (Baltimore)* **98**: e15858.
46. Carver, MP, Charleston, JS, Shanks, C, Zhang, J, Mense, M, Sharma, AK, *et al.* (2016). Toxicological Characterization of Exon Skipping Phosphorodiamidate Morpholino Oligomers (PMOs) in Non-human Primates. *J Neuromuscul Dis* **3**: 381–393.
47. Frank, DE, Schnell, FJ, Akana, C, El-Husayni, SH, Desjardins, CA, Morgan, J, *et al.* (2020). Increased dystrophin production with golodirsen in patients with Duchenne muscular dystrophy. *Neurology* **94**: e2270–e2282.
48. Heo, Y-A (2020). Golodirsen: First Approval. *Drugs* **80**: 329–333.

49. Komaki, H, Nagata, T, Saito, T, Masuda, S, Takeshita, E, Sasaki, M, *et al.* (2018). Systemic administration of the antisense oligonucleotide NS-065/NCNP-01 for skipping of exon 53 in patients with Duchenne muscular dystrophy. *Sci Transl Med* **10**.
50. Roshmi, RR and Yokota, T (2019). Viltolarsen for the treatment of Duchenne muscular dystrophy. *Drugs Today* **55**: 627–639.
51. Aartsma-Rus, A, Morgan, J, Lonkar, P, Neubert, H, Owens, J, Binks, M, *et al.* (2019). Report of a TREAT-NMD/World Duchenne Organisation Meeting on Dystrophin Quantification Methodology. *J Neuromuscul Dis* **6**: 147–159.
52. (2020). Wave Life Sciences Announces Suvodirsen Phase 1 Safety and Tolerability Data and Phase 2/3 Clinical Trial Design. *Wave Life Sciences*at <https://ir.wavelifesciences.com/news-releases/news-release-details/wave-life-sciences-announces-suvodirsen-phase-1-safety-and>.
54. Lee, T, Awano, H, Yagi, M, Matsumoto, M, Watanabe, N, Goda, R, *et al.* (2017). 2'-O-Methyl RNA/Ethylene-Bridged Nucleic Acid Chimera Antisense Oligonucleotides to Induce Dystrophin Exon 45 Skipping. *Genes (Basel)* **8**.
55. DAIICHI SANKYO COMPANY (2018). Daiichi Sankyo Announces Phase 1/2 Clinical Trial Results for DS-5141 (Therapeutic Agent for Duchenne Muscular Dystrophy) in Japanat <https://www.daiichisankyo.com/media_investors/media_relations/press_releases/detail/006840.html>.
56. Gait, MJ, Arzumanov, AA, McClorey, G, Godfrey, C, Betts, C, Hammond, S, *et al.* (2019). Cell-Penetrating Peptide Conjugates of Steric Blocking Oligonucleotides as Therapeutics for Neuromuscular Diseases from a Historical Perspective to Current Prospects of Treatment. *Nucleic Acid Ther* **29**: 1–12.
57. Moulton, HM and Moulton, JD. Morpholinos and their peptide conjugates: Therapeutic promise and challenge for Duchenne muscular dystrophy. *Biochim Biophys Acta*at <http://www.ncbi.nlm.nih.gov/entrez/query.fcgi?cmd=Retrieve&db=PubMed&dopt=Citation&list_uids=20170628>.
58. Goyenvalle, A, Griffith, G, Babbs, A, El Andaloussi, S, Ezzat, K, Avril, A, *et al.* (2015). Functional correction in mouse models of muscular dystrophy using exon-skipping tricyclo-DNA oligomers. *Nature medicine* **21**: 270–5.
59. Relizani, K, Griffith, G, Echevarría, L, Zarrouki, F, Facchinetti, P, Vaillend, C, *et al.* (2017). Efficacy and Safety Profile of Tricyclo-DNA Antisense Oligonucleotides in Duchenne Muscular Dystrophy Mouse Model. *Mol Ther Nucleic Acids* **8**: 144–157.
60. Goyenvalle, A, Vulin, A, Fougerousse, F, Leturcq, F, Kaplan, JC, Garcia, L, *et al.* (2004). Rescue of dystrophic muscle through U7 snRNA-mediated exon skipping. *Science* **306**: 1796–9.
61. Vulin, A, Barthelemy, I, Goyenvalle, A, Thibaud, JL, Beley, C, Griffith, G, *et al.* (2012). Muscle function recovery in golden retriever muscular dystrophy after AAV1-U7 exon skipping. *Mol Ther* **20**: 2120–33.
62. Wein, N, Vulin, A, Falzarano, MS, Szigyarto, CA-K, Maiti, B, Findlay, A, *et al.* (2014). Translation from a DMD exon 5 IRES results in a functional dystrophin isoform that attenuates dystrophinopathy in humans and mice. *Nat. Med.* **20**: 992–1000.
63. Verhaart, IEC, Robertson, A, Wilson, IJ, Aartsma-Rus, A, Cameron, S, Jones, CC, *et al.* (2017). Prevalence, incidence and carrier frequency of 5q-linked spinal muscular atrophy - a literature review. *Orphanet J Rare Dis* **12**: 124.
64. Calucho, M, Bernal, S, Alías, L, March, F, Venceslá, A, Rodríguez-Álvarez, FJ, *et al.* (2018). Correlation between SMA type and SMN2 copy number revisited: An analysis of 625 unrelated Spanish patients and a compilation of 2834 reported cases. *Neuromuscul. Disord.* **28**: 208–215.
65. Scholl, R, Marquis, J, Meyer, K and Schümperli, D (2007). Spinal muscular atrophy: position and functional importance of the branch site preceding SMN exon 7. *RNA Biol* **4**: 34–37.
66. Singh, RN and Singh, NN (2018). Mechanism of Splicing Regulation of Spinal Muscular Atrophy Genes. *Adv Neurobiol* **20**: 31–61.

67. Singh, NK, Singh, NN, Androphy, EJ and Singh, RN (2006). Splicing of a Critical Exon of Human Survival Motor Neuron Is Regulated by a Unique Silencer Element Located in the Last Intron. *Molecular and Cellular Biology* **26**: 1333–1346.
68. Hua, Y, Sahashi, K, Hung, G, Rigo, F, Passini, MA, Bennett, CF, *et al.* (2010). Antisense correction of SMN2 splicing in the CNS rescues necrosis in a type III SMA mouse model. *Genes Dev* **24**: 1634–1644.
69. Hua, Y, Sahashi, K, Rigo, F, Hung, G, Horev, G, Bennett, CF, *et al.* (2011). Peripheral SMN restoration is essential for long-term rescue of a severe SMA mouse model. *Nature* **478**: 123–126.
70. Chiriboga, CA, Swoboda, KJ, Darras, BT, Iannaccone, ST, Montes, J, De Vivo, DC, *et al.* (2016). Results from a phase 1 study of nusinersen (ISIS-SMNRx) in children with spinal muscular atrophy. *Neurology* **86**: 890–897.
71. Finkel, RS, Chiriboga, CA, Vajsar, J, Day, JW, Montes, J, De Vivo, DC, *et al.* (2016). Treatment of infantile-onset spinal muscular atrophy with nusinersen: a phase 2, open-label, dose-escalation study. *Lancet* **388**: 3017–3026.
72. Nusinersen initiated in infants during the presymptomatic stage of spinal muscular atrophy: Interim efficacy and safety results from the Phase 2 NURTURE study - Neuromuscular Disordersat <https://www.nmd-journal.com/article/S0960-8966(19)31127-7/fulltext>.
73. Mercuri, E, Darras, BT, Chiriboga, CA, Day, JW, Campbell, C, Connolly, AM, *et al.* (2018). Nusinersen versus Sham Control in Later-Onset Spinal Muscular Atrophy. *New England Journal of Medicine* **378**: 625–635.
74. Darras, BT, Chiriboga, CA, Iannaccone, ST, Swoboda, KJ, Montes, J, Mignon, L, *et al.* (2019). Nusinersen in later-onset spinal muscular atrophy: Long-term results from the phase 1/2 studies. *Neurology* **92**: e2492–e2506.
75. Meylemans, A and De Bleecker, J (2019). Current evidence for treatment with nusinersen for spinal muscular atrophy: a systematic review. *Acta Neurol Belg* **119**: 523–533.
76. Shababi, M, Lorson, CL and Rudnik-Schöneborn, SS (2014). Spinal muscular atrophy: a motor neuron disorder or a multi-organ disease? *J. Anat.* **224**: 15–28.
77. Bortolani, S, Stura, G, Ventilii, G, Vercelli, L, Rolle, E, Ricci, F, *et al.* (2019). Intrathecal administration of nusinersen in adult and adolescent patients with spinal muscular atrophy and scoliosis: Transforaminal versus conventional approach. *Neuromuscul. Disord.* **29**: 742–746.
78. Cordts, I, Lingor, P, Friedrich, B, Pernpeintner, V, Zimmer, C, Deschauer, M, *et al.* (2020). Intrathecal nusinersen administration in adult spinal muscular atrophy patients with complex spinal anatomy. *Ther Adv Neurol Disord* **13**.
79. Strauss, KA, Carson, VJ, Brigatti, KW, Young, M, Robinson, DL, Hendrickson, C, *et al.* (2018). Preliminary Safety and Tolerability of a Novel Subcutaneous Intrathecal Catheter System for Repeated Outpatient Dosing of Nusinersen to Children and Adults With Spinal Muscular Atrophy. *J Pediatr Orthop* **38**: e610–e617.
80. Hammond, SM, Hazell, G, Shabanpoor, F, Saleh, AF, Bowerman, M, Sleigh, JN, *et al.* (2016). Systemic peptide-mediated oligonucleotide therapy improves long-term survival in spinal muscular atrophy. *Proc. Natl. Acad. Sci. U.S.A.* **113**: 10962–10967.
81. Robin, V, Griffith, G, Carter, J-PL, Leumann, CJ, Garcia, L and Goyenvalle, A (2017). Efficient SMN Rescue following Subcutaneous Tricyclo-DNA Antisense Oligonucleotide Treatment. *Mol Ther Nucleic Acids* **7**: 81–89.
82. Ramdas, S and Servais, L (2020). New treatments in spinal muscular atrophy: an overview of currently available data. *Expert Opin Pharmacother* **21**: 307–315.
83. Harper, PS (2009). *Myotonic dystrophy*, Oxford University Press, Oxford ; New York, 106pp.
84. Overby, SJ, Cerro-Herreros, E, Llamusi, B and Artero, R (2018). RNA-mediated therapies in myotonic dystrophy. *Drug Discov. Today* **23**: 2013–2022.
85. Wheeler, TM, Lueck, JD, Swanson, MS, Dirksen, RT and Thornton, CA (2007). Correction of ClC-1 splicing eliminates chloride channelopathy and myotonia in mouse models of myotonic dystrophy. *Journal of Clinical Investigation*doi:10.1172/JCI33355.

86. Wheeler, TM, Sobczak, K, Lueck, JD, Osborne, RJ, Lin, X, Dirksen, RT, *et al.* (2009). Reversal of RNA dominance by displacement of protein sequestered on triplet repeat RNA. *Science* **325**: 336–9.
87. Lee, JE, Bennett, CF and Cooper, TA (2012). RNase H-mediated degradation of toxic RNA in myotonic dystrophy type 1. *Proc. Natl. Acad. Sci. U.S.A.* **109**: 4221–4226.
88. Wheeler, TM, Leger, AJ, Pandey, SK, MacLeod, AR, Nakamori, M, Cheng, SH, *et al.* (2012). Targeting nuclear RNA for in vivo correction of myotonic dystrophy. *Nature* **488**: 111–115.
89. Seth, PP, Siwkowski, A, Allerson, CR, Vasquez, G, Lee, S, Prakash, TP, *et al.* (2009). Short antisense oligonucleotides with novel 2'-4' conformationaly restricted nucleoside analogues show improved potency without increased toxicity in animals. *J. Med. Chem.* **52**: 10–13.
90. Pandey, SK, Wheeler, TM, Justice, SL, Kim, A, Younis, HS, Gattis, D, *et al.* (2015). Identification and Characterization of Modified Antisense Oligonucleotides Targeting DMPK in Mice and Nonhuman Primates for the Treatment of Myotonic Dystrophy Type 1. *Journal of Pharmacology and Experimental Therapeutics* **355**: 310–321.
91. Jauvin, D, Chrétien, J, Pandey, SK, Martineau, L, Revillod, L, Bassez, G, *et al.* (2017). Targeting DMPK with Antisense Oligonucleotide Improves Muscle Strength in Myotonic Dystrophy Type 1 Mice. *Mol Ther Nucleic Acids* **7**: 465–474.
92. González-Barriga, A, Kranzen, J, Croes, HJE, Bijl, S, van den Broek, WJAA, van Kessel, IDG, *et al.* (2015). Cell membrane integrity in myotonic dystrophy type 1: implications for therapy. *PLoS ONE* **10**: e0121556.
93. Prakash, TP, Mullick, AE, Lee, RG, Yu, J, Yeh, ST, Low, A, *et al.* (2019). Fatty acid conjugation enhances potency of antisense oligonucleotides in muscle. *Nucleic Acids Res.* **47**: 6029–6044.
94. Østergaard, ME, Jackson, M, Low, A, E Chappell, A, G Lee, R, Peralta, RQ, *et al.* (2019). Conjugation of hydrophobic moieties enhances potency of antisense oligonucleotides in the muscle of rodents and non-human primates. *Nucleic Acids Res.* **47**: 6045–6058.
95. Klein, AF, Varela, MA, Arandel, L, Holland, A, Naouar, N, Arzumanov, A, *et al.* (2019). Peptide-conjugated oligonucleotides evoke long-lasting myotonic dystrophy correction in patient-derived cells and mice. *J. Clin. Invest.* **129**: 4739–4744.
96. Talbott, EO, Malek, AM and Lacomis, D (2016). The epidemiology of amyotrophic lateral sclerosis. *Handb Clin Neurol* **138**: 225–238.
97. Brown, RH and Al-Chalabi, A (2017). Amyotrophic Lateral Sclerosis. *N. Engl. J. Med.* **377**: 162–172.
98. Hardiman, O, Al-Chalabi, A, Chio, A, Corr, EM, Logroscino, G, Robberecht, W, *et al.* (2017). Amyotrophic lateral sclerosis. *Nat Rev Dis Primers* **3**: 17071.
99. Andersen, PM and Al-Chalabi, A (2011). Clinical genetics of amyotrophic lateral sclerosis: what do we really know? *Nat Rev Neurol* **7**: 603–615.
100. Rothstein, JD (2009). Current hypotheses for the underlying biology of amyotrophic lateral sclerosis. *Ann. Neurol.* **65 Suppl 1**: S3-9.
101. Smith, RA, Miller, TM, Yamanaka, K, Monia, BP, Condon, TP, Hung, G, *et al.* (2006). Antisense oligonucleotide therapy for neurodegenerative disease. *J. Clin. Invest.* **116**: 2290–2296.
102. Miller, TM, Pestronk, A, David, W, Rothstein, J, Simpson, E, Appel, SH, *et al.* (2013). An antisense oligonucleotide against SOD1 delivered intrathecally for patients with SOD1 familial amyotrophic lateral sclerosis: a phase 1, randomised, first-in-man study. *Lancet Neurol* **12**: 435–442.
103. McCampbell, A, Cole, T, Wegener, AJ, Tomassy, GS, Setnicka, A, Farley, BJ, *et al.* (2018). Antisense oligonucleotides extend survival and reverse decrement in muscle response in ALS models. *J. Clin. Invest.* **128**: 3558–3567.
104. Cudkowicz, ME, McKenna-Yasek, D, Sapp, PE, Chin, W, Geller, B, Hayden, DL, *et al.* (1997). Epidemiology of mutations in superoxide dismutase in amyotrophic lateral sclerosis. *Ann. Neurol.* **41**: 210–221.

105. Bennett, CF, Krainer, AR and Cleveland, DW (2019). Antisense Oligonucleotide Therapies for Neurodegenerative Diseases. *Annu. Rev. Neurosci.* **42**: 385–406.
106. Berth, SH and Lloyd, TE (2019). How can an understanding of the C9orf72 gene translate into amyotrophic lateral sclerosis therapies? *Expert Review of Neurotherapeutics* **19**: 895–897.
107. Jiang, J and Ravits, J (2019). Pathogenic Mechanisms and Therapy Development for C9orf72 Amyotrophic Lateral Sclerosis/Frontotemporal Dementia. *Neurotherapeutics* **16**: 1115–1132.
108. Cammack, AJ, Atassi, N, Hyman, T, van den Berg, LH, Harms, M, Baloh, RH, *et al.* (2019). Prospective natural history study of C9orf72 ALS clinical characteristics and biomarkers. *Neurology* **93**: e1605–e1617.
109. Jiang, J, Zhu, Q, Gendron, TF, Saberi, S, McAlonis-Downes, M, Seelman, A, *et al.* (2016). Gain of Toxicity from ALS/FTD-Linked Repeat Expansions in C9ORF72 Is Alleviated by Antisense Oligonucleotides Targeting GGGGCC-Containing RNAs. *Neuron* **90**: 535–550.
110. Building a Neuromuscular Franchise: Progress in ALS. Biogen (June 5, 2019)at <https://investors.biogen.com/static-files/c21d50af-43ce-43a3-8e02-9fbd4a7c5558>.
111. Klim, JR, Vance, C and Scotter, EL (2019). Antisense oligonucleotide therapies for Amyotrophic Lateral Sclerosis: Existing and emerging targets. *Int. J. Biochem. Cell Biol.* **110**: 149–153.
112. Ishigaki, S and Sobue, G (2018). Importance of Functional Loss of FUS in FTLD/ALS. *Front Mol Biosci* **5**: 44.
113. Marangi, G and Traynor, BJ (2015). Genetic causes of amyotrophic lateral sclerosis: new genetic analysis methodologies entailing new opportunities and challenges. *Brain Res.* **1607**: 75–93.
114. Zhou, Y, Liu, S, Liu, G, Öztürk, A and Hicks, GG (2013). ALS-Associated FUS Mutations Result in Compromised FUS Alternative Splicing and Autoregulation. *PLoS Genet* **9**.
115. Sproviero, W, Shatunov, A, Stahl, D, Shoai, M, van Rheenen, W, Jones, AR, *et al.* (2017). ATXN2 trinucleotide repeat length correlates with risk of ALS. *Neurobiol. Aging* **51**: 178.e1-178.e9.
116. Scoles, DR, Meera, P, Schneider, MD, Paul, S, Dansithong, W, Figueroa, KP, *et al.* (2017). Antisense oligonucleotide therapy for spinocerebellar ataxia type 2. *Nature* **544**: 362–366.
117. Becker, LA, Huang, B, Bieri, G, Ma, R, Knowles, DA, Jafar-Nejad, P, *et al.* (2017). Therapeutic reduction of ataxin-2 extends lifespan and reduces pathology in TDP-43 mice. *Nature* **544**: 367–371.
118. Zhang, K and Rothstein, JD (2017). Neurodegenerative disease: Two-for-one on potential therapies. *Nature* **544**: 302–303.
119. Neumann, M, Sampathu, DM, Kwong, LK, Truax, AC, Micsenyi, MC, Chou, TT, *et al.* (2006). Ubiquitinated TDP-43 in frontotemporal lobar degeneration and amyotrophic lateral sclerosis. *Science* **314**: 130–133.
120. Ito, D and Suzuki, N (2011). Conjoint pathologic cascades mediated by ALS/FTLD-U linked RNA-binding proteins TDP-43 and FUS. *Neurology* **77**: 1636–1643.
121. Kordasiewicz, HB, Stanek, LM, Wancewicz, EV, Mazur, C, McAlonis, MM, Pytel, KA, *et al.* (2012). Sustained therapeutic reversal of Huntington's disease by transient repression of huntingtin synthesis. *Neuron* **74**: 1031–1044.
122. Martin, DDO, Kay, C, Collins, JA, Nguyen, YT, Slama, RA and Hayden, MR (2018). A human huntingtin SNP alters post-translational modification and pathogenic proteolysis of the protein causing Huntington disease. *Sci Rep* **8**: 8096.
123. Keiser, MS, Kordasiewicz, HB and McBride, JL (2016). Gene suppression strategies for dominantly inherited neurodegenerative diseases: lessons from Huntington's disease and spinocerebellar ataxia. *Hum. Mol. Genet.* **25**: R53-64.
124. Tabrizi, SJ, Leavitt, BR, Landwehrmeyer, GB, Wild, EJ, Saft, C, Barker, RA, *et al.* (2019). Targeting Huntingtin Expression in Patients with Huntington's Disease. *N. Engl. J. Med.* **380**: 2307–2316.

125. Rodrigues, FB and Wild, EJ (2018). Huntington's Disease Clinical Trials Corner: February 2018. *J Huntingtons Dis* **7**: 89–98.
126. Rodrigues, FB, Quinn, L and Wild, EJ (2019). Huntington's Disease Clinical Trials Corner: January 2019. *J Huntingtons Dis* **8**: 115–125.
127. Evers, MM, Pepers, BA, van Deutekom, JCT, Mulders, SAM, den Dunnen, JT, Aartsma-Rus, A, *et al.* (2011). Targeting several CAG expansion diseases by a single antisense oligonucleotide. *PLoS ONE* **6**: e24308.
128. Datson, NA, González-Barriga, A, Kourkouta, E, Weij, R, van de Giessen, J, Mulders, S, *et al.* (2017). The expanded CAG repeat in the huntingtin gene as target for therapeutic RNA modulation throughout the HD mouse brain. *PLoS One* **12**.
129. Kay, C, Collins, JA, Skotte, NH, Southwell, AL, Warby, SC, Caron, NS, *et al.* (2015). Huntingtin Haplotypes Provide Prioritized Target Panels for Allele-specific Silencing in Huntington Disease Patients of European Ancestry. *Mol. Ther.* **23**: 1759–1771.
130. Carroll, JB, Warby, SC, Southwell, AL, Doty, CN, Greenlee, S, Skotte, N, *et al.* (2011). Potent and Selective Antisense Oligonucleotides Targeting Single-Nucleotide Polymorphisms in the Huntington Disease Gene / Allele-Specific Silencing of Mutant Huntingtin. *Mol Ther* **19**: 2178–2185.
131. Skotte, NH, Southwell, AL, Østergaard, ME, Carroll, JB, Warby, SC, Doty, CN, *et al.* (2014). Allele-Specific Suppression of Mutant Huntingtin Using Antisense Oligonucleotides: Providing a Therapeutic Option for All Huntington Disease Patients. In: Glorioso, JC (ed.). *PLoS ONE* **9**: e107434.
132. Southwell, AL, Kordasiewicz, HB, Langbehn, D, Skotte, NH, Parsons, MP, Villanueva, EB, *et al.* (2018). Huntingtin suppression restores cognitive function in a mouse model of Huntington's disease. *Sci Transl Med* **10**.
133. Unpacking Wave's PRECISION-HD2 huntingtin-lowering trial announcement - HDBuzz - Huntington's disease research news.at <https://en.hdbuzz.net/277>.
134. Carroll, JB, Bates, GP, Steffan, J, Saft, C and Tabrizi, SJ (2015). Treating the whole body in Huntington's disease. *Lancet Neurol* **14**: 1135–1142.
135. Neil, EE and Bisaccia, EK (2019). Nusinersen: A Novel Antisense Oligonucleotide for the Treatment of Spinal Muscular Atrophy. *J Pediatr Pharmacol Ther* **24**: 194–203.
136. Joshua T. Cohen, James D. Chambers, Madison C. Silver, Pei-Jung Lin and Peter J. Neumann (2019). Putting The Costs And Benefits Of New Gene Therapies Into Perspectiveat <https://www.healthaffairs.org/do/10.1377/hblog20190827.553404/full/>.
137. Lee, BH, Collins, E, Lewis, L, Guntrum, D, Eichinger, K, Voter, K, *et al.* (2019). Combination therapy with nusinersen and AVXS-101 in SMA type 1. *Neurology* **93**: 640–641.
138. Crudele, JM and Chamberlain, JS (2019). AAV-based gene therapies for the muscular dystrophies. *Hum. Mol. Genet.* **28**: R102–R107.
139. Le Hir, M, Goyenvalle, A, Peccate, C, Précigout, G, Davies, KE, Voit, T, *et al.* (2013). AAV Genome Loss From Dystrophic Mouse Muscles During AAV-U7 snRNA-mediated Exon-skipping Therapy. *Molecular Therapy* **21**: 1551–1558.